

2017

Separate Roles of FAN1 and Fanconi Anemia Proteins in DNA Interstrand Crosslink Repair and Human Disease

Supawat Thongthip

Follow this and additional works at: http://digitalcommons.rockefeller.edu/student_theses_and_dissertations



Part of the [Life Sciences Commons](#)

Recommended Citation

Thongthip, Supawat, "Separate Roles of FAN1 and Fanconi Anemia Proteins in DNA Interstrand Crosslink Repair and Human Disease" (2017). *Student Theses and Dissertations*. 395.
http://digitalcommons.rockefeller.edu/student_theses_and_dissertations/395

This Thesis is brought to you for free and open access by Digital Commons @ RU. It has been accepted for inclusion in Student Theses and Dissertations by an authorized administrator of Digital Commons @ RU. For more information, please contact mcsweej@mail.rockefeller.edu.



SEPARATE ROLES OF FAN1 AND
FANCONI ANEMIA PROTEINS IN
DNA INTERSTRAND CROSSLINK REPAIR
AND HUMAN DISEASE

A Thesis Presented to the Faculty of

The Rockefeller University

in Partial Fulfillment of the Requirements for

the degree of Doctor of Philosophy

by

Supawat Thongthip

June 2017

SEPARATE ROLES OF FAN1 AND FANCONI ANEMIA PROTEINS IN DNA INTERSTRAND CROSSLINK REPAIR AND HUMAN DISEASE

Supawat Thongthip, Ph.D.

The Rockefeller University 2017

DNA interstrand crosslink (ICL) repair is vital for cellular proliferation and survival. Defects in the repair of DNA crosslinks have been associated with congenital abnormalities, bone marrow and kidney failure, liver dysfunction, and cancer. DNA nucleases play a significant role during the repair of ICLs and they function at multiple repair steps. Here, we assessed the contributions of FANCD2/FANCI-Associated Nuclease 1 (FAN1) to the repair of ICL lesions and studied the consequences of its deficiency, which results in rare chronic kidney disease - Karyomegalic Interstitial Nephritis (KIN). FAN1 is a highly conserved nuclease from yeast to humans. It was first identified in an RNAi screen for proteins necessary for ICL repair and also as a direct interacting partner of FANCI/FANCD2 (ID2) complex of the Fanconi anemia pathway. Using cells isolated from human KIN patients and *Fan1*-deficient mice, we showed that ICL repair function of FAN1 is non-overlapping with Fanconi anemia proteins, yet redundant with SNM1A, an exonuclease that was previously implicated in ICL

repair. Furthermore, the *Fan1* knockout mouse model recapitulates many of the phenotypes observed in human KIN patients, including renal karyomegaly and liver dysfunction. *Fan1*-deficient mice displayed hypersensitivity to ICL-inducing chemotherapeutic drugs and developed bone marrow failure following the treatment. We also demonstrated that formaldehyde and acetaldehyde are likely not the endogenous damaging agents that lead to KIN in the absence of FAN1. In parallel studies, we explored the possibility of rescuing ICL sensitivity of Fanconi anemia patient cells through an inhibition of non-homologous end joining repair (NHEJ) factors. Using both genetic and chemical approaches, we showed that NHEJ suppression could not compensate for the lack of FA pathway in the repair of ICLs.

ACKNOWLEDGEMENTS

First and foremost, I would like to thank my advisor Dr. Agata Smogorzewska, for her incredible support during all these years of graduate school. She has instilled in me the fundamentals of scientific rigor, from how good experiments should be set up and executed to how science could be effectively communicated. I have learned greatly about the good scientific practices and principles and have developed into a much more critical scientist and person, thanks to her guidance. I am also grateful to my thesis committee Dr. Titia de Lange and Dr. Nina Papavasiliou for years of advice and critical evaluation to help me focus on the important questions and experiments and ensure that I am on the right track. In addition, I would like to extend my gratitude to Dr. John Petrini who accepted the invitation to be my external examiner committee.

I would also like to express my appreciation to the past and present members of the Smogorzewska lab. I thank Frank Lach for keeping the lab functional, the utmost accurate forecasts on the weather, and generous tips on fishing. I thank Liz Garner for mentoring me during my rotation and for all the suggestions and support when experiments failed. I thank Siobhan (Gregg) Addie for introducing me to the world of mice, American pop culture and constant supplies of bake goods. I thank Anderson Wang for being approachable and

always helpful when it came to science and DNA repair. I have missed our tennis sessions and fun time exploring NYC's food scene. I thank Charlotte Cockram for being a good company who always gave practical advice on work and non-work related issues as well as for helping refresh my sense of Britishness. I especially thank Sunandini Sridhar for providing me with tremendous support. I will miss our fun time discussing sociopolitical issues, making trips to the mouse room, spending long hours with bone marrow transplant experiments, and enjoying Sukhumvit 51. I also thank her for advice on career and many other important decisions and for reading my thesis.

I would like to extend my thanks to the Funabiki lab. I thank Hiro Funabiki for many of the passionate and thoughtful discussions. I thank Cristina Ghenoiu and John Xue for persuading me to apply and come to Rockefeller in the first place. I also thank John for being extraordinarily resourceful and for being a great roommate. I am also truly thankful to Sid, Emily, Cris, Kristen, Marta, and Stephanie of the Dean's Office for being very helpful and supportive throughout the years.

Lastly, I would like to thank my family for always being my rock. I am thankful to my aunt, my dad and my mum for their unconditional love and support and for ingraining in me the invaluable life principles and discipline. I thank my two brothers, Sunthorn and Pat for their unquestionable support in whatever life

situations I am in. Finally, I would like to thank my best friend Junjuda for being with me in both joyful and difficult times and for being the best counsel one could have hoped for.

TABLE OF CONTENTS

Chapter 1: Introduction.....	1
1.1 Types and sources of DNA damage	2
1.2 Fanconi anemia	3
1.3 Fanconi anemia proteins and ICL repair	6
1.4 The identification of FANCD2/FANCI interacting protein: FAN1	13
1.5 FAN1 and ICL repair	15
1.5.1 The structure and nuclease activity of FAN1	15
1.5.2 Redundant functions of FAN1 and other structure-specific nucleases in ICL repair	19
1.5.3 The significance of the UBZ domain and the genetic interaction between FAN1 and the FA pathway.....	20
1.6 Endogenous sources of DNA damage that underlie the pathogenesis of ICL repair disorders	22
1.6.1 Acetaldehyde-induced ICL damage.....	24
1.6.2 Formaldehyde-induced ICL damage	26
1.7 FAN1 is mutated in patients with Karyomegalic Interstitial Nephritis (KIN) ...	28
Chapter 2: ICL repair functions of FAN1 in human and mice	31
2.1 Introduction.....	32

2.2 Characterization of FAN1's functions using human KIN patient cells and human tissues	32
2.2.1 FAN1 deficiency causes cellular sensitivity to DNA crosslink-inducing agents in KIN patient cells	32
2.2.2 Differential expression of FAN1 and FANCD2.....	33
2.2.3 FANCD2 Ubiquitination, G1/S and G2/M checkpoints are intact in human FAN1-deficient cells	34
2.2.4 FAN1 has ICL repair activity that is non-epistatic with FA factors in human cells.....	39
2.3 Characterization of <i>Fan1</i> knockout mouse	41
2.3.1 Verification of <i>Fan1</i> knockout in the mouse model	41
2.3.2 FAN1 participates in ICL repair independently of the UBZ domain	50
2.3.3 FAN1 can function independently of the FA pathway	52
2.3.4 Genetic interactions of <i>Fan1</i> with <i>Slx4</i> and <i>Slx4</i> -associated nuclease <i>Mus81</i>	58
2.3.5 FAN1 is functionally redundant with SNM1A.....	60
2.3.6 Lack of <i>Fan1</i> results in progressive kidney and liver karyomegaly and liver dysfunction	63
2.3.7 HSCs are unaffected in <i>Fan1</i> -deficient mice when unchallenged but severely affected when <i>Fan1</i> mice are treated with MMC	73
2.3.8 FAN1 is dispensable for the protection of bone marrow against IR induced damage	83

2.4 Summary of the findings.....	86
 Chapter 3: Elucidating the impact of aldehyde detoxification defects on	
<i>Fan1</i>-deficient mice	88
3.1 Introduction.....	89
3.2 Generation of <i>Fan1</i> ^{-/-} <i>Aldh2</i> ^{-/-} and <i>Fan1</i> ^{-/-} <i>Adh5</i> ^{-/-} mice	94
3.3 Analysis of the hematopoietic system in mice lacking <i>Fan1</i> and <i>Aldh2</i> or <i>Adh5</i>	99
3.4 Analysis of the liver and kidney function of mice lacking <i>Fan1</i> and <i>Aldh2</i> or <i>Adh5</i>	107
3.5 Impact of alcohol treatment on mice lacking <i>Fan1</i> and <i>Aldh2</i> or <i>Adh5</i>	114
3.5.1 Short-term ethanol exposure of <i>Fan1</i> / <i>Aldh2</i> mice	114
3.5.2 Long-term ethanol exposure for <i>Fan1</i> / <i>Aldh2</i> mice.....	120
3.6 Summary of the findings.....	128
 Chapter 4: Interplay between the Fanconi anemia pathway and non-	
homologous end joining in ICL repair.....	131
4.1 Introduction.....	132
4.1.1 Double strand break repair pathway choice: homologous recombination (HR) vs non-homologous end joining (NHEJ).....	132
4.1.2 Aberrant NHEJ is implicated in causing genome instability in Fanconi anemia	134

4.2 Inactivation of DNA-PKcs does not rescue MMC-induced proliferation defects in cells lacking FA pathway function.....	139
4.3 Inactivation of DNA Ligase IV or DNA Ligase III does not rescue MMC-induced proliferation defects in cells lacking FA pathway	143
4.4 Inactivation of DSB repair choice factor, 53BP1, does not rescue MMC-induced proliferation defects in <i>FANCA</i> ^{-/-} cells.....	146
4.5 Partial inactivation of Ku70 or Ku80 does not rescue ICL-induced proliferation defects in <i>FANCA</i> -deficient cells	148
4.6 Complete inactivation of NHEJ factors by CRISPR-Cas9 mediated genome-editing does not rescue MMC proliferation defects in FA cells.....	151
4.7 Summary of findings and discussion	154
Chapter 5: Discussion	159
5.1 The role of FAN1 in DNA interstrand crosslink repair	160
5.1.1 The mechanism of FAN1 in ICL repair	160
5.1.2 Genetic interaction between FAN1 and other nucleases in ICL repair ..	164
5.2 The role of FAN1 in the protection of tissue function and human disease ..	165
5.2.1 The role of FAN1 in the suppression of KIN pathogenesis.....	166
5.2.2 The role of FAN1 in the protection of bone marrow stem cells.....	169
5.2.3 FAN1 and other human diseases	171
5.3 The endogenous source of ICL damage that requires FAN1's repair activity	173

Chapter 6: Materials and Methods	179
6.1 General procedures.....	180
6.1.1 Mammalian cell culture	180
6.1.2 Viral transduction of mammalian cells	180
6.1.3 DNA damage sensitivity assays	181
6.1.4 Cell proliferation assays.....	182
6.1.5 siRNA-mediated knockdown.....	182
6.1.6 shRNA-mediated knockdown	183
6.1.7 Gene targeting	184
6.1.8 G1/S and G2/M Checkpoint analysis	184
6.1.9 Southern blotting.....	186
6.1.10 Quantitative reverse transcription-polymerase chain reaction (qRT-PCR)	186
6.1.11 Mutagenesis	187
6.1.12 Cell lysates and immunoblotting	187
6.1.13 Immunofluorescence	188
6.1.14 Chromosome breakage analysis	188
6.1.15 Histology	189
6.1.16 Fluorescent in situ hybridization (FISH)	190
6.1.17 Generation of <i>Fan1</i> -deficient mouse strain.....	190
6.1.18 Genotyping	191
6.1.19 Whole-animal MMC sensitivity.....	191

6.1.20 Alcohol administration in mice	192
6.1.21 LSK analysis	192
6.1.22 Long-term bone marrow reconstitution analysis	193
6.1.23 Micronuclei analysis of genome instability	194
6.1.24 <i>In vitro</i> analysis of hematopoietic stem cell sensitivity to MMC	195
6.2 List of primers	196
6.2.1 Genotyping primers	196
6.2.2 Mutagenesis	197
6.2.3 RT-PCR	197
6.2.4 List of shRNAs	197
6.2.5 List of sgRNAs	198
6.3 List of Antibodies	199
6.4 List of cell lines	200
Chapter 7: References	202

LIST OF FIGURES

Figure 1.1 Model of the Fanconi anemia DNA repair pathway.....	12
Figure 1.2 FAN1 domain structure and model of FAN1 nuclease activity.....	18
Figure 2.1 FAN1 deficiency causes ICL sensitivity in KIN patient cells and FAN1 is highly expressed in the kidney tissue.	36
Figure 2.2 FANCD2/FANCI ubiquitination and G1/S and G2/M checkpoints are not affected in FAN1-deficient KIN patient cells.....	38
Figure 2.3 FAN1 has ICL repair function that is non-epistatic with the FA pathway.	40
Figure 2.4 Targeting strategy to create the <i>Fan1</i> -deficient mouse.....	45
Figure 2.5 Verification of <i>Fan1</i> knockout mouse.	47
Figure 2.6 FAN1 is necessary for resistance to DNA ICL damage in MEFs.	49
Figure 2.7 The UBZ domain is dispensable for FAN1's function in ICL repair.	51
Figure 2.8 <i>Fan1</i> and FA genes are non-epistatic in MEFs in chromosome breakage assay.....	54
Figure 2.9 <i>Fan1</i> and FA genes are non-epistatic in human cells.	57
Figure 2.10 Genetic interactions of <i>Fan1</i> with <i>Slx4</i> and <i>Mus81</i>	59
Figure 2.11 FAN1 and SNM1A are redundant in conferring resistance to ICL- inducing agents.	62
Figure 2.12 <i>Fan1</i> -deficient mice are born at Mendelian ratio, grow normally and are fertile.	66

Figure 2.13 <i>Fan1</i> mice develop karyomegaly.	68
Figure 2.14 Liver function, but not kidney function is abnormal in <i>Fan1</i> -deficient mice.....	70
Figure 2.15 Karyomegaly is a result of polyploidization.	72
Figure 2.16 Blood counts are normal in the majority of <i>Fan1</i> -deficient mice.	76
Figure 2.17 FAN1 is dispensable for the bone marrow maintenance under unstressed condition.	78
Figure 2.18 <i>Fan1</i> -deficient mice are hypersensitive to MMC.	80
Figure 2.19 FAN1 is required to protect the hematopoietic stem and progenitor cells from high level of ICL damage.	82
Figure 2.20 <i>Fan1</i> deficiency does not cause bone marrow sensitivity to IR.	85
Figure 3.1 Putative sources of damage that induce KIN in the absence of FAN1.	93
Figure 3.2 Schematic of mouse interbreeding to generate mice for the study of the genetic interaction between <i>Fan1</i> and <i>Aldh2</i> or <i>Adh5</i>	96
Figure 3.3 Deficiency of <i>Adh5</i> but not <i>Aldh2</i> results in reduced pup numbers per litter in <i>Fan1</i> mutant mice.	97
Figure 3.4 Deficiency of <i>Adh5</i> but not <i>Aldh2</i> results in growth defect in <i>Fan1</i> -mutant mice.....	98
Figure 3.5 Deficiency of <i>Fan1</i> in combination with <i>Aldh2</i> or <i>Adh5</i> does not cause abnormality in the level of peripheral blood cells.	102

Figure 3.6 Deficiency of <i>Adh5</i> but not <i>Aldh2</i> compromises HSC maintenance in 3 months old <i>Fan1</i> -mutant mice.....	103
Figure 3.7 Loss of ALDH2 or ADH5 does not affect the engraftment potential of <i>Fan1</i> -deficient mice following primary transplant.	104
Figure 3.8 Loss of FAN1 or ALDH2 results in reduced engraftment potential of <i>Fan1</i> -deficient mice following the secondary transplant.	105
Figure 3.9 Deficiency of <i>Fan1</i> and <i>Aldh2</i> or <i>Adh5</i> causes insignificant increase in DNA damage in blood cells as assessed by micronuclei in normochromatic erythrocytes and reticulocytes.....	106
Figure 3.10 Kidney and liver karyomegaly are absent from mice lacking <i>Fan1</i> and <i>Aldh2</i> or <i>Adh5</i>	109
Figure 3.11 Karyomegaly in <i>Fan1</i> ^{-/-} animals is not enhanced by deficiency of <i>Aldh2</i> or <i>Adh5</i>	110
Figure 3.12 Deficiency of <i>Fan1</i> alone or in combination with <i>Aldh2</i> or <i>Adh5</i> did not cause an increase in the level of proliferating cells or cells with DNA damage.	111
Figure 3.13 Deficiency of <i>Aldh2</i> or <i>Adh5</i> did not cause liver and kidney dysfunction in young <i>Fan1</i> -deficient mice.	113
Figure 3.14 <i>Aldh2</i> -deficient mice displayed ethanol sensitivity.	117
Figure 3.15 Short-term ethanol treatment affects the hematopoietic system in <i>Aldh2</i> -deficient mice. <i>Fan1</i> ^{-/-} <i>Aldh2</i> ^{-/-} animals have slight decrease in the reticulocyte counts compared to <i>Aldh2</i> ^{-/-} animals.	119

Figure 3.16 <i>Aldh2</i> -deficient mice lose more weight after four weeks of ethanol treatment.	122
Figure 3.17 Long-term ethanol treatment moderately affects the hematopoietic system in <i>Aldh2</i> -deficient mice. No significant differences between the peripheral blood cell levels in <i>Aldh2</i> ^{-/-} and <i>Fan1</i> ^{-/-} <i>Aldh2</i> ^{-/-} deficient animals.	123
Figure 3.18 Long-term ethanol treatment did not increase the level of kidney and liver karyomegaly in <i>Fan1/Aldh2</i> double-deficient mice.	125
Figure 3.19 Long-term treatment with ethanol did not cause liver and kidney dysfunction in <i>Fan1/Aldh2</i> -deficient mice.....	127
Figure 4.1 Schematic showing proteins in the non-homologous end joining pathway.....	138
Figure 4.2 Suppression of DNA-PKcs does not rescue MMC sensitivity in FANCA-deficient cells.	142
Figure 4.3 <i>LIG4</i> or <i>LIG3</i> inactivation does not rescue MMC sensitivity in the setting of FANCA depletion.....	145
Figure 4.4 Depletion of 53BP1 does not rescue MMC sensitivity in FANCA-deficient cells.....	147
Figure 4.5 <i>Ku70</i> and <i>Ku80</i> are essential in human cells and their partial suppression does not rescue ICL sensitivity in FANCA-deficient cells.	150
Figure 4.6 Full inactivation of NHEJ factors by genome-editing does not rescue MMC sensitivity in <i>FANCA</i> ^{-/-} cells.....	153

LIST OF ABBREVIATIONS

KIN	Karyomegalic interstitial nephritis
FAN1	FANCD2/FANCI-associated nuclease 1
FANCD2	Fanconi anemia complementation group D2
FANCI	Fanconi anemia complementation group I
FANCA	Fanconi anemia complementation group A
FA-A	Fanconi anemia complementation group A
ID2	FANCD2/FANCI
ADH5	Alcohol dehydrogenase 5
ALDH2	Aldehyde dehydrogenase 2
NHEJ	Non-homologous end joining
HR	Homologous recombination
MMR	Mismatch repair
TLS	Translesion synthesis
DSBs	DNA double strand break
ssDNA	single stranded DNA
ICLs	Interstrand crosslinks
BRCA1	Breast cancer 1 susceptibility protein
BRCA2	Breast cancer 2 susceptibility protein
53BP1	Tumor suppressor p53 binding protein 1

Ku70	Ku autoantigen protein p70
Ku80	Ku autoantigen protein p80
DNA-PKcs	DNA-dependent protein kinase, catalytic subunit
LIG4	DNA Ligase 4
LIG3	DNA Ligase 3
HSC	Hematopoietic stem cell
HSPC	Hematopoietic stem and progenitor cell
MEP	Megakaryocyte erythroid progenitor
CMP	Common myeloid progenitor
GMP	Granulocyte macrophage progenitor
Lin	Lineage
Sca1	Stem cell antigen-1
c-Kit	Proto-oncogene c-Kit
LSK	Lin- Sca1+ c-Kit+
LK	Lin- Sca1- c-Kit+
RBC	Red blood cell
WBC	White blood cell
RET	Reticulocyte
PLT	Platelet
ALT	Alanine aminotransferase
AST	Aspartate aminotransferase
GLOB	Globulin

ALB	Albumin
CREA	Creatinine
BUN	Blood urea nitrogen
Pi	Phosphate ion
Mg	Magnesium ion
ROS	Reactive oxygen species
IR	Ionizing radiation
UV	Ultraviolet light
MMC	Mitomycin C
CRC	Colorectal cancer
HD	Huntington's disease
MEF	Mouse embryonic fibroblast
FISH	Fluorescence in situ hybridization
RNAi	Small interfering RNAs
shRNA	Short hairpin RNA
sgRNA	Single-guide RNA
CRISPR	Clustered regularly interspaced short palindromic repeats
s.d.	Standard deviation
n.s.	Not significant

Chapter 1: Introduction

1.1 Types and sources of DNA damage

The maintenance of genomic stability is necessary to allow the faithful transmission of the genetic information across generations. To preserve genomic integrity, DNA must be protected from damage generated spontaneously during DNA transactions or inflicted by environmental agents (Ciccia and Elledge, 2010). The spontaneous lesions can arise as a result of the nucleotide misincorporation during DNA replication, DNA base interconversions by DNA deamination or the loss of DNA bases by DNA depurination (Lindahl, 1993; Lindahl and Barnes, 2000). The environment is another important source of DNA damage. One of the most deleterious type of DNA damaging agents is ionizing radiation (IR) from x-ray or γ -ray that can induce DNA single strand breaks (SSBs) and DNA double strand breaks (DSBs). More frequently in everyday life, exposure to ultraviolet (UV) light leads to the formation of DNA-pyrimidine dimers and 6-4 photo-adducts which can account for 10^5 DNA lesions per day (Hoeijmakers, 2009). Additionally, inside the cell, DNA is frequently struck by reactive oxygen species (ROS), which can damage DNA bases and result in DNA breaks (Hoeijmakers, 2009).

The type of DNA damage that this thesis is concerned with is DNA interstrand crosslink (ICL) damage. DNA ICLs are lesions that form when the bases from opposite strands of DNA are linked together through a covalent bond. ICLs are detrimental to cells due to their ability to prevent separation of DNA

double helices, therefore interfering with processes such as DNA replication and transcription. ICLs can be induced by many of the front-line chemotherapeutic drugs including nitrogen mustard derivatives such as melphalan and cyclophosphamide, platinum-based compounds such as cisplatin and carboplatin, mitomycin C (MMC), and psoralen (Deans and West, 2011; Dunnick et al., 1987; Eastman, 1983; Gargiulo et al., 1995; Goodman et al., 1946). Additionally, ICLs can also be induced by molecules made within cells (Clauson et al., 2013). Recent studies have implicated aldehydes as well as the oxidized DNA bases and nitric oxide as their potential sources (Clauson et al., 2013; Garaycochea et al., 2012; Langevin et al., 2011; Pontel et al., 2015). Reactive aldehydes such as formaldehyde, acetaldehyde, malondialdehyde and acrolein have been shown *in vitro* and *in vivo* to be potent DNA crosslinkers (Kirchner et al., 1992; McGhee and von Hippel, 1977; Stein et al., 2006; Stone et al., 2008). Deficiency in the repair of ICLs has been associated with human genetic diseases Fanconi anemia and Karyomegalic Interstitial Nephritis (KIN) (reviewed in Kottemann and Smogorzewska, 2013; Moldovan and D'Andrea, 2009).

1.2 Fanconi anemia

Fanconi anemia (FA) is a rare genetic disease that occurs in about 1 in every 100,000 births. It is characterized by congenital abnormalities, bone marrow failure and predisposition to blood and solid cancers (Alter, 2003; Butturini et al., 1994; Fanconi, 1967; Schmid and Fanconi, 1978). FA patients

display cellular hypersensitivity to ICL inducing agents such as mitomycin C (MMC) and diepoxybutane (DEB), which results in increased cell death and characteristic chromosomal abnormalities including radial chromosomes (Auerbach et al., 1989; Scharer, 2005). Fanconi anemia disorder is genetically heterogeneous. At present, 21 genes have been found to be mutated in Fanconi anemia or Fanconi anemia-like patients. All of the identified mutated genes have been assigned a name as “*FANC*” genes, including *FANCA*, *B*, *C*, *D1*, *D2*, *E*, *F*, *G*, *I*, *J*, *L*, *M*, *N*, *O*, *P*, *Q*, *R*, *S*, *T*, *U*, and *V*. To date, there remain some patients whose complementation groups have not been assigned (Bluteau et al., 2016; Ceccaldi et al., 2016; Park et al., 2016).

FA patients are born with a range of birth defects including short stature, microcephaly, the absence of radius and thumbs, pigmentation defects, abnormalities of the cardiovascular, gastro-intestinal, and urinary systems (Auerbach, 2009; Shimamura and Alter, 2010). The developmental malformations can vary between patients and complementation groups. FA patients with complementation group D1, J and N display more severe congenital abnormalities than others (Levrin et al., 2005; Reid et al., 2007; Wagner et al., 2004). In addition, infertility is almost universal, with almost none of the male patients being reported to have offspring and the affected females developing menopause at much earlier age (Auerbach, 2009). However, the most common phenotype shared among FA patients is pancytopenia caused by progressive

bone marrow failure (Auerbach, 2009; Kutler et al., 2003b). FA patients are also presented with a high risk of developing blood malignancies such as myelodysplastic syndrome (MDS) or acute myeloid leukemia (AML) due to bone marrow abnormalities (Alter et al., 2010; Rosenberg et al., 2003).

Bone marrow failure is driven by dysfunctional hematopoietic stem cells (HSCs) and progenitor cells due to recurrent DNA damage-activated apoptosis. Disruption of FA pathway leads to elevated DNA damage in the HSCs, which in turn promotes activation of p53- and p21-mediated programmed cell death or cell cycle arrest (Ceccaldi et al., 2012; Tulpule et al., 2010). FA patients are born with lower levels of HSCs, which display lower proliferative potential and reduced repopulating and differentiating abilities (Ceccaldi et al., 2012; Kelly et al., 2007). Furthermore, exposure of hematopoietic progenitor cells to crosslinking agents intensifies their proliferation deficiency (Vinciguerra et al., 2010). These findings suggest that the FA pathway is required for the protection of hematopoietic stem cells from accumulating ICLs.

Defective DNA repair in FA cells can lead to mutations and genomic instability, which promotes tumorigenesis. In addition to blood malignancy mentioned before, FA patients are at a high risk of developing solid tumors, including several hundred-fold increase in risk of head and neck squamous cell carcinoma over that present in the general population (Kutler et al., 2003a;

Rosenberg et al., 2003). A number of FA genes, which encode proteins participating in homology-directed repair including *FANCD1 (BRCA2)*, *FANCF (BRIP1)* and *FANCN (PALB2)* are breast and ovarian cancer susceptibility genes. This association demonstrates a close link between the Fanconi anemia pathway and tumor suppression (Deans and West, 2011; Rafnar et al., 2011; Rahman et al., 2007; Seal et al., 2006; Shah et al., 2013; Tischkowitz et al., 2007; Walsh et al., 2011).

1.3 Fanconi anemia proteins and ICL repair

The products of *FANC* genes – “Fanconi anemia (FA) proteins” are necessary for the repair of ICLs. They participate in identification of the lesion and activation of repair, nucleolytic processing of the crosslink, translesion synthesis (TLS) against an unhooked lesion, and homologous recombination (HR) (Figure 1.1A-D) (reviewed in Ceccaldi et al., 2016; Kottemann and Smogorzewska, 2013). The role of FA proteins in ICL repair has been extensively studied using mammalian cells, *Xenopus* egg extracts, and the *in vitro* biochemical analysis. In the current model derived from these studies, the FA core complex proteins (A, B, C, E, F, G, L and M) and the associated proteins are involved in detection of the damage. Upon the recognition of the crosslink, FANCL, an E3 ubiquitin ligase of the FA core complex, aided by E2 ubiquitin-conjugating enzyme, FANCT/UBE2T, monoubiquitinate FANCD2 and FANCI (Figure 1.1A) (reviewed in Ceccaldi et al., 2016; Walden and Deans, 2014).

FANCD2 and FANCI are paralogs that can heterodimerize to form the ID2 complex. The dynamic association and localization of FANCI/FANCD2 are influenced by their ubiquitination status. Human FANCD2 and FANCI are monoubiquitinated at residue K561 and K523 respectively (Garcia-Higuera et al., 2001; Montes de Oca et al., 2005; Smogorzewska et al., 2007). The monoubiquitination of FANCD2 and FANCI are essential for the ICL repair function of the FA pathway (Smogorzewska et al., 2007). Additionally, phosphorylation of FANCI by ATR provides a crucial regulatory mechanism of the repair pathway (Ishiai et al., 2008; Wang, 2008). The function of the ubiquitinated ID2 complex is not fully understood. However, it has been shown to be required for the unhooking of the crosslink and for translesion synthesis-mediated bypass of the lesion in the *Xenopus* egg extract system (Figure 1.1B, C) (Douwel et al., 2014; Knipscheer et al., 2009; Raschle et al., 2008).

The DNA incisions around the ICL require SLX4 (FANCP), a Fanconi anemia protein that is associated with three structure specific nucleases, including XPF–ERCC1, MUS81–EME1 and SLX1 (Douwel et al., 2014; Fekairi et al., 2009; Munoz et al., 2009; Svendsen et al., 2009). SLX4/FANCP is a scaffold protein that can localize and modulate the activity of its associated nucleases at the site of damage (Fekairi et al., 2009; Hodskinson et al., 2014; Munoz et al., 2009; Svendsen et al., 2009; Wyatt et al., 2017). In human cells, the interaction of SLX4 with MUS81–EME1 and SLX1 are important for the Holliday junctions

(HJs) resolution during homologous recombination (Garner et al., 2013; Kim et al., 2013; Svendsen et al., 2009; Wyatt et al., 2013). In contrast, the association between SLX4 and XPF/FANCD2-ERCC1 have been shown to be essential for ICL resistance and crosslink unhooking (Crossan et al., 2011; Douwel et al., 2014; Kim et al., 2011; Kim et al., 2013; Yamamoto et al., 2011). When in complex with SLX4 *in vitro*, XPF is found to be able to completely unhook the crosslink substrates (Hodskinson et al., 2014).

A useful working model of the ICL repair has been proposed based on the study in the *Xenopus* egg extracts. According to the model, SLX4 and XPF can be recruited to the crosslink substrates upon the monoubiquitination of FANCD2 (Figure 1.1B) (Douwel et al., 2014). In this model, repair begins when two of the replication forks converge at the ICL. Once one of the leading strands arrives within 1 nucleotide of the ICL, the opposite parental strand can be incised on either side of the crosslink, resulting in the unhooking of the ICL (Raschle et al., 2008; reviewed in Zhang and Walter, 2014). To date, XPF-ERCC1 is the only nuclease known to be indispensable for the incision event in the *Xenopus* egg extracts system (Douwel et al., 2014).

The dual fork convergence model was recently challenged by an *in vivo* study from the Seidman lab using DNA-fiber based approach with fluorescently-tagged ICLs (Huang et al., 2013). Seidman and colleagues showed that the

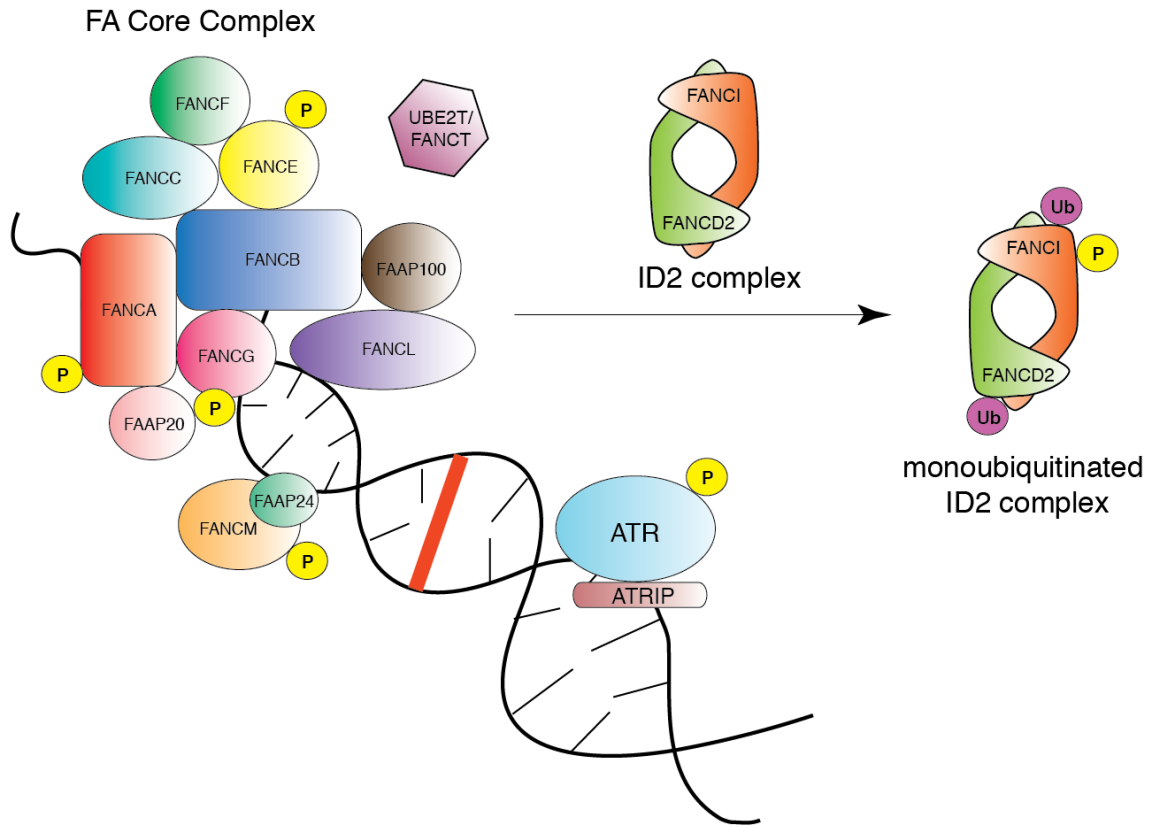
majority of replication forks can traverse (bypass) the crosslinks without prior ICL unhooking. Replication traverse of ICLs requires the DNA translocase activity of FANCM, but not other Fanconi anemia proteins. When replication transverse is blocked under FANCM deficient setting, the frequency of stalled single fork collisions with ICLs go up, suggesting that single fork collision precedes replication traverse. These results indicate that, in mammalian cells, ICLs are mostly approached by single forks rather than converging dual forks as opposed to the models proposed by the *Xenopus* studies. The questions of how FANCM facilitates replication traverse and the identity of DNA translocase distal to the ICL remain a subject of further investigation. Nevertheless, Walter and colleagues argue that, regardless of either models, both dual fork convergence and replication traverse lead to the formation of X-shape structures at ICLs, which can be recognized and processed by ICL repair nucleases such as XPF-ERCC1 (Zhang and Walter, 2014).

Following the incision, the last steps of ICL repair involve translesion synthesis and homology directed repair. The unhooked base is bypassed by translesion DNA polymerase whose identity remains unknown before being extended further by DNA polymerase ζ (REV3/REV7) (Figure 1.1C) (Raschle et al., 2008). Concurrently, the double strand break generated by ICL unhooking is repaired by homology-directed repair, a step which is facilitated by a number of FA proteins including FANCD1 (BRCA2), FANCF (BRIP1) and FANCG (PALB2),

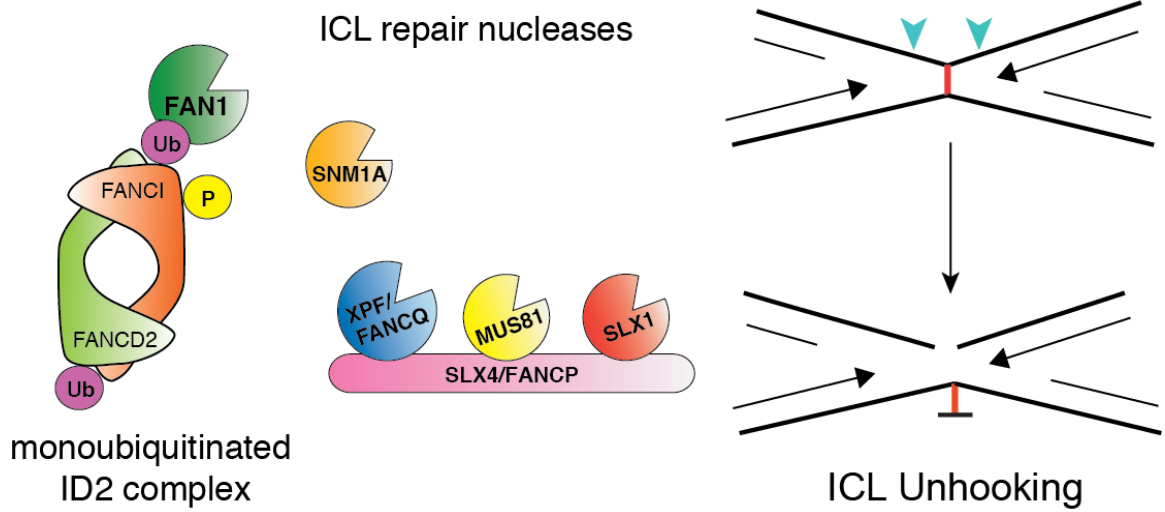
FANCO (RAD51C), FANCP (SLX4), FANCR (RAD51) and FANCS (BRCA1) (Figure 1.1D) (reviewed in Ceccaldi et al., 2016; Long et al., 2011; Walden and Deans, 2014).

Although the FA pathway plays an important role in ICL repair and human and mouse cells lacking the FA proteins are very sensitive to ICL-inducing agents, alternative ICL repair mechanisms do exist. ICL repair studies in non-replicating *Xenopus* egg extracts revealed the ICL repair pathway that depends on translesion synthesis polymerase Pol κ but not the Fanconi anemia proteins (Williams et al., 2012). This pathway of ICL repair is thought to be important for the repair of ICL damage in quiescent or slowly cycling cells that are mainly in G0/G1 phases of the cell cycle. More recently, a replication-dependent repair pathway that involves a DNA glycosylase - NEIL3 has been shown to be able to bypass the need for FA proteins (Semlow et al., 2016). Unlike nuclease-mediated ICL unhooking, NEIL3 directly cleaves the N-glycosyl bond without damaging the sugar phosphate backbone and functions independently of FANCI-FANCD2. NEIL3-mediated unhooking has been shown to be a major pathway for the repair of psoralen and abasic (AP) site ICLs. Following the cleavage of N-glycosyl bond, gaps are filled in by TLS polymerases. The significance of NEIL3-ICL repair pathway *in vivo* remains unclear as unhooking can still proceed via FANCI-FANCD2-dependent incisions when N-glycosyl bond cleavage is prevented, (Semlow et al., 2016).

A

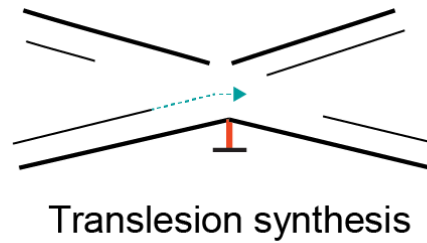
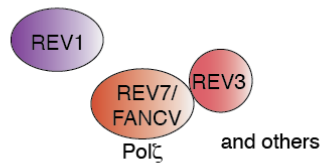


B

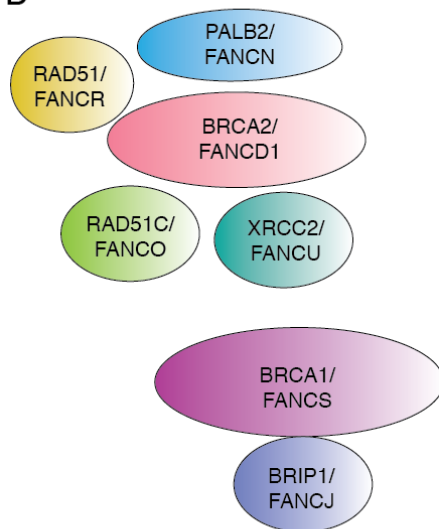


C

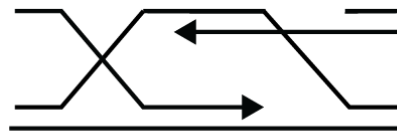
Translesion synthesis
polymerases



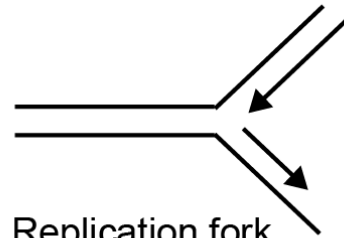
D



Homologous recombination proteins



Homologous recombination



Replication fork
protection

Figure 1.1 Model of the Fanconi anemia DNA repair pathway.

(A) Upon the detection of ICL damage, ATR phosphorylates multiple repair proteins. This together with the monoubiquitination of FANCI and FANCD2 of the ID2 complex by the Fanconi anemia (FA) core complex lead to the activation of the FA pathway. (B) ID2 complex is thought to coordinate DNA nucleases during ICL incision. (C-D) The unhooked intermediates are repaired by translesion synthesis (C) and homologous recombination (HR) (D). HR proteins are also required for the protection of the replication forks earlier during repair.

1.4 The identification of FANCD2/FANCI interacting protein: FAN1

The mechanism of how monoubiquitinated ID2 complex provides a platform for DNA nucleases or translesion synthesis polymerases for ICL processing remains unclear. Multiple studies arrived at one possible effector of the ID2 complex function, KIAA1018/FAN1 (FANCD2/FANCI-associated nuclease 1) (Kratz et al., 2010; Liu et al., 2010; MacKay et al., 2010; Smogorzewska et al., 2010). These studies show that FAN1 interacts with FANCD2 and that the depletion of FAN1 leads to ICL sensitivity. FAN1 is a structure-specific nuclease, containing four characterized domains: ubiquitin-binding domain *UBZ*, DNA binding domain *SAP* (SAF-A/B, Acinus and PIAS), protein-protein interaction domain *TPR* (tetratricopeptide repeat), and nuclease domain *VRR_nuc* (virus-type replication-repair nuclease) (Figure 1.2) (Iyer et al., 2006; Kinch et al., 2005). The UBZ domain of FAN1, which belongs to RAD18 family of zinc fingers proteins that are commonly found in DNA damage response proteins, facilitates its binding to the monoubiquitinated ID2 complex (Hofmann, 2009; Kratz et al., 2010; Liu et al., 2010; MacKay et al., 2010; Smogorzewska et al., 2010). The UBZ domain of FAN1 is not found in unicellular eukaryotes, but is highly conserved in many multicellular organisms. Interestingly, the presence of the UBZ domain is concurrent with the evolution of the majority of FA genes including FANCD2 (MacKay et al., 2010; Patel and Joenje, 2007; Smogorzewska et al., 2010). The VRR_nuc domain of FAN1 is well conserved from bacteria to humans and contains a PD-D/E(X)K motif that is often found in the active site of

many restriction endonucleases as well as MUS81 and XPF endonucleases (Kinch et al., 2005; Kosinski et al., 2005).

FAN1 is necessary for the resistance to ICL-inducing agents such as MMC, cisplatin and HN2 (nitrogen mustard derivative) in multiple model systems from *S. pombe* to mammals (Airik et al., 2016; Fontebasso et al., 2013; Kratz et al., 2010; Lachaud et al., 2016a; Liu et al., 2010; MacKay et al., 2010; Smogorzewska et al., 2010; Thongthip et al., 2016; Yoshikiyo et al., 2010; Zhou et al., 2012). Treatment of FAN1-deficient human cells with ICL-inducing agents leads to proliferation defect and chromosomal aberration that are accompanied by high level of DNA damage (Kratz et al., 2010; MacKay et al., 2010). To date, FAN1 has not been convincingly shown to be required for the repair of other types of DNA damage.

In addition to the ID2 complex, FAN1 also interacts with DNA mismatch repair proteins. The analysis of MLH1 and PMS2 interactome revealed several peptides of FAN1, while reciprocally, the top-scoring candidates from the proteomic study of FAN1's interacting partners included MLH1, MLH3, PMS1, and PMS2 (Cannavo et al., 2007; Kratz et al., 2010; MacKay et al., 2010; Smogorzewska et al., 2010). In a size exclusion study, FAN1 was found to form two subcomplexes one with FANCD2 and FANCI and the other with MLH1

(MacKay et al., 2010). It remains to be shown if FAN1 functions within the DNA mismatch repair pathway.

1.5 FAN1 and ICL repair

Although there are several lines of evidence that indicate the importance of FAN1 in the protection of cells and organisms from ICL-induced damage, its role during ICL repair remains elusive. Given the direct association between FAN1 and the monoubiquitinated ID2 complex, it has been proposed that FAN1 nuclease activity might function downstream of ID2 monoubiquitination. As such, it could contribute to ICL incision, processing of the excised crosslink, or could even function later during homology directed repair of DNA double-strand break (DSB) intermediates or in the resolution of Holliday junctions (Smogorzewska et al., 2010).

1.5.1 The structure and nuclease activity of FAN1

To date, several high-resolution structures of FAN1 have been analyzed either alone or in complex with different DNA substrates (Gwon et al., 2014; Wang et al., 2014; Zhao et al., 2014). These studies gave some insight to the mechanism of DNA binding and catalysis by FAN1. The structure solved by the Pavletich lab shows FAN1 as a monomeric protein with a bilobal structure consisting of 223-residue N-terminal domain (NTD) and a 415-residue C-terminal domain (CTD) containing a nuclease motif. The protein was crystalized with DNA

substrate with a pre-nicked 1-nucleotide 5' flap carrying 5' phosphate group and a post-nicked 4-nucleotide 3' flap. The NTD binds to the pre-nicked duplex and 3' flap, whereas the CTD binds to the 5' flap and post-nicked duplex, distorting the DNA substrate into a V-shape molecule. The authors proposed that this structure would permit sequential 3-nucleotide stepwise incisions across the crosslink (Wang et al., 2014). The structures solved by the Sung lab demonstrates the dimerization of FAN1 monomers. The binding to 5' flap DNA substrates promotes a dimerization of FAN1 in a 'head to tail' conformation. The TPR and NUC domains of one FAN1 molecule interact with the SAP domain of the other FAN1 molecule. Within the asymmetric FAN1 dimer, one of the monomers appears to have a primary role in catalysis by engaging DNA in its active site whereas the other monomer plays an ancillary role, facilitating substrate orientation and DNA flap unwinding (Zhao et al., 2014). The authors propose that the dimerization of FAN1 promotes the unwinding of the DNA duplex and guides the ssDNA towards the active site for incision (Zhao et al., 2014). Unwinding of the DNA duplex would be critical for facilitating the endonuclease activity of FAN1 on its ICL substrate, as the 5' flap incision is strongly inhibited when the crosslink is located close to the flap branch point (Zhao et al., 2014).

FAN1 possesses both endonuclease and exonuclease activity on crosslinked and non-crosslinked DNA substrates. FAN1 endonuclease activity exhibits preference for nicked and 5' flap DNA structures (Gwon et al., 2014;

MacKay et al., 2010; Smogorzewska et al., 2010; Wang et al., 2014). Structural analyses by different groups suggests that binding of FAN1 to the DNA substrate is facilitated by the positively charged surface of the SAP domain, residues flanking the SAP domain and the sugar-phosphate backbone of the DNA duplex downstream of 5' flap structure (Gwon et al., 2014; Wang et al., 2014; Zhao et al., 2014). It is proposed that the direct interaction of the SAP domain with crosslinked DNA provides proper structural remodeling of the DNA substrate, which is required for incision by the nuclease domain of FAN1 (Gwon et al., 2014; Wang et al., 2014; Zhao et al., 2014). Cleavage of 5' flap DNA of the ICL-stalled replication fork-like structures is followed by exonucleolytic processing of nicks to digest across the crosslink in 3-nucleotides stepwise incisions. This sequence of events is proposed to allow de facto ICL unhooking (Figure 1.2) (Pizzolato et al., 2015; Zhao et al., 2014).

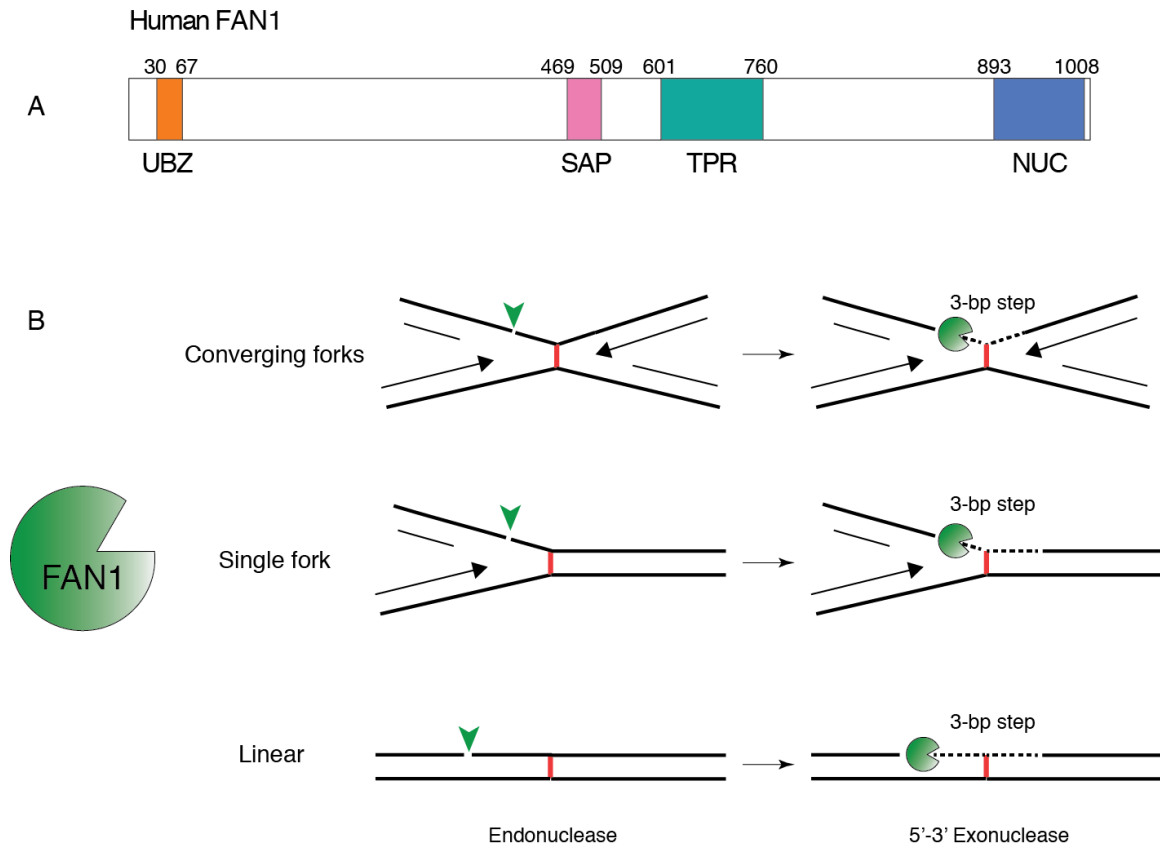


Figure 1.2 FAN1 domain structure and model of FAN1 nuclease activity.

(A) FAN1 contains 4 characterized domains including the UBZ, SAP, TPR, and NUC (nuclease) domains. (B) FAN1 is thought to participate in the ICL incision step. Potential substrates include the dual and single fork structures as well as linear DNA with an ICL. *In vitro*, FAN1 exhibits preference for the 5' flap structure via its endonuclease activity and the 5'-3' exonuclease activity allowing it to digest DNA across the ICL.

1.5.2 Redundant functions of FAN1 and other structure-specific nucleases in ICL repair

FAN1 is clearly necessary for resistance to ICL-inducing agents. However, immunodepletion of FAN1 had no effect on the incision of a cisplatin ICL in the *X. laevis* egg extract system (Douweli et al., 2014). Normal repair in this setting might be attributed to the fact that FAN1 may act on structures other than dual convergent forks that are required for repair of the damaged plasmids in this system. Alternatively, FAN1 may be functionally redundant with other ICL repair nucleases such as MUS81, SLX1 or SNM1A (reviewed in Zhang and Walter, 2014). SLX1 and MUS81-EME1 are associated with SLX4 and are genetically epistatic in ICL repair (Castor et al., 2013; Kim et al., 2013). SLX1 is a promiscuous nuclease, which like FAN1 prefers 5' flap DNA substrates *in vitro*. Therefore, it is possible that SLX1 could potentially provide 5' flap endonuclease activity required for crosslink incision in the absence of FAN1 (Fricke and Brill, 2003).

Aside from FAN1, the SNM1 family of proteins are the only crosslink repair nucleases that possess a 5'-3' exonuclease activity (Hejna et al., 2007; Wang et al., 2011). In yeast, Pso2 is the single SNM1 protein member, and is important for ICL resistance (Zhang and Walter, 2014). In higher eukaryotes, three SNM1 homologs - SNM1A, SNM1B (Apollo) and SNM1C (Artemis) exist, with SNM1A and SNM1B being implicated in ICL resistance. (Cattell et al., 2010; Ishiai et al.,

2004). SNM1A is the ortholog which has the most similarity to Pso2, and is the only one that can complement the ICL sensitivity of *pso2Δ* yeast (Hazrati et al., 2008). SNM1A deficiency, nonetheless, confers mild crosslink sensitivity in mouse and human cells (Ahkter et al., 2005; Dronkert et al., 2000; Wang et al., 2011). This suggests that SNM1A plays a minor role in mammalian ICL repair or that another ICL-repair nuclease, such as FAN1, compensates for the loss of SNM1A. Consistent with possible redundant roles of SNM1A and FAN1, the *S. pombe* *Fan1* was recently shown to be non-epistatic with *Pso2*, as *pso2Δfan1Δ* displays greater cisplatin sensitivity than a single *pso2Δ* or *fan1Δ* mutant alone (Fontebasso et al., 2013).

1.5.3 The significance of the UBZ domain and the genetic interaction between FAN1 and the FA pathway

The UBZ domain located at the N-terminus of FAN1 facilitates binding between FAN1 and the monoubiquitinated lysine residues of FANCI/FANCD2 (Figure 1.2A). However, the significance and function of this interaction has remained unclear. The UBZ-mediated interaction with the ID2 complex was first shown to be necessary for localization of FAN1 to ICL-induced DNA damage foci and psoralen-induced damage, arguing that the ICL repair activity of FAN1 may depend on the UBZ domain (Kratz et al., 2010; Liu et al., 2010; MacKay et al., 2010; Smogorzewska et al., 2010). In one of the studies, the UBZ domain was

also shown to be necessary for resistance to DNA ICLs (Liu et al., 2010).

More recent data from our and Seidman lab show that FAN1 lacking the UBZ domain can still be recruited to the site of damage (Thongthip et al., 2016). In experiments testing the recruitment of FAN1 to psoralen-induced ICLs, the Seidman lab has shown that the SAP domain was critical for rapid recruitment of FAN1 to ICLs. The UBZ-dependent phase of ICL-recruitment occurred more slowly and coincided with the localization of FANCD2 at ICLs. These observations may reflect the dependency of the UBZ-dependent recruitment or retention of FAN1 at sites of damage on the monoubiquitination of FANCI/FANCD2 (Thongthip et al., 2016; Yan et al., 2012). In our hands, this increased recruitment/retention of FAN1 was not necessary for resistance to ICL damage since expression of FAN1 with mutations in the UBZ domain fully rescued ICL sensitivity of FAN1-deficient human cells (Zhou et al., 2012). We concluded that SAP domain plays a more important role in the recruitment of FAN1 to ICLs and that FAN1 can participate in ICL repair independently of the UBZ domain.

Collectively, findings from multiple studies indicate that interaction between FAN1 and the ID2 complex is not required for ICL repair activity of FAN1 and that the crosslink repair function of FAN1 could occur independently of the FA pathway. Evidence from studies in the chicken DT40 cell line also support

this view as *FAN1*^{-/-}*FANCC*^{-/-} cells are more sensitive to cisplatin than wild-type, *FAN1*^{-/-}, or *FANCC*^{-/-} single knockout cells (Yoshikiyo et al., 2010). Whether the crosslink repair function of FAN1 is epistatic with the FA pathway in mammalian cells, is therefore a question of significant importance and will be experimentally addressed below.

1.6 Endogenous sources of DNA damage that underlie the pathogenesis of ICL repair disorders

The ICL repair pathway most likely evolved to cope with the challenges posed by endogenously produced ICL-inducing agents. Several sources of endogenous ICLs that require FA pathway's repair activity have been proposed. These include the signaling molecule nitric oxide as well as the abundant abasic sites (also known as AP or apurinic/apyrimidinic site), which can react with the opposite strand of DNA to form ICLs (Dutta et al., 2007). However, reactive aldehydes are the most well characterized sources of DNA damage that have been shown to affect bone marrow and other organ system functions *in vivo* in an FA pathway deficient setting (Garaycoechea et al., 2012; Langevin et al., 2011; Oberbeck et al., 2014; Pontel et al., 2015).

Aldehydes are reactive small molecules that can be found both in the environment and within cells as the by-products of metabolism. Examples include the products of lipid peroxidation, trans-4-hydroxy-2-nonenal, malondialdehyde, crotonaldehyde and acrolein, (Huang et al., 2010; Scharer, 2005; Stone et al.,

2008), but also formaldehyde and acetaldehyde which can be formed from the protein and nucleic acid demethylation and the metabolism of amino acids and nucleotides (Jensen et al., 2015; Loenarz and Schofield, 2008; Matsuda et al., 1999; Ogawa et al., 2000; Walport et al., 2012). Cells possess powerful detoxification systems that limit the concentration of reactive aldehydes in different organs. The majority of aldehyde detoxifying enzymes belong to the aldehyde dehydrogenase gene (ALDH) superfamily which consists of 19 gene members in humans (Jackson et al., 2011; Marchitti et al., 2008; Yoshida et al., 1998). ALDH2 is one of the most characterized ALDH family members, as it is involved in the conversion of acetaldehyde, an intermediate of ethanol metabolism, to acetate (Goedde and Agarwal, 1990; Klyosov et al., 1996). Besides ALDHs, the glutathione-dependent alcohol dehydrogenase 5 (ADH5/GSNOR), a class III alcohol dehydrogenase (ADH) plays a key role in the clearance of formaldehyde, a simpler but more toxic type of aldehyde (Sanghani et al., 2000; Staab et al., 2009).

Recent work has implicated both acetaldehyde and formaldehyde as the endogenous ICL-inducing agents that create a problem when Fanconi anemia proteins are not functional. It has been shown that an increase in endogenous acetaldehyde or formaldehyde level due to ALDH2 or ADH5 deficiency leads to chromosomal instability and results in severe proliferation defects in FA-deficient

cell lines (Langevin et al., 2011; Marietta et al., 2009; Mechilli et al., 2008; Rosado et al., 2011; Wang et al., 2000).

1.6.1 Acetaldehyde-induced ICL damage

Acetaldehyde is a toxic agent found in tobacco smoke, vehicle exhaust and some dietary products. Acetaldehyde is a common endogenous by-product of threonine, tyrosine, β -alanine and deoxyribose phosphate metabolisms (Jacobsen, 1950; Matsuda et al., 1999; Ogawa et al., 2000). Acetaldehyde can also be produced by oxidation of ethanol by the NAD-dependent alcohol dehydrogenases in the liver (Zakhari, 2006).

Acetaldehyde treatment induces H2AX phosphorylation, stimulates mutagenesis, and increases sister chromatid exchanges in cultured mammalian cells (Bird et al., 1982; Dellarco, 1988; Ristow and Obe, 1978; Wang et al., 2001). Mouse and human cells deficient for the FA pathway display aberrant chromosomes and hypersensitivity upon treatment with acetaldehyde (Langevin et al., 2011; Marietta et al., 2009; Mechilli et al., 2008; Ridpath et al., 2007).

To study the effect of acetaldehyde detoxification on cells lacking the FA pathway, the Patel lab has generated mice that lack both the FA pathway and ALDH2. *Fancd2*^{-/-}*Aldh2*^{-/-} and *Fanca*^{-/-}*Aldh2*^{-/-} mice show aberrant embryonic development as well as birth defects (Garaycochea et al., 2012; Langevin et al.,

2011; Oberbeck et al., 2014). The double *Fancd2*^{-/-}*Aldh2*^{-/-} mutant animals have a reduced survival rate, with some embryos dying between embryonic day 9.5 and 13.5. In order to produce viable pups, the pregnant females need to maintain at least one wild-type *Aldh2* allele (Langevin et al., 2011). The presence of the maternal *Aldh2* is even more significant for the development of *Fanca*^{-/-}*Aldh2*^{-/-} embryos, as they can only be born if the embryos are surgically transferred to a mother that is homozygous for wild-type *Aldh2*. Despite this rescue strategy, *Fanca*^{-/-}*Aldh2*^{-/-} mice are born with developmental defects such as eye and craniofacial abnormalities (Oberbeck et al., 2014). Additionally, treatment with ethanol during pregnancy can promote the developmental abnormalities in *Fancd2*^{-/-}*Aldh2*^{-/-} and *Fanca*^{-/-}*Aldh2*^{-/-} double-mutant pups (Langevin et al., 2011).

Fancd2^{-/-}*Aldh2*^{-/-} mice that were derived from *Aldh2*^{+/-} mothers, allowing them to develop normally, succumb to acute lymphoblastic leukemia (ALL) by 6 months of age. Majority of the remaining survivors develop spontaneous bone marrow failure due to hematopoietic stem cell attrition (Garaycochea et al., 2012; Langevin et al., 2011). The frequency and function of the hematopoietic stem and progenitor cells in *Fancd2*^{-/-}*Aldh2*^{-/-} mice are drastically reduced compared to wild-type or single mutant animals. Further analysis revealed that *Fancd2*^{-/-}*Aldh2*^{-/-} HSCs are inherently damaged and demonstrate induction of γ -H2AX that is exacerbated following ethanol feeding (Garaycochea et al., 2012).

These studies indicate a requirement for acetaldehyde detoxification by ALDH2 for the normal development, hematopoietic stem cell function, and tumor suppression, particularly in the absence of the FA pathway.

The relevance of acetaldehydes in the pathogenesis of Fanconi anemia has also been validated in human studies. Concomitant ALDH2 deficiency greatly exacerbates developmental abnormalities, bone marrow failure, and leukemia development in Japanese FA patients (Hira et al., 2013). Strikingly, FA patients with a single allele of the dominant negative ALDH2 variant (rs671) display accelerated progression to bone marrow failure. Furthermore, some FA patients with biallelic ALDH2 rs671 variant exhibit an onset of myelodysplastic syndrome and bone marrow failure at an age as young as 4 months.

1.6.2 Formaldehyde-induced ICL damage

Like acetaldehyde, formaldehyde is found in the environment as a breakdown product of compounds such as tobacco smoke, and the sweetener aspartame. It is also formed endogenously as a byproduct of metabolic reactions (Jensen et al., 2015; Trocho et al., 1998). Endogenous formaldehyde can be derived from oxidative demethylation reactions, for instance through demethylation of histones, RNA, and DNA by KDM1/JMJC or ABH family of enzymes within the nucleus (Loenarz and Schofield, 2008; Pontel et al., 2015; Walport et al., 2012). Formaldehyde is highly mutagenic and genotoxic due to its

ability to introduce DNA monoadducts (McGhee and von Hippel, 1977). DNA-protein crosslinks (DPCs) (Casanova-Schmitz and Heck, 1983; Magana-Schwencke and Ekert, 1978; Solomon and Varshavsky, 1985), and DNA interstrand crosslinks (Auerbach, 1949; Herskowitz, 1950; Lu et al., 2010).

The FA pathway has been shown to be important for the repair of formaldehyde-induced damage. FA pathway deficient DT40 chicken cells, primary mammalian cells as well as cancer cell lines are hypersensitive to formaldehyde (Pontel et al., 2015; Ridpath et al., 2007; Rosado et al., 2011). The combined inactivation of *Fancd2* and the formaldehyde detoxifying enzyme *Adh5* in the chicken DT40 cells results in synthetic lethality (Rosado et al., 2011).

The *Fancd2*^{-/-}*Adh5*^{-/-} double mutant animals display HSC dysfunction, which leads to bone marrow failure and leukemia (Pontel et al., 2015). Additionally, *Fancd2*^{-/-}*Adh5*^{-/-} animals develop liver and kidney karyomegaly which may be associated with their accelerated degeneration. The kidney failure observed in *Fancd2*^{-/-}*Adh5*^{-/-} is primarily caused by glomerular damage, which manifests as a significant change in the glomerular anatomical structure, accompanied by severe proteinuria. Animals display an increase in the level of karyomegaly (enlarged nuclei) in the renal tubular cells and liver hepatocytes.

At this point it is unclear if other reactive aldehydes will have influence on the phenotypes of Fanconi anemia pathway deficient human or mice. It is unknown if other repair pathways are involved in clearance of acetaldehyde- or formaldehyde-induced DNA damage. This question will be explored in this thesis for FAN1.

1.7 FAN1 is mutated in patients with Karyomegalic Interstitial Nephritis (KIN)

FAN1 was considered a candidate FA gene based on the observation that there is a direct association between FAN1 and the ID2 complex and the finding that its nuclease activity is required for ICL resistance. Unexpectedly, biallelic loss of function mutations in FAN1 were identified in patients with Karyomegalic Interstitial Nephritis (KIN) (Zhou et al., 2012). KIN is a chronic kidney disease, characterized by the presence of enlarged, polyploid (karyomegalic) and hyperchromatic nuclei in the proximal and distal tubules of the kidney (Godin et al., 1996; Mihatsch et al., 1979; Spoendlin et al., 1995). It is a rare disease with less than 50 cases being reported so far (Isnard et al., 2016). Patients with KIN develop progressive kidney disease, which eventually leads to early onset of end-stage kidney failure in 20-30 year olds (Mihatsch et al., 1979; Spoendlin et al., 1995; Zhou et al., 2012).

The urine of KIN patients typically show glucosuria and mild proteinuria, whereas hematuria is rare (Bhandari et al., 2002; Isnard et al., 2016; Mihatsch et al., 1979). Histologically, the kidney of KIN individuals display tubular basement membrane degeneration, tubular atrophy with significantly thicker tubular basement membrane, microcysts, interstitial infiltrations and pronounced fibrosis (Zhou et al., 2012). In addition to the renal tissue, systemic karyomegaly in other tissues such as liver, lung, brain, skin, and digestive tissues has also been observed in many patients (Burry, 1974; Mihatsch et al., 1979; Sclare, 1976). Furthermore, a number of cases exhibit elevated serum markers of hepatocyte damage, mild anemia and recurrent upper respiratory infections of unknown etiology (Bhandari et al., 2002; Godin et al., 1996; Mihatsch et al., 1979; Spoenlin et al., 1995).

Genetically, KIN is caused by autosomal recessive mutations in FAN1, with mostly nonsense mutations that lead to open reading frame truncations (Zhou et al., 2012). A number of missense mutations found in 3 of the studied families, are in the conserved functional nuclease domain, suggesting that the nuclease activity of FAN1 is important in protection against KIN development (Zhou et al., 2012). It is unclear whether KIN is driven by endogenous or exogenous sources of lesions. Viral infections and exposure to immunosuppressants or environmental genotoxins such as ochratoxin A, heavy metals or herbal medicines are typically excluded in cases described in the

literature (Bhandari et al., 2002; Godin et al., 1996; Mihatsch et al., 1979; Radha et al., 2014; Uz et al., 2011). Based on our current knowledge that FAN1 is necessary for ICL repair, the likely damage that accumulates in KIN patients are ICLs but their source is unknown.

In this thesis, I will present our studies on the ICL repair function of FAN1 and the pathogenesis of Karyomegalic Interstitial Nephritis (KIN) that develops as a result of FAN1 deficiency. Using human KIN-patient and *Fan1*-deficient mouse cell lines, we show that FAN1 is required for ICL resistance in both human and mice. FAN1 possesses ICL repair activity that is independent of the FA pathway, yet FAN1 is redundant with SNM1A, another ICL repair nuclease. I will also describe *Fan1*-deficient mouse model that displays characteristics of KIN including the presence of kidney and liver karyomegaly. The enlargement of nuclei in *Fan1*-deficient kidney and liver occurs progressively with age and is a result of genome endoreduplication. The hematopoietic stem and progenitor cells of *Fan1*-deficient animals are susceptible to crosslink-inducing agent but not to ionizing irradiation. Finally, we provide evidence that formaldehyde and acetaldehyde are unlikely the endogenous sources of damage that drive the pathogenesis of KIN.

Chapter 2: ICL repair functions of FAN1 in human and mice

2.1 Introduction

The contribution of FAN1 to ICL resistance has been firmly established (Kratz et al., 2010; Liu et al., 2010; MacKay et al., 2010; Smogorzewska et al., 2010). It is now clear that mutations in *FAN1* lead to kidney disease in humans (Zhou et al., 2012), a disease that is distinct from Fanconi anemia. This chapter describes experiments that take advantage of cell lines from KIN patients and a mouse model of the human disease, to answer questions that remain about the function of FAN1. It explores the significance of FAN1 interaction with the FANCD2 for ICL repair, the genetic interaction of FAN1 with other nucleases implicated in ICL repair, and the organismal consequences of FAN1 dysfunction with and without exogenous DNA damage.

Results

2.2 Characterization of FAN1's functions using human KIN patient cells and human tissues

2.2.1 FAN1 deficiency causes cellular sensitivity to DNA crosslink-inducing agents in KIN patient cells

Depletion of FAN1 using siRNA and shRNA has revealed that FAN1 was necessary for cellular resistance to ICLs (Kratz et al., 2010; Liu et al., 2010; MacKay et al., 2010; Smogorzewska et al., 2010). To confirm that FAN1 deficiency identified in the germline of patients with KIN also leads to sensitivity to ICL-inducing agents, patient fibroblasts were tested for sensitivity to MMC.

Patient cell line (A1170) carrying homozygous FAN1 truncation leading to lack of FAN1 protein, exhibited a survival defect and a significant induction of micronuclei, a hallmark of chromosomal instability when treated with MMC (Figure 2.1A, B). Importantly, the ICL sensitivity of the patient cells was rescued when wild-type copy of FAN1 was introduced into the cells (Figure 2.1A). This result was consistent with the proposed role of FAN1 in genome maintenance and the repair of ICLs. It is worth noting that KIN patient cells were significantly less sensitive to MMC than the Fanconi anemia (FA) patient cells lacking FANCA (RA3087) (Figure 2.1A).

2.2.2 Differential expression of FAN1 and FANCD2

The distinct phenotypes of KIN and FA could stem from the differential expression of FAN1 and FA proteins in a tissue specific manner. FAN1 could potentially be highly expressed in the kidney whereas FA proteins might be more enriched in the bone marrow, the tissues that are affected in the corresponding disorders. The study of *FAN1* and *FANCD2* gene expression revealed that *FAN1* transcripts could be detected in all tissues, although at different levels of expression (Zhou et al., 2012). *FAN1* mRNA was expressed at a higher level than *FANCD2* in parenchymatous organs, including the kidney, liver and neuronal tissues, whereas *FANCD2* expression exceeded *FAN1* in lymphatic or bone marrow-derived tissues as well as in skin and testis (Zhou et al., 2012). The fact that *FAN1* was expressed at a particularly high level in the parenchymatous

organs, raises the possibility that those tissues might depend on FAN1 for its normal function. To corroborate the findings from *FAN1* gene expression study, we examined FAN1 expression at the protein level across multiple tissues including the kidney and liver that are affected in KIN. While full-length FAN1 protein was expressed at a particularly high level in the kidney tissue, a significantly lower level was detected in the liver and the bone marrow (Figure 2.1C, D). However, as will be discussed later, MMC treatment resulted in bone marrow failure in *Fan1*-deficient mice. This observation could be explained if FAN1 is expressed in a subset of bone marrow cells (potentially the stem and progenitor cells), to protect against ICL-induced bone marrow failure.

2.2.3 FANCD2 Ubiquitination, G1/S and G2/M checkpoints are intact in human FAN1-deficient cells

To assess if DNA damage signaling and the activation of FA pathway are compromised in FAN1-deficient cells, we first tested if FAN1 was required for the monoubiquitination of FANCD2 and FANCI in FAN1 patient fibroblasts (A1170) and lymphocytes (A4466, A4486, A4385) (Zhou et al., 2012). The loss of function mutations of *FAN1* did not affect the presence of FANCD2 and FANCI monoubiquitination, suggesting that the FA pathway is activated even in the absence of FAN1 (Figure 2.2A, B)(Zhou et al., 2012).

We next examined whether FAN1 was involved in the regulation of G1/S and G2/M checkpoints following DNA damage treatments. To monitor the G1/S checkpoint, we analyzed the level of early S-phase cells after the treatment with ionizing radiation (IR) by measuring the BrdU⁺ cells with DNA content close to 2N. Cells null for ATM, kinase necessary for DNA damage signaling abated the G1/S checkpoint, allowing the progression of the IR-damaged cells into S-phase. In contrast, the absence of FAN1 or FA protein did not affect the G1/S checkpoint, as cells were effectively blocked in G1 following the IR treatment (Figure 2.2C, D). Similarly, the G2/M checkpoint appeared to be intact in cells lacking FAN1 or FANCA. FAN1- and FANCA-deficient cells were impeded from entering mitosis to the same extent as BJ wild-type cells following IR, unlike the G2/M checkpoint deficient *ATR*-depleted cells (Figure 2.2E, F).

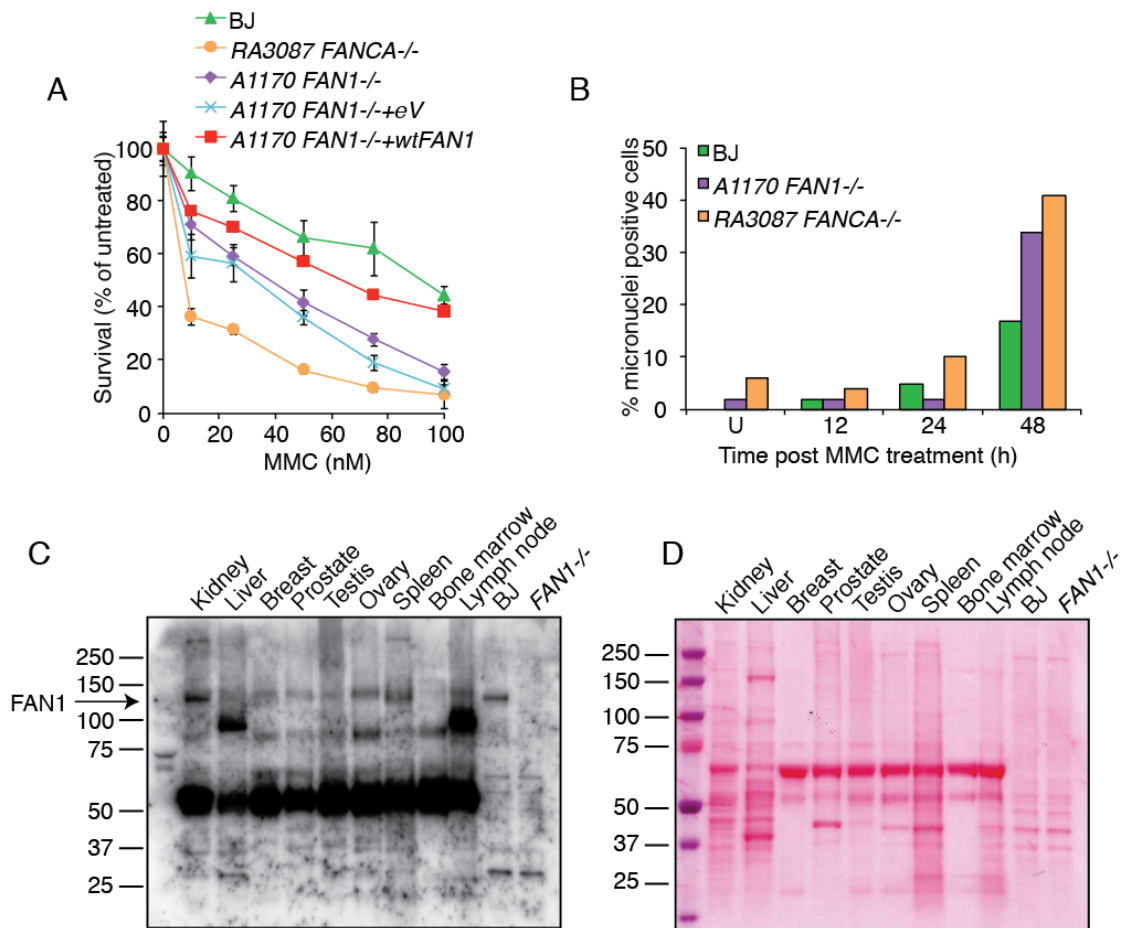
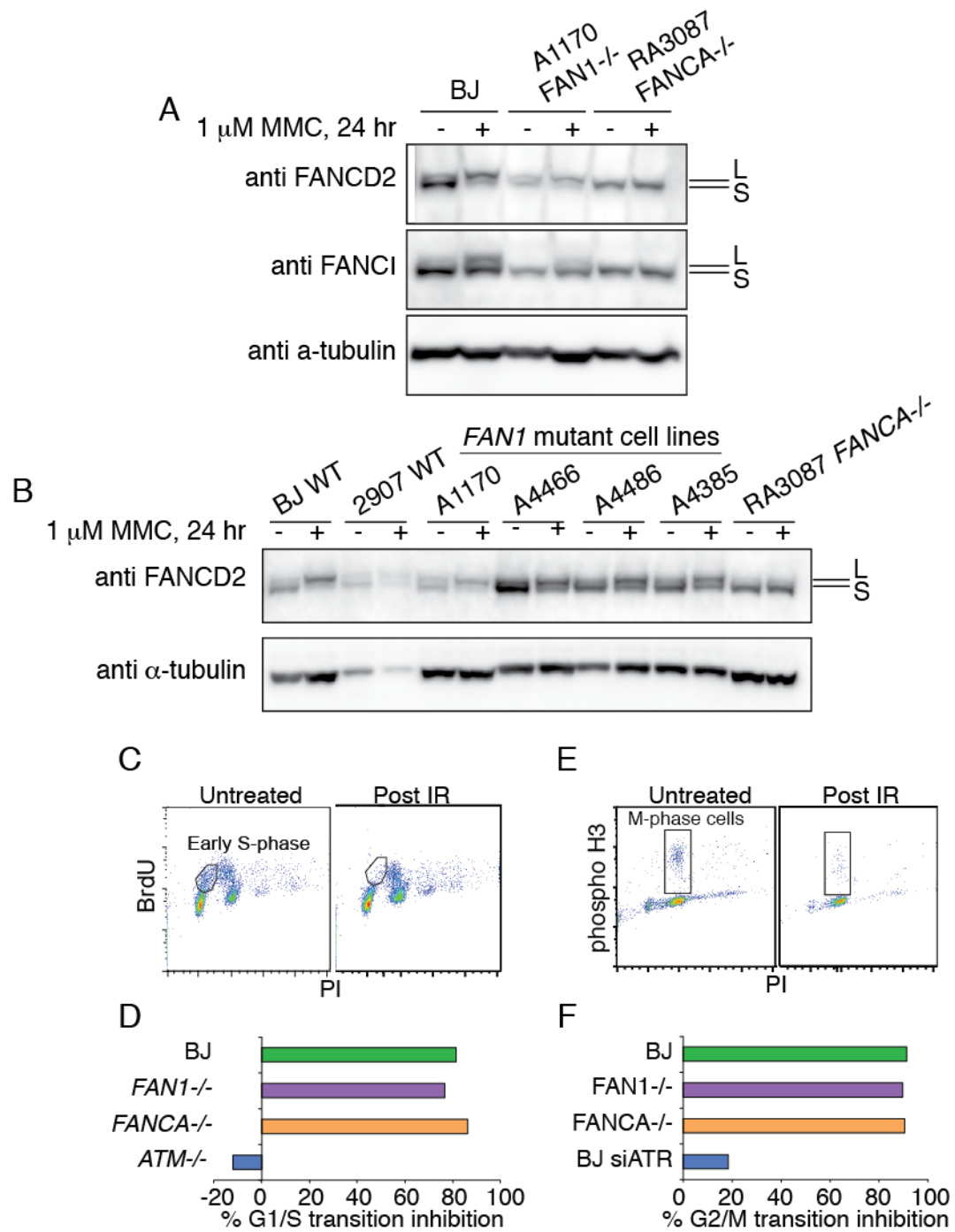


Figure 2.1 FAN1 deficiency causes ICL sensitivity in KIN patient cells and FAN1 is highly expressed in the kidney tissue.

(A) Survival of wild-type fibroblasts (BJ), RA3087 *FANCA*^{-/-}, A1170 *FAN1*^{-/-}, and A1170 cells transduced with eV (empty vector), or WT (wild-type) FAN1. Cells were treated with MMC. After 6 days, cell numbers were determined and normalized to the untreated control to calculate the percentage of survival. Error bars indicate SD. (B) Blinded quantification of cells with micronuclei following 1 hour of 1 μ M MMC treatment. (C-D) FAN1 expression in human tissues. Lysates from indicated tissues were run and immunoblotted with an antibody against FAN1 (RC394) (Left). Loading was assessed by a staining with Ponceau dye (Right).

Figure 2.2 FANCD2/FANCI ubiquitination and G1/S and G2/M checkpoints are not affected in FAN1-deficient KIN patient cells.

(A-B) Monoubiquitination status of FANCD2 in patient cell lines. Indicated cells were treated with 1 μ M MMC for 24 hours and collected for western blotting with anti-FANCD2 and anti-alpha tubulin antibodies. L indicates long, monoubiquitinated form of FANCD2 and S is a short, non-modified form. (C) Representative FACS profiles of G1/S checkpoint analysis. Cells were analyzed by BrdU and PI (propidium iodide) before and after IR. (D) Quantification of early S-phase cells with BrdU+ and DNA content around 2N. The number of early S-phase cells following IR-treatment was normalized to the untreated control to calculate the % of G1/S transition inhibition. (E) Representative FACS profiles of G2/M checkpoint analysis. Cells were analyzed by phosphorylated H3 and PI (propidium iodide) before and after IR. (F) Quantification of mitotic cells that were positive for phosphorylated H3 with DNA content close to 4N. The number of mitotic cells following IR-treatment was normalized to the untreated control to calculate the % of G2/M transition inhibition.



2.2.4 FAN1 has ICL repair activity that is non-epistatic with FA factors in human cells

It was previously shown that deletion of *FAN1* further sensitizes *FANCC*- and *FANCI*- deficient DT40 chicken cells to ICL-inducing agents. This indicates that FAN1 has FA pathway-independent function in ICL repair (Yoshikiyo et al., 2010). To examine whether this aspect of FAN1 function is conserved in human cells, we tested whether depletion of the Fanconi anemia factors including FANCD2, SLX4 or the SLX4-associated nucleases XPF and MUS81 in the *FAN1*-mutant cells led to increase in ICL sensitivity. *FAN1*-positive BJ cells were used as a control in the experiment. Depletion of *FANCD2*, *SLX4*, *XPF*, or *MUS81* in *FAN1*-deficient cells caused greater MMC sensitivity than the level observed in the corresponding FA factor-depleted BJ controls or in the non-depleted *FAN1*^{-/-} cells (Figure 2.3A-E). These results suggested that, also in human cells, FAN1 could function independently of the Fanconi anemia pathway in ICL damage response.

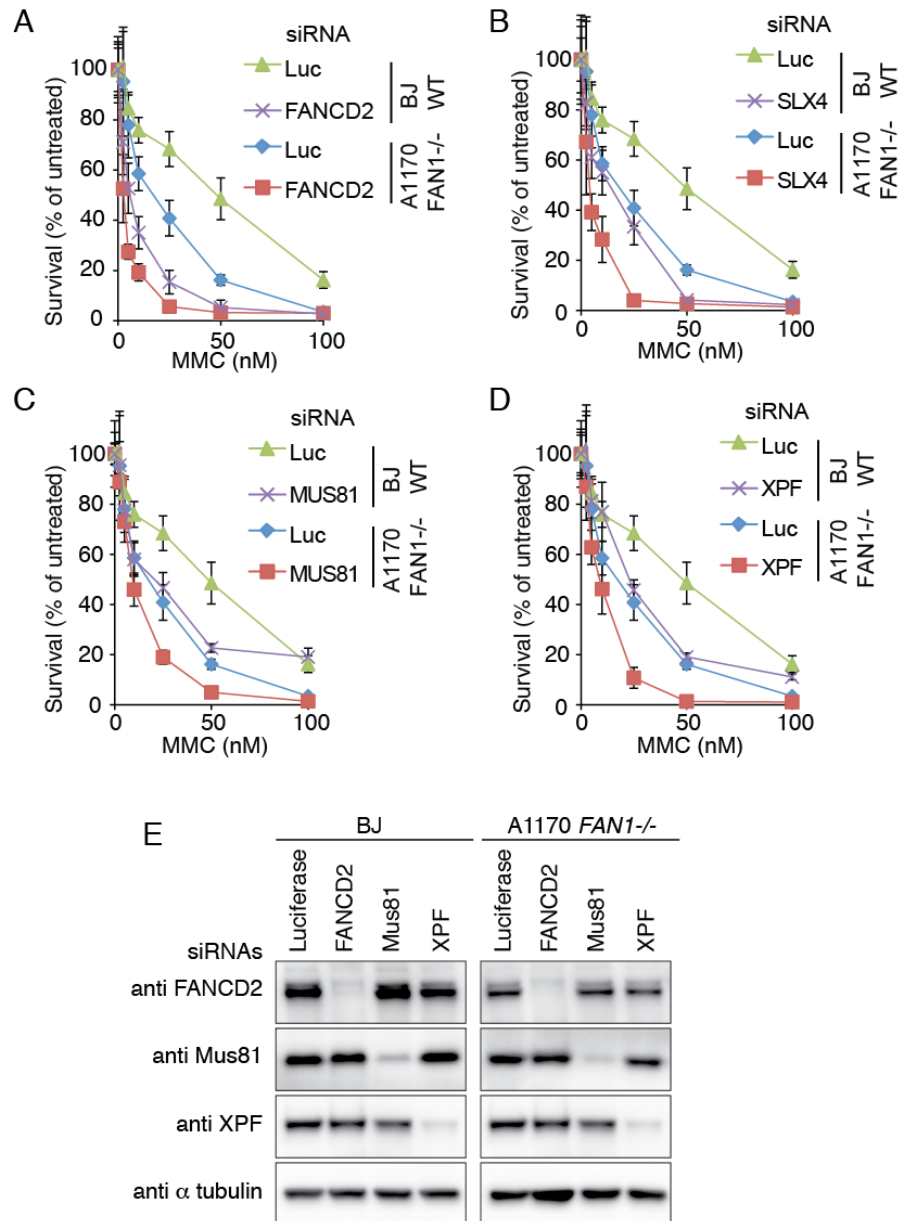


Figure 2.3 FAN1 has ICL repair function that is non-epistatic with the FA pathway.

MMC sensitivity in A1170 *FAN1*^{-/-} fibroblasts transfected with the siRNA against genes previously implicated in crosslink repair (A) FANCD2 depletion, (B) SLX4 depletion, (C) MUS81 depletion, (D) XPF depletion, (E) Immunoblot of expression levels of indicated proteins after siRNA-mediated depletion in the A1170 cells used in the experiment shown in panel A-D.

2.3 Characterization of *Fan1* knockout mouse

2.3.1 Verification of *Fan1* knockout in the mouse model

To investigate the cellular and organismal functions of FAN1, we generated *Fan1*-deficient mice. The *Fan1* locus was targeted in embryonic stem cells using a conditional *Fan1*^{tm1a} (KOMP)Wtsi (*Fan1*^{stop}) construct (Knockout Mouse Project [KOMP]) (Figure 2.4A). The correctly targeted clones were used to create a mouse with a single *Fan1*^{stop} allele, which was verified by Southern blotting using probes at 5' and 3' of the targeted site. (Figure 2.4B, C). *Fan1*^{+/stop} males were crossed with FLPe deleter female mice to generate mice carrying *Fan1*^{lox} allele (Figure 2.4A). Mice carrying the disrupted *Fan1* allele - *Fan1*^{Δex3&4}, which for ease of labeling, we refer to here as *Fan1*⁻, was generated from the cross between *Fan1*^{+/lox} male and *E2a-Cre* female mice.

Southern blotting using the probe located 5' of the targeted locus and PCR genotyping were performed to verify the generation of *Fan1*^{-/-} mice (Figure 2.5A-D). Deletion of exons 3 and 4 from *Fan1* gene resulted in low level of *Fan1* expression with *Fan1* transcript reduced to about 50% of the wild-type level in the *Fan1*^{+/-} heterozygotes and lower than 10% in *Fan1*^{-/-} animals. At the protein level, no protein expression could be detected in mouse embryonic fibroblasts (MEFs) obtained from homozygous *Fan1*^{-/-} embryonic day 13.5 (E13.5) embryos (Figure 2.5E-G). Together these results suggest that *Fan1* expression is abrogated in the *Fan1* knockout mouse that we engineered.

To assess whether FAN1 deficiency recapitulates the phenotypes observed in human cells lacking FAN1, we examined the cellular sensitivity of *Fan1*^{-/-} cells to ICL-inducing agent MMC when compared with *Fan1*^{+/+} or *Fan1*^{+/-} MEFs. Similar to human cells, *Fan1*^{-/-} MEFs displayed significant growth defects and an increase in the level of chromosome breaks and radial chromosomes when cells were treated with MMC (Figure 2.6A-C). Importantly, the cellular sensitivity and the increased breakage in *Fan1*^{-/-} MEFs after MMC treatment could be fully rescued when cells were transduced with wild-type mouse *Fan1* cDNA (Figure 2.6D, E, Figure 2.8C). These experiments show that the crosslink repair defect in *Fan1*^{-/-} MEFs is due to a lack of functional FAN1 protein.

Fan1-deficient MEFs were also more sensitive to treatment with acetaldehyde and formaldehyde, both of which have been implicated as endogenous sources of DNA ICLs (Figure 2.6F, G). However, the level of sensitivity to all tested ICL-inducing agents was significantly lower than that of MEFs deficient in SLX4 (*Slx4f3/f3*), a scaffold protein for three nucleases, including XPF, which is the major effector of the FA pathway (Figure 2.6A, F, G). Consistent with previous reports, *Fan1*-deficient MEFs did not show hypersensitivity to either camptothecin (CPT) or hydroxyurea (HU), suggesting that FAN1 is specifically required for the repair of DNA ICLs and no other S-

phase-associated replication blocks (Figure 2.6H, I; Kratz et al., 2010; Liu et al., 2010; MacKay et al., 2010; Smogorzewska et al., 2010).

Figure 2.4 Targeting strategy to create the *Fan1*-deficient mouse.

(A) Targeting strategy for *Fan1*-deficient mouse. Coding exons 1-6 of the *Fan1* genomic locus in wild type (chromosome 7), the *Fan1stop*, the *Fan1lox* and the *Fan1Δex3&4* mutant alleles generated are shown. The wild-type *Fan1* gene contains a 20.5 kb BamHI restriction fragment that hybridizes to the 5'(red) and 3'(dark green) probes. A correctly targeted *Fan1stop* locus contains a 13.8 kb fragment that hybridizes to the 5' probe and 7.5 kb fragment that hybridizes to the 3' probe. The neomycin cassette (pink), the FRT (blue), the LoxP (green), the splice acceptor (SA), and the poly A (pA) sites are also shown. The cross between *Fan1^{+/stop}* and FLP deleter mice generated *Fan1^{+/lox}*. The cross between *Fan1^{+/lox}* and FVB/N-Tg(Ella-cre)C5379Lmgd/J mice to derive *Fan1^{+/-}(Δex3&4)* are shown. The comparison between full-length wild type FAN1 transcript and *Fan1-(Δex3&4)* transcript lacking exon 3 and exon 4 are shown. Red asterisk (*), stop codon. The comparison between full-length wild type FAN1 protein with the domain architecture and the expected truncated FAN1 protein product expressed from *Fan1Δex3&4* allele are shown. (B, C) 5' and 3' Southern blot analyses of BamHI-digested genomic DNA from *Fan1^{+/+}* and *Fan1^{+/stop}* mice. CR, cross-reacting band.

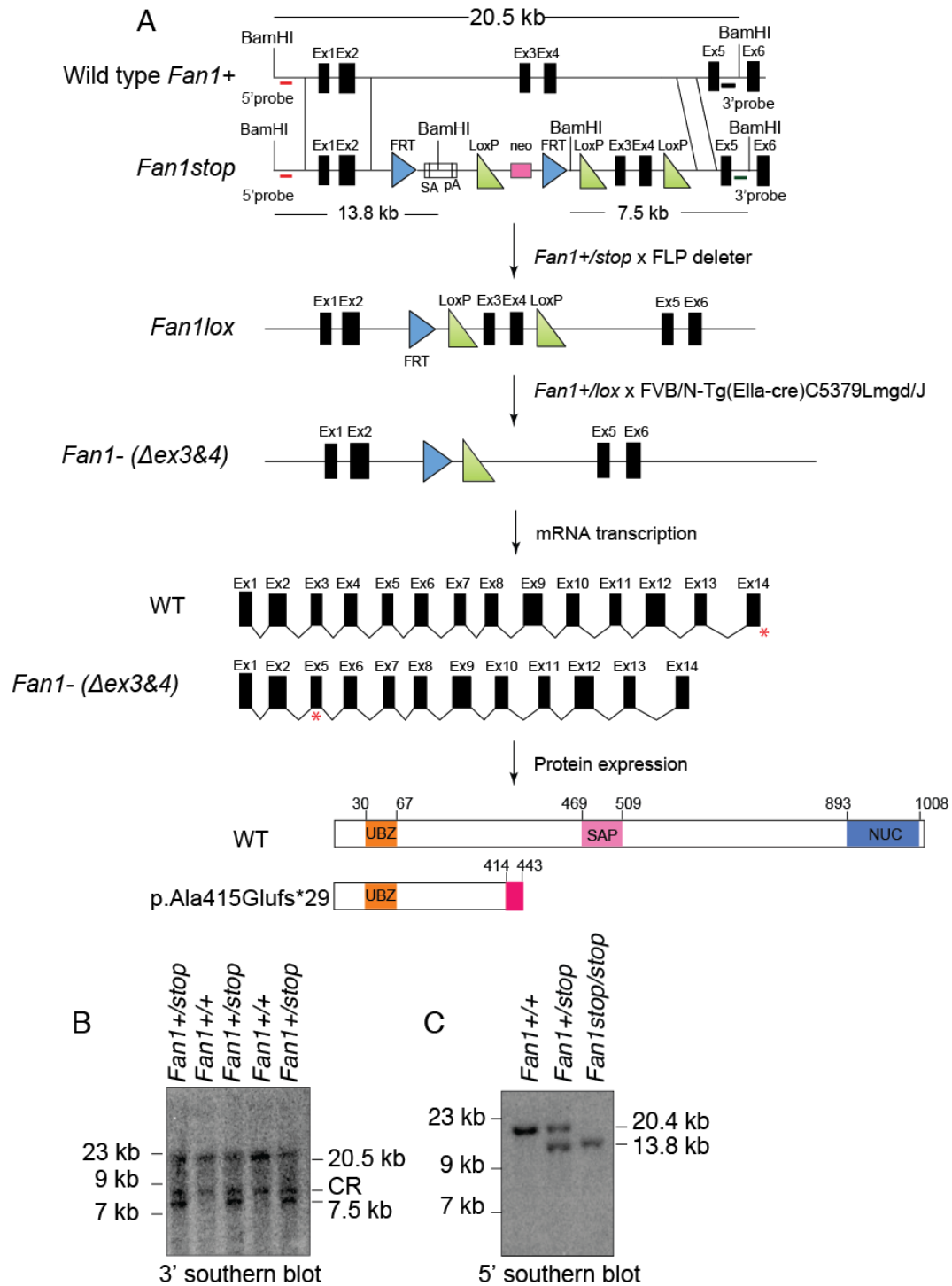


Figure 2.5 Verification of *Fan1* knockout mouse.

(A) Schematic of the wild-type and *Fan1* $\Delta ex3&4$ mutant alleles. The wild-type *Fan1* gene contains a 20.5-kb BamHI restriction fragment that can be detected with a 5' probe (red line). A correctly targeted *Fan1* locus harbors a 3.1-kb deletion, including exons 3 and 4, resulting in a 17.4-kb fragment that hybridizes to the same probe. The FRT and LoxP sites are indicated as blue and green triangles, respectively. (B) Southern blot analysis of BamHI-digested gDNA from *Fan1*^{+/+}, *Fan1*^{+/-}, and *Fan1*^{-/-} MEFs. (WT) Wild type; (Mut) mutant. (C-D) Schematic showing primer positions used for genotyping (top). Genotyping PCR for *Fan1*⁺ and *Fan1*⁻ alleles using DNA from MEFs of the indicated genotypes (bottom). (E) Schematic of exons 9-11 of *Fan1*, showing exon 10 q-PCR primers used in panel (F). (F) Quantification of *Fan1* mRNA level in MEFs of indicated genotypes. (G) Immunoblot of extracts from MEFs of the indicated genotypes using an antibody recognizing mouse FAN1. HAMFAN1 is N-terminally HA-tagged mouse FAN1 and is expressed in *Fan1*^{-/-} MEFs.

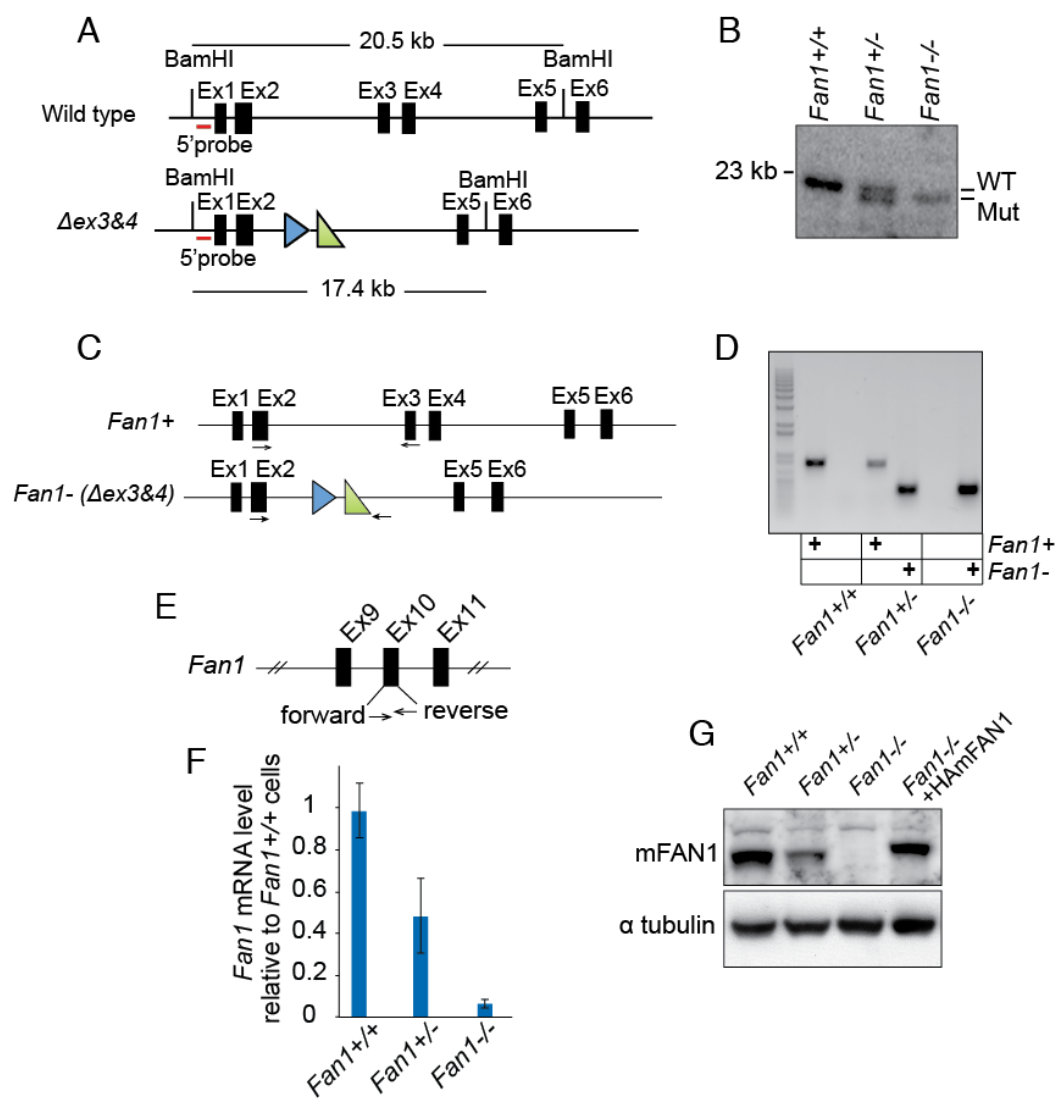
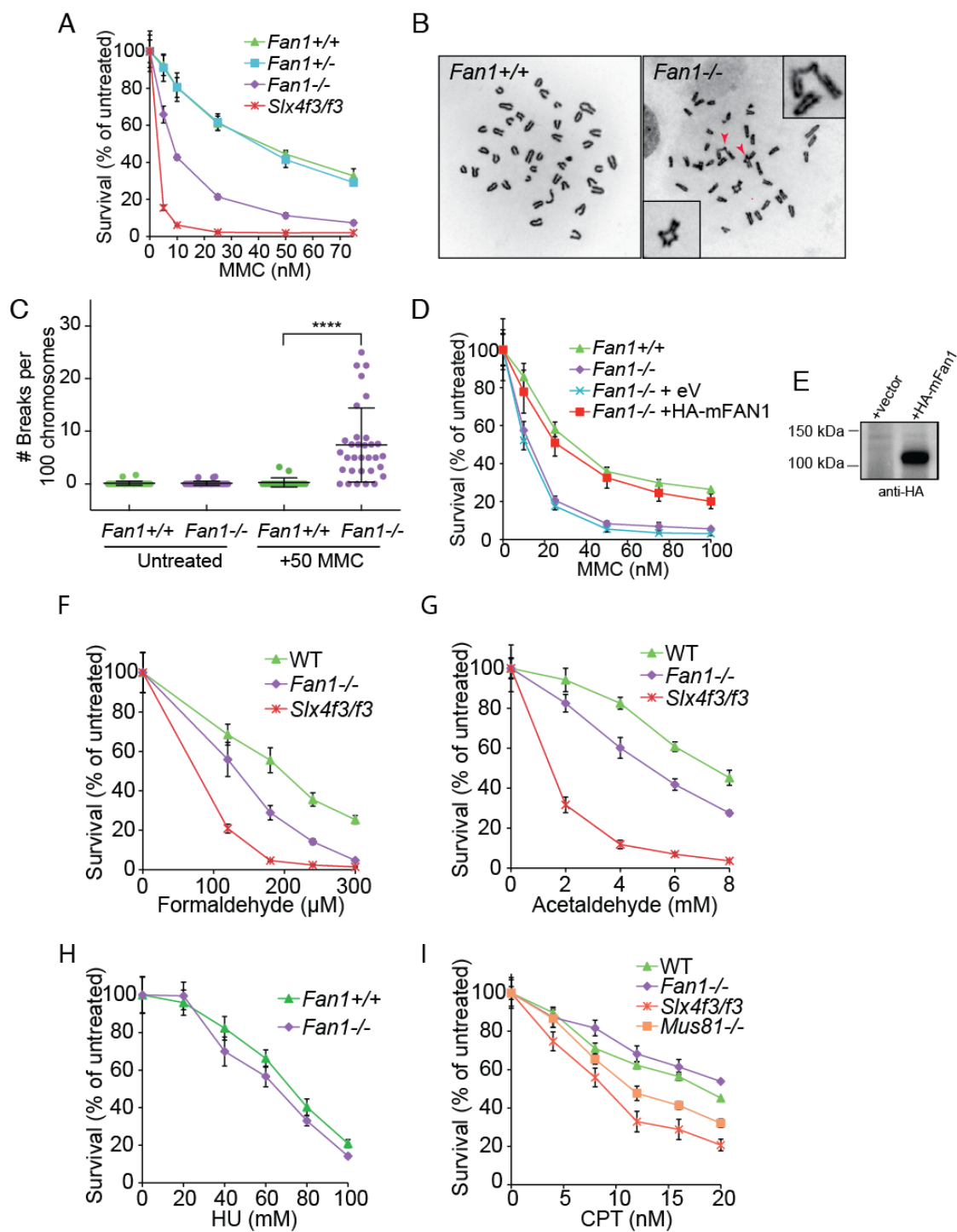


Figure 2.6 FAN1 is necessary for resistance to DNA ICL damage in MEFs.

(A) Survival of MEFs after treatment with the indicated doses of mitomycin C (MMC). MEFs were treated in triplicate with increasing concentrations of MMC. After 6 days, cell numbers were determined and normalized to untreated control to calculate the percentage of survival. Error bars indicate SD. (B) Examples of metaphase spreads of *Fan1*^{+/+} (left) and *Fan1*^{-/-} (right) after exposure to 50 nM MMC for 24 h. Arrowheads indicate radial chromosomes shown in the inset. (C) Quantification of chromosome breakage of *Fan1*^{+/+} and *Fan1*^{-/-} MEFs shown in B. (****) $P < 0.0001$, calculated using a t- test. (D) Complementation of MMC sensitivity in *Fan1*^{-/-} MEFs. *Fan1*^{-/-} MEFs stably transduced with empty vector (eV) or vector expressing HA-tagged mouse FAN1 (HA-mFAN1) were exposed to different levels of MMC, as in A. Error bars indicate SD. (E) Immunoblot showing the expression of HA-mFAN1 used in D. (F-G) Sensitivity to aldehydes of the indicated MEFs. MEFs were treated in triplicate with increasing concentrations of acetaldehyde (0–8 mM) (F) or formaldehyde (0–300 μ M) (G) for 2 h before being washed three times with PBS and were cultured for an additional 6 days in non-drug-containing medium. After 6 days, cell numbers were determined and normalized to untreated control to calculate the percentage of survival. Error bars indicate SD. (H) Survival of *Fan1*^{+/+} and *Fan1*^{-/-} MEFs treated with hydroxyurea (HU). MEFs were treated in triplicate with increasing concentrations of HU. Error bars, s.d.. (I) Survival of indicated MEFs after camptothecin (CPT) treatment (0–20 nM). MEFs were treated in triplicate with increasing concentrations of CPT. Error bars, s.d..



2.3.2 FAN1 participates in ICL repair independently of the UBZ domain

Our earlier work revealed that the UBZ domain was not important for the ability of FAN1 to confer resistance to crosslinking agents in human cells (Zhou et al., 2012). In that study, the UBZ mutated Cys44AlaCys47Ala human FAN1 fully rescued the ICL repair defect in the KIN patient cells. To assess which domains of mouse FAN1 are important for ICL resistance, we expressed mouse FAN1 with mutated UBZ (p.Cys44Ala;Cys47Ala), SAP (p.Leu480Pro), or nuclease (p.Asp963Ala) domains in *Fan1*^{-/-} MEFs and tested complementation of ICL sensitivity in a survival assay. Unlike expression of wild-type mouse *Fan1* cDNA, which was able to fully complement the MMC sensitivity of *Fan1*-deficient MEFs, expression of cDNA carrying a mutation in the SAP or nuclease domain resulted in no rescue (Figure 2.7A-C, E, F). In agreement with our previous study, the UBZ-mutated *Fan1* variant (p.Cys44Ala; Cys47Ala) behaved like the wild-type allele in this assay, indicating that FAN1-conferred ICL resistance is indeed independent of its FANCD2/FANCI interaction in mammalian cells (Figure 2.7A-D). This result was perplexing at the time, since the UBZ domain is critical for stable localization of FAN1 to the sites of DNA damage (Smogorzewska et al., 2010) and implies that a different domain of FAN1 might be important for localization of FAN1 to the ICLs.

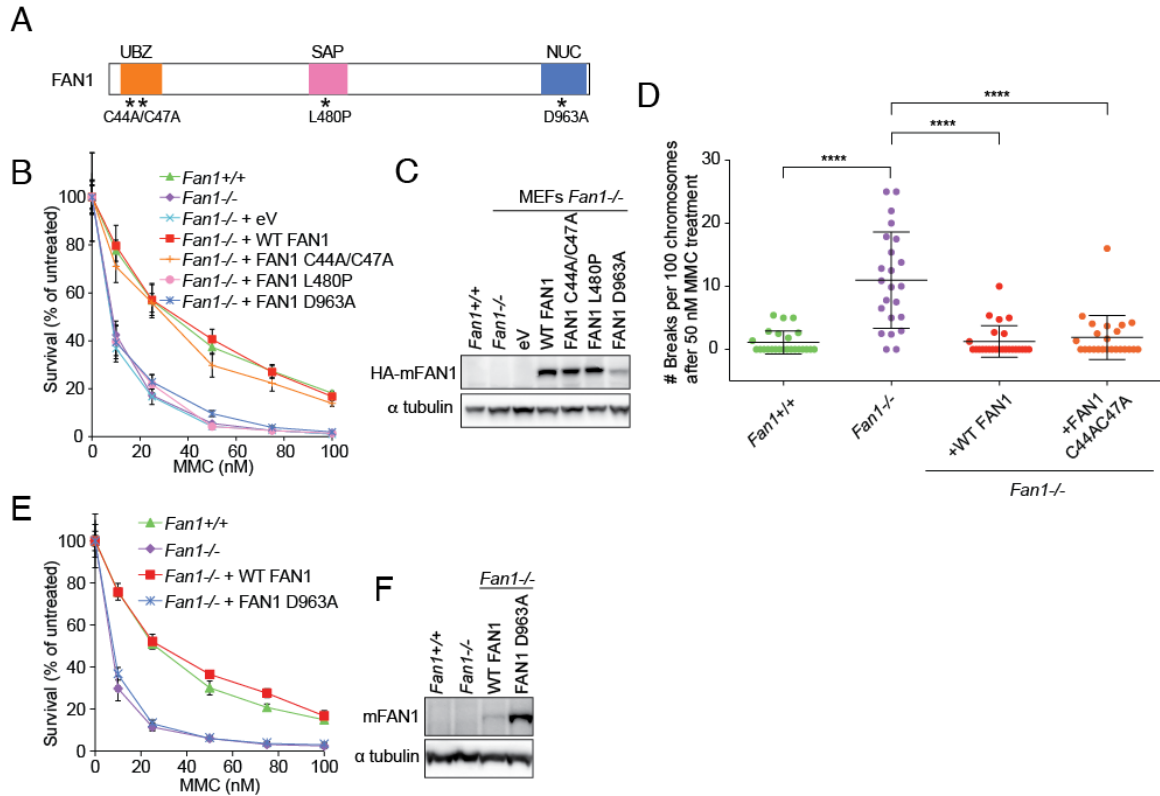


Figure 2.7 The UBZ domain is dispensable for FAN1's function in ICL repair.

(A) Schematic representation of the mouse FAN1 protein indicating the mutations in the key functional domains: C44A/C47A in the UBZ domain; p.L480P in the SAF-A/B, Acinus, and PIAS (SAP) domain; and p.D963A in (VRR- NUC) virus-type replication repair nuclease (NUC) domain. (B) MEFs stably transduced with empty vector or vector expressing *Fan1* variants with mutations shown in A were MMC-treated. Error bars indicate SD. (C) Immunoblot showing expression of mouse *Fan1* mutant cDNAs in MEFs used in B. (D) Quantification of chromosome breakage analysis of the indicated MEFs treated with 50 nM MMC for 24 hours. (E) MEFs stably transduced with vector expressing WT FAN1 or FAN1 D963A variant were exposed to MMC (0-100 nM). Error bars, s.d. (F) Immunoblot showing expression of WT FAN1 or FAN1 D963A in MEFs used in (E).

2.3.3 FAN1 can function independently of the FA pathway

Having established that FAN1 can repair ICL damage independently of its binding to FANCI/D2, we sought to determine whether FAN1 is epistatic with the FA pathway. To elucidate this genetic interaction, we generated *Fan1*^{-/-}*Fancd2*^{-/-} and *Fan1*^{-/-}*Fanca*^{-/-} double-knockout MEFs by crossing *Fan1*^{+/-} mice with *Fancd2*^{+/-} (Houghtaling et al., 2003) or *Fanca*^{+/-} (INoll et al., 2002) mice. *Fan1*^{-/-}*Fancd2*^{-/-} animals generated from the intercrosses between *Fan1*^{-/-}*Fancd2*^{+/-} mice were born at an observed ratio of 0.21, which is not significantly different from the expected ratio of 0.25. *Fancd2*^{-/-} and *Fanca*^{-/-} MEFs were more sensitive to MMC than the *Fan1*^{-/-} cells (Figure 2.8A, B), confirming that the FA pathway deficiency results in more pronounced inability to repair the MMC-induced damage. No further MMC-induced proliferation defect was apparent in the double-mutant MEF cell lines compared with cells lacking *Fancd2* or *Fanca* alone (Figure 2.8A, 2.9A). This might be due to difficulty in measuring small differences in cellular growth when cells are already very sensitive to DNA damage as is the case of FA protein deficient cells. However, a deficiency in *Fan1* enhanced the degree of MMC-induced chromosomal abnormalities in *Fancd2*^{-/-} MEFs (Figure 2.8C). FAN1 therefore has a FANCD2-independent function in the protection of cells from accruing ICL-induced chromosomal instability. To assess the epistasis in human cells, we knocked out FAN1 in *FANCA* or *FANCD2* patient cell lines (Kim et al., 2013) using CRISPR/Cas9. FAN1 deficiency further sensitized *FANCA*^{-/-} cells to MMC, which could be

complemented back to levels of MMC resistance seen in *FANCA*^{-/-} cells by exogenously expressing wild-type FAN1 (Figure 2.9A-E, H). However, human *FAN1*^{-/-}*FANCD2*^{-/-} cells did not exhibit significantly greater sensitivity to MMC than *FANCD2* single mutant cells (Figure 2.9F-H). Collectively, the analysis of the UBZ domain mutant and the epistasis analysis supports the conclusion that FAN1 has some function in ICL resistance that is independent of the FA pathway. This FAN1-specific repair function is more subtle compared with the activity of the FA-dependent pathway in mammalian cells, at least when MMC is used to introduce ICLs.

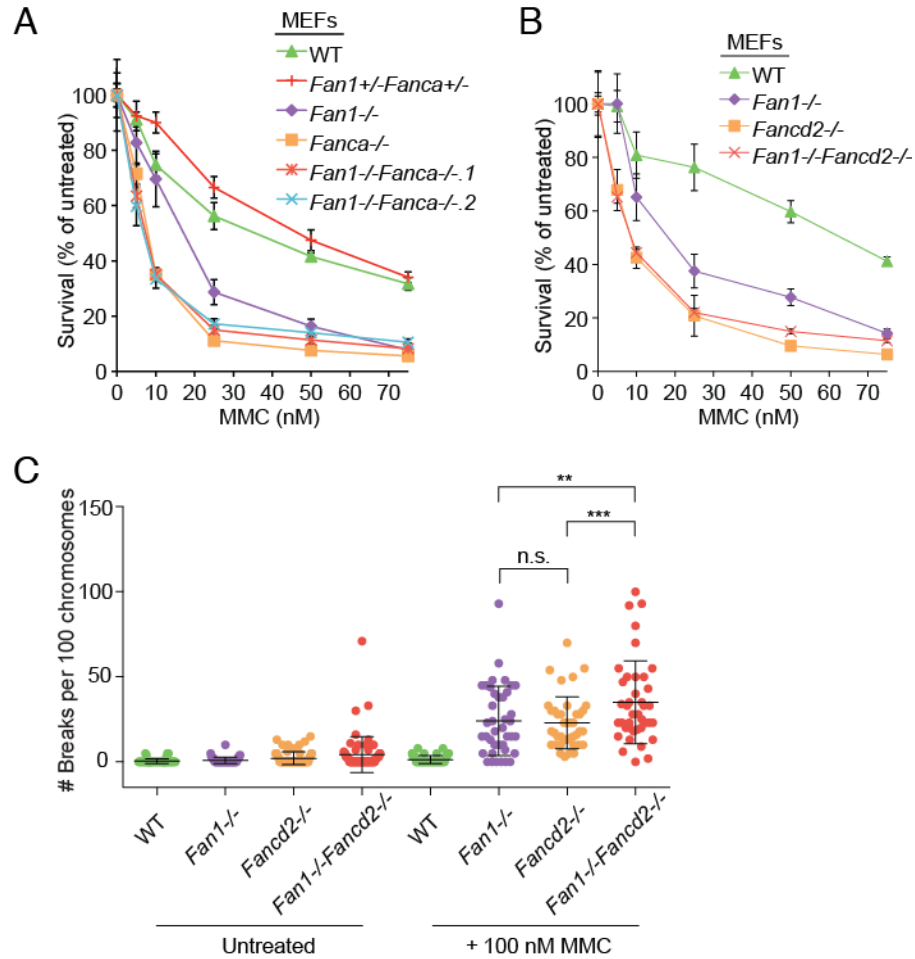
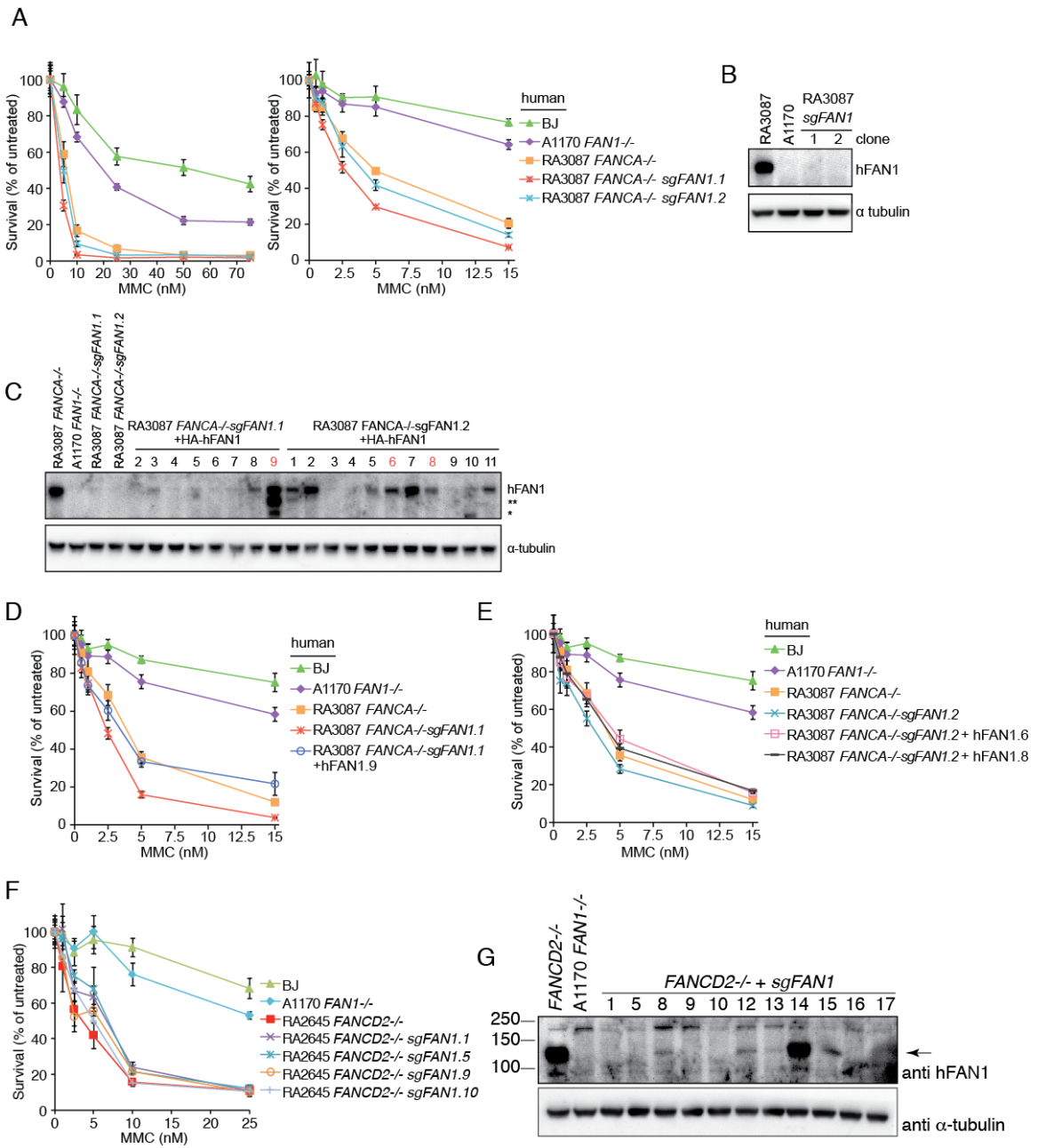


Figure 2.8 *Fan1* and FA genes are non-epistatic in MEFs in chromosome breakage assay.

(A) Survival of single *Fan1*^{-/-} and *Fancd2*^{-/-} and double *Fan1*^{-/-}*Fancd2*^{-/-} MEFs following single treatment with MMC. After 6 days, cell numbers were determined and normalized to the untreated control to calculate the percentage of survival. (WT) Wild type. Error bars indicate SD. (B) Survival of single *Fan1*^{-/-}, *Fanca*^{-/-}, and double *Fan1*^{-/-}*Fanca*^{-/-} deficient MEFs following single treatment with MMC as described in A. Error bars indicate SD. (C) Quantification of chromosome breakage analysis of the indicated MEFs collected 24 h after 100 nM MMC treatment or left untreated. (**) $P < 0.01$; (***) $P < 0.001$, calculated by one-way ANOVA.

Figure 2.9 *Fan1* and FA genes are non-epistatic in human cells.

(A) Survival of wild-type fibroblasts (BJ) and A1170-22 *FAN1*^{-/-}, RA3087 *FANCA*^{-/-}, and two clones (1 and 2) of RA3087 *FANCA*^{-/-}*FAN1*^{-/-} cells obtained by CRISPR/Cas9 gene editing. Cells were treated with MMC. After 6 days, cell numbers were determined and normalized to the untreated control to calculate the percentage of survival. Error bars indicate SD. (B) Immunoblot assessing expression of human FAN1 in human fibroblasts used in A. (C) Immunoblot assessing expression of human FAN1 transduced in RA3087 *FANCA*^{-/-}*FAN1*^{-/-} clone 1 and clone 2. The clones highlighted in red were used for the experiment outlined in (D, E). (D, E) Survival of RA3087 *FANCA*^{-/-}*FAN1*^{-/-} clone 1 and clone 2 complemented with HA-hFAN1. Cells were treated with MMC as described in A. MEFs collected 24 h after 100 nM MMC treatment or left untreated. (**) $P < 0.01$; (***) $P < 0.001$, calculated by one-way ANOVA. (F) Survival of wild-type fibroblasts (BJ) and A1170-22 *FAN1*^{-/-}, RA2645 *FANCD2*^{-/-}, and four clones (1, 5, 9 and 10) of RA2645 *FANCD2*^{-/-}*FAN1*^{-/-} cells obtained by CRISPR/Cas9 gene editing. Cells were treated with MMC. After 6 days, cell numbers were determined and normalized to the untreated control to calculate the percentage of survival. Error bars indicate SD. (G) Immunoblot assessing expression of human FAN1 in human fibroblasts used in F. (H) Sequences of the targeted clones RA3087 *FANCA*^{-/-}*FAN1*^{-/-} clone 2, RA2645 *FANCD2*^{-/-}*FAN1*^{-/-} clone 5, 9, and 10 used in A-G. The targeted region of RA3087 *FANCA*^{-/-}*FAN1*^{-/-} clone 1 and RA2645 *FANCD2*^{-/-}*FAN1*^{-/-} clone 1 could not be sequenced.



H

- i RA3087 *FANCA*^{-/-}*-sgFAN1.2*

CGTTCAAGTGGATCC -- GGCAGGTTG	g.222_223del
CGTTCAAGTGGATCCAGAGGGCAGGTTG	g.223_224insAG
CGTTCAAGTGGATCCAGGGCAGGTTG	Wild type Reference

- ii RA2645 *FANCD2*^{-/-} *-sgFAN1.5*

CGTTCAAGTGGATC ----- CAGGTTG	g.221_225del homozygous
CGTTCAAGTGGATCCAGGGCAGGTTG	Wild type Reference

- iii RA2645 *FANCD2*^{-/-} *-sgFAN1.9*

CGTTCAAGTGGATCC -- GGCAGGTTG	g.222_223del
CGTTCAAGTGGA ----- GGCAGGTTG	g.219_223del
CGTTCAAGTGGATCCAGGGCAGGTTG	Wild type Reference

- iv RA2645 *FANCD2*^{-/-} *-sgFAN1.10*

CGTTCAAG ----- TG	g.215_230del
g.35_227del (193 nt deletion)	g.35_227del
CGTTCAAGTGGATCCAGGGCAGGTTG	Wild type Reference

2.3.4 Genetic interactions of *Fan1* with *Slx4* and *Slx4*-associated nuclease *Mus81*

To determine the genetic interaction between *Slx4*, *Slx4*-associated nuclease *Mus81*, and *Fan1*, we generated *Fan1*^{-/-}*Slx4f3/f3* and *Fan1*^{-/-}*Mus81*^{-/-} MEFs through appropriate crosses. As shown earlier, *Slx4f3/f3* cells were significantly more sensitive to ICL-inducing agent compared to *Fan1*^{-/-} cells (Figure 2.6A, 2.10A). Inactivating *Fan1* in *Slx4f3/f3* cells did not have additive effect on cellular sensitivity to MMC, suggesting that *Slx4* plays a more dominant role in ICL repair and is epistatic with *Fan1* in mouse cells (Figure 2.10A).

Mus81-deficient MEFs were also significantly more sensitive to MMC than wild-type cells but less sensitive than *Fan1*^{-/-} cells (Figure 2.10B). Notably, lack of *MUS81* did not induce a remarkable increase in MMC-induced chromosomal breakage, unlike that seen in *Fan1* deficiency (Figure 2.10C). The double-knockout *Fan1*^{-/-}*Mus81*^{-/-} MEFs generated through mouse intercrosses were as sensitive to MMC as *Fan1*^{-/-} cells, suggesting that *Fan1* and *Mus81* are epistatic. Furthermore, *Mus81* knockout also did not significantly change the extent of chromosomal aberrations in MEFs lacking *Fan1* (Figure 2.10C), although there was a trend of increased abnormalities in the double-deficient cells.

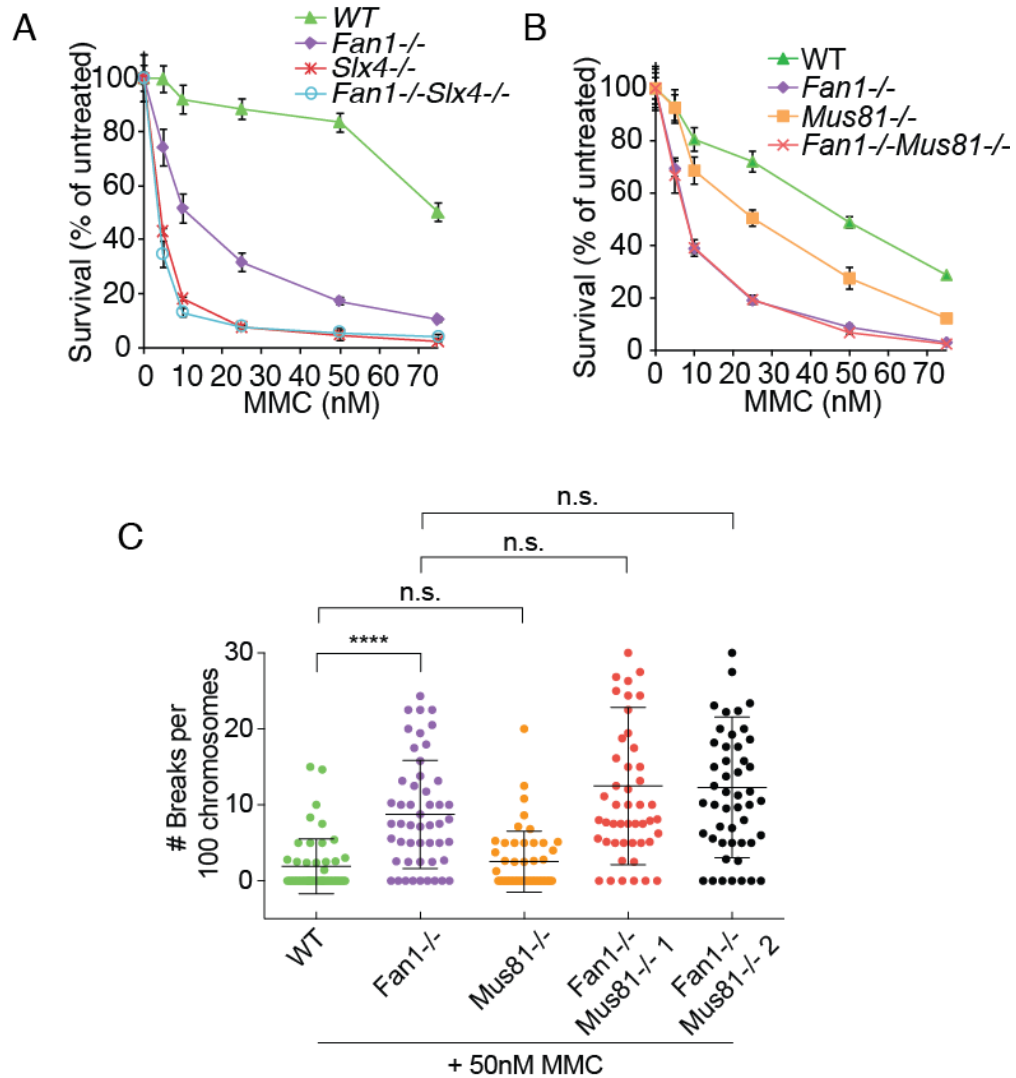


Figure 2.10 Genetic interactions of *Fan1* with *Slx4* and *Mus81*.

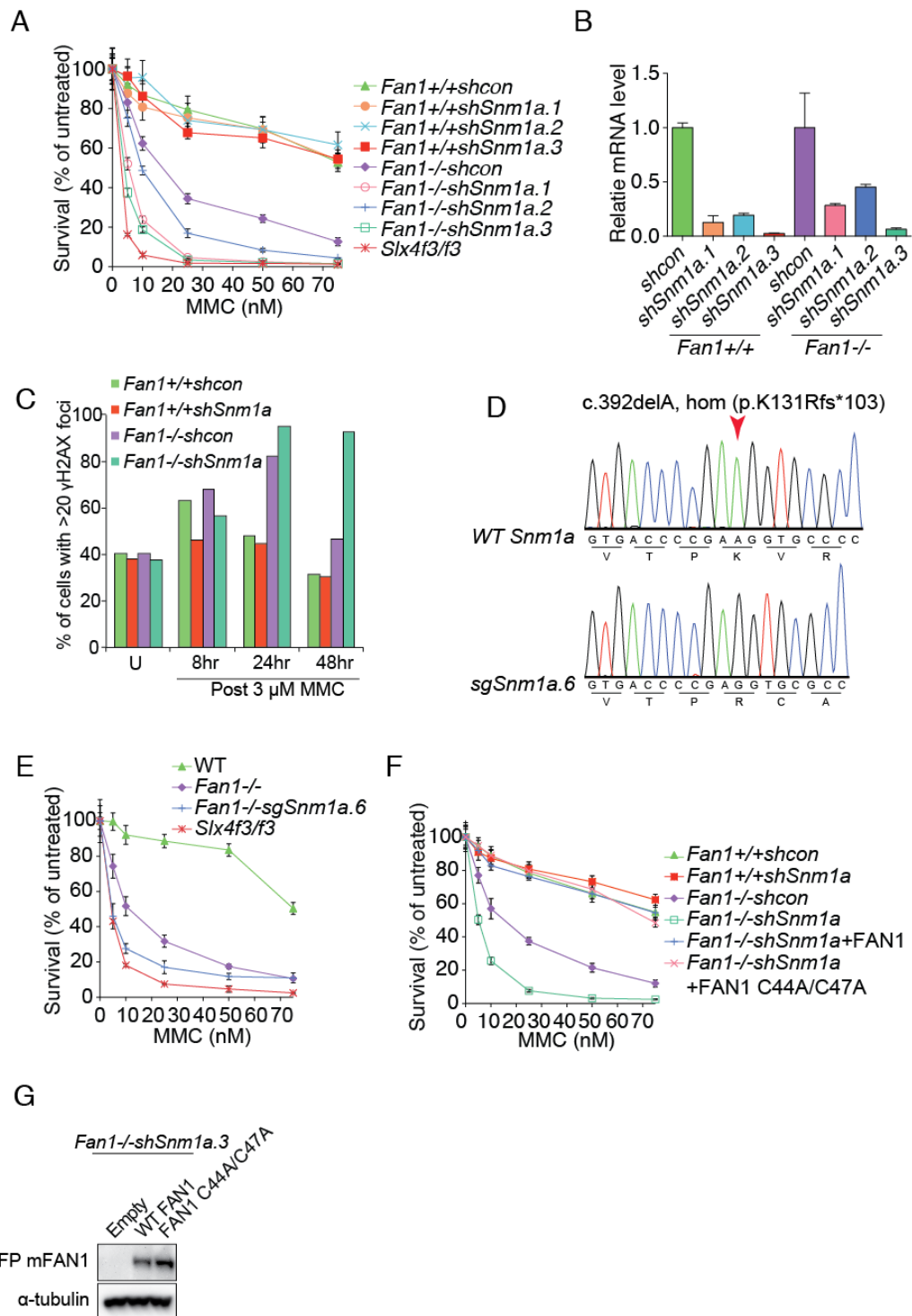
(A) Survival of *Fan1*-deficient, *Slx4*-deficient, and double-deficient MEFs treated with the indicated levels of MMC. After 6 days, cell numbers were determined and normalized to the untreated control to calculate the percentage of survival. (WT) Wild type. Error bars indicate SD. (B) Survival of *Fan1*-deficient, *Mus81*-deficient, and double-deficient MEFs treated with MMC as described in (A) (WT) Wild type. Error bars indicate SD. (C) Quantification of chromosome breakage analysis of the indicated MEFs treated with 50 nM MMC for 24 h. (****) $P < 0.0001$; (n.s.) Not significant, as determined by one-way ANOVA.

2.3.5 FAN1 is functionally redundant with SNM1A

Recent biochemical analyses revealed that *in vitro* FAN1 could incise close to a crosslink embedded in a variety of DNA substrates. In some cases, the processing of crosslink substrates by FAN1 occurred at both the 5' and 3' sides of the crosslink, leading to complete unhooking of the DNA crosslink (Pizzolato et al., 2015; Wang et al., 2014). To date, SNM1A, a homolog of yeast Pso2, is the only other known ICL-processing nuclease that is capable of digesting across an ICL, leading to the possibility that FAN1 may be functionally redundant with SNM1A in DNA ICL repair (Wang et al., 2011). To test this hypothesis, we used three different shRNAs to deplete *Snm1a* in both wild-type and *Fan1*^{-/-} MEFs. As previously reported, *Snm1a* depletion alone did not cause significant sensitivity to MMC in mouse cells (Figure 2.11A, B). However, depletion of *Snm1a* further sensitized *Fan1*-deficient cells to MMC and the level of MMC sensitization correlated with the level of *Snm1a* mRNA knockdown (Figure 2.11A-C). To confirm these results in a cell line that completely lacks both FAN1 and SNM1A, we knocked out *Snm1a* using CRISPR/Cas9. The double-deficient cells were more sensitive to MMC than *Fan1*^{-/-} cells and almost as sensitive as the SLX4-deficient cells (Figure 2.11D, E). FAN1 with an inactivated UBZ domain was able to complement an ICL repair defect in *Fan1*^{-/-}*shSnm1a* MEFs to the level of wild-type cells, indicating that the UBZ domain is also dispensable for ICL resistance in this setting. (Figure 2.11F, G).

Figure 2.11 FAN1 and SNM1A are redundant in conferring resistance to ICL-inducing agents.

(A) Survival of *Fan1*^{+/+} or *Fan1*^{-/-} stably transduced with control shRNA or shRNA targeting the *Snm1a* gene after treatment with MMC. *Slx4f3/f3* was used as a control. Error bars indicate SD. (B) Quantitative RT-PCR to assess the level of *Snm1a* transcript depletion in cell lines used in B. (C) Blinded quantification of cells with more than 20 γH2AX foci following MMC treatment. (D) Survival of wild-type, *Fan1*^{-/-}, *Fan1*^{-/-sgSnm1a.6}, and *Slx4f3/f3* MEFs after MMC. Error bars indicate SD. *Fan1*^{-/-sgSnm1a.6} is a clonal cell line with a biallelic frameshift mutation in *Snm1a* generated by CRISPR/Cas9 genome editing. (E) Sequencing of the *Fan1*^{-/-sgSnm1a.6} MEF clone used in E. (F) Survival of the indicated MEFs after MMC treatment. *Fan1*^{-/-} MEFs depleted of *Snm1a* were stably transduced with wild-type GFP-FAN1 or GFP-FAN1 C44A/C47A. Error bars indicate SD. (G) Immunoblot showing the expression of wild-type GFP-FAN1 or GFP-FAN1 C44A/C47A in *Fan1*^{-/-shSnm1a.3} MEFs used in F.



2.3.6 Lack of *Fan1* results in progressive kidney and liver karyomegaly and liver dysfunction

In order to assess if *Fan1*^{-/-} mice are a good model for human KIN, we analyzed the phenotypes of these mice. *Fan1*^{-/-} mice were born at the expected Mendelian ratio with no overt developmental abnormalities (Figure 2.12A). The growth of *Fan1*^{-/-} mice from birth until 12 weeks of age was comparable with wild-type and heterozygous littermates (Figure 2.12B). Furthermore, *Fan1*^{-/-} mice were fertile, producing on average eight pups per cross, a number comparable with those produced in crosses of heterozygous mice (Figure 2.12C).

Since one of the most pronounced characteristics of human KIN is the presence of karyomegalic nuclei in cells of multiple tissues, we monitored the histology of kidney and liver tissues in an aging cohort of mice. At 3 months, we did not observe any remarkable differences in the distribution of nuclear areas (cross-sectional area of nucleus) in renal tubular cells between *Fan1*^{-/-} and wild-type animals (Figure 2.13A, B). Increased nuclear area became detectable in *Fan1* mice at 6 months of age (Figure 2.13B). The level of renal karyomegaly further intensified with age, as the proportion of cells with larger than median nuclear area rose more than twofold to ~29% in 12-month-old *Fan1* mice (Figure 2.13B, C). Notably, the number of tubular cells with nuclei larger than the median area also went up to ~10% in 12-month-old wild-type animals. However, the nuclear area in this cohort did not exceed 1.2 times the median, unlike *Fan1*^{-/-}

animals at an equivalent age, which displayed a significant fraction (17%) that were >1.2 of the median. Significant karyomegaly was absent from glomeruli of *Fan1*^{-/-} mice (Figure 2.13D)

Despite the presence of karyomegaly, we detected no significant elevation in the level of blood urea nitrogen, creatinine, phosphorus, and magnesium in *Fan1*^{-/-} mice throughout the experiment (Figure 2.14A-D). These results indicate that, even with apparent karyomegaly, the kidneys of the 18-month-old *Fan1*^{-/-} animals still retain sufficient function to support homeostasis. Additional experimental manipulations to induce kidney injury may be necessary to elicit overt kidney failure in this model.

Similar to the kidney, there was no discernible difference in the distribution of the hepatocyte nuclear area between 3-month-old wild-type and *Fan1*^{-/-} mice. However, in 18-month-old mice without functional FAN1, a large fraction (>50%) of nuclei became significantly enlarged (Figure 2.13E, F). In order to determine whether the liver morphology had an impact on liver function, we analyzed liver enzymes and serum proteins in 3- to 18-month-old animals. *Fan1*^{-/-} animals displayed elevated alanine transaminase and aspartate transaminase while exhibiting lowered albumin and globulin levels (Figure 2.14E-H). The rise in serum liver enzyme and concurrent reduction in serum proteins synthesized

within the liver tissue indicate that the increase in karyomegalic hepatocytes coincides with the deterioration of liver function.

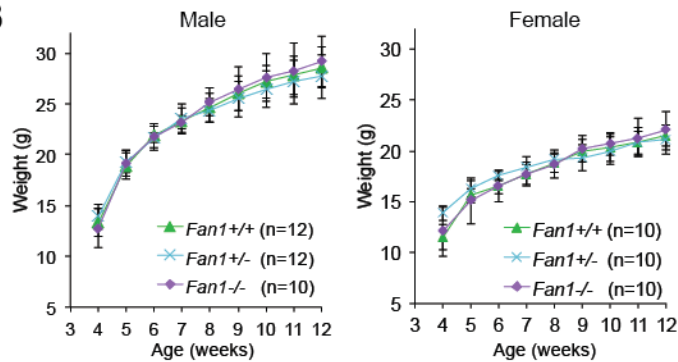
Consistent with the polyploidization of the cells in KIN patients, the enlarged cells in the kidney and liver tissue had increased numbers of hybridization signals of fluorescence in situ hybridization (FISH) probes recognizing three different chromosomes. In contrast, the spleen, which did not display karyomegaly, had very few cells with more than two signals (Figure 2.15A-E).

Taken together, these results strongly support that FAN1 is required to suppress age-dependent development of karyomegaly in the kidney and liver. The *Fan1*^{-/-} mouse model thus phenocopies the KIN conditions observed in humans and will be instrumental in understanding human disease and potentially the aging-associated changes in these tissues.

A

Genotype	# of pups	Observed ratio	Expected Ratio
<i>Fan1</i> ^{+/+}	49	0.24	0.25
<i>Fan1</i> ^{+/-}	107	0.51	0.50
<i>Fan1</i> ^{-/-}	51	0.25	0.25
Total number	207	p-value	0.8714

B



C

Maternal genotype	Paternal genotype	Number of Mating tested	Number of litters	Number of pups	Pups/ litters
<i>Fan1</i> ^{+/-}	<i>Fan1</i> ^{+/-}	15	15	110	7.3
<i>Fan1</i> ^{-/-}	<i>Fan1</i> ^{-/-}	8	8	65	8.1

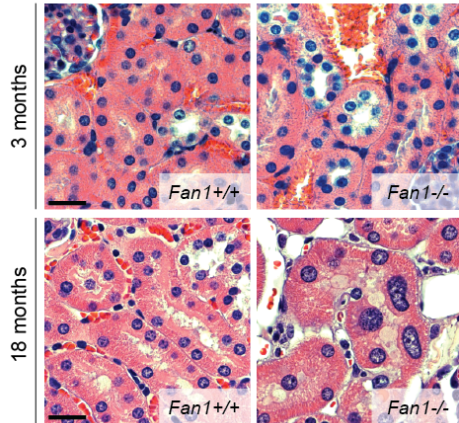
Figure 2.12 *Fan1*-deficient mice are born at Mendelian ratio, grow normally and are fertile.

(A) *Fan1*^{-/-} mice are born at the expected Mendelian ratio. Viability of *Fan1*^{-/-} mice was determined by genotyping the progeny from crosses of *Fan1*^{+/+} female and *Fan1*^{+/-} male at 21 days of age. p-value was calculated using the χ^2 -test. (B) Weight of male and female *Fan1*^{+/+}, *Fan1*^{+/-}, and *Fan1*^{-/-} mice from 3-12 weeks of age. (C) *Fan1*-deficient mice are fertile as assessed by the comparison of litter size from *Fan1*^{+/-} x *Fan1*^{+/-} and *Fan1*^{-/-} x *Fan1*^{-/-} crosses.

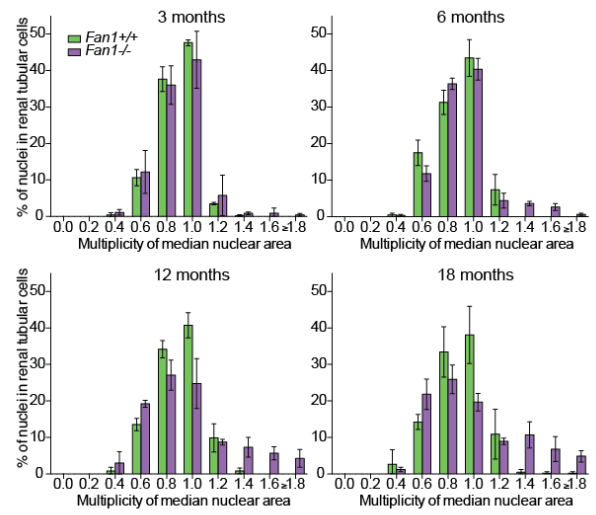
Figure 2.13 *Fan1* mice develop karyomegaly.

(A) Hematoxylin and eosin (H&E) staining of kidneys from *Fan1*^{+/+} and *Fan1*^{-/-} mice at 3 and 18 months. (B) Quantification of the nuclear area (cross-sectional area) of tubular epithelial cells in the cortex of kidneys from *Fan1*^{+/+} and *Fan1*^{-/-} mice at 3, 6, 12, and 18 months. The area of each nucleus was normalized to the median nuclear area present in the section to control for fixation and embedding conditions. Data were then plotted and grouped according to area. n = 3. Error bars indicate SD. (C) Percentage of karyomegalic nuclei larger than the median nuclear area in *Fan1*^{+/+} and *Fan1*^{-/-} mice at 3, 6, 12, and 18 months. (*) P < 0.05; (**) P < 0.01, calculated by one-way ANOVA. n = 3. Error bars indicate SD. (D) Quantification of the nuclear area of glomerular cells in *Fan1*^{+/+} and *Fan1*^{-/-} mice at 18 months. The area of each nucleus was normalized to the median nuclear area of each section. Data were then plotted and grouped according to area. n = 3. Error bars indicate SD. (E) H&E staining of liver sections from *Fan1*^{+/+} and *Fan1*^{-/-} animals at 3 and 18 months. (F) Quantification of the area of nuclei in the liver isolated from *Fan1*^{+/+} and *Fan1*^{-/-} mice at 3 and 18 months. n = 3. Error bars indicate SD.

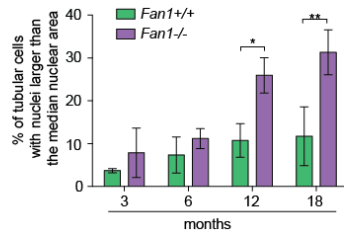
A



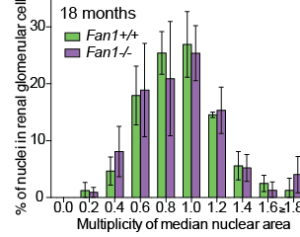
B



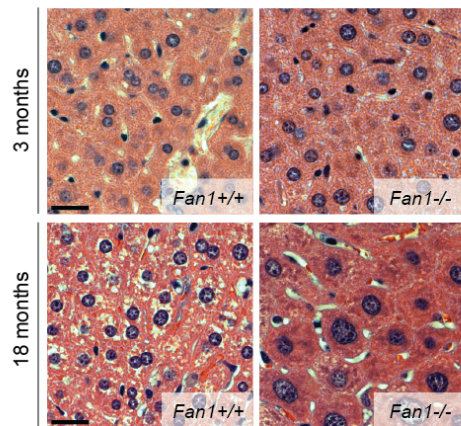
C



D



E



F

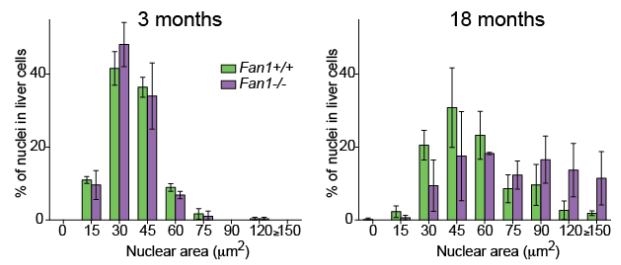


Figure 2.14 Liver function, but not kidney function is abnormal in *Fan1*-deficient mice.

(A-D) Analysis of serum level of (A) blood urea nitrogen (BUN), (B) creatinine, (C) phosphorus, and (D) magnesium to monitor kidney function of *Fan1*^{+/+} and *Fan1*^{-/-} mice at indicated ages. (E-H) Analysis of serum level of liver enzymes and markers of liver function: (E) alanine transaminase (ALT), (F) aspartate transaminase (AST), (G) albumin (ALB), and (H) globulin (GLOB). Bars represent mean \pm SD; ***p < 0.001, **p < 0.01 were calculated using F-test.

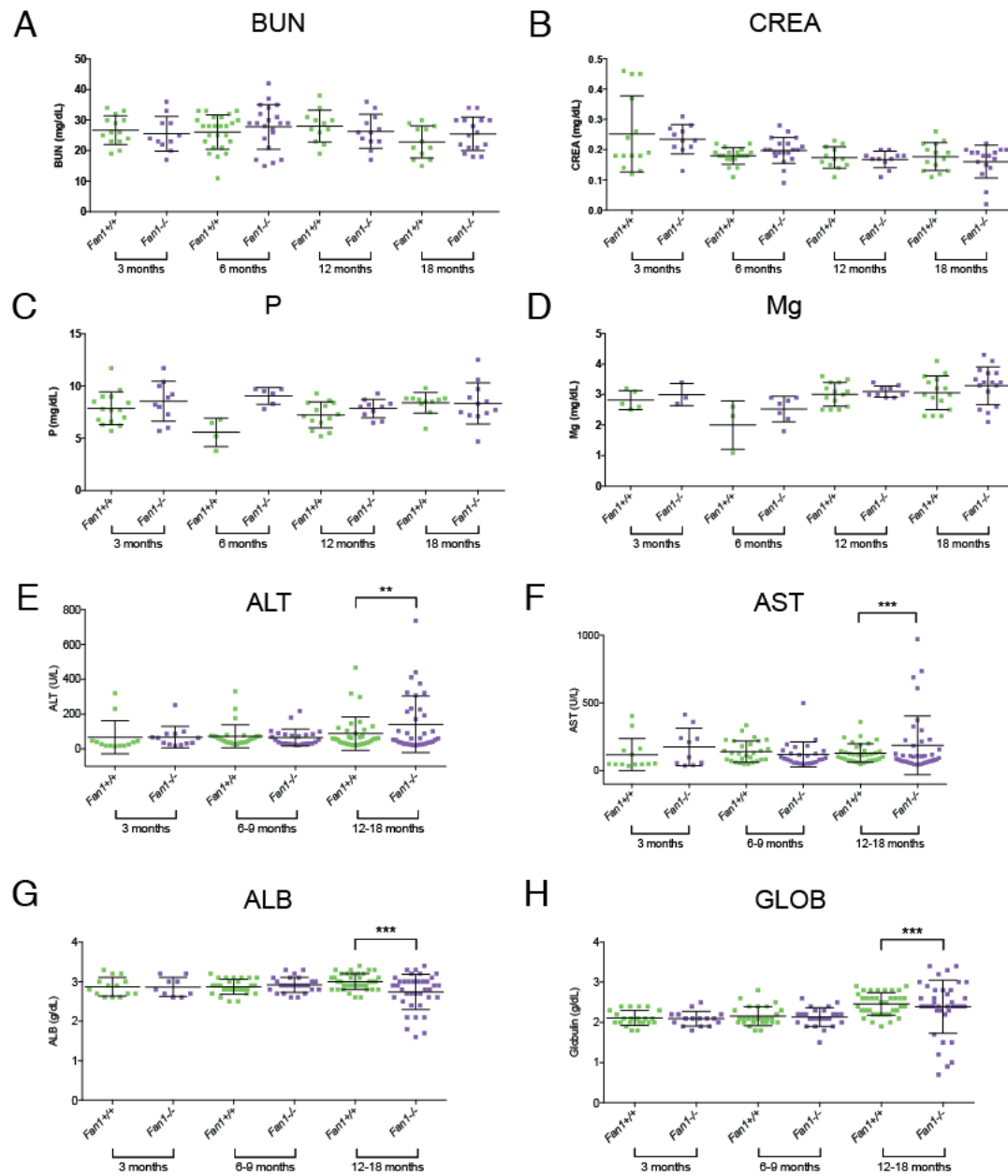
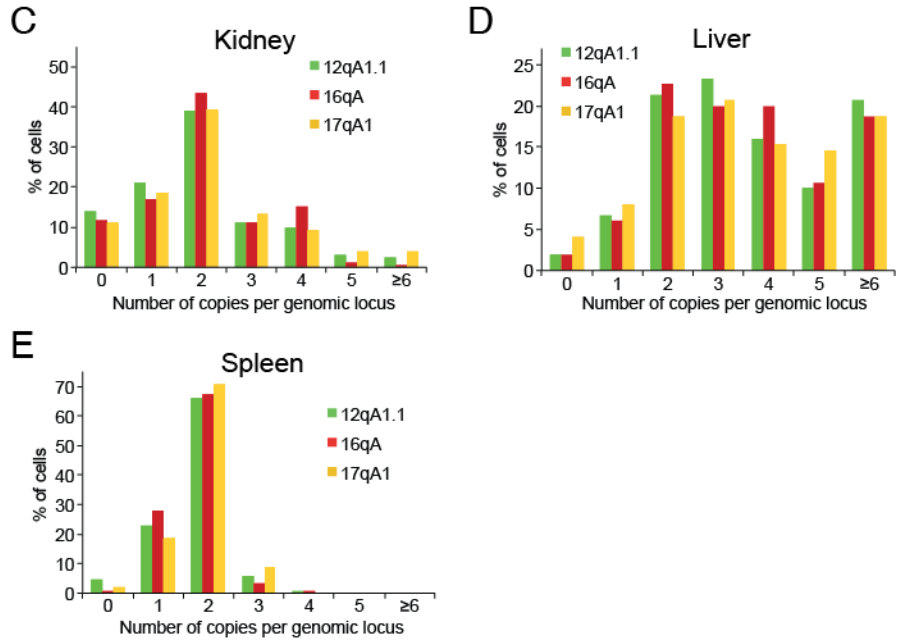
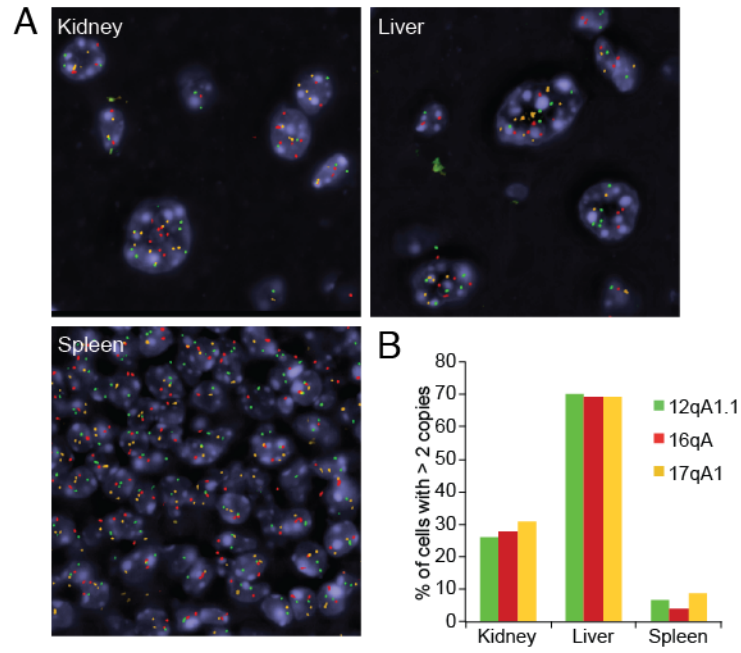


Figure 2.15 Karyomegaly is a result of polyploidization.

(A) Representative images of fluorescent in situ hybridization (FISH) performed with probes against the indicated loci in the kidneys, livers, and spleens of 18-month-old *Fan1*^{-/-} animals. The detail of the probes is given in Section 6.1.16. (B) Quantification of the cells with more than two signals per nucleus in 18-month-old *Fan1*^{-/-} animals. The analysis was restricted to tubular epithelial cells in the kidney and liver hepatocytes. (C-E) Quantification of FISH signals per nucleus in 18 months old *Fan1*^{-/-} animals. Tubular epithelial cells in the kidney (C), liver hepatocytes (D) and cells in the spleen (E) were assessed.



2.3.7 HSCs are unaffected in *Fan1*-deficient mice when unchallenged but severely affected when *Fan1* mice are treated with MMC

Anemia has been reported in a number of human KIN cases, prompting us to investigate the possible hematological dysfunction in *Fan1*-deficient mice. At the peripheral blood level, *Fan1*^{-/-} mice did not show obvious signs of cytopenia at a young age (Figure 2.16A-E). To explore the possibility of bone marrow abnormalities in *Fan1* animals, we analyzed the hematopoietic stem cell (HSC) population in the bone marrow of young (3 month) and old (18 month) mice with or without *Fan1* deficiency. We could not detect any changes in the level of the Lineage (Lin)⁻ Sca-1⁺ c-Kit⁺ (LSK) or Lin⁻ Sca-1⁻ c-Kit⁺ (LK) populations between *Fan1*^{+/+} and *Fan1*^{-/-} mice (Figure 2.17A, B). The numbers of long-term, short-term, and multipotent HSCs as well as the more differentiated progenitor cells-(megakaryocyte/erythroid progenitors, granulocyte/monocyte progenitors, and common myeloid progenitors) in *Fan1*^{-/-} animals were also similar to that of the wild-type control in the same age groups (Figure 2.17C, D). Inactivation of *Fan1* in mice with *Fancd2* deficiency did not significantly reduce the level of hematopoietic progenitor cells compared with *Fancd2* single-mutant mice (Figure 2.17E, F). Collectively, these results indicated that the activity of FAN1 is not required for the protection of early HSCs under unstressed conditions.

Although the bone marrow was not functionally compromised in *Fan1*^{-/-} mice, we asked whether FAN1 was required upon exogenous treatment with ICL-

inducing agents. *Fan1*^{-/-} and control mice were treated with a single intraperitoneal injection of 10 mg/kg MMC and were followed over the next 3 weeks. Some wild-type and heterozygous *Fan1*^{+/-} mice showed a minor drop in body weight after receiving the MMC. Most eventually regained the initial weight and tolerated the dose of MMC given until the end of the experiment (20 days post injection) (Figure 2.18A). In contrast, all *Fan1*^{-/-} mice reacted acutely to MMC, displaying a significant drop in body weight (10%–30%) following the treatment (Figure 2.18A). Ninety percent of *Fan1*^{-/-} mice tested died within two weeks after MMC treatment (Figure 2.18B). On day 7 after treatment with MMC, a parallel cohort of *Fan1*^{-/-} mice displayed depletion of the hematopoietic progenitor cells, as shown by a decrease in total cell number in the femurs and a complete disappearance of c-Kit⁺ bone marrow cells following MMC treatment (Figure 2.19A-D). Furthermore, MMC-treatment caused significantly greater reduction in the level of LSK cells in *Fan1*-deficient c-Kit⁺ cells cultured *in vitro* compared to wild-type (Figure 2.19E). In agreement, the histological analysis revealed pronounced hypocellularity in the bone marrow and the thymus of *Fan1*^{-/-} mice (Figure 2.18C). The effect of ICL repair deficiency on the hematopoietic system of *Fan1*^{-/-} animals was further supported by significant neutropenia and thrombocytopenia. Although the red blood cell (RBC) count was largely unaltered due to the long half-life of RBCs, the reticulocyte counts of *Fan1*^{-/-} mice was significantly lower than *Fan1*^{+/+} mice at day 7 after MMC treatment (Figure 2.19F-I). These results illustrate the necessity of FAN1 for the maintenance of

hematopoiesis and survival of animals exposed to high levels of exogenous crosslink damage.

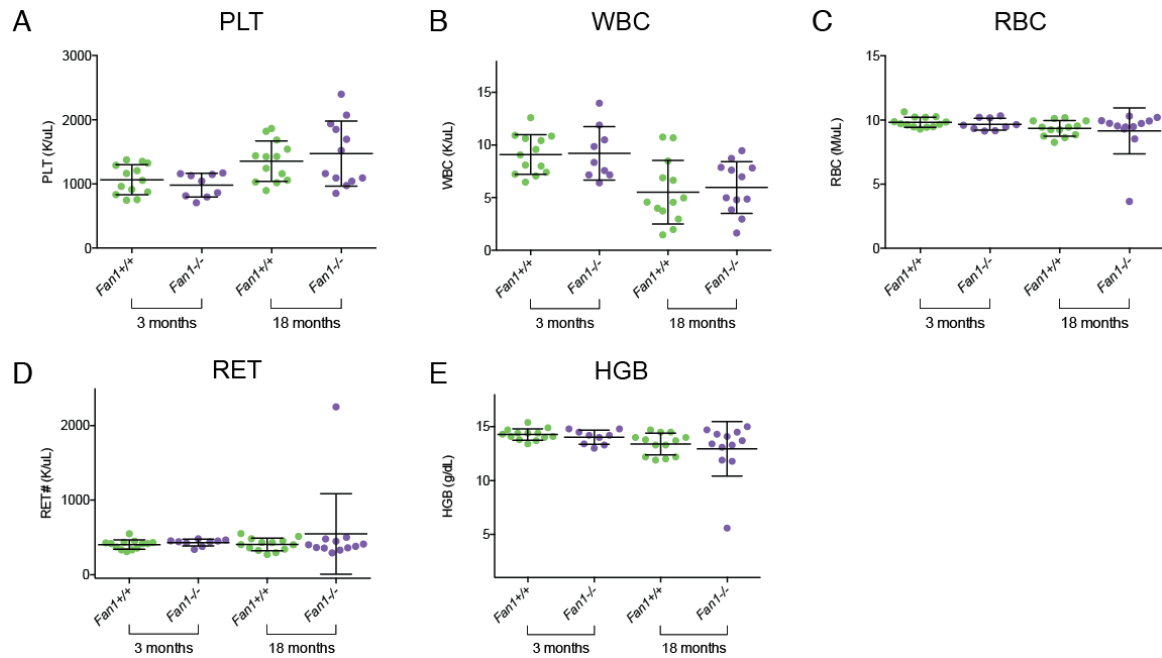


Figure 2.16 Blood counts are normal in the majority of *Fan1*-deficient mice.

(A-E) Blood analysis in *Fan1*^{+/+} and *Fan1*^{-/-} mice: (A) platelets (PLT), (B) white blood cells (WBC), (C) red blood cells (RBC), (D) reticulocytes (RET), and (E) hemoglobin concentration (HGB).

Figure 2.17 FAN1 is dispensable for the bone marrow maintenance under unstressed condition.

(A) Representative FACS profiles of HSCs isolated from bone marrow of *Fan1*^{+/+} and *Fan1*^{-/-} mice, indicating LSK and LK population. (B) Quantification of hematopoietic stem cells (HSCs) isolated from *Fan1*^{+/+} and *Fan1*^{-/-} mice assessed by FACS. n = 3 per genotype. Error bars indicate SD. (C) Analysis of LT-HSC, ST-HSC and MPP isolated from femurs and tibiae of *Fan1*^{+/+} and *Fan1*^{-/-} mice at indicated ages assessed by FACS. Error bars, s.d., n = 3 per genotype. (D) Analysis of MEP (megakaryocyte/erythroid progenitors), GMP (granulocyte/monocyte progenitors), and CMP (common-myeloid progenitors) isolated from femurs and tibiae of *Fan1*^{+/+} and *Fan1*^{-/-} mice at indicated ages assessed by FACS. Error bars, s.d., n = 3 per genotype. (E) Quantification of HSCs isolated from mice of the indicated genotypes, assessed by FACS. n = 3 per genotype. (WT) Wild type. Error bars indicate SD. (F) D) Analysis of LT-HSC, ST-HSC, and MPP (left) and MEP, GMP, and CMP (right) isolated from femurs and tibiae of 6 months old WT, *Fan1*^{-/-}, *Fancd2*^{-/-}, and *Fan1*^{-/-} *Fancd2*^{-/-} mice assessed by FACS. Error bars, s.d., n = 3 per genotype.

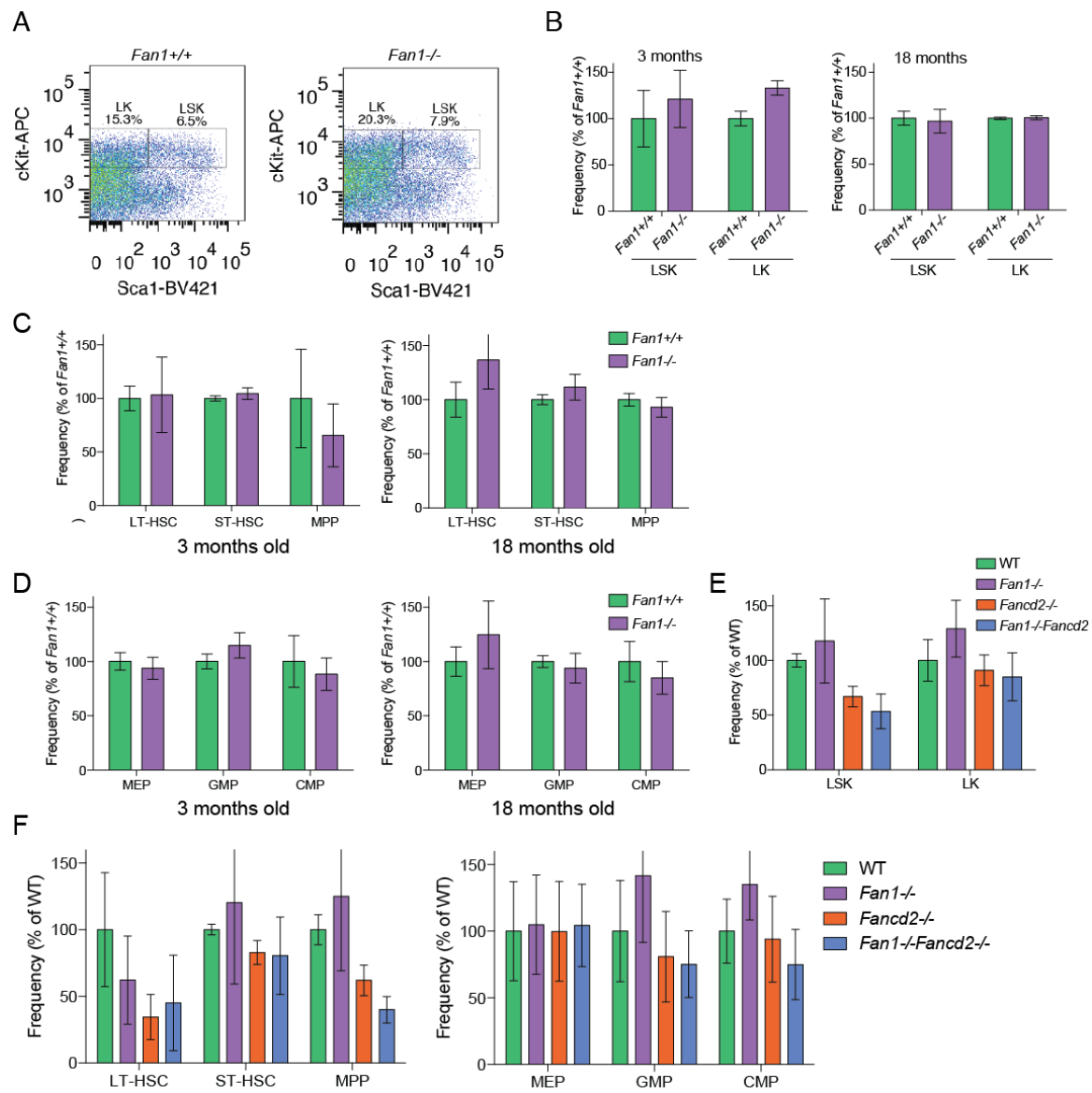


Figure 2.18 *Fan1*-deficient mice are hypersensitive to MMC.

(A) Weight monitoring of mice after treatment with MMC. Following intraperitoneal injection of 10 mg of MMC per kg, *Fan1*^{+/+}, *Fan1*^{+/-}, and *Fan1*^{-/-} mice were weighed every 2 days for 20 days or until death. Weight is expressed as % of original weight on the day of MMC injection. (B) Survival of *Fan1*^{+/+}, *Fan1*^{+/-}, and *Fan1*^{-/-} mice (n = 10 per genotype) after a single treatment with 10 mg/kg MMC. Mice from each genotype were monitored up to 20 days following MMC intraperitoneal injection. Bone marrow and thymus histology from *Fan1*^{+/+} and *Fan1*^{-/-} mice treated 1 week prior with 10 mg/kg MMC. Representative images at 10× and 63× are shown.

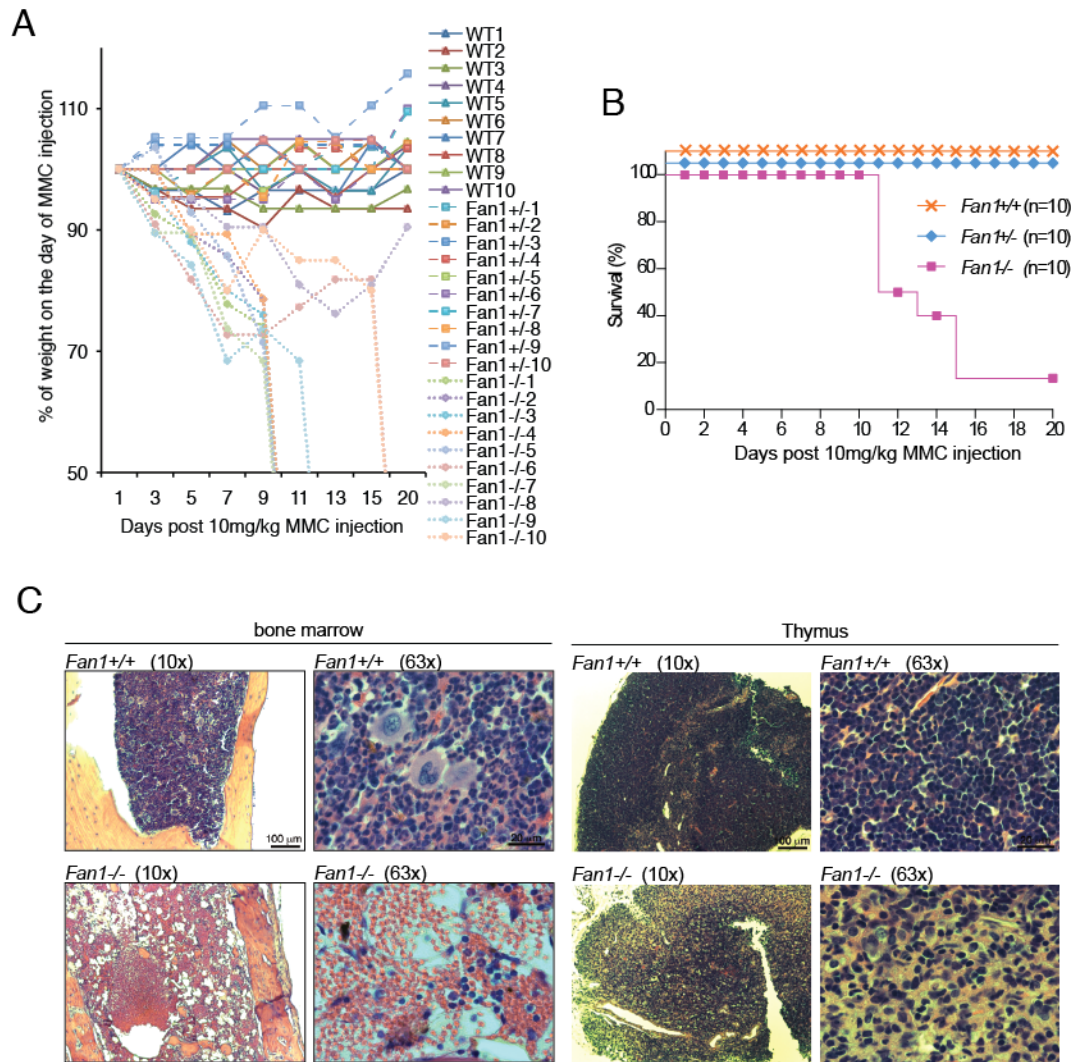
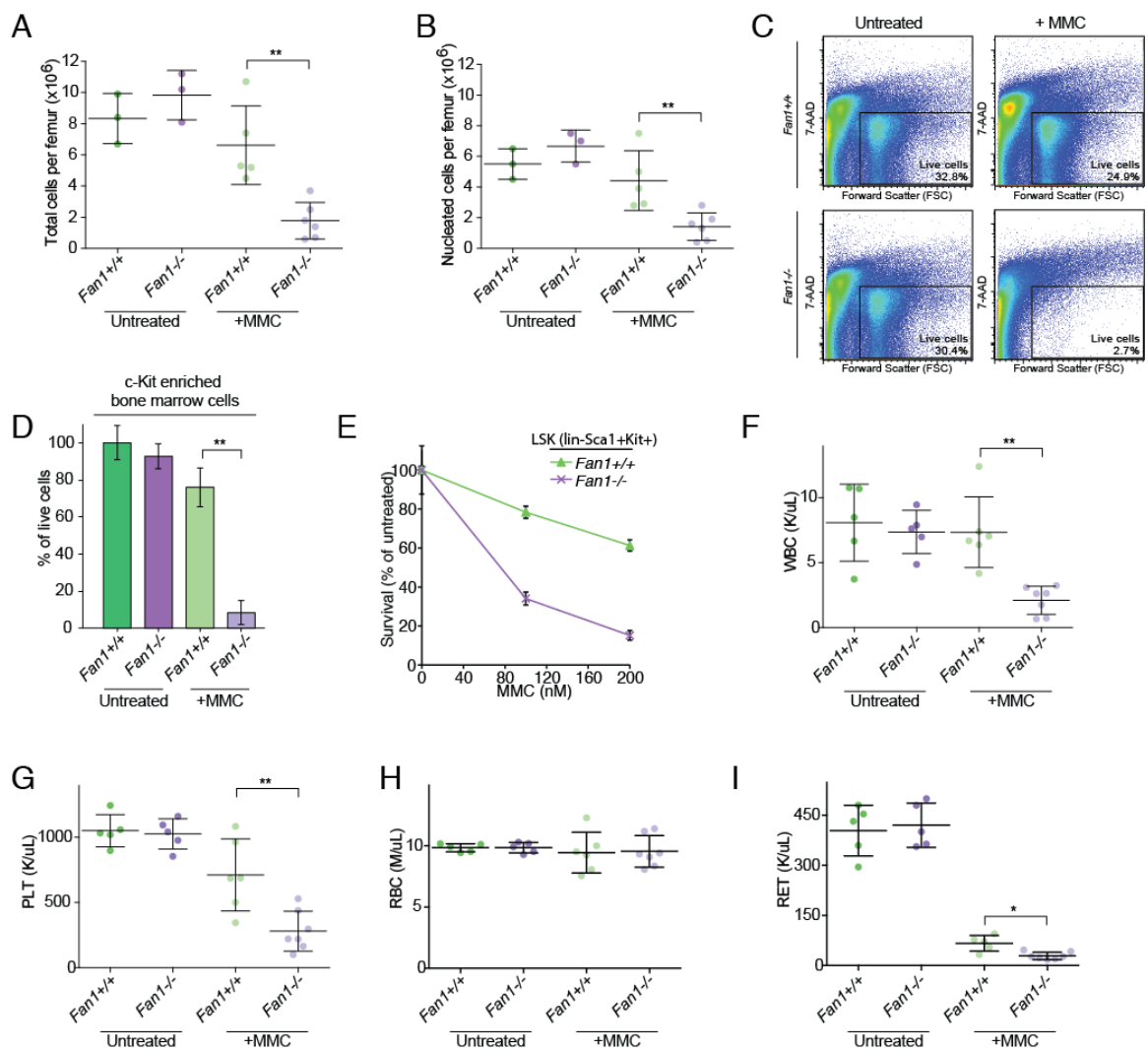


Figure 2.19 FAN1 is required to protect the hematopoietic stem and progenitor cells from high level of ICL damage.

(A) Total number of cells per femur of *Fan1*^{+/+} and *Fan1*^{-/-} mice untreated or treated 1 week prior with 10 mg/kg MMC. Bars represent mean \pm SD. (**) $P < 0.01$, calculated using unpaired t-test. (B) Number of nucleated cells per femur of *Fan1*^{+/+} and *Fan1*^{-/-} mice untreated or treated 1 week prior with 10 mg/kg MMC. Bars represent mean \pm SD; ** $p < 0.01$ were calculated using unpaired t-test. (C) Representative FACS profile of bone marrow cells that were enriched for c-Kit positive population, determined by FSC and 7-ADD (7-amino-actinomycin D) viability gate. The bone marrow cells were isolated from *Fan1*^{+/+} and *Fan1*^{-/-} mice untreated or treated 1 week prior with 10 mg of MMC per kg. (D) Percentage of live bone marrow cells that were enriched for c-Kit⁺ population. The bone marrow cells were isolated from *Fan1*^{+/+} and *Fan1*^{-/-} mice untreated or treated 1 week prior with 10 mg/kg MMC. Bars represent mean \pm SD. (**) $P < 0.01$, calculated using unpaired t-test. (E) Survival of *Fan1*^{+/+} and *Fan1*^{-/-} LSK population within the *in vitro* culture c-Kit⁺ cells following a single treatment with MMC. After 48 hours, LSK frequency were determined and normalized to the untreated control to calculate the percentage of survival. Error bars indicate SD. (F-I) White blood cell (WBC) (F), platelet (PLT) (G), Red blood cell (RBC) (H), and Reticulocyte (RET) (I) counts of *Fan1*^{+/+} and *Fan1*^{-/-} mice untreated or treated 1 week prior with 10 mg/kg MMC. Bars represent mean \pm SD. (**) $P < 0.01$, calculated using unpaired t-test.



2.3.8 FAN1 is dispensable for the protection of bone marrow against IR induced damage

To examine whether *Fan1* deficiency renders bone marrow sensitivity to DNA damaging agents in a non-specific manner, we analyzed the effect of ionizing radiation (IR) on the hematopoietic system in wild-type and *Fan1*^{-/-} animals. Mice were treated with a sublethal dose of 450 cGy X-ray that has been shown to cause severe bone marrow abnormalities in mice models with defects in the repair of IR-induced DNA damage (Nussenzweig et al., 1997). The changes in the peripheral blood cells and hematopoietic stem and progenitor cell function were monitored to assess the requirement of FAN1 in the protection of bone marrow against IR-induced lesions. A significant drop in the body weight among wild-type or *Fan1*^{-/-} cohorts was not observed within 6 weeks following the irradiation. However, the body weight of both groups of animals remained relatively constant until 3 week following the treatment (Figure 2.20A). As previously described, IR treatment induced significant damage to the bone marrow progenitor cells, leading to a drastic depletion of WBC, platelets and reticulocytes level in the peripheral blood analyzed 1 week after the treatment. The level of red blood cell count reduced more gradually, most likely owing to its longer half-life. At around week 4-5, most of the blood cell counts in both wild-type and *Fan1*^{-/-} mice returned back to one observed in the untreated controls (Figure 2.20B-E). These results indicated that the hematopoietic progenitor cells were not significantly more damaged in IR-treated *Fan1*-deficient animals. To

specifically assess the level of HSCs in the bone marrow, we analyzed the level of c-Kit⁺ and LSK cells two weeks following IR treatment and found no significant alternation in wild-type and *Fan1*-deficient animals (Figure 2.20F). These results suggest that FAN1 is dispensable for the repair of IR-inflicted damage and that its role in the protection of the hematopoietic system is specifically against DNA crosslinking agents.

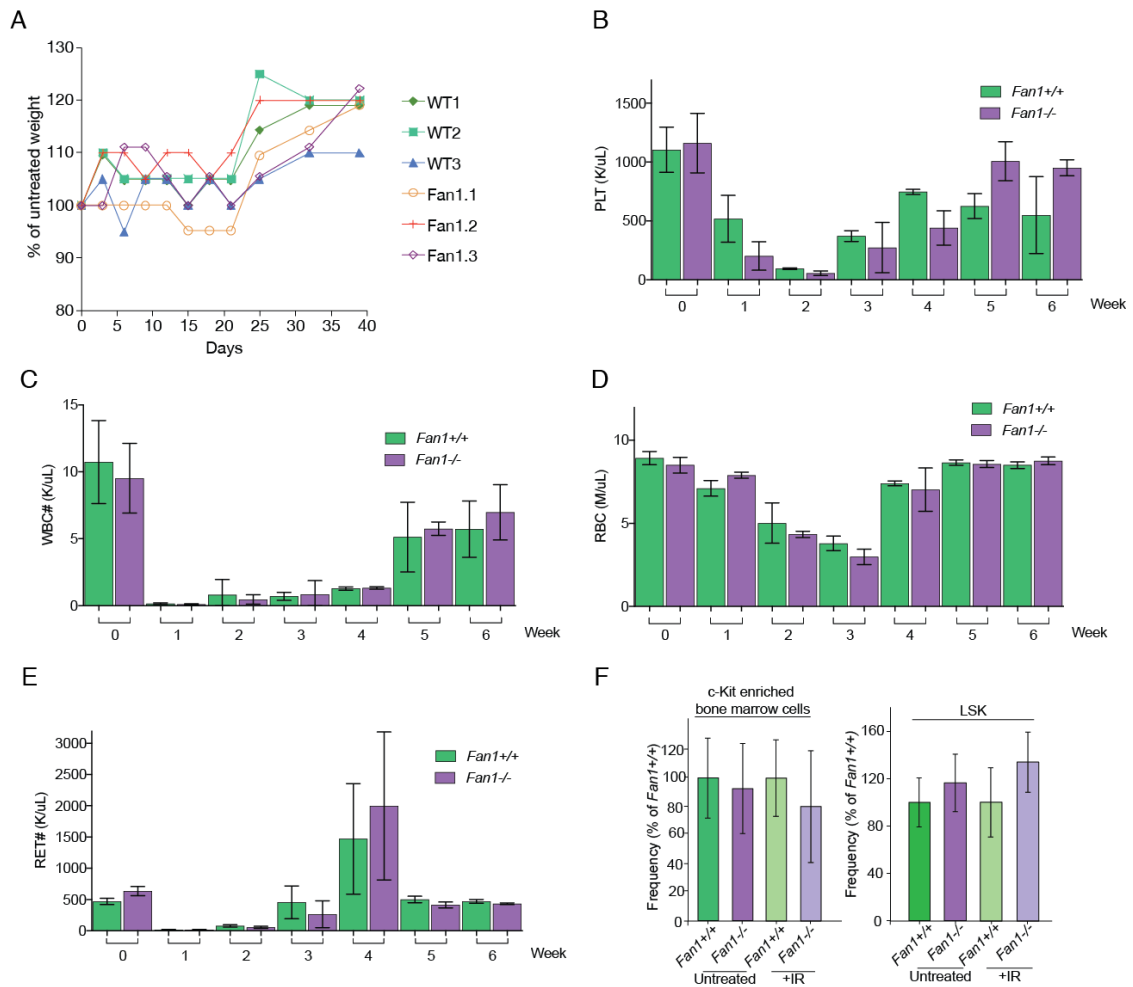


Figure 2.20 *Fan1* deficiency does not cause bone marrow sensitivity to IR.

(A) Weight monitoring of mice after treatment with IR. Following 450 cGy of x-ray treatment, *Fan1*^{+/+} and *Fan1*^{-/-} mice were weighed every 3 days for 6 weeks. Weight is expressed as % of original weight on the day of irradiation. (B-E) White blood cell (WBC) (B), platelet (PLT) (C), Red blood cell (RBC) (D), and Reticulocyte (RET) (E) counts of *Fan1*^{+/+} and *Fan1*^{-/-} mice untreated or IR-treated monitored weekly for 6 weeks following IR treatment. Bars represent mean \pm SD. (F) Percentage of live bone marrow cells that were enriched for c-Kit⁺ (left) or LSK (right) populations. The bone marrow cells were isolated from *Fan1*^{+/+} and *Fan1*^{-/-} mice untreated or treated 2 weeks prior with 450 cGy of x-ray. Bars represent mean \pm SD.

2.4 Summary of the findings

FAN1 expression could not be detected in fibroblasts of human KIN patient or the *Fan1* knockout mouse embryonic fibroblasts that were generated for the study. Using cells from both species, we showed that FAN1 deficiency results in cellular sensitivity to ICL-inducing agents. The level of ICL sensitivity in FAN1-negative cells is significantly lower than cells lacking Fanconi anemia proteins, suggesting that the ICL repair function of FAN1 and FANC proteins are not equivalent. Using the *Fan1*-deficient MEFs, we showed that the UBZ mutant FAN1 could rescue the proliferation defects and suppress chromosomal aberration induced by MMC. Therefore, FAN1 can participate in ICL repair independently of its interaction with the ID2 complex. This finding is also corroborated by the epistasis analysis, which revealed that FAN1 has FANCD2 independent function in the suppression of MMC-induced chromosomal abnormalities. When analyzed for the genetic interactions with other ICL repair nucleases, we found that FAN1 and MUS81 are epistatic, whereas FAN1 is redundant with SNM1A. The requirement of SNM1A in ICL resistance is only apparent when FAN1 is co-inactivated, suggesting that FAN1 can substitute for SNM1A in ICL repair. The SNM1A-redundant function of FAN1 does not depend on its UBZ domain.

At the whole organism level, *Fan1*-deficient mice recapitulate the KIN phenotypes including the presence of renal and liver karyomegaly and liver

dysfunction, both of which are age-dependent. We showed that the karyomegalic cells are polyploid, which likely results from genome endoreduplication. Nevertheless, the renal function was found to be intact even at 18 months of age, potentially due to the high buffering capacity of the kidney. *Fan1*-deficient mice are fertile, display no obvious developmental defects, and show normal bone marrow function. However, *Fan1*-deficient hematopoietic tissues including bone marrow and thymus are sensitive to MMC, with *Fan1*^{-/-} mice developing MMC-induced bone marrow failure due to hematopoietic stem and progenitor cell depletion. The dependency of FAN1 in the protection of bone marrow cells is specific to ICL challenge as ionizing radiation failed to inflict more severe phenotypes in *Fan1*^{-/-} than in wild-type animals.

Chapter 3: Elucidating the impact of aldehyde detoxification defects on *Fan1*-deficient mice

3.1 Introduction

The pathophysiology of KIN disease development is not understood. *Fan1*-deficient animals develop KIN characteristics despite being accommodated in a very controlled environment, with no exposure to exogenous nephrotoxins (see section 2.3.6) (Airik et al., 2016; Lachaud et al., 2016b; Thongthip et al., 2016). Based on this finding, we hypothesize that it is the endogenously produced toxin that is the culprit in KIN pathogenesis.

Recently, endogenous aldehydes have been shown to contribute to the pathology of Fanconi anemia, another disorder of ICL repair deficiency (Garaycoechea et al., 2012; Langevin et al., 2011; Oberbeck et al., 2014; Pontel et al., 2015). Increased load of acetaldehyde or formaldehyde resulting from *Aldh2* or *Adh5* deficiency dramatically exacerbates Fanconi anemia phenotypes in a mouse model of the disease. *Fancd2*^{-/-}*Adh5*^{-/-} mice develop glomerular diseases and karyomegaly in the kidney (Pontel et al., 2015).

The direct association between the genotoxic effect of formaldehyde on the kidney and liver tissues in humans has not been widely explored. The toxicity of formaldehyde and its breakdown product formate is typically attributed to their effect on the central nervous system and to their potential as carcinogenic agents (Humans, 2006; Songur et al., 2010). The most direct evidence that formaldehyde metabolism is critical for the protection of the kidney and liver

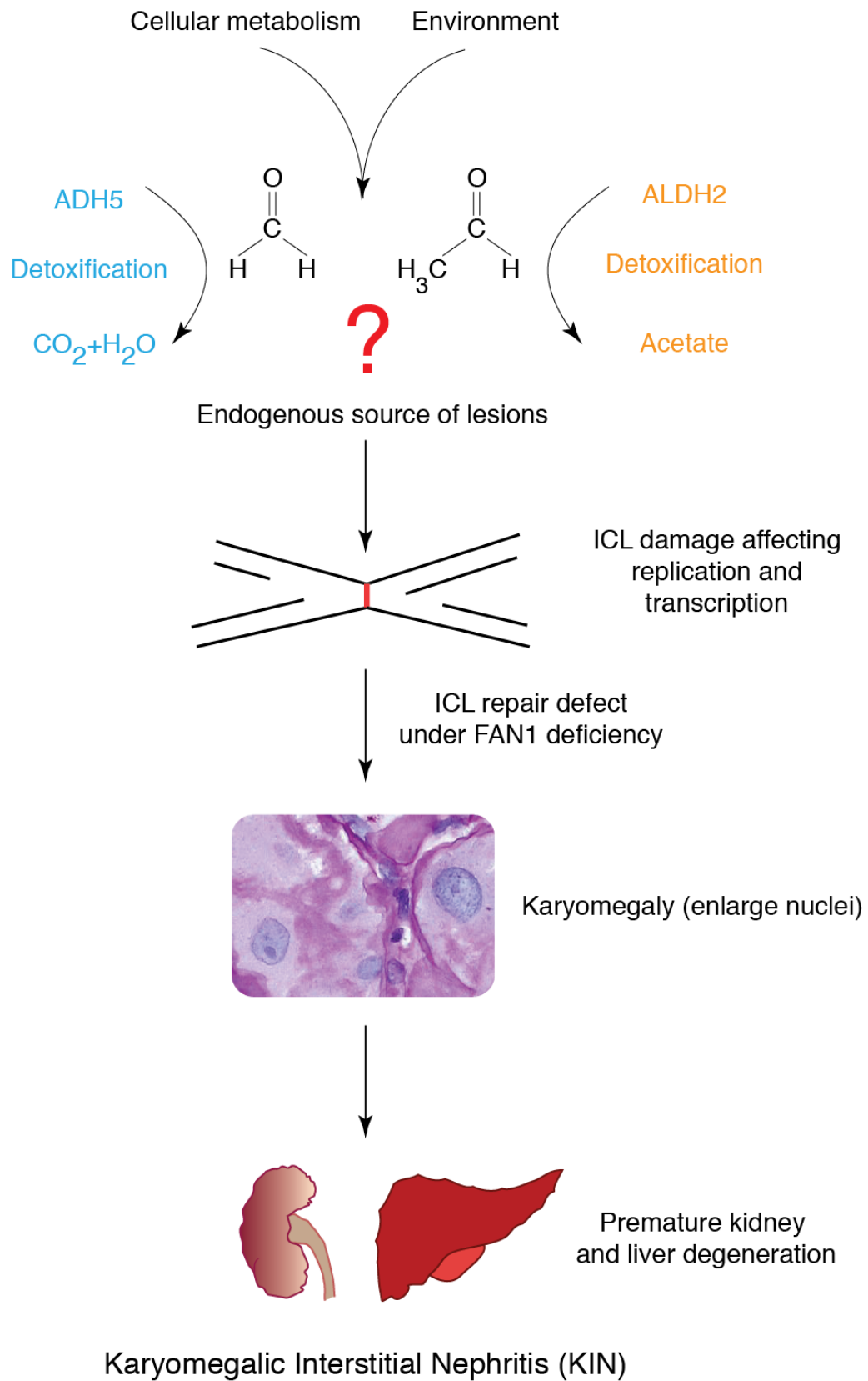
tissues came from the study of *Fancd2*^{-/-}*Adh5*^{-/-} mice (see section 1.6.2) (Pontel et al., 2015). The presence of renal and liver karyomegaly in the double mutant mice raises a possibility that formaldehyde is a potential *in vivo* damaging agent in the kidney and liver.

Another connection between aldehydes and human disease is that excessive acetaldehyde derived from chronic alcohol consumption causes liver damage (Chuang et al., 2009; Mills and Harrison, 2005; Seitz and Becker, 2007; Voigt, 2005). Alcohol consumption has also been shown to compromise the kidney function by promoting interstitial edema and renal hypertrophy in alcohol-fed animals (Epstein, 1997; Van Thiel et al., 1977). Additionally, alcohol-induced free radical production from the oxidation of acetaldehyde intermediates has been linked to deterioration of the Na⁺/K⁺-ATPase carrier in the proximal tubular epithelial cells (Laitinen et al., 1991; Parenti et al., 1991; Rodrigo et al., 1991; Rothman et al., 1992). This phenomenon is potentially linked to the observation that some chronic alcoholics have increased urinary levels of beta-2-microglobulin, N-Acetyl- β -D-glucosaminidase (NAG) and alanine aminopeptidase (AAP), markers of proximal tubular damage (Jung et al., 1987; Schardijn and Statius van Eps, 1987). Furthermore, prenatal ethanol exposure has detrimental effects on postnatal kidney function (De Marchi et al., 1993). Whether any of these effects on the renal function are derived from ICL damage caused by ethanol or its acetaldehyde intermediate, remains to be determined.

Considering the above evidence of potential links between aldehyde-inflicted ICL damage and blood, kidney, and liver dysfunction, we set out to test if increased levels of acetaldehydes or formaldehydes would exacerbate the KIN phenotypes of *Fan1*^{-/-} mice. We generated *Fan1*^{-/-}*Aldh2*^{-/-} and *Fan1*^{-/-}*Adh5*^{-/-} double mutant mouse models. We hypothesized that by inactivating *Aldh2* or *Adh5*, the increased basal level of ICLs may lead to an acceleration or exacerbation of KIN phenotypes, particularly in *Fan1*-deficient mice (Figure 3.1). If acetaldehyde and formaldehyde play a role in KIN pathology, *Fan1*^{-/-}*Aldh2*^{-/-} or *Fan1*^{-/-}*Adh5*^{-/-} double-deficient mice would display worsening of the phenotypes present in *Fan1*-deficient mice.

Figure 3.1 Putative sources of damage that induce KIN in the absence of FAN1.

The sources of presumed endogenous damage leading to Karyomegalic Interstitial Nephritis (KIN) is unknown. Formaldehyde and acetaldehyde are two ICL-inducing agents that have been shown to play a role in the pathogenesis of Fanconi anemia, which is a disorder of unrepaired ICL-damage. It is possible that these agents would also be deleterious in the setting of FAN1 deficiency.



Results

3.2 Generation of *Fan1*^{-/-}*Aldh2*^{-/-} and *Fan1*^{-/-}*Adh5*^{-/-} mice

To test the hypothesis that lack of detoxification of acetaldehyde or formaldehyde would exacerbate the phenotypes of *Fan1*-deficient mice, the *Fan1*^{-/-} were crossed with *Aldh2*^{-/-} or *Adh5*^{-/-} to generate *Fan1*^{+/-}*Aldh2*^{+/-} and *Fan1*^{+/-}*Adh5*^{+/-} double heterozygotes (Figure 3.2A). The double heterozygotes were crossed to derive *Fan1*^{-/-}*Aldh2*^{-/-} or *Fan1*^{-/-}*Adh5*^{-/-} double homozygous mutants (Figure 3.2A). The male and female *Fan1*^{-/-}*Aldh2*^{-/-} or *Fan1*^{-/-}*Adh5*^{-/-} double homozygotes were then used to establish the cohorts of double homozygotes for subsequent study. In order to enrich animals for the experiments, we generated WT, or single mutant animals: *Fan1*^{-/-}, *Aldh2*^{-/-}, and *Adh5*^{-/-} through the crosses from the homozygous parental breeding pairs (Figure 3.2B).

The crosses between *Fan1*^{-/-}*Aldh2*^{-/-} yielded pups at similar ratios to wild-type and *Fan1* single mutant breeding pairs, suggesting that deficiency in *Aldh2* did not affect the fertility of the male and female *Fan1*-deficient animals, nor did it impair embryogenesis or fetal viability (Figure 3.3). Interestingly, loss of ADH5 alone caused a reduction in the number of pups produced in comparison to wild-type animals (Figure 3.3). This was in contrast to the published data, which revealed no differences in terms of the litter size at weaning (Liu et al., 2004). The reason for this difference is unclear. Inactivation of *Fan1* in *Adh5*^{-/-} animals

resulted in further decrease in the litter size compared to *Adh5*^{-/-} single mutant (Figure 3.3). Deficiency in *Aldh2* did not compromise the growth of mice lacking *Fan1* as *Fan1*^{-/-}*Aldh2*^{-/-} DKO displayed normal growth with the 12-weeks weight comparable to wild-type and *Fan1*^{-/-} animals. *Fan1*^{-/-}*Adh5*^{-/-} on the other hand, exhibited moderate growth defect when compared with *Fan1*^{-/-} or *Adh5*^{-/-} single mutants (Figure 3.4A, B).

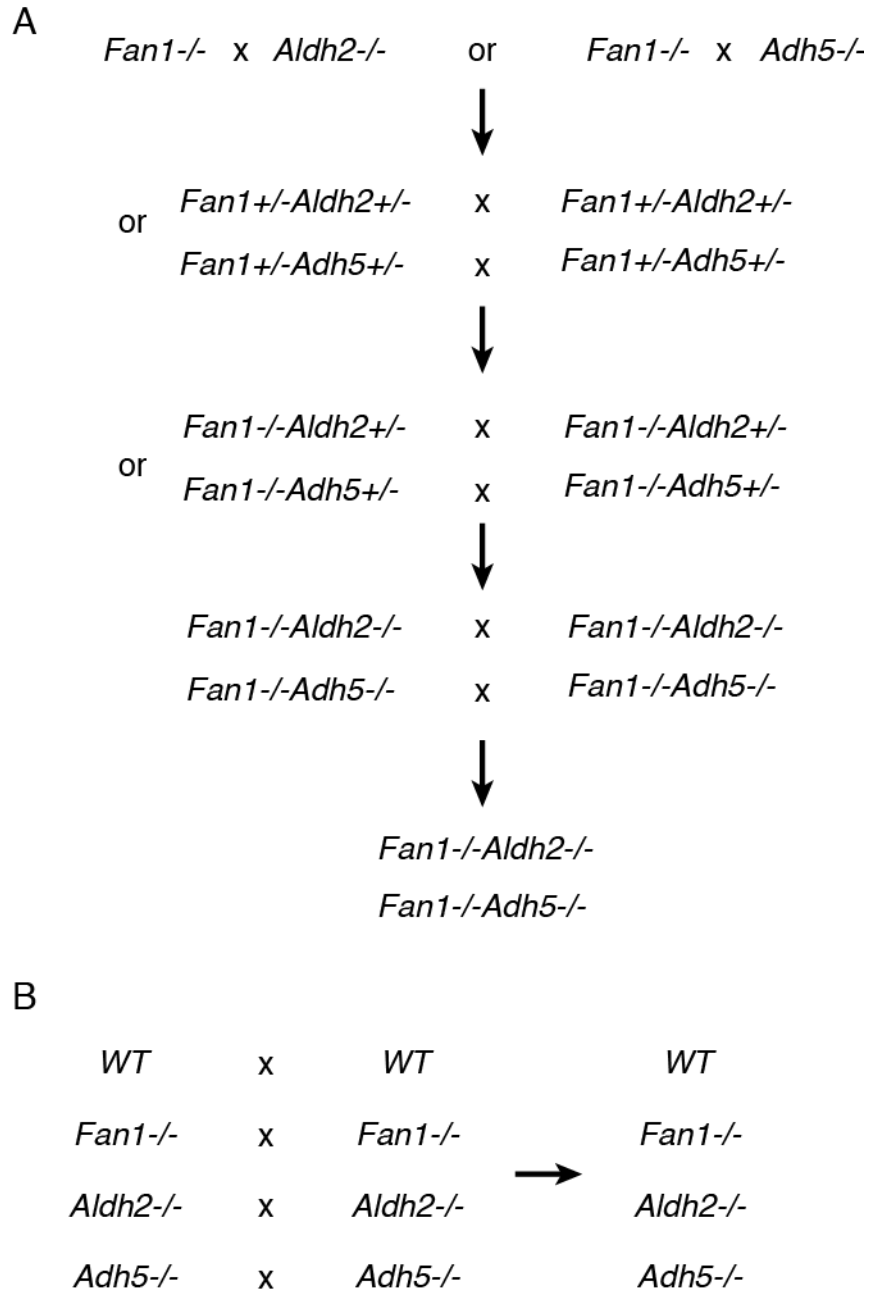


Figure 3.2 Schematic of mouse interbreeding to generate mice for the study of the genetic interaction between *Fan1* and *Aldh2* or *Adh5*.

(A) The generation of double knockout *Fan1*^{-/-}*Aldh2*^{-/-} or *Fan1*^{-/-}*Adh5*^{-/-} mice for the study. (B) The generation of wild-type (WT) and single knockout *Fan1*^{-/-}, *Aldh2*^{-/-}, or *Adh5*^{-/-} mice for the study.

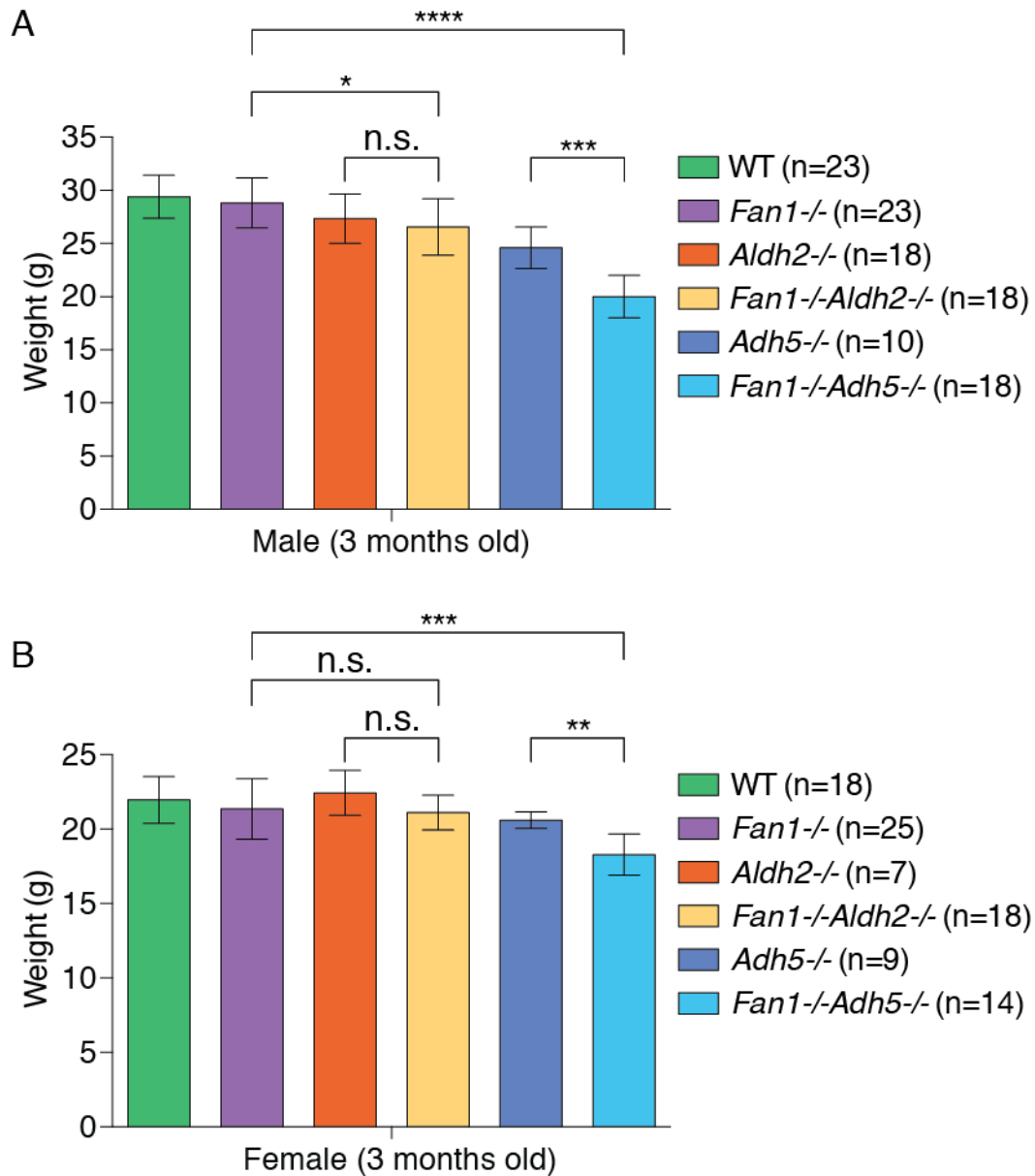


Figure 3.4 Deficiency of *Adh5* but not *Aldh2* results in growth defect in *Fan1*-mutant mice.

(A-B) Weight of male (A) and female (B) WT, *Fan1*^{-/-}, *Aldh2*^{-/-}, *Fan1*^{-/-}*Aldh2*^{-/-}, *Adh5*^{-/-} and *Fan1*^{-/-}*Adh5*^{-/-} mice from 12 weeks of age. Error bars, s.d., *p < 0.05, **p < 0.01, ***p < 0.001, ****p < 0.0001, and n.s., not significant, were calculated by Mann-Whitney U test.

3.3 Analysis of the hematopoietic system in mice lacking *Fan1* and *Aldh2* or *Adh5*

Aldh2 or *Adh5* deficiency did not lead to a significant change in the level of peripheral blood cells irrespective of *Fan1* status and age (Figure 3.5A-H). We next assessed the state of the hematopoietic system in mice with deficiency in FAN1 and aldehyde detoxification enzymes by analyzing the level of LSK (Lin-Sca1+ cKit+) population in of *Fan1*^{-/-}*Aldh2*^{-/-} and *Fan1*^{-/-}*Adh5*^{-/-} mice and the appropriate corresponding controls. We found that *Adh5* but not *Aldh2* deficiency led to a significant reduction of the LSK population of 3 months old mice under *Fan1*-deficient background (Figure 3.6A). The 12 months old *Fan1*^{-/-}*Aldh2*^{-/-} and *Fan1*^{-/-}*Adh5*^{-/-} mice, however, displayed wild-type level of LSK population (Figure 3.6B).

In order to assess the functionality of HSCs, we adopted the competitive repopulation assay to quantify the engraftment potential of the HSCs from WT, *Fan1*^{-/-}, *Aldh2*^{-/-}, *Fan1*^{-/-}*Aldh2*^{-/-}, *Adh5*^{-/-}, *Fan1*^{-/-}*Adh5*^{-/-} animals. The transplant was performed from the donor with CD45.2 isotype into the congenic recipients with CD45.1 isotype pre-conditioned with lethal dosage of 850 cGy of x-ray. By quantifying the frequency of CD45.2/CD45.1 ratio of the leukocytes in the recipient animals, we were able to derive the engraftment efficiency of HSCs under various combined genetic backgrounds at 1, 2 and 4 months post-transplant as previously described (Katayama et al., 1999; Morrison et al., 1996).

The primary transplant revealed that the engraftment potential was not compromised in *Fan1*-deficient mice (Figure 3.7A-C). Furthermore, inactivating *Aldh2* or *Adh5* did not affect the engraftment of long term HSCs (LT-HSCs) after a single transplantation cycle (Figure 3.7A-C). We further challenged the HSCs by performing the second round of bone marrow transplant using the total bone marrow isolated from the primary recipients two months post-transplant and transferred into the secondary recipients that were also pre-conditioned with x-ray. Notably, mice lacking FAN1 displayed poorer engraftment compared to WT control after the secondary transplant experiment (Figure 3.8). This observation supports the conclusion that FAN1 is required for the protection of HSCs under stressed condition (Section 2.3.7). *Aldh2* deficiency also led to a significant reduction in the engraftment potential of HSCs in the secondary transplant (Figure 3.8) but *Aldh2* deficiency did not exacerbate the defect in engraftment in *Fan1*-deficient animals.

We next assessed whether deficiency in either of the aldehyde detoxification enzyme would lead to an increase in the DNA damage level manifested as micronuclei in the peripheral RBC or RET. The level of micronucleated RBC (MN-RBC) and micronucleated RET (MN-RET) based on positive propidium iodine (PI) staining did not increase in *Fan1*^{-/-}*Aldh2*^{-/-} or *Fan1*^{-/-}*Adh5*^{-/-} animals in comparison to the wild-type or single mutant controls. This leads us to conclude that FAN1 is dispensable for the protection of the

erythropoietic compartment from micronuclei formation under wild-type or acetaldehyde/formaldehyde-detoxification deficient conditions (Figure 3.9A-C).

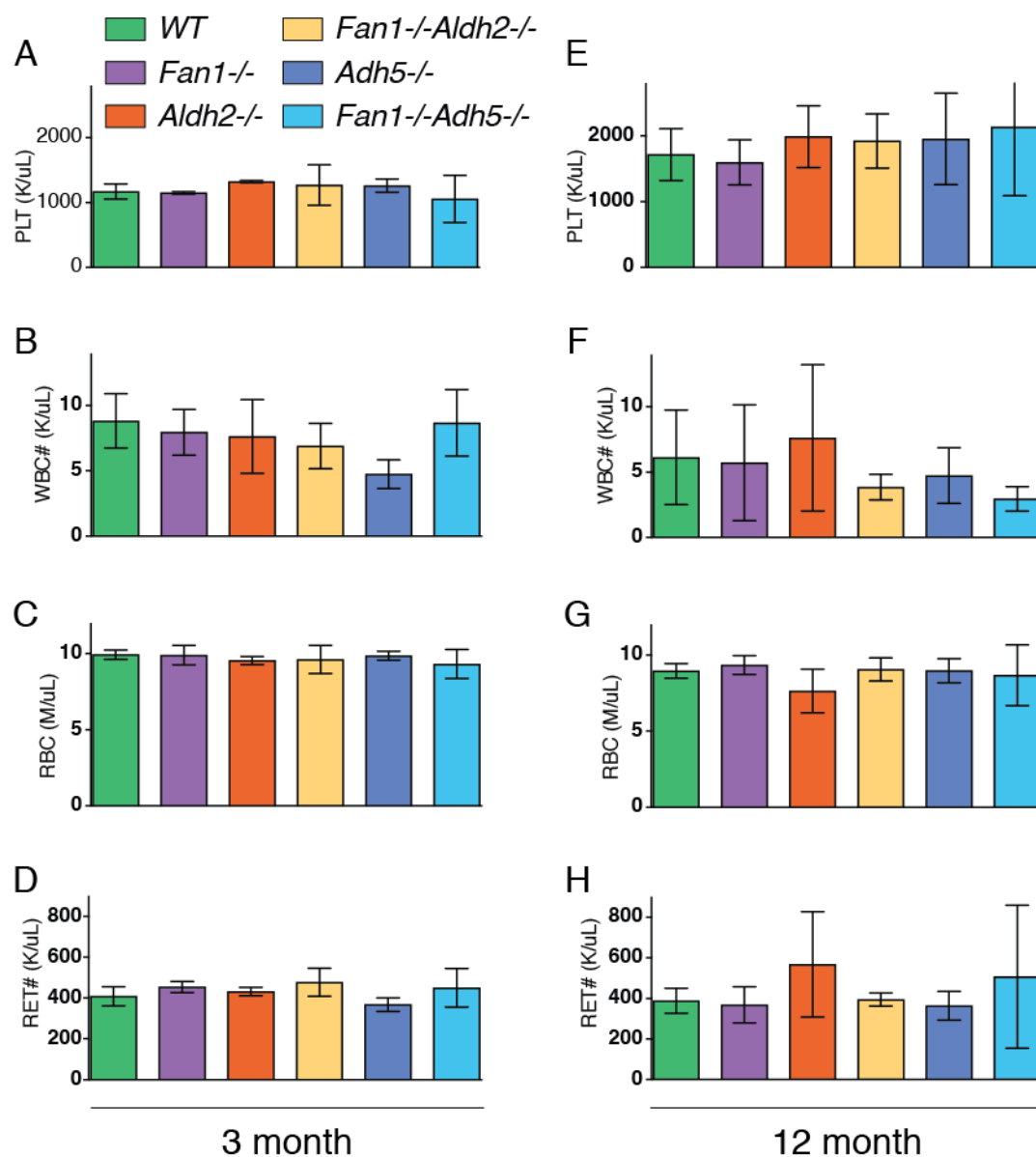
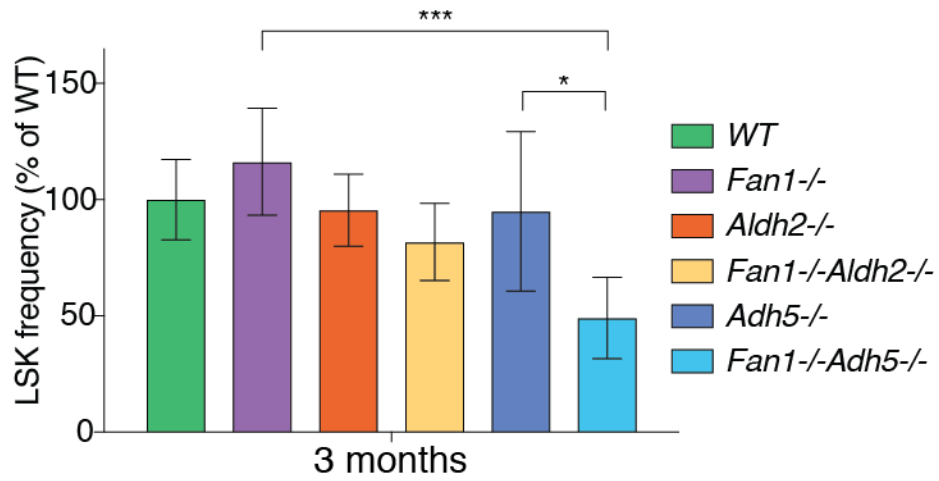


Figure 3.5 Deficiency of *Fan1* in combination with *Aldh2* or *Adh5* does not cause abnormality in the level of peripheral blood cells.

(A-H) Blood analysis mice of indicated genotypes at 3 months (A-D) or 12 months (E-H) of age: (A/E) platelets (PLT), (B/F) white blood cells (WBC), (C/G) red blood cells (RBC), (D/H) reticulocytes (RET). Error bars, s.d., n=3.

A



B

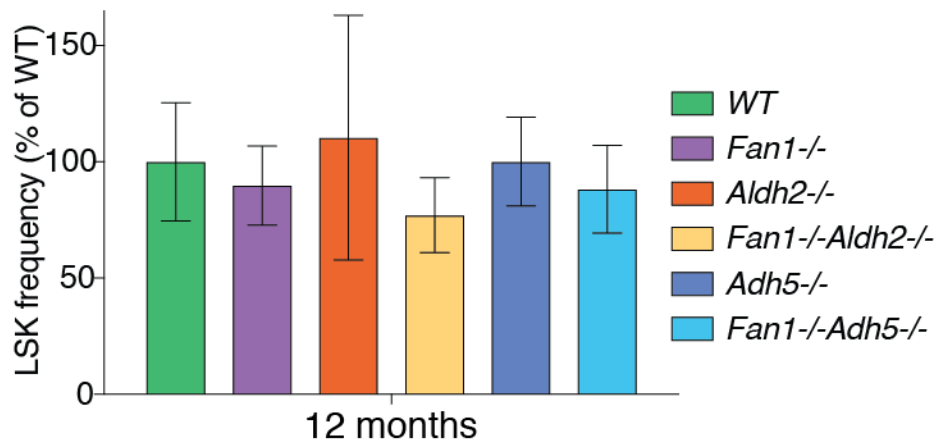


Figure 3.6 Deficiency of *Adh5* but not *Aldh2* compromises HSC maintenance in 3 months old *Fan1*-mutant mice.

(A-B) Quantification of HSCs isolated from 3 months (A) or 12 months (B) WT, *Fan1*^{-/-}, *Aldh2*^{-/-}, *Fan1*^{-/-}*Aldh2*^{-/-}, *Adh5*^{-/-} and *Fan1*^{-/-}*Adh5*^{-/-} mice assessed by FACS. Error bars, s.d., n=6 for (A) and n=3 for (B) per genotype. *p < 0.05 and ***p < 0.001 were calculated by one-way ANOVA.

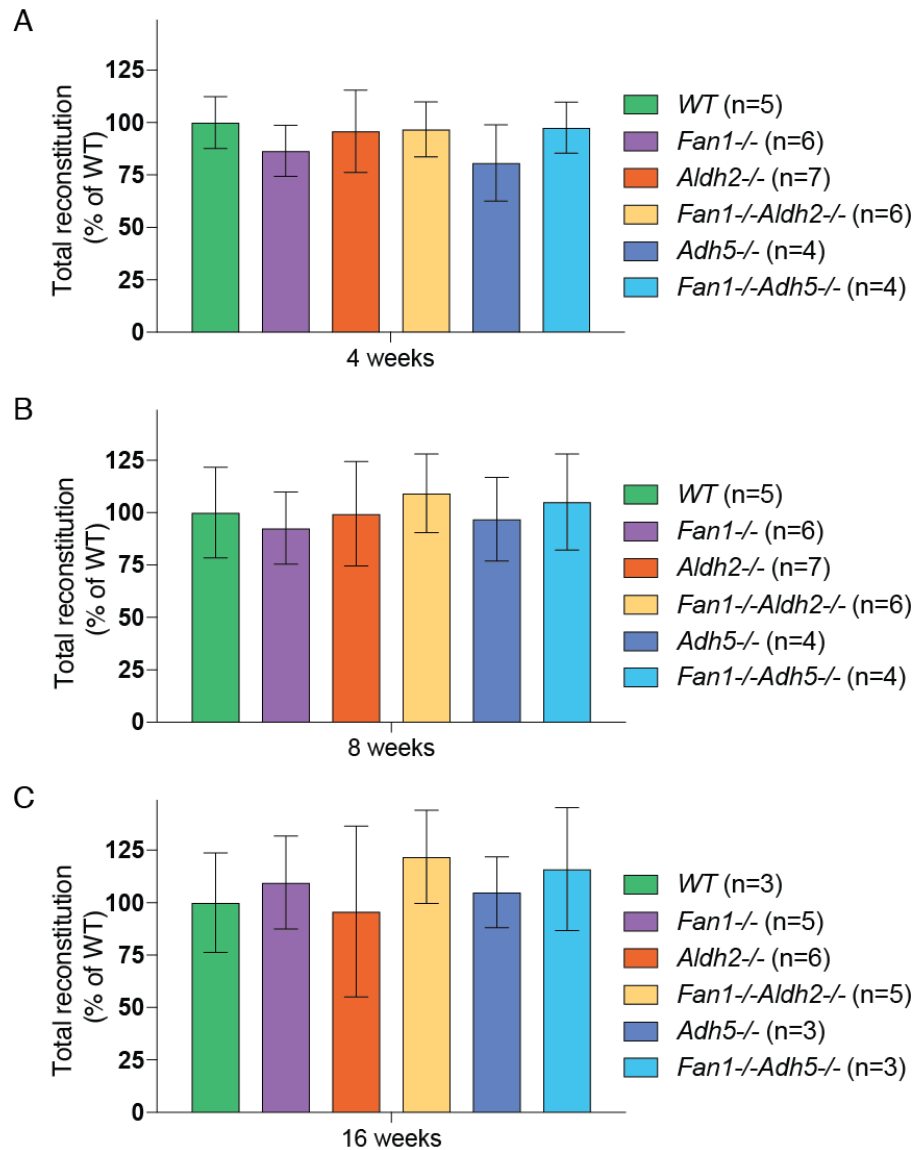


Figure 3.7 Loss of ALDH2 or ADH5 does not affect the engraftment potential of *Fan1*-deficient mice following primary transplant.

(A-C) Quantification of HSC function based on percent engraftment of CD45.2 donor bone marrow cells over the CD45.1 competitor bone marrow cells following the primary transplant calculated by the percent of CD45.2 donor leukocytes (CD45.2/D45.2+CD45.1 or Total reconstitution) of donor mice of different genotypes relative to the percent of CD45.2 donor leukocytes of WT analyzed at 4-weeks (A), 8-weeks (B), or 12-weeks (C) after the transplant. The number of sample (n) is shown in the figure.

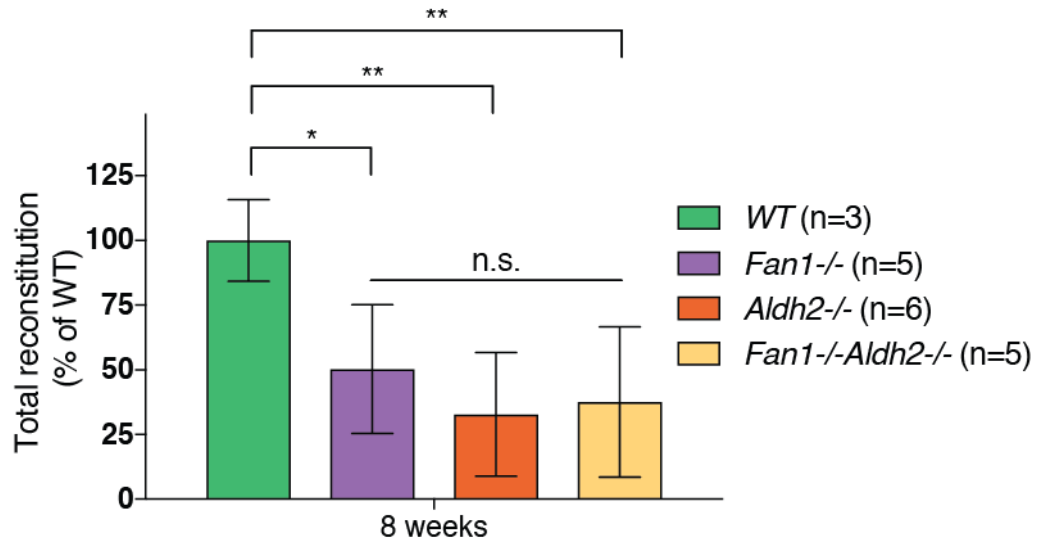


Figure 3.8 Loss of FAN1 or ALDH2 results in reduced engraftment potential of *Fan1*-deficient mice following the secondary transplant.

Quantification of HSC function based on percent engraftment of CD45.2 donor bone marrow cells over the CD45.1 competitor bone marrow cells following the secondary transplant. Percentage of CD45.2 donor leukocytes (CD45.2/CD45.2+CD45.1) of donor mice of different genotypes relative to the percent of CD45.2 donor leukocytes of WT at 8-weeks after the transplant is shown. The number of sample (n) was as described in the figure. *p < 0.05 and **p < 0.01 were calculated by one-way ANOVA.

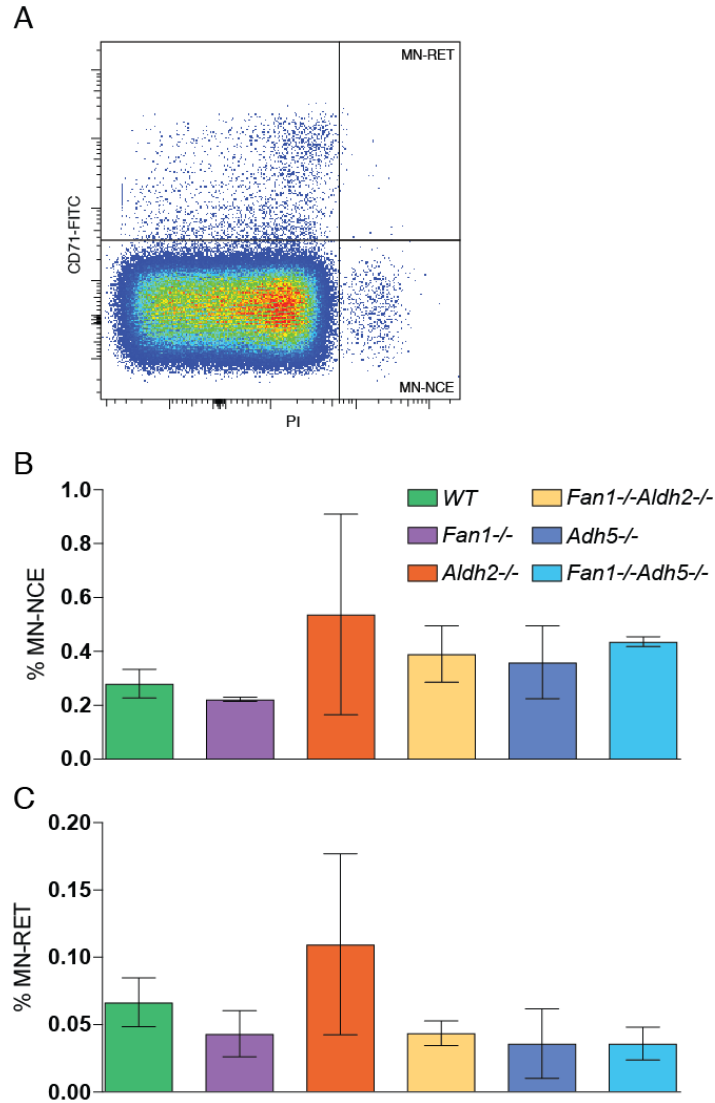


Figure 3.9 Deficiency of *Fan1* and *Aldh2* or *Adh5* causes insignificant increase in DNA damage in blood cells as assessed by micronuclei in normochromatic erythrocytes and reticulocytes.

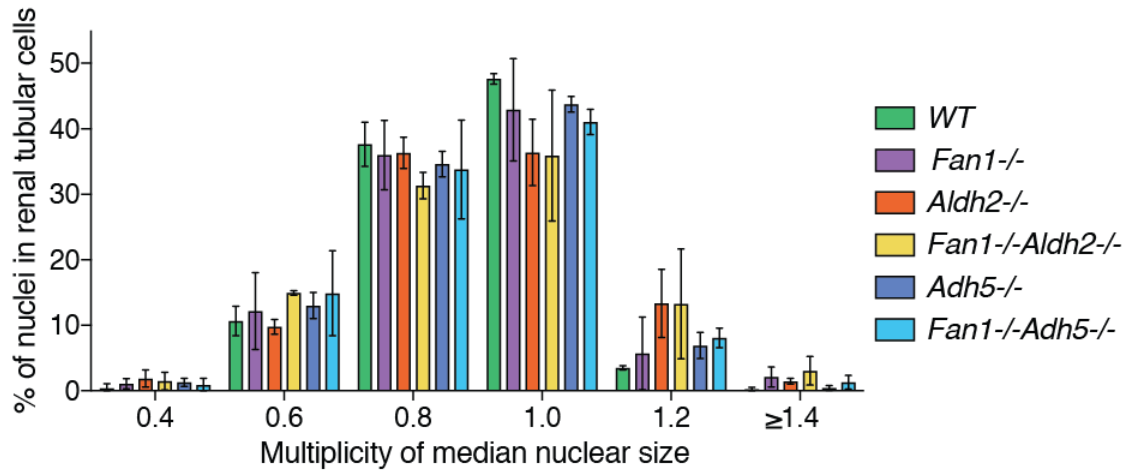
(A) Representative FACS profiles of micronucleated (PI⁺) or non-micronucleated (PI⁻) normochromatic erythrocytes (MN-NCE) (CD71⁻) or Reticulocytes (RET) (CD71⁺) cells isolated from blood. (B-C) Percent of MN-NCE (B) or MN-RET (C) analyzed in blood collected from mice of indicated genotypes.

3.4 Analysis of the liver and kidney function of mice lacking *Fan1* and *Aldh2* or *Adh5*

In order to assess the impact of concomitant loss of FAN1 and aldehyde detoxifying enzymes on the pathogenesis of KIN in mice, we monitored the level of karyomegaly and function of the kidney and liver in aging cohorts at 3 months and 12 months of age. As expected from our earlier study, karyomegaly is absent from kidney or liver tissue at 3 months of age (Figure 3.10A,B). Additional inactivation of either *Aldh2* or *Adh5* in *Fan1*-deficient cohorts did not result in significant increase in the proportion of karyomegalic nuclei in either tissues (Figure 3.10A,B). Karyomegaly was apparent in 12 months-old *Fan1*^{-/-} animals, but we did not observe an additional increase in the level of enlarged nuclei when *Aldh2* or *Adh5* was inactivated in *Fan1*^{-/-} mice (Figure 3.11). Furthermore, the kidney from *Fan1*^{-/-}*Aldh2*^{-/-} and *Fan1*^{-/-}*Adh5*^{-/-} mice did not show signs of increased level of DNA damage as determined by γ H2AX staining or increased level of proliferating cells as marked by Ki67 (Figure 3.12A, B). However, we did not observe a significant difference in the level of γ H2AX positive staining of renal tubular epithelium between wild-type and *Fan1*^{-/-} animals as reported in (Lachaud et al., 2016b) (Figure 3.12B). It is unclear why this discrepancy exists. It is possible that presence of the nuclease-inactive FAN1 in the other mouse model leads to different cellular effects than complete lack of FAN1.

In parallel to the histological study, we monitored the function of kidney and liver of *Fan1* mice lacking ALDH2 or ADH5 by analyzing the serum level of their corresponding enzyme and metabolite markers. Again, we failed to notice any significant changes in the serum level of liver enzymes or liver-produced proteins as well as the serum markers of the kidney function such as BUN, creatinine, Mg and Phosphorus (Pi) in *Fan1*^{-/-}*Aldh2*^{-/-} or *Fan1*^{-/-}*Adh5*^{-/-} mice (Figure 3.13A-H).

A



B

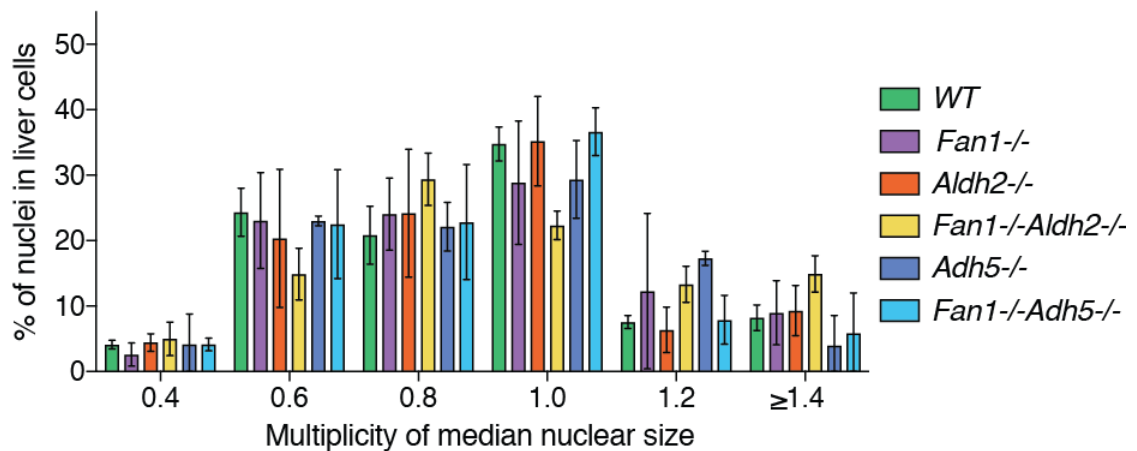


Figure 3.10 Kidney and liver karyomegaly are absent from mice lacking *Fan1* and *Aldh2* or *Adh5*.

(A-B) Quantification of the nuclear area (cross-sectional area) of tubular epithelial cells (A) or liver hepatocyte (B) in the cortex of kidney from mice of indicated genotypes at 3 months. The area of each nucleus was normalized to the median nuclear area. Data were then plotted and grouped according to area (n=3, Error bars, s.d.).

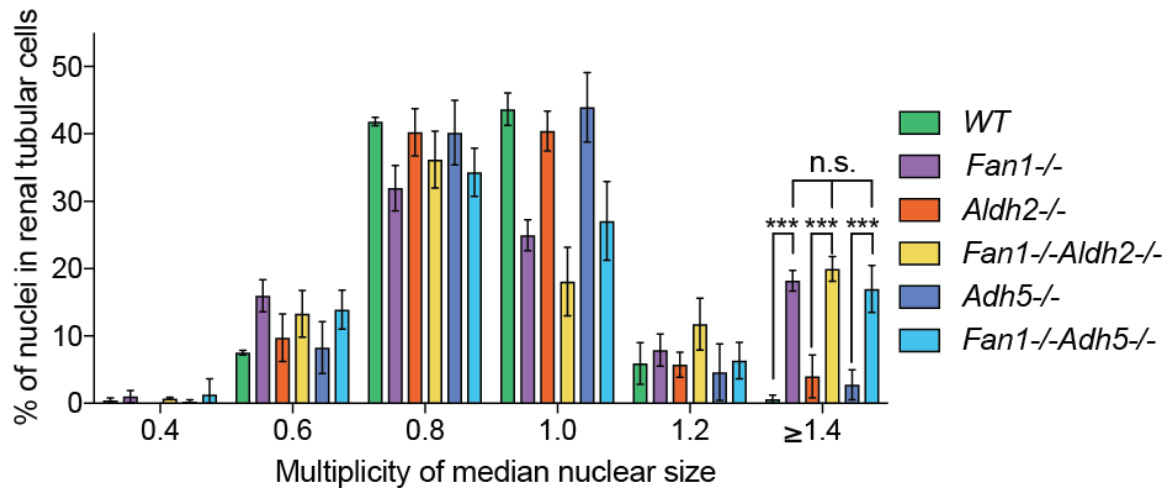


Figure 3.11 Karyomegaly in *Fan1*^{-/-} animals is not enhanced by deficiency of *Aldh2* or *Adh5*.

Quantification of the nuclear area (cross-sectional area) of tubular epithelial cells in mice of indicated genotypes at 12 months. The area of each nucleus was normalized to the median nuclear area of each section. Data were then plotted and grouped according to area (n=3, Error bars, s.d.).

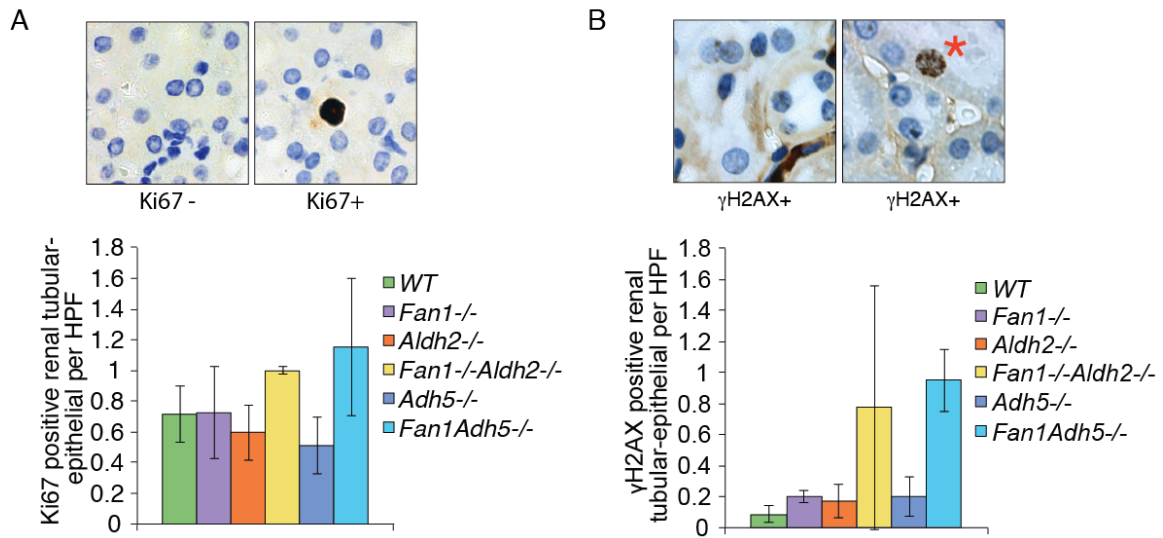
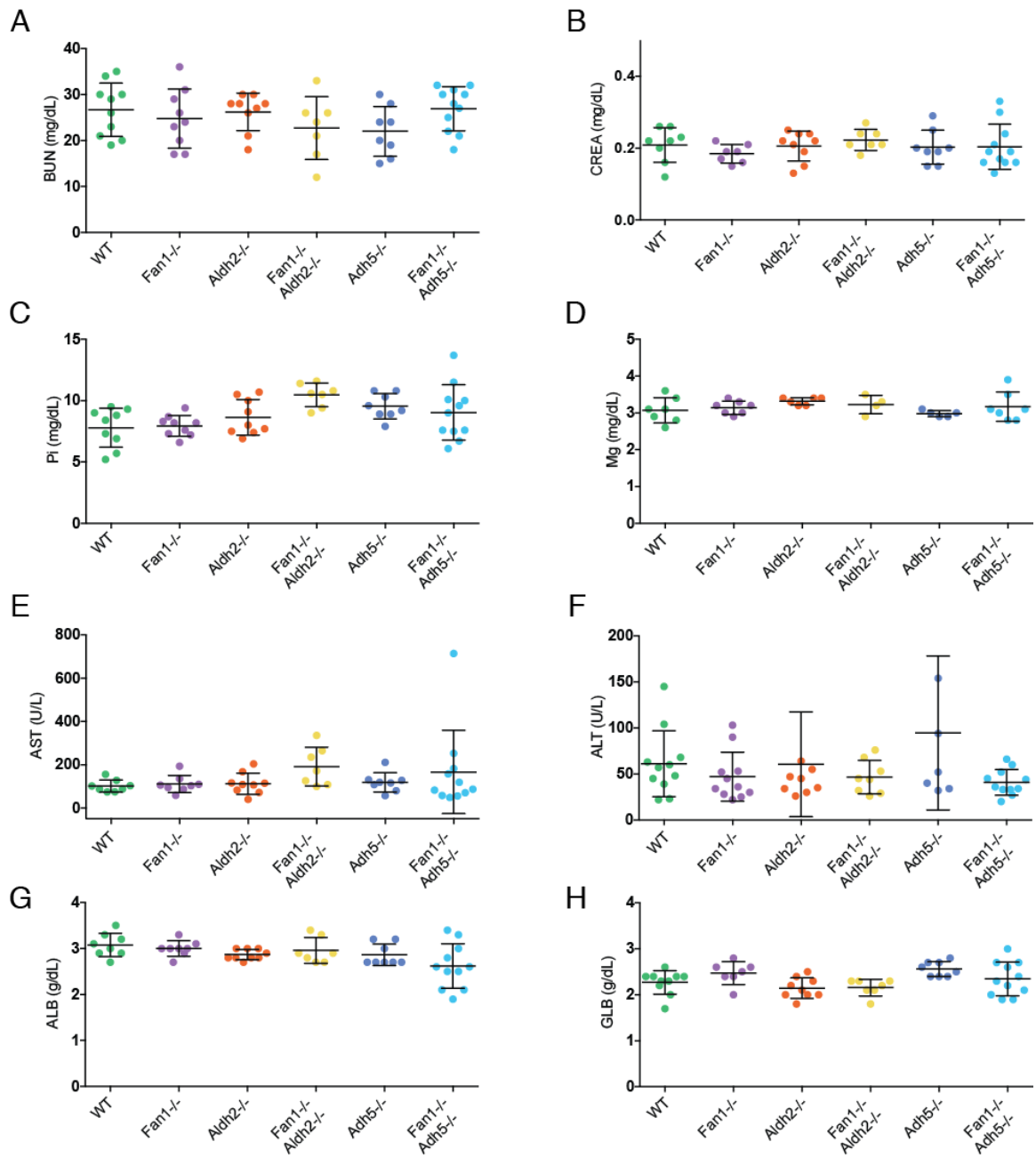


Figure 3.12 Deficiency of *Fan1* alone or in combination with *Aldh2* or *Adh5* did not cause an increase in the level of proliferating cells or cells with DNA damage.

(A-B) Representative images of Ki67- or Ki67+ (A, top) or γH2AX- or γH2AX+ (B, top) renal tubular epithelial cells and the quantification of Ki67+ (A, bottom) or γH2AX+ (B, bottom) renal tubular epithelial cells in mice of indicated genotypes at 12 months. The quantification was performed in a blinded manner from 35-45 high power field (HPF) (40x) images. Error bars, s.d., n=3 per genotype.

Figure 3.13 Deficiency of *Aldh2* or *Adh5* did not cause liver and kidney dysfunction in young *Fan1*-deficient mice.

(A-D) Analysis of serum level of (A) blood urea nitrogen (BUN), (B) creatinine, (C) phosphorus, and (D) magnesium to monitor kidney function in mice of indicated genotypes at 3-6 months. (F-I) Analysis of serum level of liver enzymes and markers of liver function: (F) alanine transaminase (ALT), (G) aspartate transaminase (AST), (H) albumin (ALB), and (I) globulin (GLOB) in mice of indicated genotypes at 3-6 months. Bars represent mean \pm SD.



3.5 Impact of alcohol treatment on mice lacking *Fan1* and *Aldh2* or *Adh5*

One of the possible explanations for the lack of significant exacerbation of KIN phenotypes in *Fan1*-deficient mice lacking ALDH2 or ADH5 is that the increase in the basal level of acetaldehyde or formaldehyde was below the threshold required to elicit sufficient damage that would necessitate the repair activity of FAN1. To further enhance the level of aldehyde-inflicted damage, we performed alcohol feeding experiments in the *Aldh2* or *Adh5*-deficient animals. Metabolism of ethanol leads to the formation of acetaldehyde intermediate whereas the metabolism of methanol leads to the generation of formaldehyde. Therefore, the administration of ethanol or methanol in mice lacking the corresponding aldehyde detoxifying enzyme should elicit a greater level of damage. This is the case with the Fanconi anemia mouse models, as ethanol or methanol ad libitum feeding leads to stronger hematopoietic defect in *Aldh2*^{-/-} or *Adh5*^{-/-} mice lacking FANCD2 respectively (Langevin et al., 2011; Pontel et al., 2015). If either of the two aldehydes contribute to the pathogenesis of KIN, this strategy could expose the phenotypes previously hidden in the untreated *Fan1*^{-/-} *Aldh2*^{-/-} or *Fan1*^{-/-}*Adh5*^{-/-} double mutant mice.

3.5.1 Short-term ethanol exposure of *Fan1/Aldh2* mice

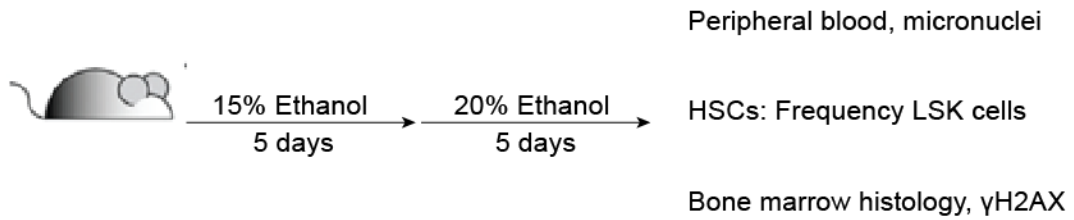
To test the effect of ethanol-induced acetaldehyde in the expression of KIN phenotypes, we employed two separate ethanol treatment schemes. In the first regimen, ethanol was added to the drinking water at a final concentration of

15% for 5 days before being changed to 20% for another 5 days. The second treatment scheme involved supplying 10% of ethanol in the drinking water for one month. With the high dose treatment of ethanol, the animals lacking ALDH2 regardless of *Fan1* status exhibited severe sensitivity with their weight being drastically reduced to around 80% of the original weight by day 10 of the treatment (Figure 3.14A, B).

High-dose ethanol treatment regimen resulted in a significant deficiency in hematopoiesis following ethanol feeding in *Aldh2*-deficient animals. There was a reduction in the level of WBC and RET (reticulocytes) in the treated *Aldh2*^{-/-} and *Fan1*^{-/-}*Aldh2*^{-/-} mice, suggesting that hematopoietic progenitors are negatively affected by ethanol-induced acetaldehyde (Figure 3.15A, B). *Fan1*^{-/-}*Aldh2*^{-/-} displayed a greater reduction in the WBC and RET levels than the *Aldh2*^{-/-} mice alone. However, only the difference in the reticulocyte count between *Aldh2*^{-/-} single mutant and *Fan1*^{-/-}*Aldh2*^{-/-} double mutants were statistically significant (Figure 3.15B). The level of RBC was unchanged most likely due to their longer half-life compared to other types of blood cells (Figure 3.15C). The level of platelets went up significantly in *Aldh2*^{-/-} and *Fan1*^{-/-}*Aldh2*^{-/-} (Figure 3.15D). The cause of thrombocytosis (high platelet count) was unclear, albeit this trend was in contrast to the commonly known effect of ethanol in promoting thrombocytopenia symptom in human with alcoholism (Ballard, 1997; Girard et al., 1987).

Ethanol treatment led to a significant depletion of the LSK population in *Aldh2*^{-/-} and *Fan1*^{-/-}*Aldh2*^{-/-} animals (Figure 3.15E). However, the difference in the LSK frequencies between *Aldh2*^{-/-} and *Fan1*^{-/-}*Aldh2*^{-/-} was not statistically significant. We conclude that the absence of *Aldh2* was driving hematopoietic defect following high dose of ethanol treatment. Furthermore, we were able to detect a significant increase in the level of micronucleated normochromatic erythrocytes (MN-NCE) in *Aldh2*^{-/-} and *Fan1*^{-/-}*Aldh2*^{-/-} animals compared to wild-type or *Fan1*^{-/-} mutant mice (Figure 3.15F). Yet again, the difference between the micronuclei level of *Aldh2*^{-/-} and *Fan1*^{-/-}*Aldh2*^{-/-} was not statistically significant, indicating that the observed DNA damage phenotype was caused by deficiency in *Aldh2* not *Fan1*. With these results, we can conclude that the ethanol-induced damage on the hematopoietic system in the *Fan1*/*Aldh2* cohorts was primarily driven by the absence of *Aldh2* not *Fan1*.

A



B

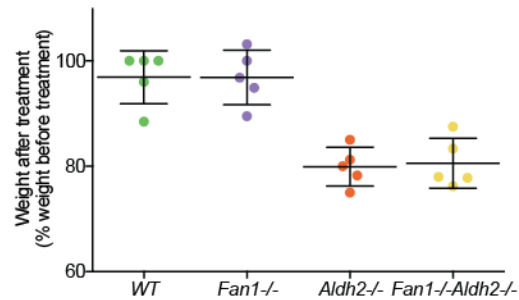
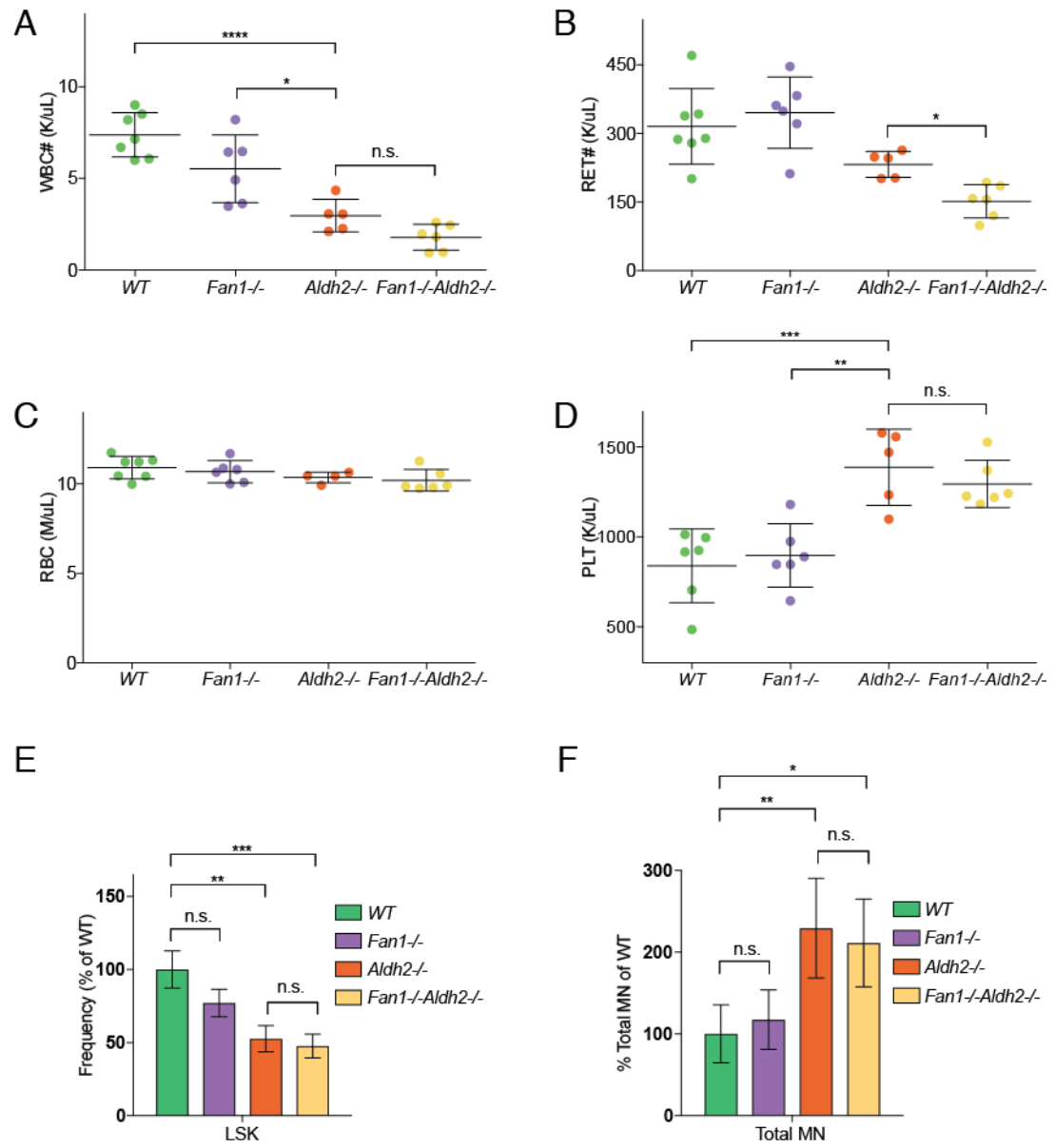


Figure 3.14 *Aldh2*-deficient mice displayed ethanol sensitivity.

(A) Schematic of ethanol treatment regimen. Mice were treated with 15% ethanol for 5 days and 20% for another 5 days before being sacrificed for analysis. (B) Weight of mice measured after the ethanol treatment scheme in (A). Weight is expressed as % of original weight before the treatment. Bars represent mean \pm SD.

Figure 3.15 Short-term ethanol treatment affects the hematopoietic system in *Aldh2*-deficient mice. *Fan1*^{-/-}*Aldh2*^{-/-} animals have slight decrease in the reticulocyte counts compared to *Aldh2*^{-/-} animals.

(A-D) White blood cell (WBC) (A), Reticulocyte (RET) (B), Red blood cell (RBC) (C), and platelet (PLT) (D) counts from mice of indicated genotypes after the ethanol treatment (Figure 3.12A). Bars represent mean \pm SD; * $p < 0.05$, ** $p < 0.01$, *** $p < 0.001$, **** $p < 0.0001$, n.s., not significant were calculated by one-way ANOVA. (E) Quantification of HSCs isolated from 3-month-old mice of indicated genotypes treated with ethanol as in (A-D) assessed by FACS. Error bars, s.d., $n=3$. ** $p < 0.01$, *** $p < 0.001$, n.s., not significant, were calculated by one-way ANOVA. (F) Percent of total MN (MN-NCE + MN-RET) analyzed in blood collected from mice of indicated genotypes treated with ethanol as in (A-D). Error bars, s.d., $n=3$. * $p < 0.05$, ** $p < 0.01$, n.s., not significant, were calculated by one-way ANOVA.



3.5.2 Long-term ethanol exposure for *Fan1/Aldh2* mice

To assess the effect of increased acetaldehyde production in the *Fan1Aldh2* cohorts over longer treatment time, drinking water was replaced with 10% ethanol solution for 1 month (Figure 3.16A). At week 4, mice with deficiency in *Aldh2* lost weight to 80% of the starting weight (Figure 3.16B). The use of reduced ethanol concentration caused a mild increase in the level of RET and PLT in mice lacking *Aldh2*. This was likely a prolonged response to ethanol-induced anemia. However, the differences in the RET and PLT levels between *Aldh2*^{-/-} single mutants and *Fan1*^{-/-}*Aldh2*^{-/-} double mutants were not statistically significant. (Figure 3.17A, B). The differences in the level of WBC and RBC counts between *Fan1Aldh2* cohorts were not statistically significant (Figure 3.17C, D).

Next, we analyzed the histology of kidney and liver under long-term ethanol treatment. We did not detect a significant difference in the number of karyomegalic nuclei in kidney epithelial or liver cells among mice regardless of *Fan1* and *Aldh2* status (Figure 3.18A, B). The ethanol-treated *Fan1*^{-/-}*Aldh2*^{-/-} double mutant mice displayed normal kidney and liver functions compared to WT and single mutant animals (Figure 3.19A-H). Additionally, we did not detect an increase in the level of Ki67⁺ renal tubular epithelial cells in the alcohol treated kidney irrespective of *Fan1* or *Aldh2* status (Figure 3.18C), indicating that the ethanol treatment employed in the study did not stimulate cell division in the

kidney tissue as was reported with the treatment with crosslink-inducing agent cisplatin (Airik et al., 2016).

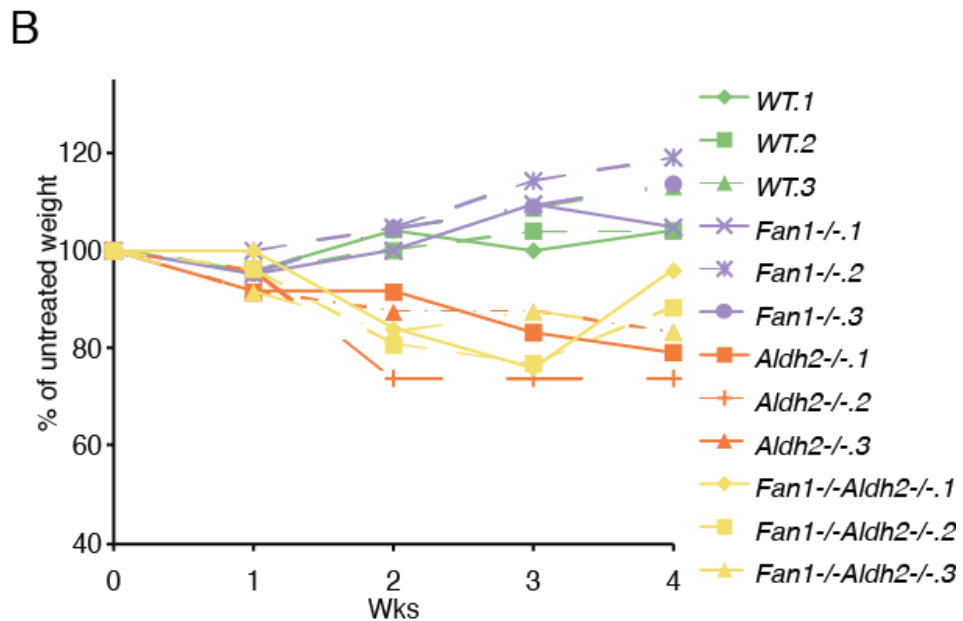
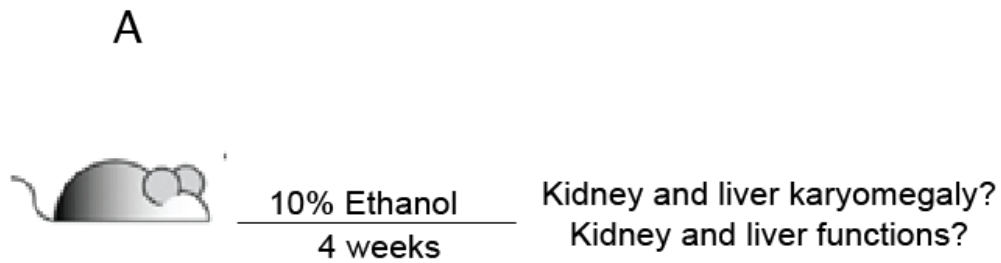


Figure 3.16 *Aldh2*-deficient mice lose more weight after four weeks of ethanol treatment.

(A) Schematic of ethanol treatment scheme. Mice were treated with 10% ethanol for 4 weeks, and then sacrificed for analysis. (B) Weight of mice measured weekly after the ethanol treatment scheme in (A). Weight is expressed as % of original weight before the treatment.

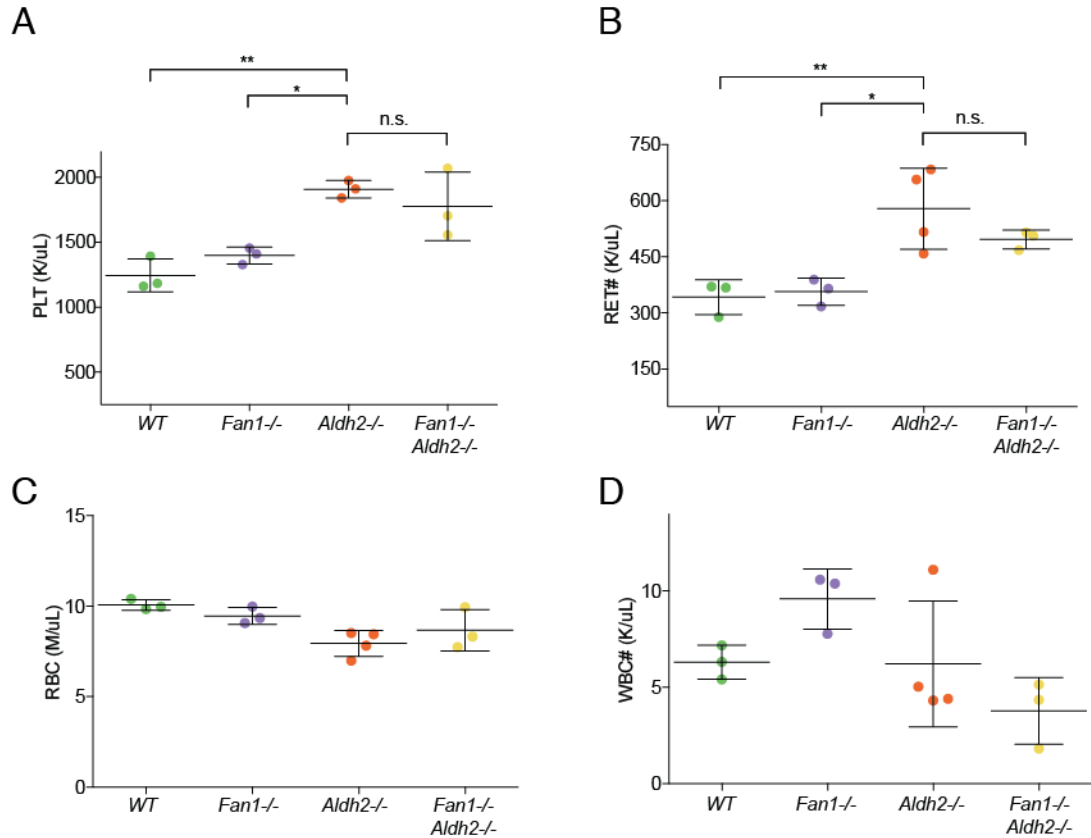


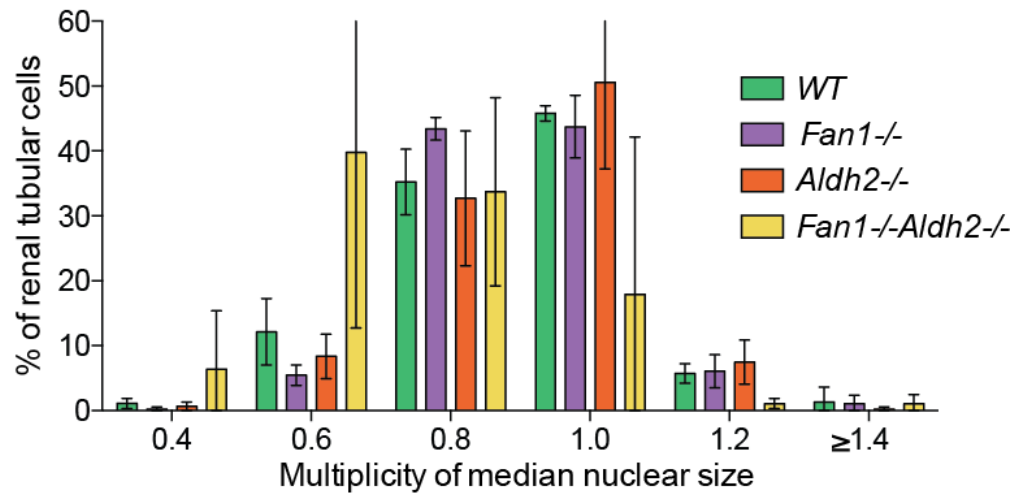
Figure 3.17 Long-term ethanol treatment moderately affects the hematopoietic system in *Aldh2*-deficient mice. No significant differences between the peripheral blood cell levels in *Aldh2*^{-/-} and *Fan1*^{-/-}*Aldh2*^{-/-} deficient animals.

(A-D) Platelet (PLT) (A), Reticulocyte (RET) (B), Red blood cell (RBC) (C), and white blood cell (WBC) (D) counts from mice of indicated genotypes after the ethanol treatment (Figure 3.14A). Bars represent mean \pm SD; * $p < 0.05$, ** $p < 0.01$, n.s., not significant was calculated by one-way ANOVA.

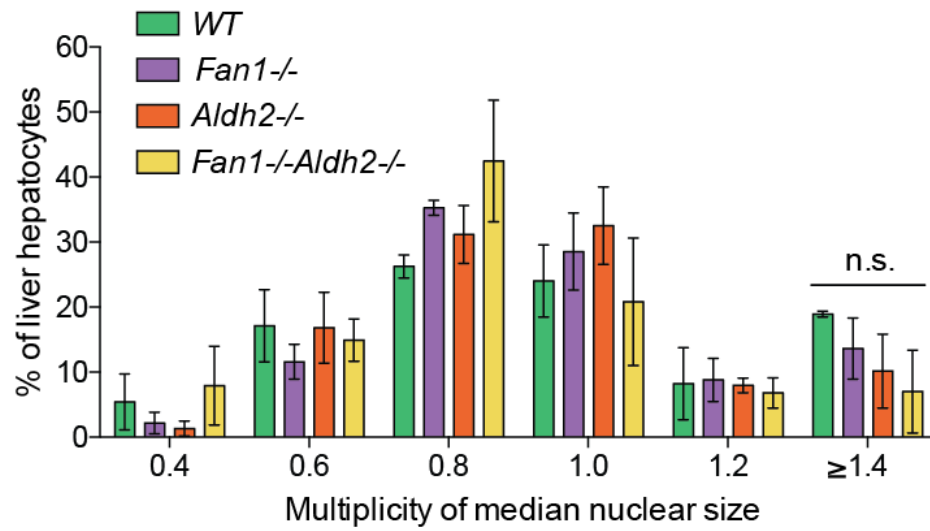
Figure 3.18 Long-term ethanol treatment did not increase the level of kidney and liver karyomegaly in *Fan1/Aldh2* double-deficient mice.

(A-B) Quantification of the nuclear area of tubular epithelial cells (A) or liver hepatocyte (B) in the cortex of kidney from 4 months old mice of indicated genotypes at 1 month after the ethanol treatment (Figure 3.14A). The area of each nucleus was normalized to the median nuclear area. Data were then plotted and grouped according to area (n=3, Error bars, s.d.). (C) The quantification of Ki67+ tubular epithelial cells after the alcohol treatment as in (Figure 3.14A) performed in a blinded manner from 35-45 high power field (HPF) (40x) images. Error bars, s.d., n=3 per genotype.

A



B



C

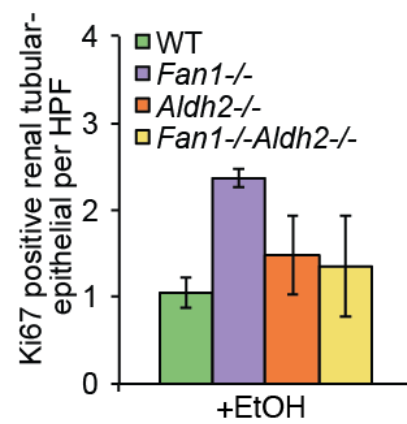
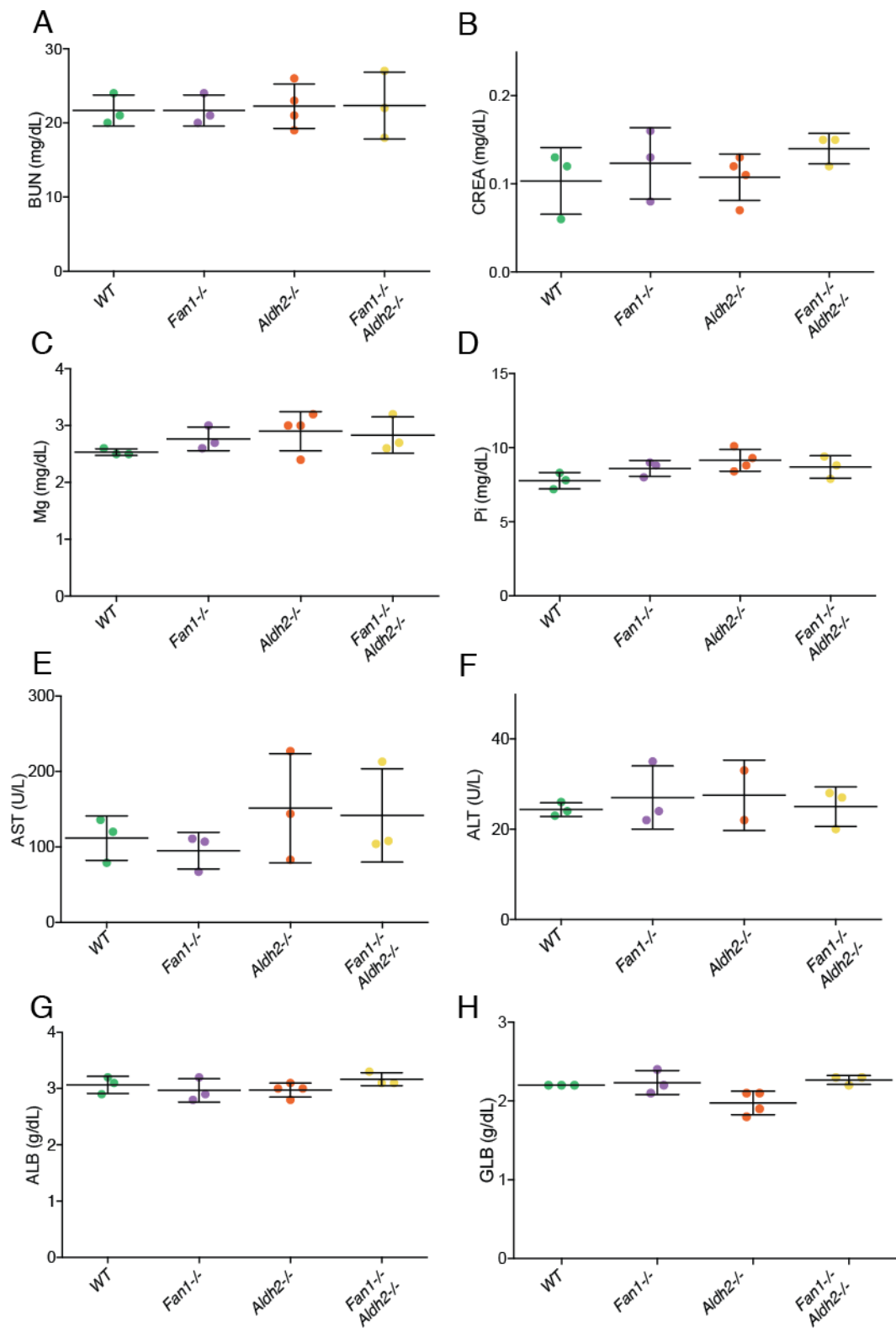


Figure 3.19 Long-term treatment with ethanol did not cause liver and kidney dysfunction in *Fan1/Aldh2*-deficient mice.

(A-D) Analysis of serum level of (A) blood urea nitrogen (BUN), (B) creatinine, (C) phosphorus, and (D) magnesium to monitor kidney function in 4 months mice of indicated genotypes after 1 months of ethanol treatment. (F-I) Analysis of serum level of liver enzymes and markers of liver function: (F) alanine transaminase (ALT), (G) aspartate transaminase (AST), (H) albumin (ALB), and (I) globulin (GLOB) in 4 months mice of indicated genotypes after 1 months of ethanol treatment. Bars represent mean \pm SD.



3.6 Summary of the findings

Concomitant lack of *Aldh2* in *Fan1* did not affect growth or fertility of the animals. In contrast, *Fan1/Adh5* double deficiency caused significant growth defect and reduced number of pups produced per litter. This result underlines a possible requirement of FAN1 to counteract the damage inflicted by increased formaldehyde due to the absence of ADH5 to maintain normal growth and embryonic development. The LSK population in 3 month-old *Fan1/Adh5* double mutant animals was decreased compared to levels in wild-type animals, however the remaining level of LSK in *Fan1^{-/-}Adh5^{-/-}* was sufficient to support the production of peripheral blood cells. The reduction in LSK level was not observed in *Fan1^{-/-}Adh5^{-/-}* animals at 12 months. This could be due to an age-related increase in the cycling activity of hematopoietic stem cells as previously reported (Rossi et al., 2007). Deficiency of *Fan1* alone or in combination with *Aldh2* or *Adh5* did not result in reduced engraftment potential after the first transplant. Secondary transplant revealed that combination of *Aldh2* and *Fan1* deficiency resulted in decreased HSC engraftment. Secondary engraftment was not yet tested in *Fan1^{-/-}Adh5^{-/-}* animals.

We did not observe a significant increase in the level of karyomegaly in the kidney or liver tissues in 3 month-old animals lacking FAN1 and ALDH2 or ADH5. FAN1 status appeared to be a determinant on the level of renal karyomegaly in 12 months old animals as the deficiency of *Aldh2* or *Adh5* did not

lead to increased karyomegaly in kidney or liver. In line with tissue histology, the concomitant absence of FAN1 and ALDH2 or ADH5 did not cause further functional decline in the kidney and liver. When treated with ethanol, lack of FAN1 caused a stronger peripheral blood abnormality in *Aldh2*-deficient animals, although the severity was much less compared to that observed in *Fancd2/Aldh2* double-mutant animals (Langevin et al., 2011). This result suggests that FAN1 functions in the repair of ethanol-induced damage in the bone marrow, although to a lesser extent than the proteins of the Fanconi anemia pathway. The ethanol treatment failed to exacerbate kidney and liver karyomegaly phenotype in *Fan1*^{-/-} or *Fan1*^{-/-}*Aldh2*^{-/-} double-deficient animals in our experiments suggesting that acetaldehyde may not be the endogenous agent that leads to karyomegaly in the absence of FAN1. Experiments with methanol treatment of *Fan1*^{-/-}*Adh5*^{-/-} animals will be necessary to further assess possible role of increased formaldehyde levels on the pathogenesis of karyomegalic interstitial nephritis.

Overall our data highlight the fact that increased level of formaldehyde but not acetaldehyde could moderately compromise the maintenance of HSC level in young *Fan1*-deficient animals. However, under stressed condition, for instance through successive bone marrow transplantations, the presence of FAN1 or ALDH2 is necessary for the protection of HSCs from the transplant-induced stress. In terms of the KIN phenotypes, we conclude that the heightened level of endogenous acetaldehyde or formaldehyde present due to *Aldh2* or *Adh5*

deficiency, is insufficient to enhance the level of tissue karyomegaly or to incite kidney and liver dysfunctions in *Fan1*-deficient animals. Acetaldehyde and formaldehyde are unlikely to be the endogenous sources of damage that promote KIN-associated phenotypes in the absence of FAN1.

Chapter 4: Interplay between the Fanconi anemia pathway and non-homologous end joining in ICL repair

4.1 Introduction

Several recent studies suggest that ICL sensitivity and genomic instability, two major hallmarks of Fanconi anemia are a result of inappropriate repair activity of another DNA repair pathway, the non-homologous end joining (NHEJ). It was shown that suppression of NHEJ could rescue ICL hypersensitivity and chromosomal aberration in FA-deficient cells in multiple model organisms (Adamo et al., 2010; Bouwman et al., 2010; Pace et al., 2010). There are; however, a number of conflicting reports among the results from different model systems, with paucity of data from the human Fanconi anemia patient cells (reviewed in Kottemann and Smogorzewska, 2013). This prompted us to analyze whether inactivating NHEJ can suppress ICL repair defects in FA patient cells.

4.1.1 Double strand break repair pathway choice: homologous recombination (HR) vs non-homologous end joining (NHEJ)

DSBs are repaired by one of two repair processes – homologous recombination (HR) or non-homologous end joining (NHEJ). Several FA proteins, including BRCA1/FANCS, BRCA2/FANCD1, PALB2/FANCN, RAD51/FANCR and SLX4/FANCP, are key regulators of important steps during the process (Howlett et al., 2002; Vaz et al., 2010; Wang et al., 2015; Xia et al., 2007). BRCA1 is required for the resection of DSB, to promote HR by preparing DNA ends for the BRCA2-dependent loading of RAD51. RAD51, a recombinase,

forms RAD51-ssDNA nucleoprotein filaments to facilitate homology search and strand invasion. Some of the D-loop structures formed following the strand invasion can be resolved by SLX4-associated nucleases SLX1 and MUS81 (Garner et al., 2013; Li and Heyer, 2008; Wyatt et al., 2013). In addition, FANCD1 proteins of the core and the ID2 complexes have been shown to have a modulatory role in the control of HR proficiency, although the mechanism is still unclear (Nakanishi et al., 2005; Smogorzewska et al., 2007). Homology directed repair is considered to be an error-free process since the template for the repair is a sister chromatid.

In the NHEJ pathway, DSB ends are captured by the Ku70/80 heterodimers (Blier et al., 1993; Falzon et al., 1993; Mimori and Hardin, 1986). DNA-dependent protein kinase catalytic subunit (DNA-PKcs), a serine/threonine kinase is recruited and its kinase activity promotes endonucleolytic processing of DSB ends by Artemis and subsequent ligation by DNA Ligase IV (LIG4)/XRCC4 complex with the help of a stimulatory factor XLF (Ciccia and Elledge, 2010; Goodarzi et al., 2006; Grawunder et al., 1997; Yannone et al., 2008). The endonucleolytic processing and the ability of NHEJ machinery to directly rejoin two broken DNA ends together regardless of the sequence homology, make the repair outcome error-prone, leading to accumulation of genomic mutations and chromosomal translocations (Chiruvella et al., 2013; Lieber, 2008, 2010).

4.1.2 Aberrant NHEJ is implicated in causing genome instability in Fanconi anemia

The repair of ICL-induced DSBs generated by ICL unhooking have been shown to depend on homologous recombination (Long et al., 2011). This preference for repair via HR instead of NHEJ is thought to be a consequence of the activity of FA pathway and HR during S/G2 phases (Moore and Haber, 1996; Sonoda et al., 2006), as well as the type of substrate that is created during ICL repair. Recent studies suggest the FA pathway may play an active role in inhibiting aberrant NHEJ activity at the ICL-induced DSBs and protect cells from accumulating chromosomal abnormalities (Adamo et al., 2010; Pace et al., 2010; Zhang et al., 2016). Suppression of NHEJ has been shown to relieve ICL sensitivity in a number of FA-deficient model systems. In *Caenorhabditis elegans* with a germline defects in *fcd-2* (*FANCD2*), sensitivity to crosslinking agents and abnormal meiotic crossovers can be ameliorated after the deletion of *lig-4* (Adamo et al., 2010). A knockout of Ku70 in FANCC-deficient DT40 chicken cells as well as depletion of Ku80 in human FA-D2 or FA-C patient cells using RNAi also result in a partial rescue of ICL hypersensitivity (Adamo et al., 2010; Pace et al., 2010). Furthermore, treatment with DNA-PKcs inhibitor fully or partially alleviated sensitivity to ICL-inducing compounds in FANCA or FANCD2-depleted human HeLa cells and *Fanca* or *Fancc* mutant mouse embryonic fibroblasts (MEFs). Depletion of FANCD2 failed to sensitize DNA-PKcs-deficient M059J human glioblastoma cells to ICL-inducing agents (Adamo et al., 2010). More

recently, inhibition of TGF- β signaling was shown to promote ICL resistance of FA patient cell lines and to suppress hematopoietic stem cell (HSC) defects in FA mouse and human cells. This inhibition was correlated with up-regulation of HR factors and down-regulation of NHEJ factors (Zhang et al., 2016).

The finding of NHEJ inhibition rescuing phenotypes of Fanconi anemia deficiency, raised a number of interesting questions. One would want to know the mechanism of how the FA pathway functions to counteract the inappropriate engagement of NHEJ proteins and a more profound question of how the ICL repair proceeds in the absence of FA and NHEJ pathways. Mutagenicity of such a process would be of interest. Therapeutically, it would be important to determine whether NHEJ inhibition could be a potential medical treatment for the patients with Fanconi anemia, even in the short term while a patient is awaiting a bone marrow transplant, and whether the effect of NHEJ inhibition is specific to particular crosslinking agents, or complementation groups of FA patients.

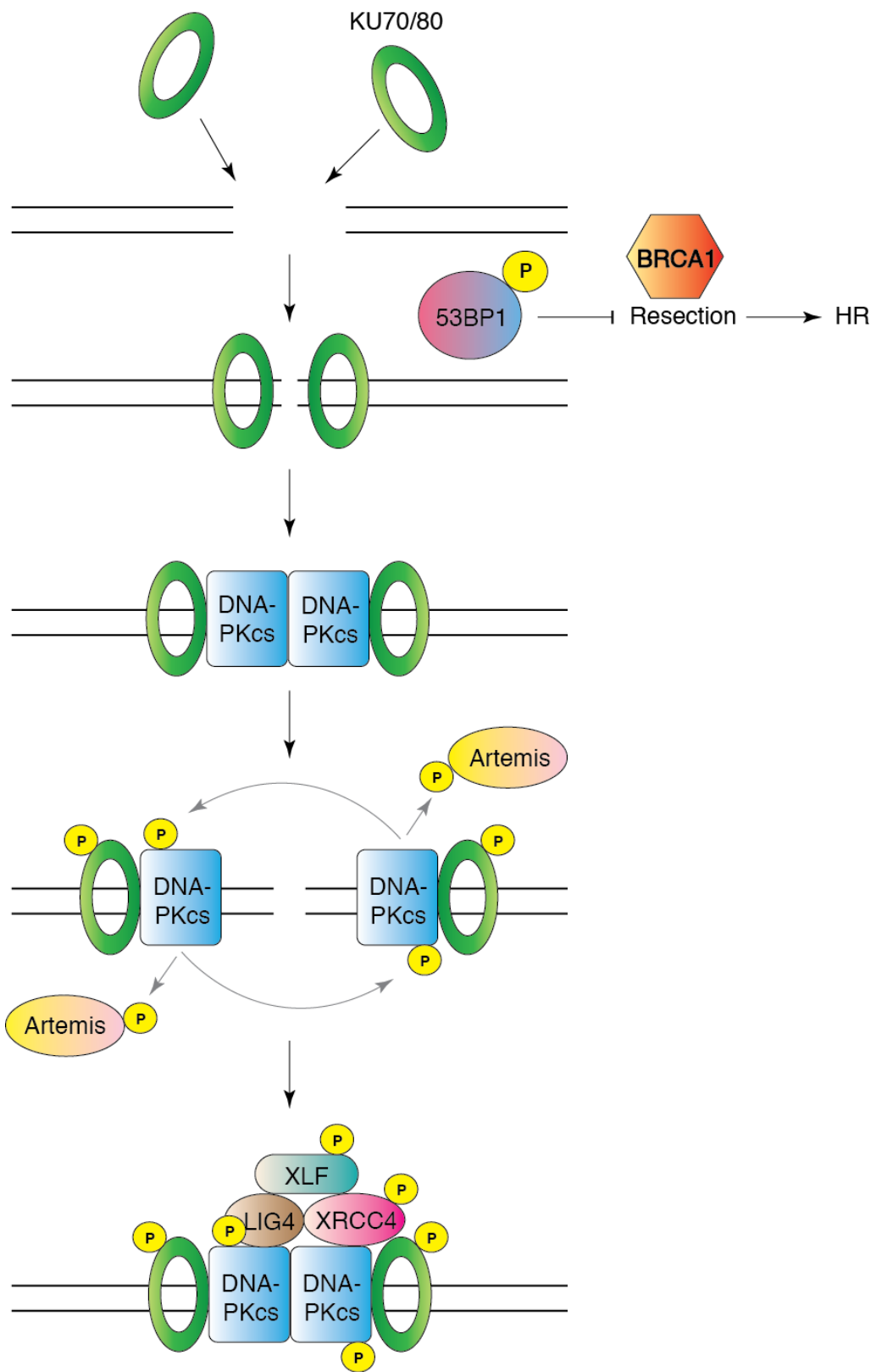
The implication that NHEJ underlies the ICL sensitivity and chromosomal aberration in FA-deficient cells has, however, been challenged by contradicting results of other studies. Knockout of LIG4 or DNA-PKcs does not rescue of crosslink sensitivity in DT40 cell lines (Pace et al., 2010). In very convincing genetic knockout studies, MEFs lacking FANCD2 and Ku80, DNA-PKcs, or

53BP1 were as sensitive to ICL-inducing agents as FANCD2-deficient cells alone (Bunting et al., 2012; Houghtaling et al., 2005).

The disparity between results of different studies that assessed the genetic interaction of FA and NHEJ pathways prompted our studies that use human patient cell lines. In this study, we assessed whether disrupting components of NHEJ with chemical inhibitors, RNAi or CRISPR-Cas9 could rescue the ICL hypersensitivity of human *FANCA*^{-/-} patient fibroblasts. All of our experiments led to a conclusion that abrogation of major NHEJ factors does not alleviate crosslink repair defect phenotypes of *FANCA*^{-/-} cells.

Figure 4.1 Schematic showing proteins in the non-homologous end joining pathway.

Ku70/Ku80 heterodimer complex recruited to DSB ends activates DNA-PKcs. In parallel, 53BP1 is recruited to promote NHEJ by suppressing extensive DNA end resection and enhancing DNA end mobility. DNA-PK regulates the stability of DSB ends through phosphorylation of Artemis and other protein substrates. Artemis facilitates DNA end processing and, subsequently, LIG4/XRCC4 complex and XLF catalyze the ligation of the broken ends to complete NHEJ repair.



Results

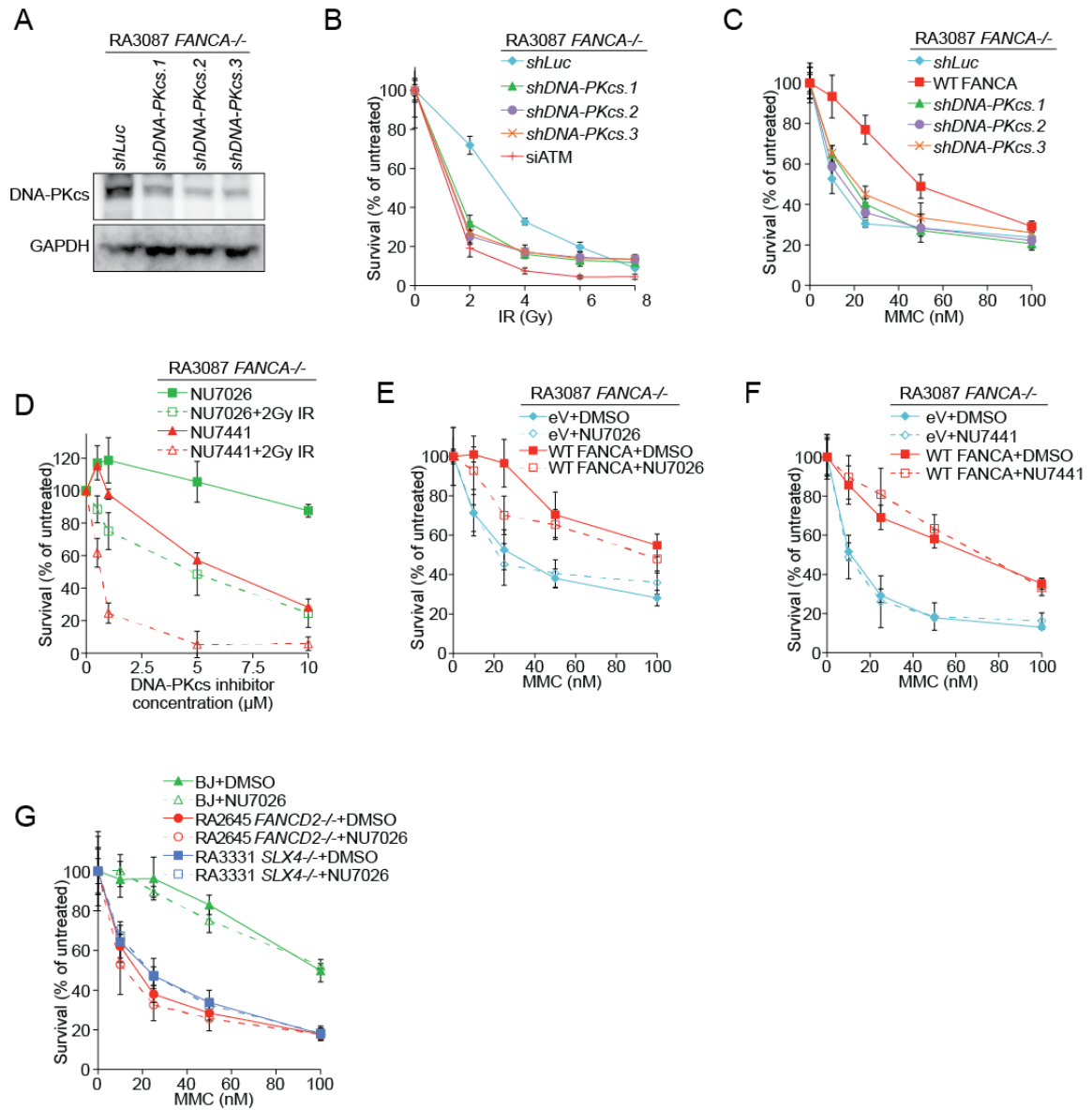
4.2 Inactivation of DNA-PKcs does not rescue MMC-induced proliferation defects in cells lacking FA pathway function.

FANCA^{-/-} (RA3087) human patient fibroblasts with biallelic deletion of *FANCA* (Kim et al., 2013), were used for studies to examine whether suppressing essential NHEJ factors could rescue crosslink repair defects in FA patient cells. We first used RNAi-mediated knockdown to deplete *DNA-PKcs* in RA3087 cells (Figure 4.2A). Three independent hairpins to *DNA-PKcs* efficiently suppressed NHEJ activity as determined by increased sensitization of *shDNA-PKcs* expressing RA3087 cells to ionizing irradiation (IR) (Figure 4.2A, B). However, these cells were still as sensitive to MMC as the control *FANCA*^{-/-} cells expressing control shRNA (Figure 4.2C). We next chemically inhibited DNA-PKcs activity in RA3087 cells using DNA-PKcs inhibitors. Both DNA-PKcs inhibitors, NU7026 and NU7441, efficiently inhibited NHEJ as demonstrated by dosage-dependent IR-induced survival defect in inhibitor-treated RA3087 cells (Figure 4.2D). RA3087 cells treated with the inhibitors at dosages that induced NHEJ suppression without significant growth defects (10 μ M for NU7026 or 1 μ M for NU7441) did not exhibit resistance to MMC (Figure 4.2E, F). DNA-PKcs inhibitor NU7026 treatment also failed to reduce MMC sensitivity of FA patient cells lacking FANCD2 or SLX4, FA proteins that act downstream of FANCA (Figure 4.2G). These results show that shRNA-depletion or chemical inhibition of DNA-

PKcs to inactivate NHEJ did not restore crosslink repair proficiency in FA patient cells.

Figure 4.2 Suppression of DNA-PKcs does not rescue MMC sensitivity in FANCA-deficient cells.

(A) Survival of RA3087 FANCA-deficient patient cells stably transduced with shRNA targeting Luciferase (control) or *DNA-PKcs* after IR treatment (0-8 Gy). FA-A patient cells with siRNA treatment against ATM was used as IR sensitive-control. Error bars, s.d.. (B) Survival of RA3087 cells stably transduced with shRNA targeting Luciferase (control) or *DNA-PKcs* and RA3087 cells complemented with FANCA after MMC treatment (0-100 nM). Error bars, s.d.. (C) Immunoblot showing the expression of DNA-PKcs in the shRNA transduced RA3087 cells used in A and B. (D) Survival of RA3087 cells under untreated or treated with 2 Gy IR after the pretreatment with NU7026 (0-10 μ M) or NU7441 (0-10 μ M). Error bars, s.d.. (E) Survival of RA3087 cells stably transduced with empty vector or with FANCA under chronic treatment with MMC (0-100 nM). The cells were pretreated with 10 μ M NU7026 or DMSO. Error bars, s.d.. (F) Survival of RA3087 cells stably transduced with empty vector or with FANCA after treatment with MMC (0-100 nM). The cells were pretreated with 1 μ M NU7441 or DMSO. Error bars, s.d.. (G) Survival of wild type fibroblasts (BJ), RA2645 *FANCD2*-deficient cells, RA3331 *SLX4*-deficient cells after treatment with MMC (0-100 nM). The cells were pretreated with 10 μ M NU7026 or DMSO. Error bars, s.d..



4.3 Inactivation of DNA Ligase IV or DNA Ligase III does not rescue MMC-induced proliferation defects in cells lacking FA pathway

We next examined whether suppression of DNA Ligase IV would rescue ICL hypersensitivity in FANCA-deficient cells. *FANCA* depletion in *LIG4*^{+/+}, *LIG4*^{+/-}, or *LIG4*^{-/-} HCT116 cell lines (Oh et al., 2013) led to a significant reduction of FANCA protein level and a disappearance of FANCI monoubiquitination in all *shFANCA* transduced HCT116 cell lines, indicating a successful inhibition of the FA pathway. FANCA depletion in all cell lines, regardless of the *LIG4* status resulted in no change to MMC sensitivity from the parental cell lines expressing control shRNA (Figure 4.3A, B), leading to conclusion that absence of Ligase IV could not rescue sensitivity to MMC in the setting of FA pathway deficiency. We have noted, however, that cells lacking one allele of *LIG4* were more sensitive to MMC than the *LIG4*^{+/+} HCT116 cells and that the *LIG4*^{-/-} HCT116 were even more sensitive than the *LIG4*^{+/-} HCT116 cells. This finding will have to be confirmed in other, non-HCT116 cells.

In parallel, we assessed impact of DNA Ligase III deficiency on MMC sensitivity in the setting of FANCA deficiency. Ligase III function is essential in mitochondria (Simsek et al., 2011). To examine the impact of LIG3 and alternative NHEJ suppression on the outcome of ICL repair in FA-deficient cells, we used *FANCA* shRNAs in HCT116 cell lines with *LIG3* being inactivated in the nucleus but active in the mitochondria (Jones et al., 2014; Oh et al., 2014).

Absence of nuclear LIG3 did not rescue the MMC sensitivity of *FANCA*-depleted HCT116, indicating that alternative end joining pathway is unlikely to be responsible for ICL-inflicted genomic instability in cells deficient in FA pathway (Figure 4.3C, D).

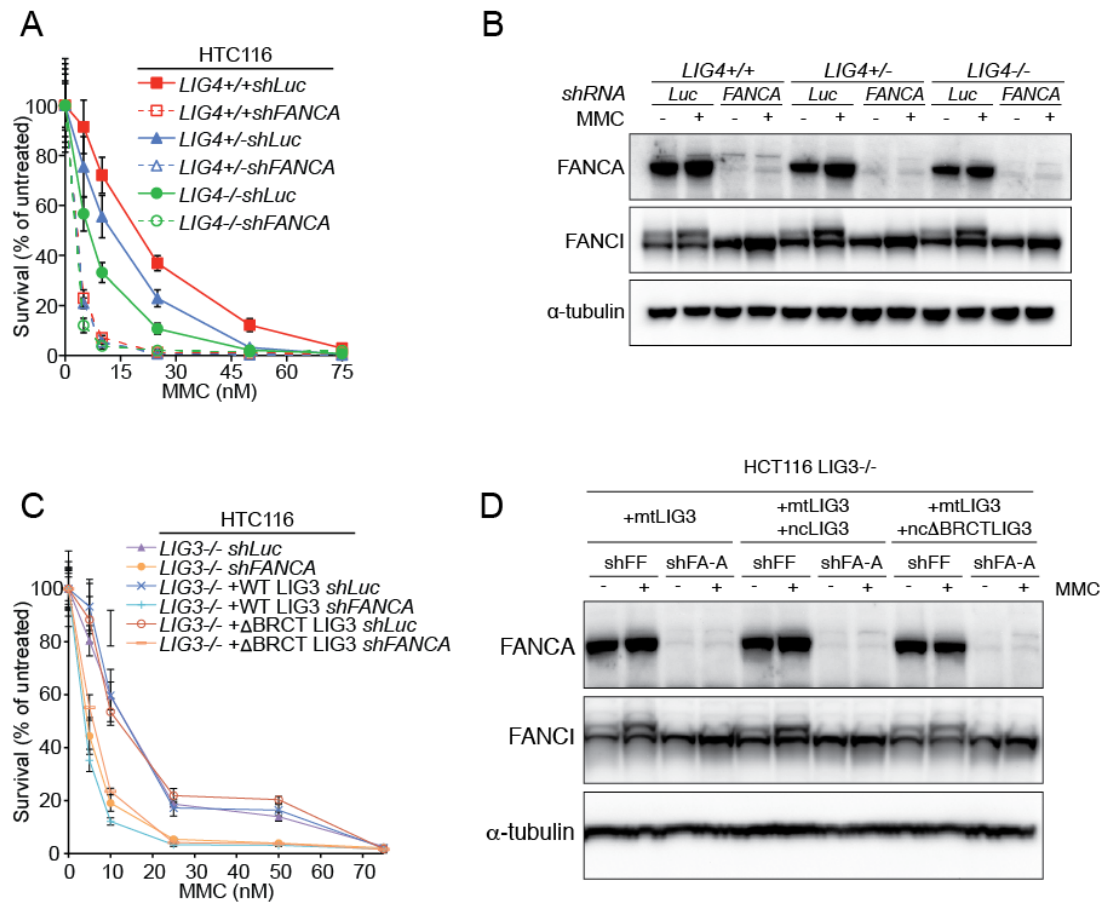


Figure 4.3 *LIG4* or *LIG3* inactivation does not rescue MMC sensitivity in the setting of *FANCA* depletion.

(A) Survival of *LIG4*^{+/+}, *LIG4*^{+/-}, and *LIG4*^{-/-} HCT116 cells stably transduced with shRNA targeting Luciferase (control) or *FANCA* after MMC treatment (0-75 nM). Error bars, s.d.. (B) Immunoblot showing expression of *FANCA* and *FANCI* in the shRNA transduced cells used in A with or without 24 hours 1 μ M MMC treatment. (C) Survival of *LIG3*^{+/+}, *LIG3*^{-/-}, *LIG3*^{-/-} +WT *LIG3*, and *LIG3*^{-/-} + Δ BRCT *LIG3* HCT116 cells stably transduced with shRNA targeting Luciferase (control) or *FANCA* after MMC treatment (0-75 nM). Error bars, s.d.. (D) Immunoblot showing expression of *FANCA* and *FANCI* in the shRNA cells used in C with or without 24 hours 1 μ M MMC treatment.

4.4 Inactivation of DSB repair choice factor, 53BP1, does not rescue MMC-induced proliferation defects in *FANCA*^{-/-} cells

We next assessed if 53BP1, factor that functions upstream of the core NHEJ machinery to promote the choice between NHEJ and HR in DNA DSB repair, would rescue MMC sensitivity of *FANCA*^{-/-} cells. There are conflicting reports on whether 53BP1 inactivation could rescue the ICL-repair defect in BRCA1-deficient mouse cells (Bouwman et al., 2010; Bunting et al., 2012). Notably, 53BP1 deletion cannot rescue ICL-induced chromosomal aberrations in *Fancd2*-deficient MEFs (Bunting et al., 2012). As all of these studies were performed in mouse cells, we generated an equivalent human system with *FANCA*/53BP1 double deficiency. In agreement with published data, which suggests that 53BP1 does not play a major role in resistance to IR-induced DSBs, we did not observe a significant IR sensitivity in 53BP1-depleted FA-A patient cell lines despite efficient protein depletion (Figure 4.4A) (Chapman et al., 2012; Iwabuchi et al., 2006; Nakamura et al., 2006; Riballo et al., 2004; Ward et al., 2004). 53BP1 knockdown did not lead to a suppression of MMC sensitivity in human *FANCA*-deficient cells (Figure 4.4B, C). These results provide strong support for the finding in the mouse system that loss of 53BP1 is not sufficient to rescue defective ICL repair in FA deficient cells.

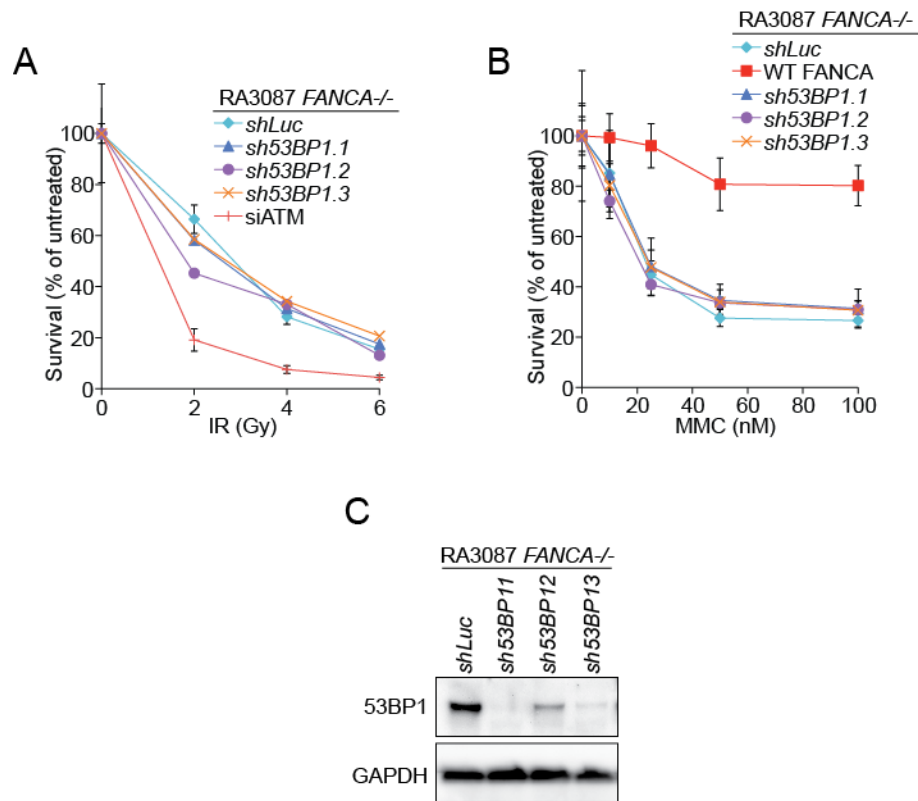


Figure 4.4 Depletion of 53BP1 does not rescue MMC sensitivity in FANCA-deficient cells.

(A) Survival of RA3087 FANCA-deficient patient cells stably transduced with shRNA targeting Luciferase (control) or 53BP1 after IR treatment (0-6 Gy). RA3087 cells transfected with siRNA against ATM were used as positive control for outcome after IR treatment. Error bars, s.d.. (B) Survival of RA3087 cells stably transduced with shRNA targeting Luciferase (control) or 53BP1 or RA3087 cells complemented with FANCA after MMC treatment (0-100 nM). Error bars, s.d.. (C) Immunoblot showing the expression of 53BP1 in the shRNA transduced RA3087 cells used in A and B.

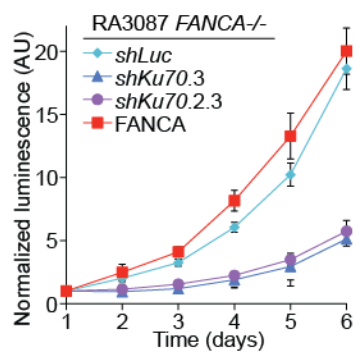
4.5 Partial inactivation of Ku70 or Ku80 does not rescue ICL-induced proliferation defects in FANCA-deficient cells

We analyzed the possibility of suppressing ICL sensitivity of FANCA-deficient human cells by Ku70 (XRCC6) and Ku80 (XRCC5) inactivation. By stably expressing three independent shRNA hairpins and their combinations to target Ku70 or Ku80 in FA-A patient cells, we were able to partially but never completely deplete Ku70 and Ku80. We found that RA3087 cells with Ku70 or Ku80 knockdown grew slower than control cells (Figure 4.5A-D). This growth arrest induced upon Ku70 or Ku80 depletion is consistent with data showing that Ku70 and Ku80 are essential genes for human but not mouse cells (Fattah et al., 2008b; Li et al., 2002). Ku70 and Ku80 have been shown to be required for telomere maintenance and their absence leads to genomic instability and cell death (Myung et al., 2004; Wang et al., 2009). We used cells with the best Ku70 depletion and did not detect a significant suppression of MMC sensitivity in Ku70-depleted RA3087 cells (Figure 4.5E).

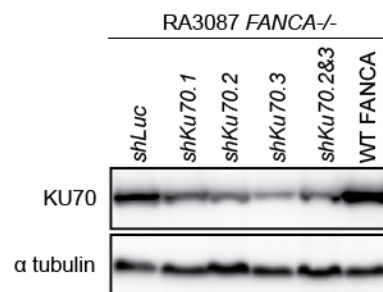
Figure 4.5 *Ku70* and *Ku80* are essential in human cells and their partial suppression does not rescue ICL sensitivity in FANCA-deficient cells.

(A) Growth of RA3087 *FANCA*^{-/-} cells stably transduced with shRNA targeting Luciferase (control) or *Ku70* or complemented with FANCA. Error bars, s.d.. (B) Immunoblot showing the expression of Ku70 in cells used in A. (C) Growth of RA3087 cells stably transduced with shRNA targeting Luciferase (control) or *Ku80* or complemented with FANCA. Error bars, s.d.. (D) Immunoblot showing the expression of *Ku80* in cells used in C. (E) Survival of *FANCA*^{-/-} patient cells stably transduced with shRNA targeting Luciferase (control) or *Ku70* and *FANCA*^{-/-} patient cells complemented with FANCA after MMC treatment (0-100 nM). Error bars, s.d..

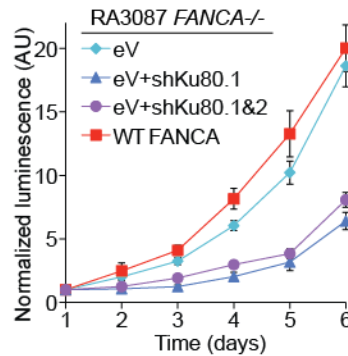
A



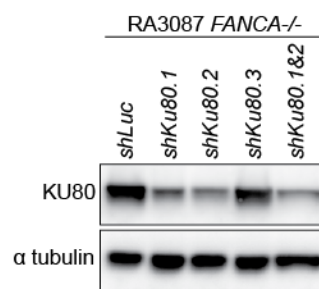
B



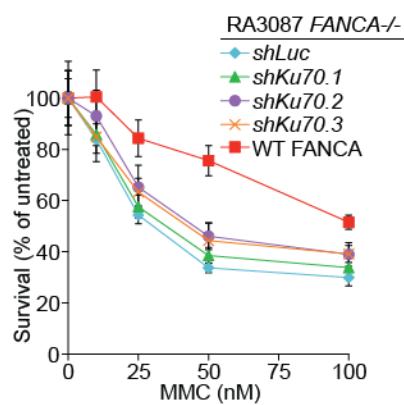
C



D



E

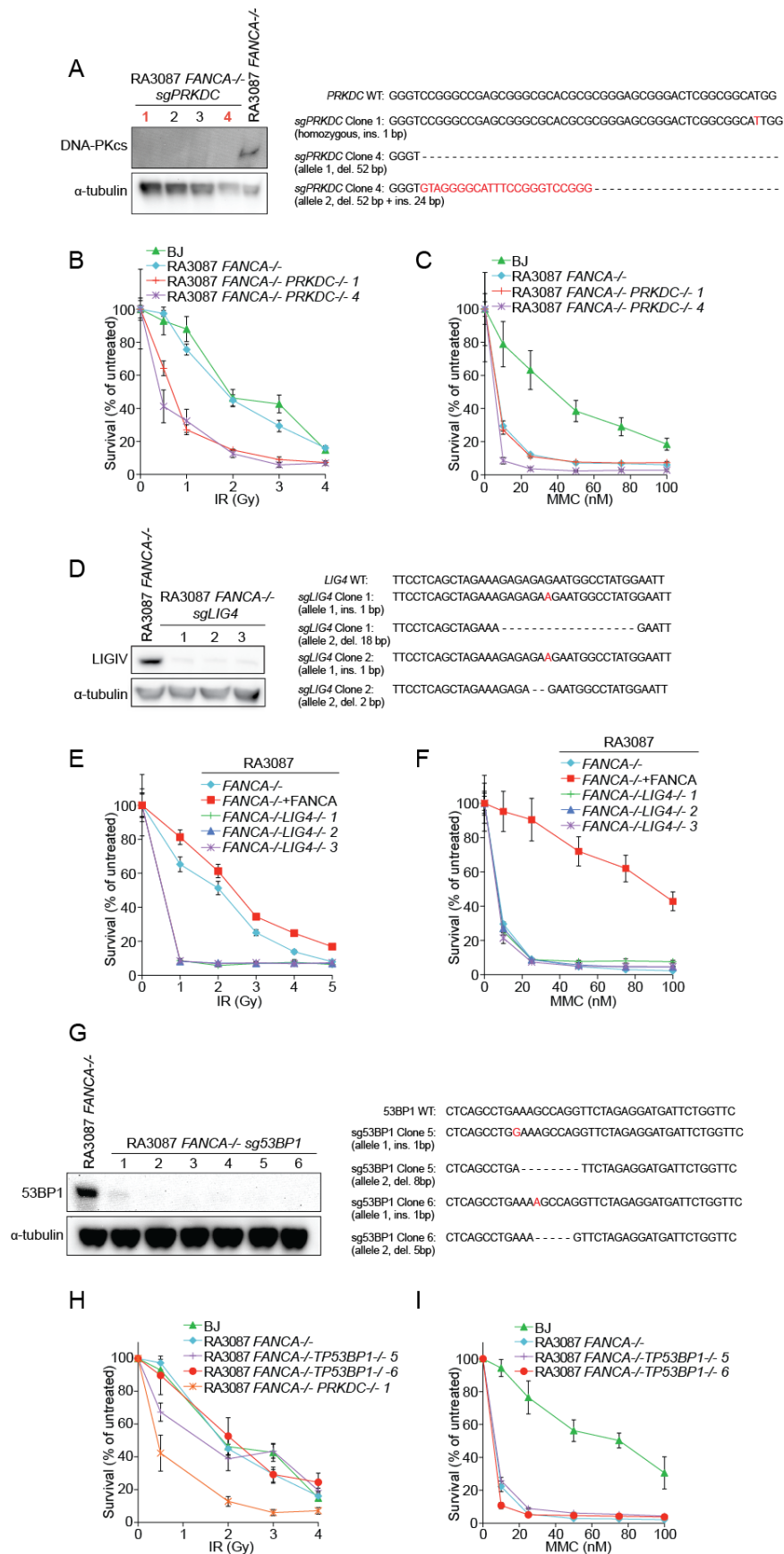


4.6 Complete inactivation of NHEJ factors by CRISPR-Cas9 mediated genome-editing does not rescue MMC proliferation defects in FA cells

To eliminate the possibility that lack of rescue of MMC sensitivity in FA-pathway-deficient cells was due to the residual NHEJ activity after shRNA-mediated knockdown or chemical inhibition, Clustered Regularly Interspaced Short Palindromic Repeat (CRISPR)-Cas9-dependent gene engineering was employed to completely inactivate components of NHEJ including DNA-PKcs, LIG4, and 53BP1 in *FANCA*^{-/-} patient cells. Successful inactivation of the three NHEJ factors was verified at the protein level as the expressions of DNA-PKcs, LIG4, and 53BP1 were not detected in the isolated clones (Brooke Conti, Figure 4.6 A, D, G). Furthermore, as expected, the DNA-PKcs (Clone 1 and 4) and LIG4 (Clone 1, 2, and 3) knockout cells exhibited sensitivity to IR, confirming that NHEJ was abrogated in these clones (Brooke Conti, Figure 4.6B, E). Similar to the shRNA-mediated depletion experiment (Figure 4.4A), full removal of 53BP1 by genome editing did not result in significant IR sensitivity (Brooke Conti, Figure 4.6H). Nonetheless, CRISPR-Cas9-mediated complete removal of DNA-PKcs, LIG4, or 53BP1 did not improve the MMC-induced survival defect in RA3087 cells (Brooke Conti, Figure 4.6C, F, I). These experiments are consistent with the conclusion that NHEJ suppression does not rescue ICL repair defect in Fanconi anemia patient cells.

Figure 4.6 Full inactivation of NHEJ factors by genome-editing does not rescue MMC sensitivity in *FANCA*^{-/-} cells.

(A) Immunoblot showing expression of DNA-PKcs in RA3087 *FANCA*^{-/-} cells and the RA3087 *FANCA*^{-/-}*DNA-PKcs*^{-/-} clones obtained by CRISPR/Cas9 gene editing. Sequences at the targeting site of clone 1 and 4 are shown. (B) Survival of wild type fibroblasts (BJ), *FANCA*^{-/-}, and 2 clones (1 and 4) of *FANCA*^{-/-}*DNA-PKcs*^{-/-} cells after IR treatment (0-4 Gy). Error bars, s.d.. (C) Survival of wild type fibroblasts (BJ), *FANCA*^{-/-}, and 2 clones (1 and 4) of *FANCA*^{-/-}*DNA-PKcs*^{-/-} cells after MMC treatment (0-100 nM). Error bars, s.d.. (D) Immunoblot showing expression of LIG4 in RA3087 *FANCA*^{-/-} cells and the RA3087 *FANCA*^{-/-}*LIG4*^{-/-} clones. Sequences around the targeting site of clone 1 and 2 are shown. (E) Survival of *FANCA*^{-/-}, *FANCA*^{-/-} complemented with *FANCA*, and 3 clones of *FANCA*^{-/-}*LIG4*^{-/-} cells (1, 2, and 3) after IR treatment (0-5 Gy). Error bars, s.d.. (F) Survival of *FANCA*^{-/-}, *FANCA*^{-/-} complemented with *FANCA*, and 3 clones of *FANCA*^{-/-}*LIG4*^{-/-} cells (1, 2, and 3) after MMC treatment (0-100 nM). Error bars, s.d.. (G) Immunoblot showing expression of 53BP1 in *FANCA*^{-/-} cells and the *FANCA*^{-/-}*53BP1*^{-/-} clones. Sequences around the targeting site of clone 5 and 6 are shown. (H) Survival of wild type fibroblasts (BJ), *FANCA*^{-/-}, and 2 clones (5 and 6) of *FANCA*^{-/-}*53BP1*^{-/-} cells after IR treatment (0-4 Gy). *FANCA*^{-/-}*DNA-PKcs*^{-/-}.1 CRISPR-targeted clone from (A-C) was used as IR sensitive-control. Error bars, s.d.. (I) Survival of wild type fibroblasts (BJ), *FANCA*^{-/-}, and 2 clones (5 and 6) of *FANCA*^{-/-}*53BP1*^{-/-} cells after MMC treatment (0-100 nM). Error bars, s.d..
All experiments shown in the figure were performed by Brooke Conti, a fellow student in the lab.



4.7 Summary of findings and discussion

The observation that NHEJ inhibition could suppress ICL-inducing agent sensitivity in FA deficient cells has triggered excitement for potential new therapeutic avenues for FA and novel mechanistic insight into ICL repair. However, there have been inconsistencies between published studies (Adamo et al., 2010; Bunting et al., 2012; Chapman et al., 2012; Houghtaling et al., 2005; Kottemann and Smogorzewska, 2013; Pace et al., 2010). Here we performed an extensive analysis in cells derived from FA patients to identify whether inactivating NHEJ factors could rescue ICL-induced proliferation defects. We found that inactivation of classical NHEJ proteins, including DNA-PKcs, DNA Ligase IV, and Ku70/80, as well as pathway choice protein 53BP1 or Ligase III necessary for alternative NHEJ, do not alleviate the ICL sensitivity in FA patient cells.

Our findings directly contradict published studies including the observation that DNA-PKcs deficiency could suppress ICL-inducing agent sensitivity in FA pathway-deficient human cells. The rescue of MMC sensitivity with DNA-PKcs inhibitor was previously illustrated in HeLa cells with RNAi to deplete FANCA or FANCD2 (Adamo et al., 2010). However, we failed to rescue MMC sensitivity of *FANCA*^{-/-} patient cells by shRNA-mediated depletion of DNA-PKcs or through chemical inhibitors of DNA-PKcs. It is possible that this inconsistency was a result of different experimental set-ups. The rescue effect observed in the

previous studies could be a non-specific effect of the DNA-PKcs inhibitor or incomplete depletion of the FA transcripts by RNAi treatment. We did not attain similar observation, despite using the same type and treatment of DNA-PKcs inhibitor. As evidenced by the pronounced IR sensitivity upon depletion or chemical inhibition of DNA-PKcs, we are confident that inactivation of DNA-PKcs does not rescue ICL repair defects in the human FA patient cells. Yet there remains a possibility that the remnant DNA-PKcs activity from incomplete depletion or inhibition could still contribute to the MMC sensitivity observed. To discard that possibility, we characterized the CRISPR/Cas9-generated full genetic knockout of *DNA-PKcs* in FA-A patient cells and observed no rescue of MMC sensitivity (Brooke Conti, Figure 4.6A-C), leading us to conclude that DNA-PKcs suppression does not promote ICL resistance in FANCA-deficient human patient cells. Our findings are consistent with mouse genetic data that showed that ICL sensitivity of *Fancd2* mutant MEFs could not be rescued by DNA-PKcs deficiency (Houghtaling et al., 2005).

Divergent relationship between NHEJ and ICL repair among experimental systems appears to be a common theme. This is well illustrated by the contradictory effects of LIG4 suppression on ICL-induced drug resistance in *C. elegans* and chicken DT-40 cells, reflecting potential differential regulations of DSB repair pathway choice and the FA pathway in different organisms (Adamo et al., 2010; Pace et al., 2010). Our analysis provides the first genetic evidence

against a rescue of crosslink repair defects by *LIG4* inactivation in human cells. Ablation of *LIG4* did not promote ICL resistance in *FANCA*-depleted HCT116 cells. It should be noted that the HCT116 cells lack functional MLH1 and MSH3 proteins, whose role in ICL repair remains incompletely understood. We thus tested the effect of CRISPR-mediated *LIG4* inactivation directly in *FANCA*^{-/-} patient cell lines and observed no evidence for a rescue of ICL sensitivity (by Brooke Conti, Figure 4.6D-F).

In this study, we showed that 53BP1 inactivation did not restore ICL repair proficiency in *FANCA*-deficient cells, in agreement with the previous study in the mouse (Bunting et al., 2012). This observation indicates that a potential increase in DSB end resection with 53BP1 deficiency, which disfavors NHEJ could not compensate for the lack of *FANCA*-dependent ICL repair (Bunting et al., 2012; Knipscheer et al., 2009; Raschle et al., 2008).

The analysis of rescue of FA cellular phenotypes by Ku70/Ku80 inactivation in human cells is challenging, as Ku70 and Ku80 function is essential at human telomeres (Fattah et al., 2008a; Li et al., 2002). Depletion of Ku80 was nonetheless shown previously to partially rescue ICL sensitivity in FA-C and FA-D2 patient cells (Adamo et al., 2010; Pace et al., 2010). In mouse cells, *Ku80* is not essential and its knockout leads not only to lack of rescue, but to an increase in sensitivity to ICL-inducing agents when combined with *Fancd2* deficiency

(Bunting et al., 2012). Here, we did not observe a rescue of ICL sensitivity in FANCA-deficient cells when Ku70 or Ku80 were partially depleted. Until Ku70 or Ku80 mutants that retain the telomere protection function but lose specifically the NHEJ activity are identified, we will not know for sure if full inhibition of the KU complex would lead to rescue of FA phenotypes.

It should be noted that in most of our experiments, we focused our attention on the effect of NHEJ suppression on the proliferation of FA-patient cells under ICL treatment without additional analysis on the state of crosslinking-induced chromosomal abnormality, which is a diagnostic feature of FA cells. NHEJ is thought to contribute to the chromosomal translocation and the formation of radial chromosomes. Therefore, there is a possibility that NHEJ inactivation could rescue the radial chromosomes phenotype or could change the types of chromosomal aberrations without rescuing the proliferation defect in ICL-treated FA-patient cells. There is in fact some recent evidence in support of such phenomenon that chromosomal translocation/radial chromosomes may not be the direct cause of cellular sensitivity to crosslinks or defective DSB repair (Bunting et al., 2010). This merits further investigation in the future.

It should also be noted that our genetic experiments were mostly undertaken in *FANCA*^{-/-} fibroblasts because as a member of the core complex its abrogation leads to a full inactivation of FA pathway. We also took into

consideration that majority of FA patients carry FANCA mutations. While it is possible that other members of the FA pathway may have unique relationships with NHEJ, we showed that DNA-PKs inhibitors did not rescue the ICL sensitivity of human patient cells lacking FANCD2 or SLX4, the downstream components of the FA pathway. Aberrant NHEJ activity is thereby unlikely to be responsible for the ICL-inducing agent sensitivity of FA-deficient cells. In addition, our study was performed on human patient fibroblasts rather than hematopoietic stem cells (HSCs), which may be more relevant to FA-associated bone marrow failure. A recent report proposes a correlation between the effect of NHEJ down-regulation and a rescue of HSCs defects in FA-deficient mouse and human models via an inhibition of TGF- β signaling (Zhang et al., 2016). Whether direct NHEJ suppression would produce a similar rescue effect on FA-deficient HSCs needs to be explored.

Together our findings have significant implications for the care of FA patients. With our current results, we conclude that inhibition of NHEJ would not be able to suppress cellular sensitivity to crosslinking agents in FA-patient cells and hence it would not be a viable treatment option for FA patients. It is still important to continue to identify and understand the pathways that may crosstalk with FA pathway and which could be involved in the aberrant processes in FA-deficient cells so that the relevant targeted therapy could be developed in the future.

Chapter 5: Discussion

5.1 The role of FAN1 in DNA interstrand crosslink repair

In this study, we analyzed FAN1 function in human and mouse cells. Cell lines derived from KIN patients and *Fan1*-deficient mouse embryos, provide a powerful genetic tool to study the molecular mechanisms of FAN1 function in DNA interstrand crosslink (ICL) repair. Our work demonstrates that FAN1 is necessary for cellular resistance to DNA ICL-inducing agents as FAN1-deficient cells display decreased proliferation and aberrant chromosomal structures after treatment with them. Our study also highlights that the ICL repair function of FAN1 is independent of the FA pathway and is not contingent upon interaction with the ID2 complex. This finding provides a plausible explanation for the phenotypic differences observed between FA and KIN patients.

5.1.1 The mechanism of FAN1 in ICL repair

Our study demonstrates that the sensitivity of cells derived from KIN patients to ICL-inducing agents can be complemented by ectopic expression of wild-type FAN1. Further analysis revealed that KIN patient cells have intact DNA damage G1/S and G2/M checkpoints, as well as robust FANCD2 ubiquitination especially following ICL treatment. These results suggest that FAN1 might function downstream of DNA damage response and FA pathway activation. To further characterize the mechanism of FAN1 in ICL repair, we generated *Fan1*-deficient mouse embryonic fibroblasts. The study showed that *Fan1*-knockout mouse cells recapitulate the behavior of human cells deficient for FAN1. Namely,

the nuclease activity of FAN1 proved necessary for protection against various ICL inducing agents - MMC, acetaldehyde and formaldehyde, but not to non-crosslink replication stress inducers such as hydroxyurea or camptothecin. Our analysis also suggests that FAN1 is not haploinsufficient for ICL repair as MEFs heterozygous for the *Fan1*-deficient allele were resistant to the same drug treatments. These findings are consistent with karyomegalic interstitial nephritis (KIN) being a recessive disease in humans (Zhou et al., 2012).

The UBZ domain-mediated interaction between FAN1 and the ID2 complex is believed to be crucial for the recruitment of FAN1 to the sites of crosslinked DNA and its involvement in ICL repair (Kratz et al., 2010; Liu et al., 2010; MacKay et al., 2010; Smogorzewska et al., 2010). However, our data indicate that FAN1 can facilitate ICL repair independently of the UBZ domain. Our work in collaboration with the Seidman lab demonstrates that the UBZ domain is not necessary for the localization of FAN1 to the site of crosslinks (Thongthip et al., 2016). The recruitment of FAN1 relies primarily on the SAP domain, with the UBZ domain playing an auxiliary role in the additional enrichment of FAN1 at the site of damage. Based on the structural analysis of FAN1, the direct interaction of the SAP domain with crosslinked DNA provides proper structural remodeling of the DNA substrate, which is required for appropriate incision by the nuclease domain of FAN1 and subsequent ICL repair (Gwon et al., 2014; Wang et al., 2014; Zhao et al., 2014). Consistent with the

SAP domain being important for recruitment to the ICL, we found that ectopic expression of FAN1 with mutations in its SAP domain failed to rescue ICL repair defect in *Fan1*-deficient mouse cells. The observation that the SAP domain is sufficient for the efficient recruitment of FAN1 to the damage site raises the possibility that FAN1 could function in cellular contexts where the FA proteins are unable to act efficiently; for example, in the G0 or G1 stage of the cell cycle or at a subset of DNA lesions that have structures other than convergent replication forks.

The fact that the UBZ of FAN1 is not necessary for resistance to ICL inducing agents, prompts a question of the significance and function of the UBZ domain and the FAN1- FANCD2 interaction. It is possible that the UBZ domain is required for the functions of FAN1 and the ubiquitinated FANCD2/FANCI that are unrelated to the repair of ICLs. The UBZ domain is a more recent evolutionary extension of FAN1 protein architecture (MacKay et al., 2010; Smogorzewska et al., 2010). In yeast, Fan1 is capable of conferring ICL repair activity in the absence of the UBZ domain (Fontebasso et al., 2013). Study from John Rouse laboratory showed that the UBZ domain of FAN1 is essential for processing replication forks and for protection against chromosomal instability after treatment with HU and MMC (Lachaud et al., 2016a). Our experimental conditions however, did not reveal a similar requirement for UBZ domain in maintenance of chromosomal stability after MMC treatment. One potential

difference is that we are working with a knockout model of FAN1 and the Rouse lab works with a nuclease dead allele of FAN1. Nevertheless, it remains to be determined whether defects in the fork-protective function of FAN1 could contribute to KIN development. Another possibility that remains to be explored is the role of the UBZ domain in the potential functions of FAN1 in regulation of DNA mismatch repair (MMR) and nucleotide repeat expansion pathways, which are associated with diseases like hereditary colorectal cancer (CRC) and Huntington's disease (HD) (Bettencourt et al., 2016; Segui et al., 2015) (see section 5.2.3).

Consistent with the UBZ domain not being necessary for ICL resistance, we showed that FAN1 has ICL repair functions outside of the FA pathway. Our data are consistent with studies in DT40 chicken cells, which report that FAN1 is not epistatic with FANCC and FANCI in ICL resistance (Yoshikiyo et al., 2010). Based on the MMC-induced proliferation defect, the FA protein network represents the predominant ICL repair pathway in mammalian cells (Lachaud et al., 2016b; Thongthip et al., 2016; Zhou et al., 2012). However, we found that FAN1 depletion/inactivation can further enhance the ICL-induced sensitivity of FANCD2-depleted BJ cells, SLX4-depleted BJ cells, and FANCA-patient cells. Similarly, we observed that FAN1 depletion could also exacerbate chromosomal aberrations in MEF cells lacking FANCD2 upon exposure to a high level of ICLs. These results firmly establish the presence of an FA pathway-independent

functions of FAN1 that can protect cells from accruing extensive genomic alterations upon exposure to ICL agents.

5.1.2 Genetic interaction between FAN1 and other nucleases in ICL repair

In vitro biochemical analyses of SLX4/FANCP and XPF/FANCD1-dependent processing of the crosslinks and the ICL unhooking studies from *Xenopus* egg extracts, strongly support the major involvement of the 3' flap endonuclease activity of XPF/FANCD1, but not FAN1, in performing ICL unhooking (Douwel et al., 2014; Hodskinson et al., 2014). Lack of SLX4-interacting XPF sensitizes human cells to ICL-inducing agents to a greater extent than the depletion of FAN1. However, it is evident from the published biochemical analyses as well as from our own unpublished data, that FAN1 is very effective in incising and unhooking different types of crosslink substrates *in vitro* through its endonuclease and exonuclease activities (Pizzolato et al., 2015; Zhao et al., 2014)(A. Wang, L. Timashev, and A. Smogorzewska, unpublished). This suggests that the true function of FAN1 has not yet been identified. FAN1 may be involved in repair at stalled forks, which do not look like the converging replication forks formed on plasmids in the *Xenopus* egg extracts. It is also possible that FAN1 predominantly works in G1 unlike typical FA-associated proteins that function in S phase as illustrated by the experiments in *Xenopus* (Raschle et al., 2008). Another explanation for the lack of a discernible ICL unhooking defect in egg extracts depleted of FAN1, could be the presence of

redundant nucleases in the extracts. In our study, we identified SNM1A as being redundant with FAN1 during the ICL damage response. Unlike FAN1, SNM1A deficiency alone exhibits very mild crosslink sensitivity in mammalian cells (Ahkter et al., 2005; Dronkert et al., 2000). In fact, our analysis demonstrated that depletion of SNM1A in fibroblasts did not elicit any significant sensitization to ICLs. On the other hand, cells lacking both FAN1 and SNM1A became as sensitive to crosslinking agents as cells lacking the FA proteins such as SLX4 or FANCD2. This result suggests that the ICL repair could be severely compromised when both SNM1A and FAN1 are absent. The analysis of ICL incision and repair after co-depletion of FAN1 and SNM1A in the *Xenopus* egg extracts could shed further light on the unhooking of the ICLs. The long-term *in vivo* effects of a combined SNM1A and FAN1 deficiency have not been studied. It is possible that the redundant functions of the two nucleases contribute to the protection of kidney and liver tissues. It will be interesting to determine if the *Snm1a* knockout animals develop KIN and whether combined inactivation of *Fan1* and *Snm1a* could exacerbate KIN phenotypes.

5.2 The role of FAN1 in the protection of tissue function and human disease

The *Fan1* knockout mouse model exhibits karyomegaly in the kidney and liver. This phenomenon demonstrates age-dependence, as stronger phenotypes become more apparent in the older mice. Moreover, even though the *Fan1*-deficient mice display normal hematopoiesis under unstressed conditions, they

develop acute bone marrow dysfunction when challenged with MMC, which severely affects animal survival. Overall, our mouse model recapitulates the pathology of human KIN in which FAN1 mutations have been identified (Zhou et al., 2012). Although FAN1 mutations in the general population are rare, patients with such mutations are predicted to have an adverse reaction if they were treated ICL-inducing chemotherapeutics.

5.2.1 The role of FAN1 in the suppression of KIN pathogenesis

FAN1 protein appears to be ubiquitously expressed in various human tissues with a significant level detected in the kidney and liver, two of the tissues affected in KIN patients. *Fan1*-deficient mice display karyomegaly in epithelial cells lining the renal tubules in the kidney as well as in the hepatocytes in the liver, as early as at six months of age. Moreover, the number as well as the average area of the enlarged nuclei increases with time, suggesting that this phenomenon is a continuous and chronic process. The FISH analysis of 18-month-old mice revealed increased ploidy at three independent genomic loci consistent with reduplication of the genome in the karyomegalic nuclei. This observation implies that affected cells undergo replication cycles, which are not followed by successful mitoses. It is unclear at this point if the whole genome, or only parts of the genome are reduplicated in the absence of FAN1. In KIN patients, the karyomegalic nuclei in kidney tissue have also been shown to contain polyploid DNA. This supports our finding in *Fan1*-deficient mice, that the

enlargement of nuclei is a result of polyploidization that takes place in the absence of FAN1 (Bhandari et al., 2002; Spoendlin et al., 1995).

One possible reason for endoreduplication is exit from prolonged cell cycle arrest in the setting of persistent DNA damage. The arrest may not last permanently and is eventually overcome by mitosis and/or cytokinesis bypass with a new round of replication licensing and initiation cycle (Davoli et al., 2010). Alternatively, the absence of FAN1 may directly interfere with chromosome segregation or cytokinesis preventing the division of the duplicated genomes and cells, leading to an increase in ploidy level. More work is needed to understand the polyploidization of different tissues affected in KIN patients. The question of how polyploidization is allowed to take place in *Fan1*-deficient animals despite the presence of p53 also merits further investigation. The extensive karyomegaly seen in the liver in this mouse model could be useful for understanding the mechanism of polyploidization in normal hepatic tissue during aging.

Analysis of 18 months old *Fan1*-deficient mice revealed that, similar to KIN patients, the mice exhibit liver function abnormality as determined by an increase in AST and ALT and a reduction in the level of serum albumin and globulin, which are synthesized in the liver. Hepatocytes are especially prone to increasing their ploidy during development and in response to insults including DNA damage (reviewed in Gentric and Desdouets, 2014). The proportion of

karyomegalic polyploid hepatocytes is significantly higher in livers of *Fan1*-deficient mice compared to that of wild-type animals at 18 months. Based on our observation that the polyploidization is a progressive event and that there is a strong correlation between ploidy increase and functional decline of the animals, it is highly likely that polyploidization is a pathogenic and not an adaptive event in *Fan1*-deficient animals.

Although both the liver and the kidney of the *Fan1*-deficient mice display karyomegaly at 18 months, we only observe liver but not kidney dysfunction. The serum level of urea nitrogen, creatinine and electrolytes that we measured are more representative of glomerular function and are not specialized markers of proximal tubule function, the primary subtype of kidney tissues affected in *Fan1*-deficient mice (Hall et al., 2014; Labarga et al., 2009; Norden et al., 2000). Other markers that more accurately correspond with changes in proximal tubule function such as the urine level of glucose, amino acids and tubular proteins (e.g. retinol-binding protein) might be more appropriate for future assessment of functional impairment (Hall et al., 2014).

The kidney is a very resilient organ with high buffering capacity of tissue function and usually its functional decline only becomes apparent upon loss of the majority of kidney tissue. Our study was done in mice with C57BL/6J genetic background, and this strain is known to be less susceptible to developing kidney

deficiency. Another factor is a relatively short lifespan of mice which might not have allowed for sufficient kidney impairment despite the absence of FAN1. Additional insults including nephrectomy of one kidney or increase in the endogenous DNA damage load (see section 5.3), may be necessary to see effects of FAN1 deficiency on kidney function. Alternately, the genetic differences between mice and humans might be responsible for the less severe phenotypes exhibited by *Fan1*-deficient mice. It is possible that additional gene inactivation of a redundant nuclease such as SNM1A might expose kidney dysfunction in mice.

5.2.2 The role of FAN1 in the protection of bone marrow stem cells

In contrast to patients with Fanconi anemia, KIN patients do not develop pancytopenia at a young age (Zhou et al., 2012). However, when diagnosed with kidney failure, some KIN patients exhibit mild anemia of a presently unknown origin (Godin et al., 1996). The anemic phenotype observed in KIN patients could be an outcome of prolonged kidney dysfunction or alternatively a direct consequence of bone marrow abnormalities, prompting us to evaluate the bone marrow function of *Fan1*^{-/-} mice. These mice at either young or old age, display normal levels of peripheral blood cells compared to wild-type animals. The analysis of bone marrow histology and quantification of hematopoietic stem cell (HSC) frequency in 3 and 18 months old *Fan1*^{-/-} mice do not reveal a discernible change from the wild type levels. In competitive reconstitution experiments, LT-HSCs derived from bone marrow of *Fan1*^{-/-} mice were able to engraft with the

same efficiency as their wild-type counterparts. This result suggests that the function of hematopoietic stem cells is not compromised in *Fan1*-deficient mice. Additionally, we also determined that *Fan1* deficiency does not significantly enhance the HSC defect observed in *Fancd2*^{-/-} animals. Taken together, these data imply that the activity of FAN1 is dispensable for the protection of hematopoietic stem cells from DNA damage under unperturbed conditions.

Only one *Fan1*^{-/-} mouse in our study cohort exhibited signs of blood cytopenia during the first 18 months of life, which is most likely a sporadic event. Despite not being required under unstressed conditions, FAN1 is essential for the maintenance of hematopoiesis when animals are challenged with doses of crosslinking agents that can be well tolerated by the wild type animals. We determined that the bone marrow and thymus were particularly prone to ICL-induced toxicity in *Fan1*-deficient animals and that injection of these animals with MMC resulted in 90% mortality. Moreover, analysis of the c-Kit⁺ cells, which represent the hematopoietic stem cell population, revealed that the frequency of these cells, including the LSK and the LK populations is severely affected by the treatment with MMC. This result indicates that FAN1 is indispensable for the protection of both the stem and progenitor cells in the bone marrow upon exposure to an ICL-challenge. The sensitivity of the HSCs was specific to the ICL-induced damage, as ionizing radiation did not elicit the same level of pathology. Defects in the kidney and liver were not detected under the acute

MMC treatment used in this study. More chronic, low dose treatments might be necessary to induce kidney and liver dysfunction in young *Fan1*^{-/-} animals.

5.2.3 FAN1 and other human diseases

Other than KIN, mutations in FAN1 have been implicated as a pathogenic factor in a number of diseases including polyglutamine diseases such as Huntington's disease (HD) and multiple spinocerebellar ataxias (SCAs), hereditary colorectal cancer (CRC) and high-risk pancreatic cancer (PC) (Bettencourt et al., 2016; Segui et al., 2015; Smith et al., 2015). Occurrences of pulmonary carcinoma and hepatic lymphoma have also been reported in *Fan1* knockout mice at 20 months of age (Lachaud et al., 2016a). Additionally, a deletion of 15q13.2-13.3 which includes FAN1 and 4 other genes, has been identified in patients with Schizophrenia (SZ) (Chen et al., 2016; Forsingdal et al., 2016).

It is unclear how FAN1 variants are involved in the pathogenesis of these diseases. In the case of hereditary CRC, mutations associated are either truncation mutations such as p.Cys47* and p.Arg952* or missense mutations including p.Asp140Thr, p.Pro340Ser, and p.Arg591Trp. *FAN1*^{+/-} heterozygous cells with p.Cys47* variant were reported to have almost wild-type level of ICL resistance whereas among all the missense mutations, the p.Asp140Thr FAN1 variant was the only one to display ICL-repair defects as shown by its failure to

complement the ICL sensitivity of FAN1-deficient 293T cells (Segui et al., 2015). The ICL repair efficiency of cells carrying the pancreatic cancer variant p.Met50Arg of FAN1 has yet to be assessed (Smith et al., 2015). Nonetheless, this is the first time that the UBZ domain of FAN1 has been implicated to be functionally significant in human studies. To date, there is no evidence indicating the loss of heterozygosity or reduced level of FAN1 expression in CRC or PC tumor samples that harbor FAN1 variants (Broderick et al., 2017; Segui et al., 2015; Smith et al., 2015). These observations suggest a possibility that the FAN1 variants act as dominant alleles. Alternatively, the mutations could potentially affect the function of FAN1 outside of ICL repair, which may be affected by a haploinsufficiency of FAN1.

DNA mismatch repair (MMR) is one of the likely cellular processes that may require the activity of FAN1 for the protection against CRC and Huntington's disease (Bettencourt et al., 2016; Segui et al., 2015). The function of FAN1 in MMR has not been formally demonstrated, however, FAN1 was shown by multiple labs to be able to interact with MMR components including MLH1, MLH3, PMS2 and PMS1 (Kratz et al., 2010; Liu et al., 2010; MacKay et al., 2010; Smogorzewska et al., 2010). In accordance with this idea, mutations in MMR factors have been implicated in the control of DNA repeat stability that is known to underlie CRC and polyglutamine disease predisposition syndromes (Iyer et al., 2015; Mirkin, 2007; Tome et al., 2013; Wheeler et al., 2003). Given that the type

of CRC described in patients with FAN1 variants is MMR proficient, FAN1 might not be directly involved in the main MMR pathway (Segui et al., 2015). However, its function might be important for the modulation of the pathway to ensure that faithful DNA replication and repair occur, especially within the repetitive regions of the genome. In order to verify the plausible function of FAN1 in MMR and in the protection against repeat-instability disorders, more data need to be collected with larger control populations and the hypothesized functions of FAN1 need to be tested in cellular and animal models.

5.3 The endogenous source of ICL damage that requires FAN1's repair activity

The major unanswered question in the pathophysiology of KIN is the nature of lesions that FAN1 repairs. Given the recent data implicating acetaldehyde and formaldehyde in the pathogenesis of Fanconi anemia (Garaycochea et al., 2012; Hira et al., 2013; Langevin et al., 2011; Pontel et al., 2015), aldehydes are attractive candidates as endogenous sources of damage that could promote KIN in the absence of FAN1. Based on the sensitivity of *Fan1*-deficient MEFs to aldehydes, there was a possibility that FAN1 was involved in the repair of acetaldehyde- or formaldehyde- induced damage, particularly in the kidney and liver that are affected in KIN patients.

Our data indicate a mild growth defect in *Fan1*^{-/-}*Adh5*^{-/-} double-deficient animals, which implies that an increased basal formaldehyde level in *Adh5*-deficient mice could lead to the accumulation of formaldehyde-induced DNA damage that affects growth. The absence of ADH5 also results in smaller number of pups produced per litter, a phenotype which is slightly worsened upon inactivation of FAN1. Given that the testis and ovary from *Fan1*^{-/-}*Adh5*^{-/-} animals are within normal limits histologically (data not shown), we hypothesize that FAN1 might be required to maintain normal embryonic development, protecting developing embryos from formaldehyde insults, which arise in the absence of ADH5.

Kidney and liver function in *Fan1* mutant animals with *Aldh2* or *Adh5* inactivation are no different than in the wild-type or other single mutant control mice. The histology of kidney and liver from 3-month-old *Fan1*^{-/-}*Aldh2*^{-/-} or *Fan1*^{-/-}*Adh5*^{-/-} animals is within normal limits with no significant presence of karyomegalic cells. This result suggests that KIN phenotypes cannot be accelerated by ablating either acetaldehyde or formaldehyde detoxification in *Fan1*-deficient animals. Moreover, we can attribute the karyomegaly phenotype primarily to the absence of FAN1. At 12 months of age, *Fan1* single or the DKO mice lacking both *Fan1* and *Aldh2* or *Adh5* mice displayed similar levels of renal karyomegaly. Also, there was no sign of enhanced proliferation or DNA damage in the kidney tissue of *Fan1*^{-/-}*Aldh2*^{-/-} or *Fan1*^{-/-}*Adh5*^{-/-} animals. The fact that

suppression of *Aldh2* or *Adh5* in *Fan1*-deficient mice did not promote tissue karyomegaly and tissue damage, challenges the idea that acetaldehyde and formaldehyde contribute to KIN pathogenesis. Furthermore, even when *Fan1*^{-/-} *Aldh2*^{-/-} animals were additionally stressed with increased levels of acetaldehyde due to ethanol feeding in the absence of the detoxification pathway, no renal karyomegaly or kidney/liver functional decline was observed. The stress-enhancing experiment with *Fan1/Adh5* series is still on-going.

Lack of synergy between Fan1 and Adh5 in promoting kidney disease was unexpected. Recent work demonstrated that inactivation of ADH5, which is responsible for formaldehyde detoxification, resulted in tissue karyomegaly, kidney failure, and abnormal liver function when combined with *Fancd2* deficiency (Pontel et al., 2015). It is possible that the synergy was not seen because the etiology of karyomegaly in the absence of FANCD2 is different from its etiology in the absence of FAN1. *Fancd2*^{-/-}*Adh5*^{-/-} mice develop glomerular damage before they develop karyomegaly and this damage is absent in KIN patients and *Fan1*-deficient mice. Future experiments will be required to identify the mechanism of karyomegaly in both genetic backgrounds.

Besides effects on growth, ADH5 deficiency also had an adverse effect on the maintenance of the hematopoietic stem and progenitor populations in young 3 months old *Fan1*^{-/-}*Adh5*^{-/-}. This effect was not seen in *Fancd2*^{-/-}*Aldh2*^{-/-} mice.

The stronger phenotypes observed in *Fan1*^{-/-} mice lacking ADH5 when compared to mice lacking ALDH2, are reminiscent of the effects of these two aldehyde detoxification deficiencies in Fanconi anemia mice with *Fancd2*^{-/-}*Adh5*^{-/-} mice exhibiting more severe defects compared with *Fancd2*^{-/-}*Aldh2*^{-/-}. This could stem from the more severe nature of formaldehyde induced lesions or alternatively due to the increased number of lesions when ADH5 was absent.

Despite a reduction in the LSK frequency, the remaining *Fan1*^{-/-}*Adh5*^{-/-} HSCs can effectively function to support sufficient production of peripheral blood cells. We further assessed HSC function by testing the ability of the long-term HSCs to reconstitute hematopoiesis after serial transplantation. While there is no discernible functional compromise in the engraftment efficiency of the bone marrow lacking FAN1 in combination with ADH5 or ALDH2 after the first transplant, the secondary transplant revealed that both FAN1 and ALDH2 are required for long-term reconstitution of blood cells. Secondary transplant studies are still ongoing with *Fan1*^{-/-}*Adh5*^{-/-} mice.

Taken together, our results show that FAN1 contributes very subtly, to the protection of the bone marrow against acetaldehyde and formaldehyde-induced damage in the bone marrow. It is possible that in the bone marrow, nucleases associated with the Fanconi anemia pathway such as XPF are more active at clearing out aldehyde-induced crosslinks. Furthermore, SNM1A, a redundant

nuclease may be able to efficiently compensate for the lack of FAN1 in the bone marrow, masking the contribution of FAN1 to the repair of aldehyde-induced crosslinks. The generation and characterization of *Fan1*^{-/-}*Snm1a*^{-/-}*Aldh2*^{-/-} and *Fan1*^{-/-}*Snm1a*^{-/-}*Adh5*^{-/-} triple mutant mice would be of interest to examine such hypothesis.

Several questions regarding the contributions of FAN1 to KIN pathophysiology remain unanswered. We still do not know the endogenous source of lesions that leads to KIN pathogenesis. Based on our studies, it is unlikely that these are acetaldehyde or formaldehyde. It is still possible that FAN1 is required for the repair of damage inflicted by other reactive aldehydes. Therefore, investigating the contributions of other members of the aldehyde dehydrogenase/alcohol dehydrogenase family might of value. In addition, other metabolites that cause ICLs are possible candidates. To address this possibility, performing an unbiased screen for metabolic genes whose inactivation in combination with FAN1 deficiency produces a synthetic lethality or a synthetically reduced fitness at the cellular level and an acceleration of KIN phenotypes at the whole organism level, may prove to be a fruitful approach. Furthermore, the possibility of KIN being driven by lesions other than ICLs should not be overlooked. For instance, ischemia reperfusion model, which induces significant oxidative damage, could be used to stress the kidney to examine its impact on the maintenance of renal tubular cells and kidney function in the presence and

absence of FAN1. Identification of the endogenous lesion that needs FAN1 for its removal will be important not only for the basic understanding of FAN1 function but may also lead to therapeutic strategies to protect liver and kidney function in more general population.

Chapter 6: Materials and Methods

6.1 General procedures

6.1.1 Mammalian cell culture

Human patient fibroblasts were transformed by HPV16 E6E7 and immortalized by expression of catalytic subunit of human telomerase (hTERT). Cells were cultured at 3% oxygen and maintained in DMEM containing 15% FBS, 100 U/mL penicillin, 0.1 µg/mL streptomycin, 0.1 mM nonessential amino acids, and 0.1 mM glutamax (Life Technologies).

Primary MEFs were isolated from E13.5 embryos using standard techniques and cultured at 3% oxygen and in DMEM containing 15% FBS, 100 U/mL penicillin, 0.1 µg/mL streptomycin, 0.1 mM non-essential amino acids and glutamax (Life Technologies). MEFs were immortalized at passage 2 using pMSCVNeo HPV16E6E7.

6.1.2 Viral transduction of mammalian cells

For viral infections, 293T cells plated in 10 cm dishes the day before were transfected with 6 µg of plasmid DNA and the viral packaging vectors using TransIT reagent (Mirus). The media was changed once, 24 hours after transfection. The virus-containing supernatants were harvested at 24 hours and 48 hours later and filtered (0.45 µM filter). Polybrene was added at a final concentration of 4 µg/mL before used to infect the targeted cells. Cells were infected 2-3 at 12 hours intervals for each experimental condition. 24 hours after the infection, the infected cells were put under selection with the appropriate

antibiotic (puromycin (2 µg/mL), blasticidin (500 µg/mL), hygromycin (100 µg/mL) or neomycin (600 µg/mL). Selection was deemed completed after all uninfected control cells had died in the presence of antibiotic.

6.1.3 DNA damage sensitivity assays

Analyses of cell survival under DNA damaging agent treatment were performed in a 6-well plate format (except the experiments from Figure 4.2B-E, Figure 4.4A-B, and Figure 4.5E that were performed in a 96-well plate format) as previously described (Kim et al., 2013). Cells were seeded in triplicate at a density of $3.5-4 \times 10^4$ per well in a 6-well plate or 500 cells per well in a 96-well plate (Opaque White Microtest™ plate (BD, 353296)) before treatment with DNA damaging drugs (MMC (0-75 nM), HU (0-100 nM), CPT (0-20 nM)) 24 hours later. For cell survival assay following ionizing radiation, cells were first irradiated in suspension before plating. In the case of NU7026 or NU7441 pre-treatment for inhibition of DNA-PKcs, cells were first pre-treated with 10 µM NU7026 or 1 µM NU7441 for 3 hours before being subjected to MMC treatment in a media containing the corresponding DNA-PKcs inhibitor for the duration of the survival assay.

In the 6-well plate format, the cells were split once after 3 days of drug treatment. After additional 3–4 days of further culturing, cell numbers were determined using the Z2 Coulter Counter (Beckman Coulter). For the 96-well

plate format, cell viability was determined after 5 days in culture using the CellTiter-Glo reagent (Promega). 500 cells were plated per well in a 96-well plate (Opaque White Microtest™ plate (BD, 353296) and allowed to grow following the DNA damaging agent treatment for 4-5 days until the most confluent well reached ~ 80-90% confluency. 50 µl CellTiter-Glo reagent were added to each well, which contained 100 µl of media, mixed well by repeated pipetting and allowed to incubate at room temperature for 15 minutes before the luminescence signals were read. Luminescence signal/cell viability post-treatment were normalized to Luminescence signal /cell viability of the untreated samples to give the percentage of survival.

6.1.4 Cell proliferation assays

Cell proliferation was determined using the 96-well plate format. 500 cells were plated per well in a 96-well plate (Opaque White Microtest™ plate (BD, 353296)). Cell viability as determined by the luminescence signal was measured daily for 6 days using the CellTiter-Glo reagent (Promega). The luminescence signals were normalized to the luminescence signals measured on day 1 to give the percentage of cell proliferation.

6.1.5 siRNA-mediated knockdown

For siRNA transfection, cells were subjected to reverse transfection, using RNAiMax (Thermo Fisher). siRNAs were prepared at a final concentration of 25

nM in 500 μ l of Opti-MEM medium (Gibco) before mixing with 5 μ l of Lipofectamine RNAimax (Thermo) and transferred to empty 6-well plate. After 20 minutes of incubation at RT, ~ 150,000 cells diluted in 2 mL of media with no added antibiotic were added on top of the RNAi complexes per well. The media was changed once 24 hours later, and the RNAi-transfected cells were used at 72 hours following the transfection for each experiment.

6.1.6 shRNA-mediated knockdown

DNA-PKcs, 53BP1, Ku70 and Ku80 shRNA targeting sequences were amplified from ssDNA template using miRXhoF (cagaaggctcgagaaggtatattgctgttgacagtgagcg) and miREcoRIR (ctaaagtagcccccttgaattccgaggcagtagca) primers. The original shRNA expression vector pAHM - (pALPS-Hygro-miR30) vector was mutagenized to remove the EcoRI site within the hygromycin gene to leave only a unique EcoRI cut site within the miR30 cassette of the vector. The XhoI/EcoRI-digested amplified products were then ligated to the XhoI/EcoRI digested pAHM vector. FANCA was stably knocked down using pAHM-UltramiR generated by inserting MluI-HpaI fragments of shFANCA pGipz-UltramiR (Transomics) into pAHM. Sequences of shRNAs are given in 6.2.4. Cells were transduced with shRNA-expressing lentiviruses and selected for 1 week with 200 μ g/mL hygromycin until the selection was deemed completed after all uninfected control cells had died in the presence of antibiotic.

6.1.7 Gene targeting

RA3087 *FANCA*^{-/-} human fibroblasts and *Fan1*^{-/-} MEFs were transduced with lentivirus expressing of pCW-Cas9 vector encoding dox-inducible Cas9 expression cassette (Wang et al. 2014b) (plasmid 50661, Addgene, originally from Lander and Sabatini labs, MIT). After selection with 50 µg/mL hygromycin (for MEFs) or 3 µg/mL puromycin (for human fibroblasts), a single clone with undetected basal level of pCW-Cas9 but showed increased in expression following dox-induction was selected before being transduced with lentivirus expressing single guide RNA (sgRNA) (Sanjana et al. 2014; Wang et al. 2015) targeting *FAN1* in *FANCA*^{-/-} human fibroblasts or *Snm1a* in the *Fan1*^{-/-} MEFs. Following selection in 3 µg/mL puromycin (for MEFs) or 5 µg/mL blasticidin (for human fibroblasts), cells were treated with 100 ng/mL doxycyclin for 48 hours before single cells were plated in 96-well plates. Isolated clones were screened for CRISPR-mediated genome editing at target region by sequencing of genomic DNA. The reduction of the corresponding mRNA transcripts determined by RT-PCR or protein level was used to validate knockout. Sequences of sgRNAs are listed in 6.2.5.

6.1.8 G1/S and G2/M Checkpoint analysis

G1/S checkpoint

Cells were treated with 10 Gy IR. After resting for 10 hours, cells were pulsed by 10 µM BrdU for 30 minutes. The cells were then trypsinized and

harvested for fixation and analysis. Cells were fixed in ice-cold 100% methanol slowly while vortexing. After fixation, the fixed cells were stored at -20 °C at least 24 hours before staining. Methanol were then replaced by 1 mL 2 N HCl plus 0.2 mg/mL of pepsin and cells were incubated for 30 minutes at room temperature. To neutralized HCL, 3 mL of 0.1 M sodium tetraborate (pH 8.5) were added. Cells were then washed once in PBS before a second washed with 1%BSA/0.5% Tween-20/PBS. The staining was done with 1:20 FITC-conjugated anti-BrdU antibody (BD) in 1%BSA/0.5% Tween-20/PBS at room temperature for 30 minutes in the dark. Cells were washed once with PBS before resuspended in 500 µl of PBS/PI (20µg/mL)/RNase (200µg/mL) solution, incubated for 15-20 minutes at 37 °C and analyzed by LSRII flow cytometer (BD Pharmingen).

G2/M checkpoint

Cells were treated with 10 Gy IR and rested for 1 hour before arrested with 100 ng/µl nocodazole for 18 hours. The cells were then trypsinized and harvested for fixation and analysis. Cells were fixed in ice-cold 70% ethanol solution slowly while vortexing. After fixation, the fixed cells were stored at -20 °C at least 24 hours before staining. Cells were washed once with PBS before being permeabilized with 0.2%Triton X-100 in PBS for 10 minutes. Cells were then washed once in PBS before being blocked in 1%FBS/PBS for 30 minutes. After blocking cells were stained with 1 µg/ml anti-phospho H3 antibody (Upstate Rabbit) for 1 hour at 4 °C. Cells were washed once with PBS before being

stained with 1:1000 Secondary antibody 30 minutes at 4 °C in the dark. Cells were washed once with PBS before resuspended in 500 µL of PBS/PI (20µg/mL)/RNase (200µg/mL) solution, incubated for 15-20 minutes at 37 °C and analyzed by LSRII flow cytometer (BD Pharmingen).

6.1.9 Southern blotting

Cells were collected by trypsinization, washed once in PBS and processed for genomic DNA isolation. Genomic DNA was extracted as previously described (de Lange et al., 1990). Genomic DNA was digested by a restriction enzymes BamHI overnight before being run on a 0.7% agarose gel overnight. The gels were depurinated with 0.25N HCl, denatured and neutralized using standard Southern blotting protocol and transferred to nitrocellulose membrane. The probes were synthesized by Klenow-based labeling using random hexamers and α -³²P-dCTP. Membranes were exposed to PhosphorImager screens and quantified with ImageQuant software.

6.1.10 Quantitative reverse transcription-polymerase chain reaction (qRT-PCR)

RNA was isolated using the RNeasyPlus extraction kit (Qiagen). cDNA was synthesized using the SuperScript III First-Strand Synthesis System (Life Technologies) and qRT-PCR was performed using the Platinum SYBR Green qPCR SuperMix-UDG (Life Technologies) on an Applied Biosystems 7900HT

Sequence Detection System. All steps were carried out as per the manufacturers' instructions. Differences between samples calculated using QuantStudio software (Applied Biosystems) using the Δ CT method and were normalized to actin. Primers used for qRT-PCR are listed in 6.2.3.

6.1.11 Mutagenesis

Mouse *Fan1* cDNA was prepared by SuperScript III Reverse Transcriptase (Thermo)-mediated cDNA synthesis using wild type mouse embryonic fibroblasts (MEFs) RNA extract. The cDNA was cloned into pENTR™/D-TOPO (Lifetechnologies). Mutagenesis was performed using the QuikChange Multi Site-Directed mutagenesis kit (Agilent) as per the manufacturer's instructions using oligonucleotides listed in 6.2.2.

6.1.12 Cell lysates and immunoblotting

Cells were lysed in 2X Laemmli buffer (125 mM Tris-HCl, pH 6.8, 200 mM DTT, 4% SDS, 20% glycerol, 0.02% bromophenol blue) at 10^6 cells per 100 μ l, sonicated at Amplitude 20 for 30 seconds (S-4000, MISONIX), and boiled for 5 minutes at 100 °C. The processed lysates were loaded at the equivalent of 1.5-2 10^5 cells per lane. Protein samples were separated by SDS-PAGE and blotted onto PVDF blotting membranes (GE healthcare Life Sciences). Membranes were blocked in 3% milk in t-BST (0.1% Tween-20 in 50mM Tris, 150mM NaCl, pH 7.6) for 1 hour at RT and incubated with primary antibody in 3% milk containing t-

BST overnight at 4 °C or for 2-3 hours at RT. Membranes were washed 3 times in t-BST, 10 minutes each and incubated with secondary antibody in t-BST for 1 hour at RT, and washed 3 times 10 minutes each with t-BST at RT. Blots were developed with enhanced chemiluminescence (Perkin Elmer) on Multimage II FlourChem HD2 Imaging system (Alpha Innotech).

6.1.13 Immunofluorescence

Cells were grown on autoclaved-round coverslips. Cells were rinsed once with PBS, before being fixed with 3.7% formaldehyde in PBS for 10 minutes at RT and washed three times with PBS. Cells were blocked with PBG (0.2% (w/v) cold water fish gelatin (Sigma), 0.5% (w/v) BSA (Sigma) in PBS) for 20 minutes at RT, before being incubated with primary antibody diluted in PBG for 2 h at RT or overnight at 4 °C. Afterwards, cells were washed 3 times with PBG at RT, incubated with secondary antibody diluted 1:500 in PBG for 1 hour at RT, and washed 2 times with PBG and 1 time with PBS. Coverslips were sealed onto glass sides with mounting medium (VECTASHIELD with DAPI, Vector). Images were captured with a Zeiss Axio Observer A1 microscope using Axiovision software.

6.1.14 Chromosome breakage analysis

Cells were plated at around 75% confluency before being exposed to 50-100 nM MMC 12 hours later for 24 hours. Afterwards, cells were arrested

for 2 hours with 0.167 $\mu\text{g/mL}$ of colcemid (EMD) (without media change). Cells were harvested, incubated in 0.075 M KCl for 15 minutes at 37°C, and fixed in freshly prepared methanol:glacial acetic acid (3:1). Metaphase spreads were prepared by dropping cells onto pre-wetted microscope slides. Slides were air-dried overnight at 40°C before staining with 6% Karyomax Giemsa (Life Technologies) in Gurr buffer (Life Technologies) for 3 min. After rinsing with fresh Gurr buffer and distilled water, slides were fully dried at room temperature and scanned using the Metasystems Metafer. One-way ANOVA test was used to determine the statistical significance. The quantification was blinded.

6.1.15 Histology

Tissues were harvested and fixed in 10% neutral buffered formalin for 20 hours at 4 °C. They were then washed twice with water before transferred to 70% ethanol solution. The bone decalcification (femur/tibia), paraffin embedding, sectioning and hematoxylin & eosin (H&E) staining were performed at the Center for Comparative Medicine and Pathology at MSKCC. Quantification of nuclear area in tissues was performed blinded to the genotype of the sample. Images were captured at 40X objective on a Zeiss Axiovert 40 microscope and then analyzed in ImageJ. The area (cross-sectional area) of at least 150 nuclei from renal tubular epithelial cells or glomerular cells were measured and normalized to the median nuclear area of each section. Data were then plotted and grouped according to area.

6.1.16 Fluorescent in situ hybridization (FISH)

FISH analysis was performed by the MSKCC Molecular Cytogenetics Core. It is analyzed on a 5 µm-thick formalin fixed paraffin section using an in-house 3-color probe for chromosomal regions: 12qA1.1, 16qA and 17qA1. The probe mix consisted of the following BAC clones: 12qA1.1 (clones RP23-168O9, RP23-54G4 & RP23-41E22; labeled with Green dUTP); 16qA (clones RP23-290E4, RP23-356A24 & RP23-258J4; labeled with Red dUTP); and 17qA1 (clones RP23-73N16, RP23-354J18 & RP23-202G20; labeled with Orange dUTP). Probe labeling, hybridization, post-hybridization washing, and fluorescence detection were performed according to standard procedures. Slides were scanned using a Zeiss Axioplan 2i epifluorescence microscope equipped with a megapixel CCD camera (CV-M4+CL, JAI) controlled by Isis 5.5.9 imaging software (MetaSystems Group Inc, Waltham, MA).

6.1.17 Generation of *Fan1*-deficient mouse strain

All of the animals were handled according to the Rockefeller University institutional animal care and use committee (IACUC) protocols. *Fan1* gene targeting construct (Fan1tm1a(KOMP)Wtsi; MGI code: 4940765) was generated by the Knockout Mouse Project KOMP. The construct was electroporated into albino B6 mice-derived embryonic stem cells (ES) and the targeted ES cells were injected into C57BL/6J blastocyst to generate chimeric animals by the Gene Targeting and the Transgenic services at the Rockefeller University. Germline

transmission of the targeted allele - *Fan1(stop)* was verified by the 5' and 3' probes on Southern blots (Figure 2.4) and used to generate *Fan1lox* from the cross with FLPe deleter mouse strain (Jackson Labs). *Fan1 Δ ex3&4* allele was generated from the cross between *Fan1+/lox* and E2a-Cre mice (Jackson Labs). *Fanca* and *Fancd2*-deficient mice of 129SV background were obtained from Marcus Grompe (Noll et al. 2002; Houghtaling et al. 2003). *Slx4* and *Mus81*-deficient mice of C57/Bl6 background were obtained from Paula Cohen (Dendouga et al. 2005; Holloway et al. 2011). *Aldh2*- and *Adh5*- deficient mice of C57/Bl6 background were obtained from KJ Patel (Langevin et al. 2011; Pontel et al. 2015).

6.1.18 Genotyping

Genotyping was carried out by PCR on DNA isolated from mouse tail samples digested overnight in 250 µl Direct PCR Lysis reagent (Yolk Sac, Viagenbiotech supplemented with 0.4 mg/mL Proteinase K. PCR was performed in 20 µl reaction containing 1.5 µl of DNA extract, 10x PCR buffer (Qiagen), 0.2 mM dNTP, 1% DMSO, 0.15 U of Taq polymerase (Qiagen) and 0.25/0.5 µM of each individual primer. Genotyping primers are shown in 6.2.1.

6.1.19 Whole-animal MMC sensitivity

12 weeks old mice were injected intraperitoneally with a single dose of 10 mg of MMC per kg of body weight. Survival and body weight measurements were

recorded daily. The percentage of survival was calculated according to the Kaplan and Meier method (Kaplan and Meier 1958). Differences in survival between the different genotypes were tested for significance by the Log-Rank test. The hematopoietic analyses were done seven days following MMC treatment in an independent cohort of mice. The blood was collected by cardiac puncture and analyzed for complete blood count (CBC) and serum level of liver and kidney marker analytes at the Center for Comparative Medicine and Pathology at MSKCC. The bone marrow cells were collected for LSK analysis.

6.1.20 Alcohol administration in mice

Ethanol was provided to mice ad libitum in two different administration schemes. For short-term exposure, water supply was replaced by a 15% Ethanol solution for 5 days, followed by a 20% ethanol solution for another 5 days. Alternatively, a 10% ethanol solution was provided to mice for 1 month in a long-term treatment scheme. To administer methanol, mice were gavage-fed with methanol solution to a final dose of 80 mg/kg, 5 days per week for 4 weeks. Following the treatments, mice were sacrificed for histological examination, hematopoietic and genome instability analysis.

6.1.21 LSK analysis

Bone marrow cells were isolated from the femurs and tibiae of mice by crushing the bone in FACs buffer (2% FBS in 1X PBS) followed by an additional

wash in FACs buffer, before being filtered through a 40-mm cell strainer. The early progenitor cells (c-Kit⁺) were enriched by a 30-minute incubation with CD117 (c-Kit) microbeads (Miltenyi Biotec) before passing through the LS column (Miltenyi Biotec) placed under magnetic field. The column was washed once with FACs buffer, followed by an elution outside of the magnetic field. The c-Kit⁺ enriched cells were stained for 1 hour at 4 °C with the following antibodies – PerCP-Cyanine5.5-conjugated lineage cocktail with antibodies anti-CD4 (Clone: RM4-5 eBioscience), CD3e (Clone: 145-2C11 eBioscience), Ly-6G/Gr-1 (RB6-8C5 eBioscience), CD11b/Mac-1 (Clone: M1/70 eBioscience), CD45R/B220 (RA3-6B2 eBioscience), CD8a (Clone: 53-6.7 eBioscience), and TER-119 (eBioscience), anti-c-Kit (APC, Clone: 2B8 eBioscience), anti-Sca-1 (BV421, Clone: D7 biolegend), anti-CD150 (SLAM) (PE, Clone: TC15-12F12.2 biolegend) and anti-CD34 (FITC, Clone: RAM34 eBioscience) and anti- CD16/32 (AF700, Clone: 93 ebioscience) (Frascoli et al. 2012). After one wash with FACs buffer, the samples were resuspended in FACs buffer with 7-AAD (ebioscience) before run on a LSRII flow cytometer (BD Pharmingen) and the data were analyzed with the FlowJo software.

6.1.22 Long-term bone marrow reconstitution analysis

The bone marrow cells were isolated from donor animals (CD45.2) and prepared as described in 6.1.21. To count the number of live nucleated cells, a fraction of cells was treated with ACK lysing buffer (Life technologies) for 10

minutes, followed by Trypan blue staining, and counted using a Countess Cell counter (Life Technologies). 5×10^5 (primary transplant) or 2×10^6 (secondary transplant) total bone marrow cells from femur/tibia of donor (CD45.2) mixed with 2.5×10^5 total bone marrow competitor cells (CD45.1) in PBS were transplanted to the recipient animals (CD45.1) through retro-orbital injection. The recipient animals were pre-conditioned with 2 doses of 450 cGy x-ray irradiation with a 3-hour resting interval. The level of reconstitution efficiency was determined by the ratio of CD45.2 to CD45.1 white blood cells using the following antibodies cocktail – anti-Ter119 (APC eBioscience), anti-Gr-1 (PE eBioscience), anti-Mac1 (PB Biolegend), anti-B220 (BV521 Biolegend), anti-CD3 (APC-Cy7 Biolegend), anti-CD45.1 (PE-Cy7 eBioscience), anti-CD45.2 (Pecp-Cy5.5 eBioscience), and Propidium iodide (PI Sigma) and analyzed with before run on a LSRII flow cytometer (BD Pharmingen) at 1, 2, or 4 months.

6.1.23 Micronuclei analysis of genome instability

The analysis was done as described in (Balmus et al., 2015). The blood was collected through retro-orbital bleeding by heparinized capillary tubes (Fisher) or cardiac puncture (if the animals were sacrificed) into the EDTA-coated tubes (Greiner Bio-One). The blood was then resuspended in heparin solution before fixed in cold methanol and stored directly at -80°C for at least 12 hours. After one wash with bicarbonate buffer, the cells were stained with anti-CD71 (FITC SouthernBiotech) in a solution containing 5 mg/mL RNase (Sigma). After 1

wash with bicarbonate buffer, the cells were resuspended in bicarbonate buffer containing 5 mg/mL PI and analyzed with a LSRII flow cytometer (BD Pharmingen).

6.1.24 *In vitro* analysis of hematopoietic stem cell sensitivity to MMC

c-Kit⁺ enriched cells were isolated as described in 6.1. The cells were then cultured in DMEM/F12 (Gibco) containing 100 U/mL penicillin, murine recombinant cytokines including TPO (100 ng/mL Peprotech), SCF (100 ng/mL Peprotech), FLT-3 (100 ng/mL Peprotech), IL-3 (20 ng/mL Peprotech), IL-6 (20 ng/mL Peprotech). 24 hours later, the MMC were added at different concentrations (0 nM, 100 nM, 200 nM) and the cells were cultured for additional 48 hours. The cells were then harvested and washed once with FACs buffer before stained for the LSK markers as described in 6.1.21.

6.2 List of primers

6.2.1 Genotyping primers

Mouse genotyping primers		
Genotype	Primer sequences	Amplicon size (bp)
<i>Fan1+</i>	5'-AAGGTCTGTGGTCATCGTGTCTCAG-3' 5'-AAACGATCCCTGTCTGGCTGA-3'	292
<i>Fan1-</i>	5'-TGAGACAGCTCAACTGGCACT-3' 5'-AAACGATCCCTGTCTGGCTGA-3'	543
<i>Fancd2+</i>	5'-TCAGCCTCACATGGAGTTTAACG-3' 5'-AA TTCGCCAATGACAAGACGC-3'	300
<i>Fancd2-</i>	5'-TCAGCCTCACATGGAGTTTAACG-3' 5'-CAGGGATGAAAGGGTCTTACGC-3'	550
<i>Fanca+</i>	5'-TTCCTTCAAAGCTGCTGGGG-3' 5'-CAGTGACATCTTCCTTCCTAACTCC-3'	350
<i>Fanca-</i>	5'- TTCCTTCAAAGCTGCTGGGG-3' 5'- GGTGAACGTTACAGAAAAGCAGGCT-3'	600
<i>Slx4+</i>	5'-CACTGAGCCATCTCACCAGC-3' 5'-GGAGCCCAGTCTGGGACTCTG-3'	475
<i>Slx4f3</i>	5'-CACTGAGCCATCTCACCAGC-3' 5'-TCGTGGTATCGTTATGCGCC-3'	298
<i>Mus81+</i>	5'-CTAGCCGCTTGCGTTCCACAATGT-3' 5'-GGAGCTAAGGCCTAGCGAGTACAG-3'	418
<i>Mus81-</i>	5'-GGTGTGGCCCTGATGGAAGAG-3' 5'-GGAGCTAAGGCCTAGCGAGTACAG-3'	380
<i>Aldh2+</i>	5'-AAACTTTGCACACACTGTCCC-3' 5'-CCCAGATCCAAGTGTAGGAATAC-3'	212
<i>Aldh2-</i>	5'-AAACTTTGCACACACTGTCCC-3' 5'-GCTTCACTGAGTCTCTGGCATCTC-3'	441
<i>Adh5+</i>	5'-TCAAGAGGTGAGGCTACAAGTT-3' 5'-GGCATGTCTTCATTTAGCTCAC-3'	200
<i>Adh5-</i>	5'-CCTGCCGAGAAAGTATCCATCATG-3' 5'-CCAAGCTCTTCAGCAATATCACG-3'	374

6.2.2 Mutagenesis

Mutagenesis primers	
Mutation	Primer sequences
FAN1 C44A/C47A	5'-CAGTGCACCACCTGCTAAACTTGCAGCT TCAACTGCTCATAAAATGGTGCCCA-3'
FAN1 L480P	5'-TCTGCTCCTGAGCCGAAAGCCCTGGCC-3'
FAN1 D963A	5'-GGGGCCTCCCAGCCTTGGTGGTGTG-3'

6.2.3 RT-PCR

RT-PCR primers	
Gene	Primer sequences
Mouse <i>Fan1</i>	5'-CACAGTCCTGTGTTCTGTGGA-3' 5'-TCAAAGCCACTCTGCCTGTA-3'
Mouse <i>Snm1a</i>	5'-GCAAAGTCCACACACTGTTCC-3' 5'-CTGCTGTGACGGGAAGGTAT-3'
Mouse Actin	5'-CTAAGGCCAACCGTGAAAAG-3' 5'-ACCAGAGGCATACAGGGACA-3'

6.2.4 List of shRNAs

shRNA target sequences	
shRNA	Target sequences
Mouse <i>Snm1a.1</i>	5'-TGACTCTTTTCTGCTTCT-3'
Mouse <i>Snm1a.2</i>	5'-CAGAATCTGTTGAAAAATCA-3'
Mouse <i>Snm1a.3</i>	5'-CATGTCCGTTCTATAAGAGA-3'
Human <i>DNA-PKcs.1</i>	5'- AAAGCATGTTTCTTTAAATAA-3'

Human <i>DNA-PKcs.2</i>	5'-CCCGGTAAAGATCCTAATTCT-3'
Human <i>DNA-PKcs.3</i>	5'-CCACCATGGATGTGTTTGTCA-3'
Human <i>Ku70.1</i>	5'-AACGGATCTGACTACTCACTC-3'
Human <i>Ku70.2</i>	5'-ACAGGTTAAAGCTGAAGCTCA-3'
Human <i>Ku70.3</i>	5'-CAGGGAAAGTTACCAAGAGAA-3'
Human <i>Ku80.1</i>	5'-CCAGCTGGATATTATAATTCAT-3'
Human <i>Ku80.2</i>	5'-CCCCGCTGAGGTGACAACAAA-3'
Human <i>Ku80.3</i>	5'-CAAGAGAGAAAGTTTCGTTAT-3'
Human <i>53BP1.1</i>	5'-CAAGGATGTACATGTTGTAAA-3'
Human <i>53BP1.2</i>	5'-AAAGGAGAAGAGGAGAAAGAA-3'
Human <i>53BP1.3</i>	5'-AACGATTATGTTTCTCACTAA-3'
Human <i>FANCA.1</i>	5'-CCTGCAGAGAATGCTGATTTT-3'
Human <i>FANCA.2</i>	5'-AACAGTATGTTCTCCCGTCTT-3'

6.2.5 List of sgRNAs

sgRNA target sequences	
Gene	Target sequences
Mouse <i>Snm1a</i>	5'-CGAAGGTGCGCCCTGTTTAT-3'
Human <i>FAN1</i>	5'-CGTTCAAGTGGATCCAGGG-3'

6.3 List of Antibodies

Antigen	ID	Source	Uses
mFAN1	S101D	John Rouse lab	WB
mFANCD2	EPR2302	Abcam	WB
HA	MMS-101R	Covance	WB, IF
hFAN1	AP394	In-house	WB
GFP	Clones 7.1 and 13.1	Roche	WB, IF
γ H2AX	JBW301/05-636	Upstate	WB, IF
H2AX	A300-082A	Bethyl	WB
hDNA-PKcs	Clone: 25-4	Fisher	WB
h53BP1	NB100-304	Novus	WB, IF
hKu70	N3H10	NeoMarkers	WB
hKu80	C-ter Ku80	Lisa Postow Funabiki lab	WB
hFANCA	A301-980A	Bethyl	WB
hFANCI	AP583	In-house	WB
hFANCD2	NB100-182	Novus	WB, IF
hXPF/ERCC4	Bethyl	A301-315A	WB
hMUS81	M1445	Sigma	WB
α tubulin	T9026	Sigma	WB

6.4 List of cell lines

Cell lines	Organism
BJ	Human, Fibroblasts
A1170-22 (KIN patients)	Human, Fibroblasts
A4466 (KIN patients)	Human, Lymphocytes
A4486 (KIN patients)	Human, Lymphocytes
A4385 (KIN patients)	Human, Lymphocytes
RA3087 (FA-A patients)	Human, Fibroblasts
RA2645 (FA-D2 patients)	Human, Fibroblasts
RA3331 (FA-P/SLX4 patients)	Human, Fibroblasts
RA3087 pcwCAS9	Human, Fibroblasts
RA2645 pcwCAS9	Human, Fibroblasts
RA3087 $sgFAN1$	Human, Fibroblasts
RA2645 $sgFAN1$	Human, Fibroblasts
WT HCT 116	Human, Colorectal carcinoma
$LIG4^{+/-}$ HCT 116	Human, Colorectal carcinoma
$LIG4^{-/-}$ HCT 116	Human, Colorectal carcinoma
$LIG3^{-/-}$ +mtLIG3 HCT 116	Human, Colorectal carcinoma
$LIG3^{-/-}$ +mtLIG3+ncLIG3 HCT 116	Human, Colorectal carcinoma
$LIG3^{-/-}$ +mtLIG3+nc Δ BRCTLIG3 HCT 116	Human, Colorectal carcinoma

Cell lines	Organism
<i>Fan1</i> ^{+/+}	Mouse, E13.5 MEFs
<i>Fan1</i> ^{+/-}	Mouse, E13.5 MEFs
<i>Fan1</i> ^{-/-}	Mouse, E13.5 MEFs
<i>Fancd2</i> ^{-/-}	Mouse, E13.5 MEFs
<i>Fan1</i> ^{-/-} <i>Fancd2</i> ^{-/-}	Mouse, E13.5 MEFs
<i>Fanca</i> ^{-/-}	Mouse, E13.5 MEFs
<i>Fan1</i> ^{-/-} <i>Fanca</i> ^{-/-}	Mouse, E13.5 MEFs
<i>Fan1</i> ^{-/-} <i>sgSnm1a.6</i>	Mouse, E13.5 MEFs
<i>Slx4f3/f3</i>	Mouse, E13.5 MEFs
<i>Fan1</i> ^{-/-} <i>Slx4f3/f3</i>	Mouse, E13.5 MEFs
<i>Mus81</i> ^{-/-}	Mouse, E13.5 MEFs
<i>Fan1</i> ^{-/-} <i>Mus81</i> ^{-/-}	Mouse, E13.5 MEFs

Chapter 7: References

Adamo, A., Collis, S.J., Adelman, C.A., Silva, N., Horejsi, Z., Ward, J.D., Martinez-Perez, E., Boulton, S.J., and La Volpe, A. (2010). Preventing nonhomologous end joining suppresses DNA repair defects of Fanconi anemia. *Mol Cell* 39, 25-35.

Ahkter, S., Richie, C.T., Zhang, N., Behringer, R.R., Zhu, C., and Legerski, R.J. (2005). Snm1-Deficient Mice Exhibit Accelerated Tumorigenesis and Susceptibility to Infection. *Mol Cell Biol* 25, 10071-10078.

Airik, R., Schueler, M., Airik, M., Cho, J., Porath, J.D., Mukherjee, E., Sims-Lucas, S., and Hildebrandt, F. (2016). A FANCD2/FANCI-Associated Nuclease 1-Knockout Model Develops Karyomegalic Interstitial Nephritis. *J Am Soc Nephrol* 27, 3552-3559.

Alter, B.P. (2003). Cancer in Fanconi anemia, 1927-2001. *Cancer* 97, 425-440.

Alter, B.P., Giri, N., Savage, S.A., Peters, J.A., Loud, J.T., Leathwood, L., Carr, A.G., Greene, M.H., and Rosenberg, P.S. (2010). Malignancies and survival patterns in the National Cancer Institute inherited bone marrow failure syndromes cohort study. *Br J Haematol* 150, 179-188.

Auerbach, A.D. (2009). Fanconi anemia and its diagnosis. *Mutation Research/Fundamental and Molecular Mechanisms of Mutagenesis* 668, 4-10.

Auerbach, A.D., Rogatko, A., and Schroeder-Kurth, T.M. (1989). International Fanconi Anemia Registry: relation of clinical symptoms to diepoxybutane sensitivity. *Blood* 73, 391-396.

Auerbach, C. (1949). The Mutagenic Mode of Action of Formalin. *Science* 110, 419-420.

Ballard, H.S. (1997). The hematological complications of alcoholism. *Alcohol Health Res World* 21, 42-52.

Balmus, G., Karp, N.A., Ng, B.L., Jackson, S.P., Adams, D.J., and McIntyre, R.E. (2015). A high-throughput in vivo micronucleus assay for genome instability screening in mice. *Nat Protoc* 10, 205-215.

Bettencourt, C., Hensman-Moss, D., Flower, M., Wiethoff, S., Brice, A., Goizet, C., Stevanin, G., Koutsis, G., Karadima, G., Panas, M., *et al.* (2016). DNA repair pathways underlie a common genetic mechanism modulating onset in polyglutamine diseases. *Ann Neurol* 79, 983-990.

Bhandari, S., Kalowski, S., Collett, P., Cooke, B.E., Kerr, P., Newland, R., Dowling, J., and Horvath, J. (2002). Karyomegalic nephropathy: an uncommon cause of progressive renal failure. *Nephrol Dial Transplant* 17, 1914-1920.

Bird, R.P., Draper, H.H., and Basrur, P.K. (1982). Effect of malonaldehyde and acetaldehyde on cultured mammalian cells. Production of micronuclei and chromosomal aberrations. *Mutat Res* 101, 237-246.

Blier, P.R., Griffith, A.J., Craft, J., and Hardin, J.A. (1993). Binding of Ku protein to DNA. Measurement of affinity for ends and demonstration of binding to nicks. *J Biol Chem* 268, 7594-7601.

Bluteau, D., Masliah-Planchon, J., Clairmont, C., Rousseau, A., Ceccaldi, R., Dubois d'Enghien, C., Bluteau, O., Cuccuini, W., Gachet, S., Peffault de Latour, R., *et al.* (2016). Biallelic inactivation of REV7 is associated with Fanconi anemia. *J Clin Invest* 126, 3580-3584.

Bouwman, P., Aly, A., Escandell, J.M., Pieterse, M., Bartkova, J., van der Gulden, H., Hiddingh, S., Thanasoula, M., Kulkarni, A., Yang, Q., *et al.* (2010). 53BP1 loss rescues BRCA1 deficiency and is associated with triple-negative and BRCA-mutated breast cancers. *Nat Struct Mol Biol* 17, 688-695.

Broderick, P., Dobbins, S.E., Chubb, D., Kinnersley, B., Dunlop, M.G., Tomlinson, I., and Houlston, R.S. (2017). Validation of Recently Proposed Colorectal Cancer Susceptibility Gene Variants in an Analysis of Families and Patients-a Systematic Review. *Gastroenterology* 152, 75-77 e74.

Bunting, S.F., Callen, E., Kozak, M.L., Kim, J.M., Wong, N., Lopez-Contreras, A.J., Ludwig, T., Baer, R., Faryabi, R.B., Malhowski, A., *et al.* (2012). BRCA1 functions independently of homologous recombination in DNA interstrand crosslink repair. *Mol Cell* 46, 125-135.

Bunting, S.F., Callen, E., Wong, N., Chen, H.T., Polato, F., Gunn, A., Bothmer, A., Feldhahn, N., Fernandez-Capetillo, O., Cao, L., *et al.* (2010). 53BP1 inhibits homologous recombination in Brca1-deficient cells by blocking resection of DNA breaks. *Cell* 141, 243-254.

Burry, A.F. (1974). Extreme dysplasia in renal epithelium of a young woman dying from hepatocarcinoma. *J Pathol* 113, 147-150.

Butturini, A., Gale, R.P., Verlander, P.C., Adler-Brecher, B., Gillio, A.P., and Auerbach, A.D. (1994). Hematologic abnormalities in Fanconi anemia: an International Fanconi Anemia Registry study. *Blood* 84, 1650-1655.

Cannavo, E., Gerrits, B., Marra, G., Schlapbach, R., and Jiricny, J. (2007). Characterization of the interactome of the human MutL homologues MLH1, PMS1, and PMS2. *J Biol Chem* 282, 2976-2986.

Casanova-Schmitz, M., and Heck, H.D. (1983). Effects of formaldehyde exposure on the extractability of DNA from proteins in the rat nasal mucosa. *Toxicol Appl Pharmacol* 70, 121-132.

Castor, D., Nair, N., Déclais, A.-C., Lachaud, C., Toth, R., MacArtney, T.J., Lilley, D.M.J., Arthur, J.S.C., and Rouse, J. (2013). Cooperative control of holliday junction resolution and DNA repair by the SLX1 and MUS81-EME1 nucleases. *Mol Cell* 52, 221-233.

Cattell, E., Sengerova, B., and McHugh, P.J. (2010). The SNM1/Pso2 family of ICL repair nucleases: from yeast to man. *Environ Mol Mutagen* 51, 635-645.

Ceccaldi, R., Parmar, K., Mouly, E., Delord, M., Kim, J.M., Regairaz, M., Pla, M., Vasquez, N., Zhang, Q.S., Pondarre, C., *et al.* (2012). Bone marrow failure in Fanconi anemia is triggered by an exacerbated p53/p21 DNA damage response that impairs hematopoietic stem and progenitor cells. *Cell Stem Cell* 11, 36-49.

Ceccaldi, R., Sarangi, P., and D'Andrea, A.D. (2016). The Fanconi anaemia pathway: new players and new functions. *Nat Rev Mol Cell Biol* 17, 337-349.

Chapman, J.R., Taylor, M.R., and Boulton, S.J. (2012). Playing the end game: DNA double-strand break repair pathway choice. *Mol Cell* 47, 497-510.

Chen, J., Calhoun, V.D., Perrone-Bizzozero, N.I., Pearlson, G.D., Sui, J., Du, Y., and Liu, J. (2016). A pilot study on commonality and specificity of copy number variants in schizophrenia and bipolar disorder. *Transl Psychiatry* 6, e824.

Chiruvella, K.K., Liang, Z., and Wilson, T.E. (2013). Repair of double-strand breaks by end joining. *Cold Spring Harb Perspect Biol* 5, a012757.

Chuang, S.C., La Vecchia, C., and Boffetta, P. (2009). Liver cancer: descriptive epidemiology and risk factors other than HBV and HCV infection. *Cancer Lett* 286, 9-14.

Ciccia, A., and Elledge, S.J. (2010). The DNA damage response: making it safe to play with knives. *Mol Cell* 40, 179-204.

Clauson, C., Scharer, O.D., and Niedernhofer, L. (2013). Advances in understanding the complex mechanisms of DNA interstrand cross-link repair. *Cold Spring Harb Perspect Biol* 5, a012732.

Crossan, G.P., van der Weyden, L., Rosado, I.V., Langevin, F., Gaillard, P.-H.L., McIntyre, R.E., Gallagher, F., Kettunen, M.I., Lewis, D.Y., Brindle, K., *et al.* (2011). Disruption of mouse Slx4, a regulator of structure-specific nucleases, phenocopies Fanconi anemia. *Nat Genet* 43, 147-152.

Davoli, T., Denchi, E.L., and de Lange, T. (2010). Persistent telomere damage induces bypass of mitosis and tetraploidy. *Cell* *141*, 81-93.

de Lange, T., Shiue, L., Myers, R.M., Cox, D.R., Naylor, S.L., Killery, A.M., and Varmus, H.E. (1990). Structure and variability of human chromosome ends. *Mol Cell Biol* *10*, 518-527.

De Marchi, S., Cecchin, E., Basile, A., Bertotti, A., Nardini, R., and Bartoli, E. (1993). Renal tubular dysfunction in chronic alcohol abuse--effects of abstinence. *N Engl J Med* *329*, 1927-1934.

Deans, A.J., and West, S.C. (2011). DNA interstrand crosslink repair and cancer. *1-14*.

Dellarco, V.L. (1988). A mutagenicity assessment of acetaldehyde. *Mutat Res* *195*, 1-20.

Douwel, D.K., Boonen, R.A.C.M., Long, D.T., Szypowska, A.A., Räschle, M., Walter, J.C., and Knipscheer, P. (2014). XPF-ERCC1 Acts in Unhooking DNA Interstrand Crosslinks in Cooperation with FANCD2 and FANCP/SLX4. *Mol Cell*, *1-12*.

Dronkert, M.L., de Wit, J., Boeve, M., Vasconcelos, M.L., van Steeg, H., Tan, T.L., Hoeijmakers, J.H., and Kanaar, R. (2000). Disruption of mouse SNM1 causes increased sensitivity to the DNA interstrand cross-linking agent mitomycin C. *Mol Cell Biol* 20, 4553-4561.

Dunnick, J.K., Forbes, P.D., Davies, R.E., and Iverson, W.O. (1987). Toxicity of 8-methoxypsoralen, 5-methoxypsoralen, 3-carbethoxypsoralen, or 5-methylisopsoralen with ultraviolet radiation in the hairless (HRA/Skh) mouse. *Toxicol Appl Pharmacol* 89, 73-80.

Dutta, S., Chowdhury, G., and Gates, K.S. (2007). Interstrand cross-links generated by abasic sites in duplex DNA. *J Am Chem Soc* 129, 1852-1853.

Eastman, A. (1983). Characterization of the adducts produced in DNA by cis-diamminedichloroplatinum(II) and cis-dichloro(ethylenediamine)platinum(II). *Biochemistry* 22, 3927-3933.

Epstein, M. (1997). Alcohol's impact on kidney function. *Alcohol Health Res World* 21, 84-92.

Falzon, M., Fewell, J.W., and Kuff, E.L. (1993). EBP-80, a transcription factor closely resembling the human autoantigen Ku, recognizes single- to double-strand transitions in DNA. *J Biol Chem* 268, 10546-10552.

Fanconi, G. (1967). Familial constitutional panmyelocytopathy, Fanconi's anemia (F.A.). I. Clinical aspects. *Semin Hematol* 4, 233-240.

Fattah, F.J., Lichter, N.F., Fattah, K.R., Oh, S., and Hendrickson, E.A. (2008a). Ku70, an essential gene, modulates the frequency of rAAV-mediated gene targeting in human somatic cells. *Proc Natl Acad Sci U S A* 105, 8703-8708.

Fattah, K.R., Ruis, B.L., and Hendrickson, E.A. (2008b). Mutations to Ku reveal differences in human somatic cell lines. *DNA Repair (Amst)* 7, 762-774.

Fekairi, S., Scaglione, S., Chahwan, C., Taylor, E.R., Tissier, A., Coulon, S., Dong, M.-Q., Ruse, C., Yates, I., John R, Russell, P., *et al.* (2009). Human SLX4 Is a Holliday Junction Resolvase Subunit that Binds Multiple DNA Repair/Recombination Endonucleases. *Cell* 138, 78-89.

Fontebasso, Y., Etheridge, T.J., Oliver, A.W., Murray, J.M., and Carr, A.M. (2013). The conserved Fanconi anemia nuclease Fan1 and the SUMO E3 ligase Pli1 act in two novel Pso2-independent pathways of DNA interstrand crosslink repair in yeast. *DNA repair* 12, 1011-1023.

Forsingdal, A., Fejgin, K., Nielsen, V., Werge, T., and Nielsen, J. (2016). 15q13.3 homozygous knockout mouse model display epilepsy-, autism- and schizophrenia-related phenotypes. *Transl Psychiatry* 6, e860.

Fricke, W.M., and Brill, S.J. (2003). Slx1-Slx4 is a second structure-specific endonuclease functionally redundant with Sgs1-Top3. *Genes Dev* 17, 1768-1778.

Garaycoechea, J.I., Crossan, G.P., Langevin, F., Daly, M., Arends, M.J., and Patel, K.J. (2012). Genotoxic consequences of endogenous aldehydes on mouse haematopoietic stem cell function. *Nature* 489, 571-575.

Garcia-Higuera, I., Taniguchi, T., Ganesan, S., Meyn, M.S., Timmers, C., Hejna, J., Grompe, M., and D'Andrea, A.D. (2001). Interaction of the Fanconi anemia proteins and BRCA1 in a common pathway. *Mol Cell* 7, 249-262.

Gargiulo, D., Kumar, G.S., Musser, S.S., and Tomasz, M. (1995). Structural and function modification of DNA by mitomycin C. Mechanism of the DNA sequence specificity of mitomycins. *Nucleic Acids Symp Ser*, 169-170.

Garner, E., Kim, Y., Lach, F.P., Kottemann, M.C., and Smogorzewska, A. (2013). Human GEN1 and the SLX4-associated nucleases MUS81 and SLX1 are essential for the resolution of replication-induced Holliday junctions. *Cell Rep* 5, 207-215.

Gentric, G., and Desdouets, C. (2014). Polyploidization in liver tissue. *Am J Pathol* 184, 322-331.

Girard, D.E., Kumar, K.L., and McAfee, J.H. (1987). Hematologic effects of acute and chronic alcohol abuse. *Hematol Oncol Clin North Am* 1, 321-334.

Godin, M., Francois, A., Le Roy, F., Morin, J.P., Creppy, E., Hemet, J., and Fillastre, J.P. (1996). Karyomegalic interstitial nephritis. *Am J Kidney Dis* 27, 166.

Goedde, H.W., and Agarwal, D.P. (1990). Pharmacogenetics of aldehyde dehydrogenase (ALDH). *Pharmacol Ther* 45, 345-371.

Goodarzi, A.A., Yu, Y., Riballo, E., Douglas, P., Walker, S.A., Ye, R., Harer, C., Marchetti, C., Morrice, N., Jeggo, P.A., *et al.* (2006). DNA-PK autophosphorylation facilitates Artemis endonuclease activity. *EMBO J* 25, 3880-3889.

Goodman, L.S., Wintrobe, M.M., and *et al.* (1946). Nitrogen mustard therapy; use of methyl-bis (beta-chloroethyl) amine hydrochloride and tris (beta-chloroethyl) amine hydrochloride for Hodgkin's disease, lymphosarcoma, leukemia and certain allied and miscellaneous disorders. *J Am Med Assoc* 132, 126-132.

Grawunder, U., Wilm, M., Wu, X., Kulesza, P., Wilson, T.E., Mann, M., and Lieber, M.R. (1997). Activity of DNA ligase IV stimulated by complex formation with XRCC4 protein in mammalian cells. *Nature* 388, 492-495.

Gwon, G.H., Kim, Y., Liu, Y., Watson, A.T., Jo, A., Etheridge, T.J., Yuan, F., Zhang, Y., Kim, Y., Carr, A.M., *et al.* (2014). Crystal structure of a Fanconi anemia-associated nuclease homolog bound to 5' flap DNA: basis of interstrand cross-link repair by FAN1. *Genes Dev* 28, 2276-2290.

Hall, A.M., Bass, P., and Unwin, R.J. (2014). Drug-induced renal Fanconi syndrome. *QJM* 107, 261-269.

Hazrati, A., Ramis-Castellort, M., Sarkar, S., Barber, L.J., Schofield, C.J., Hartley, J.A., and McHugh, P.J. (2008). Human SNM1A suppresses the DNA repair defects of yeast *pso2* mutants. *DNA repair* 7, 230-238.

Hejna, J., Philip, S., Ott, J., Faulkner, C., and Moses, R. (2007). The hSNM1 protein is a DNA 5'-exonuclease. *Nucleic Acids Res* 35, 6115-6123.

Herskowitz, I.H. (1950). The differential induction of lethal mutations by formalin in the two sexes of *Drosophila*. *Science* 112, 302-303.

Hira, A., Yabe, H., Yoshida, K., Okuno, Y., Shiraishi, Y., Chiba, K., Tanaka, H., Miyano, S., Nakamura, J., Kojima, S., *et al.* (2013). Variant ALDH2 is associated with accelerated progression of bone marrow failure in Japanese Fanconi anemia patients. *Blood* 122, 3206-3209.

Hodskinson, M.R.G., Silhan, J., Crossan, G.P., Garaycochea, J.I., Mukherjee, S., Johnson, C.M., Schärer, O.D., and Patel, K.J. (2014). Mouse SLX4 Is a Tumor Suppressor that Stimulates the Activity of the Nuclease XPF-ERCC1 in DNA Crosslink Repair. *Mol Cell*, 1-33.

Hoeijmakers, J.H. (2009). DNA damage, aging, and cancer. *N Engl J Med* 361, 1475-1485.

Hofmann, K. (2009). Ubiquitin-binding domains and their role in the DNA damage response. *DNA Repair (Amst)* 8, 544-556.

Houghtaling, S., Newell, A., Akkari, Y., Taniguchi, T., Olson, S., and Grompe, M. (2005). Fancd2 functions in a double strand break repair pathway that is distinct from non-homologous end joining. *Hum Mol Genet* 14, 3027-3033.

Houghtaling, S., Timmers, C., Noll, M., Finegold, M.J., Jones, S.N., Meyn, M.S., and Grompe, M. (2003). Epithelial cancer in Fanconi anemia complementation group D2 (Fancd2) knockout mice. *Genes Dev* 17, 2021-2035.

Howlett, N.G., Taniguchi, T., Olson, S., Cox, B., Waisfisz, Q., De Die-Smulders, C., Persky, N., Grompe, M., Joenje, H., Pals, G., *et al.* (2002). Biallelic inactivation of BRCA2 in Fanconi anemia. *Science* 297, 606-609.

Huang, H., Kozekov, I.D., Kozekova, A., Wang, H., Lloyd, R.S., Rizzo, C.J., and Stone, M.P. (2010). DNA cross-link induced by trans-4-hydroxynonenal. *Environ Mol Mutagen* 51, 625-634.

Huang, J., Liu, S., Bellani, M.A., Thazhathveetil, A.K., Ling, C., de Winter, J.P., Wang, Y., Wang, W., and Seidman, M.M. (2013). The DNA translocase FANCM/MHF promotes replication traverse of DNA interstrand crosslinks. *Mol Cell* 52, 434-446.

Humans, I.W.G.o.t.E.o.C.R.t. (2006). Formaldehyde, 2-butoxyethanol and 1-tert-butoxypropan-2-ol. *IARC Monogr Eval Carcinog Risks Hum* 88, 1-478.

INoll, M., Battaile, K.P., Bateman, R., Lax, T.P., Rathbun, K., Reifsteck, C., Bagby, G., Finegold, M., Olson, S., and Grompe, M. (2002). Fanconi anemia group A and C double-mutant mice: functional evidence for a multi-protein Fanconi anemia complex. *Exp Hematol* 30, 679-688.

Ishiai, M., Kimura, M., Namikoshi, K., Yamazoe, M., Yamamoto, K., Arakawa, H., Agematsu, K., Matsushita, N., Takeda, S., Buerstedde, J.-M., *et al.* (2004). DNA cross-link repair protein SNM1A interacts with PIAS1 in nuclear focus formation. *Mol Cell Biol* 24, 10733-10741.

Ishiai, M., Kitao, H., Smogorzewska, A., Tomida, J., Kinomura, A., Uchida, E., Saberi, A., Kinoshita, E., Kinoshita-Kikuta, E., Koike, T., *et al.* (2008). FANCI phosphorylation functions as a molecular switch to turn on the Fanconi anemia pathway. *Nat Struct Mol Biol* *15*, 1138-1146.

Isnard, P., Rabant, M., Labaye, J., Antignac, C., Knebelmann, B., and Zaidan, M. (2016). Karyomegalic Interstitial Nephritis: A Case Report and Review of the Literature. *Medicine (Baltimore)* *95*, e3349.

Iwabuchi, K., Hashimoto, M., Matsui, T., Kurihara, T., Shimizu, H., Adachi, N., Ishiai, M., Yamamoto, K., Tauchi, H., Takata, M., *et al.* (2006). 53BP1 contributes to survival of cells irradiated with X-ray during G1 without Ku70 or Artemis. *Genes Cells* *11*, 935-948.

Iyer, L.M., Babu, M.M., and Aravind, L. (2006). The HIRAN domain and recruitment of chromatin remodeling and repair activities to damaged DNA. *Cell Cycle* *5*, 775-782.

Iyer, R.R., Pluciennik, A., Napierala, M., and Wells, R.D. (2015). DNA triplet repeat expansion and mismatch repair. *Annu Rev Biochem* *84*, 199-226.

Jackson, B., Brocker, C., Thompson, D.C., Black, W., Vasiliou, K., Nebert, D.W., and Vasiliou, V. (2011). Update on the aldehyde dehydrogenase gene (ALDH) superfamily. *Hum Genomics* 5, 283-303.

Jacobsen, E. (1950). Is acetaldehyde an intermediary product in normal metabolism? *Biochim Biophys Acta* 4, 330-334.

Jensen, R.P., Luo, W., Pankow, J.F., Strongin, R.M., and Peyton, D.H. (2015). Hidden formaldehyde in e-cigarette aerosols. *N Engl J Med* 372, 392-394.

Jones, R.E., Oh, S., Grimstead, J.W., Zimbric, J., Roger, L., Heppel, N.H., Ashelford, K.E., Liddiard, K., Hendrickson, E.A., and Baird, D.M. (2014). Escape from telomere-driven crisis is DNA ligase III dependent. *Cell Rep* 8, 1063-1076.

Jung, K., Schulze, B.D., and Sydow, K. (1987). Diagnostic significance of different urinary enzymes in patients suffering from chronic renal diseases. *Clin Chim Acta* 168, 287-295.

Katayama, Y., Mahmut, N., Takimoto, H., Maeda, Y., Yano, T., Kojima, K., Azuma, T., Hara, M., Imajyo, K., Takahashi, S., *et al.* (1999). Hematopoietic progenitor cells from allogeneic bone marrow transplant donors circulate in the very early post-transplant period. *Bone Marrow Transplant* 23, 659-665.

Kelly, P.F., Radtke, S., Kalle, C.V., Balcik, B., Bohn, K., Mueller, R., Schuesler, T., Haren, M., Reeves, L., Cancelas, J.A., *et al.* (2007). Stem Cell Collection and Gene Transfer in Fanconi Anemia. *Mol Ther* 15, 211-219.

Kim, Y., Lach, F.P., Desetty, R., Hanenberg, H., Auerbach, A.D., and Smogorzewska, A. (2011). Mutations of the SLX4 gene in Fanconi anemia. *Nat Genet* 43, 142-146.

Kim, Y., Spitz, G.S., Veturi, U., Lach, F.P., Auerbach, A.D., and Smogorzewska, A. (2013). Regulation of multiple DNA repair pathways by the Fanconi anemia protein SLX4. *Blood* 121, 54-63.

Kinch, L.N., Ginalski, K., Rychlewski, L., and Grishin, N.V. (2005). Identification of novel restriction endonuclease-like fold families among hypothetical proteins. *Nucleic Acids Res* 33, 3598-3605.

Kirchner, J.J., Sigurdsson, S.T., and Hopkins, P.B. (1992). Interstrand Cross-Linking of Duplex DNA by Nitrous-Acid - Covalent Structure of the Dg-to-Dg Cross-Link at the Sequence 5'-Cg. *J Am Chem Soc* 114, 4021-4027.

Klyosov, A.A., Rashkovetsky, L.G., Tahir, M.K., and Keung, W.M. (1996). Possible role of liver cytosolic and mitochondrial aldehyde dehydrogenases in acetaldehyde metabolism. *Biochemistry* 35, 4445-4456.

Knipscheer, P., Raschle, M., Smogorzewska, A., Enoiu, M., Ho, T.V., Scharer, O.D., Elledge, S.J., and Walter, J.C. (2009). The Fanconi Anemia Pathway Promotes Replication-Dependent DNA Interstrand Cross-Link Repair. *Science* 326, 1698-1701.

Kosinski, J., Feder, M., and Bujnicki, J.M. (2005). The PD-(D/E)XK superfamily revisited: identification of new members among proteins involved in DNA metabolism and functional predictions for domains of (hitherto) unknown function. *BMC Bioinformatics* 6, 172.

Kottemann, M.C., and Smogorzewska, A. (2013). Fanconi anaemia and the repair of Watson and Crick DNA crosslinks. *Nature* 493, 356-363.

Kratz, K., Schöpf, B., Kaden, S., Sendoel, A., Eberhard, R., Lademann, C., Cannavó, E., Sartori, A.A., Hengartner, M.O., and Jiricny, J. (2010). Deficiency of FANCD2-Associated Nuclease KIAA1018/FAN1 Sensitizes Cells to Interstrand Crosslinking Agents. *Cell* 142, 77-88.

Kutler, D.I., Auerbach, A.D., Satagopan, J., Giampietro, P.F., Batish, S.D., Huvos, A.G., Goberdhan, A., Shah, J.P., and Singh, B. (2003a). High incidence of head and neck squamous cell carcinoma in patients with Fanconi anemia. *Arch Otolaryngol Head Neck Surg* 129, 106-112.

Kutler, D.I., Singh, B., Satagopan, J., Batish, S.D., Berwick, M., Giampietro, P.F., Hanenberg, H., and Auerbach, A.D. (2003b). A 20-year perspective on the International Fanconi Anemia Registry (IFAR). *Blood* 101, 1249-1256.

Labarga, P., Barreiro, P., Martin-Carbonero, L., Rodriguez-Novoa, S., Solera, C., Medrano, J., Rivas, P., Albalater, M., Blanco, F., Moreno, V., *et al.* (2009). Kidney tubular abnormalities in the absence of impaired glomerular function in HIV patients treated with tenofovir. *AIDS* 23, 689-696.

Lachaud, C., Moreno, A., Marchesi, F., Toth, R., Blow, J.J., and Rouse, J. (2016a). Ubiquitinated Fancd2 recruits Fan1 to stalled replication forks to prevent genome instability. *Science*.

Lachaud, C., Slean, M., Marchesi, F., Lock, C., Odell, E., Castor, D., Toth, R., and Rouse, J. (2016b). Karyomegalic interstitial nephritis and DNA damage-induced polyploidy in Fan1 nuclease-defective knock-in mice. *Genes Dev* 30, 639-644.

Laitinen, K., Lamberg-Allardt, C., Tunninen, R., Karonen, S.L., Tahtela, R., Ylikahri, R., and Valimaki, M. (1991). Transient hypoparathyroidism during acute alcohol intoxication. *N Engl J Med* 324, 721-727.

Langevin, F., Crossan, G.P., Rosado, I.V., Arends, M.J., and Patel, K.J. (2011). Fancd2 counteracts the toxic effects of naturally produced aldehydes in mice. *Nature* 475, 53-58.

Levrn, O., Attwooll, C., Henry, R.T., Milton, K.L., Neveling, K., Rio, P., Batish, S.D., Kalb, R., Velleuer, E., Barral, S., *et al.* (2005). The BRCA1-interacting helicase BRIP1 is deficient in Fanconi anemia. *Nat Genet* 37, 931-933.

Li, G., Nelsen, C., and Hendrickson, E.A. (2002). Ku86 is essential in human somatic cells. *Proc Natl Acad Sci U S A* 99, 832-837.

Li, X., and Heyer, W.D. (2008). Homologous recombination in DNA repair and DNA damage tolerance. *Cell Res* 18, 99-113.

Lieber, M.R. (2008). The mechanism of human nonhomologous DNA end joining. *J Biol Chem* 283, 1-5.

Lieber, M.R. (2010). The mechanism of double-strand DNA break repair by the nonhomologous DNA end-joining pathway. *Annu Rev Biochem* 79, 181-211.

Lindahl, T. (1993). Instability and decay of the primary structure of DNA. *Nature* 362, 709-715.

Lindahl, T., and Barnes, D.E. (2000). Repair of endogenous DNA damage. *Cold Spring Harb Symp Quant Biol* 65, 127-133.

Liu, L., Yan, Y., Zeng, M., Zhang, J., Hanes, M.A., Ahearn, G., McMahon, T.J., Dickfeld, T., Marshall, H.E., Que, L.G., *et al.* (2004). Essential roles of S-nitrosothiols in vascular homeostasis and endotoxic shock. *Cell* 116, 617-628.

Liu, T., Ghosal, G., Yuan, J., Chen, J., and Huang, J. (2010). FAN1 Acts with FANCI-FANCD2 to Promote DNA Interstrand Cross-Link Repair. *Science* 329, 693-696.

Loenarz, C., and Schofield, C.J. (2008). Expanding chemical biology of 2-oxoglutarate oxygenases. *Nat Chem Biol* 4, 152-156.

Long, D.T., Raschle, M., Joukov, V., and Walter, J.C. (2011). Mechanism of RAD51-dependent DNA interstrand cross-link repair. *Science* 333, 84-87.

Lu, K., Collins, L.B., Ru, H., Bermudez, E., and Swenberg, J.A. (2010). Distribution of DNA adducts caused by inhaled formaldehyde is consistent with induction of nasal carcinoma but not leukemia. *Toxicol Sci* 116, 441-451.

MacKay, C., Déclais, A.-C., Lundin, C., Agostinho, A., Deans, A.J., MacArtney, T.J., Hofmann, K., Gartner, A., West, S.C., Helleday, T., *et al.* (2010).

Identification of KIAA1018/FAN1, a DNA Repair Nuclease Recruited to DNA Damage by Monoubiquitinated FANCD2. *Cell* 142, 65-76.

Magana-Schwencke, N., and Ekert, B. (1978). Biochemical analysis of damage induced in yeast by formaldehyde. II. Induction of cross-links between DNA and protein. *Mutat Res* 51, 11-19.

Marchitti, S.A., Brocker, C., Stagos, D., and Vasiliou, V. (2008). Non-P450 aldehyde oxidizing enzymes: the aldehyde dehydrogenase superfamily. *Expert Opin Drug Metab Toxicol* 4, 697-720.

Marietta, C., Thompson, L.H., Lamerdin, J.E., and Brooks, P.J. (2009). Acetaldehyde stimulates FANCD2 monoubiquitination, H2AX phosphorylation, and BRCA1 phosphorylation in human cells in vitro: implications for alcohol-related carcinogenesis. *Mutat Res* 664, 77-83.

Matsuda, T., Terashima, I., Matsumoto, Y., Yabushita, H., Matsui, S., and Shibutani, S. (1999). Effective utilization of N2-ethyl-2'-deoxyguanosine triphosphate during DNA synthesis catalyzed by mammalian replicative DNA polymerases. *Biochemistry* 38, 929-935.

McGhee, J.D., and von Hippel, P.H. (1977). Formaldehyde as a probe of DNA structure. 3. Equilibrium denaturation of DNA and synthetic polynucleotides. *Biochemistry* 16, 3267-3276.

Mechilli, M., Schinoppi, A., Kobos, K., Natarajan, A.T., and Palitti, F. (2008). DNA repair deficiency and acetaldehyde-induced chromosomal alterations in CHO cells. *Mutagenesis* 23, 51-56.

Mihatsch, M.J., Gudat, F., Zollinger, H.U., Heierli, C., Tholen, H., and Reutter, F.W. (1979). Systemic karyomegaly associated with chronic interstitial nephritis. A new disease entity? *Clin Nephrol* 12, 54-62.

Mills, S.J., and Harrison, S.A. (2005). Comparison of the natural history of alcoholic and nonalcoholic fatty liver disease. *Curr Gastroenterol Rep* 7, 32-36.

Mimori, T., and Hardin, J.A. (1986). Mechanism of interaction between Ku protein and DNA. *J Biol Chem* 261, 10375-10379.

Mirkin, S.M. (2007). Expandable DNA repeats and human disease. *Nature* 447, 932-940.

Moldovan, G.-L., and D'Andrea, A.D. (2009). How the Fanconi Anemia Pathway Guards the Genome. In *Genetics*, pp. 223-249.

Montes de Oca, R., Andreassen, P.R., Margossian, S.P., Gregory, R.C., Taniguchi, T., Wang, X., Houghtaling, S., Grompe, M., and D'Andrea, A.D. (2005). Regulated interaction of the Fanconi anemia protein, FANCD2, with chromatin. *Blood* *105*, 1003-1009.

Moore, J.K., and Haber, J.E. (1996). Cell cycle and genetic requirements of two pathways of nonhomologous end-joining repair of double-strand breaks in *Saccharomyces cerevisiae*. *Mol Cell Biol* *16*, 2164-2173.

Morrison, S.J., Wandycz, A.M., Akashi, K., Globerson, A., and Weissman, I.L. (1996). The aging of hematopoietic stem cells. *Nat Med* *2*, 1011-1016.

Munoz, I.M., Hain, K., Declais, A.C., Gardiner, M., Toh, G.W., Sanchez-Pulido, L., Heuckmann, J.M., Toth, R., Macartney, T., Eppink, B., *et al.* (2009). Coordination of structure-specific nucleases by human SLX4/BTBD12 is required for DNA repair. *Mol Cell* *35*, 116-127.

Myung, K., Ghosh, G., Fattah, F.J., Li, G., Kim, H., Dutia, A., Pak, E., Smith, S., and Hendrickson, E.A. (2004). Regulation of telomere length and suppression of genomic instability in human somatic cells by Ku86. *Mol Cell Biol* *24*, 5050-5059.

Nakamura, K., Sakai, W., Kawamoto, T., Bree, R.T., Lowndes, N.F., Takeda, S., and Taniguchi, Y. (2006). Genetic dissection of vertebrate 53BP1: a major role in

non-homologous end joining of DNA double strand breaks. *DNA Repair (Amst)* 5, 741-749.

Nakanishi, K., Yang, Y.G., Pierce, A.J., Taniguchi, T., Digweed, M., D'Andrea, A.D., Wang, Z.Q., and Jasin, M. (2005). Human Fanconi anemia monoubiquitination pathway promotes homologous DNA repair. *Proc Natl Acad Sci U S A* 102, 1110-1115.

Norden, A.G., Scheinman, S.J., Deschodt-Lanckman, M.M., Lapsley, M., Nortier, J.L., Thakker, R.V., Unwin, R.J., and Wrong, O. (2000). Tubular proteinuria defined by a study of Dent's (CLCN5 mutation) and other tubular diseases. *Kidney Int* 57, 240-249.

Nussenzweig, A., Sokol, K., Burgman, P., Li, L., and Li, G.C. (1997). Hypersensitivity of Ku80-deficient cell lines and mice to DNA damage: the effects of ionizing radiation on growth, survival, and development. *Proc Natl Acad Sci U S A* 94, 13588-13593.

Oberbeck, N., Langevin, F., King, G., de Wind, N., Crossan, G.P., and Patel, K.J. (2014). Maternal aldehyde elimination during pregnancy preserves the fetal genome. *Mol Cell* 55, 807-817.

Ogawa, H., Gomi, T., and Fujioka, M. (2000). Serine hydroxymethyltransferase and threonine aldolase: are they identical? *Int J Biochem Cell Biol* 32, 289-301.

Oh, S., Harvey, A., Zimbric, J., Wang, Y., Nguyen, T., Jackson, P.J., and Hendrickson, E.A. (2014). DNA ligase III and DNA ligase IV carry out genetically distinct forms of end joining in human somatic cells. *DNA Repair (Amst)* 21, 97-110.

Oh, S., Wang, Y., Zimbric, J., and Hendrickson, E.A. (2013). Human LIGIV is synthetically lethal with the loss of Rad54B-dependent recombination and is required for certain chromosome fusion events induced by telomere dysfunction. *Nucleic Acids Res* 41, 1734-1749.

Pace, P., Mosedale, G., Hodkinson, M.R., Rosado, I.V., Sivasubramaniam, M., and Patel, K.J. (2010). Ku70 corrupts DNA repair in the absence of the Fanconi anemia pathway. *Science* 329, 219-223.

Parenti, P., Giordana, B., and Hanozet, G.M. (1991). In vitro effect of ethanol on sodium and glucose transport in rabbit renal brush border membrane vesicles. *Biochim Biophys Acta* 1070, 92-98.

Park, J.Y., Virts, E.L., Jankowska, A., Wiek, C., Othman, M., Chakraborty, S.C., Vance, G.H., Alkuraya, F.S., Hanenberg, H., and Andreassen, P.R. (2016).

Complementation of hypersensitivity to DNA interstrand crosslinking agents demonstrates that XRCC2 is a Fanconi anaemia gene. *J Med Genet* 53, 672-680.

Patel, K.J., and Joenje, H. (2007). Fanconi anemia and DNA replication repair. *DNA Repair (Amst)* 6, 885-890.

Pizzolato, J., Mukherjee, S., Schärer, O.D., and Jiricny, J. (2015). FANCD2-associated Nuclease 1, but Not Exonuclease 1 or Flap Endonuclease 1, Is Able to Unhook DNA Interstrand Cross-links in Vitro. *Journal of Biological Chemistry* 290, 22602-22611.

Pontel, L.B., Rosado, I.V., Burgos-Barragan, G., Garaycochea, J.I., Yu, R., Arends, M.J., Chandrasekaran, G., Broecker, V., Wei, W., Liu, L., *et al.* (2015). Endogenous Formaldehyde Is a Hematopoietic Stem Cell Genotoxin and Metabolic Carcinogen. *Mol Cell* 60, 177-188.

Radha, S., Tameem, A., and Rao, B.S. (2014). Karyomegalic interstitial nephritis with focal segmental glomerulosclerosis: A rare association. *Indian J Nephrol* 24, 117-119.

Rafnar, T., Gudbjartsson, D.F., Sulem, P., Jonasdottir, A., Sigurdsson, A., Jonasdottir, A., Besenbacher, S., Lundin, P., Stacey, S.N., Gudmundsson, J., *et*

al. (2011). Mutations in BRIP1 confer high risk of ovarian cancer. *Nat Genet* 43, 1104-1107.

Rahman, N., Seal, S., Thompson, D., Kelly, P., Renwick, A., Elliott, A., Reid, S., Spanova, K., Barfoot, R., Chagtai, T., *et al.* (2007). PALB2, which encodes a BRCA2-interacting protein, is a breast cancer susceptibility gene. *Nat Genet* 39, 165-167.

Raschle, M., Knipscheer, P., Enoiu, M., Angelov, T., Sun, J., Griffith, J.D., Ellenberger, T.E., Scharer, O.D., and Walter, J.C. (2008). Mechanism of replication-coupled DNA interstrand crosslink repair. *Cell* 134, 969-980.

Reid, S., Schindler, D., Hanenberg, H., Barker, K., Hanks, S., Kalb, R., Neveling, K., Kelly, P., Seal, S., Freund, M., *et al.* (2007). Biallelic mutations in PALB2 cause Fanconi anemia subtype FA-N and predispose to childhood cancer. *Nat Genet* 39, 162-164.

Riballo, E., Kuhne, M., Rief, N., Doherty, A., Smith, G.C., Recio, M.J., Reis, C., Dahm, K., Fricke, A., Krempler, A., *et al.* (2004). A pathway of double-strand break rejoining dependent upon ATM, Artemis, and proteins locating to gamma-H2AX foci. *Mol Cell* 16, 715-724.

Ridpath, J.R., Nakamura, A., Tano, K., Luke, A.M., Sonoda, E., Arakawa, H., Buerstedde, J.M., Gillespie, D.A., Sale, J.E., Yamazoe, M., *et al.* (2007). Cells deficient in the FANC/BRCA pathway are hypersensitive to plasma levels of formaldehyde. *Cancer Res* 67, 11117-11122.

Ristow, H., and Obe, G. (1978). Acetaldehyde induces cross-links in DNA and causes sister-chromatid exchanges in human cells. *Mutat Res* 58, 115-119.

Rodrigo, R., Vergara, L., and Oberhauser, E. (1991). Effect of chronic ethanol consumption on postnatal development of renal (Na + K)-ATPase in the rat. *Cell Biochem Funct* 9, 215-222.

Rosado, I.V., Langevin, F., Crossan, G.P., Takata, M., and Patel, K.J. (2011). Formaldehyde catabolism is essential in cells deficient for the Fanconi anemia DNA-repair pathway. *Nat Struct Mol Biol* 18, 1432-1434.

Rosenberg, P.S., Greene, M.H., and Alter, B.P. (2003). Cancer incidence in persons with Fanconi anemia. *Blood* 101, 822-826.

Rossi, D.J., Bryder, D., Seita, J., Nussenzweig, A., Hoeijmakers, J., and Weissman, I.L. (2007). Deficiencies in DNA damage repair limit the function of haematopoietic stem cells with age. *Nature* 447, 725-729.

Rothman, A., Proverbio, T., Fernandez, E., and Proverbio, F. (1992). Effect of ethanol on the Na(+)- and the Na⁺,K(+)-ATPase activities of basolateral plasma membranes of kidney proximal tubular cells. *Biochem Pharmacol* 43, 2034-2036.

Sanghani, P.C., Stone, C.L., Ray, B.D., Pindel, E.V., Hurley, T.D., and Bosron, W.F. (2000). Kinetic mechanism of human glutathione-dependent formaldehyde dehydrogenase. *Biochemistry* 39, 10720-10729.

Schardijn, G.H., and Statius van Eps, L.W. (1987). Beta 2-microglobulin: its significance in the evaluation of renal function. *Kidney Int* 32, 635-641.

Scharer, O.D. (2005). DNA interstrand crosslinks: natural and drug-induced DNA adducts that induce unique cellular responses. *Chembiochem* 6, 27-32.

Schmid, W., and Fanconi, G. (1978). Fragility and spiralization anomalies of the chromosomes in three cases, including fraternal twins, with Fanconi's anemia, type Estren-Dameshek. *Cytogenet Cell Genet* 20, 141-149.

Sclare, G. (1976). A case of unexplained karyomegaly. *Beitr Pathol* 157, 301-306.

Seal, S., Thompson, D., Renwick, A., Elliott, A., Kelly, P., Barfoot, R., Chagtai, T., Jayatilake, H., Ahmed, M., Spanova, K., *et al.* (2006). Truncating mutations in the

Fanconi anemia J gene BRIP1 are low-penetrance breast cancer susceptibility alleles. *Nat Genet* 38, 1239-1241.

Segui, N., Mina, L.B., Lazaro, C., Sanz-Pamplona, R., Pons, T., Navarro, M., Bellido, F., Lopez-Doriga, A., Valdes-Mas, R., Pineda, M., *et al.* (2015). Germline Mutations in FAN1 Cause Hereditary Colorectal Cancer by Impairing DNA Repair. *Gastroenterology* 149, 563-566.

Seitz, H.K., and Becker, P. (2007). Alcohol metabolism and cancer risk. *Alcohol Res Health* 30, 38-41, 44-37.

Semlow, D.R., Zhang, J., Budzowska, M., Drohat, A.C., and Walter, J.C. (2016). Replication-Dependent Unhooking of DNA Interstrand Cross-Links by the NEIL3 Glycosylase. *Cell* 167, 498-511 e414.

Shah, S., Kim, Y., Ostrovnaya, I., Murali, R., Schrader, K.A., Lach, F.P., Sarrel, K., Rau-Murthy, R., Hansen, N., Zhang, L., *et al.* (2013). Assessment of SLX4 Mutations in Hereditary Breast Cancers. *PLoS One* 8, e66961.

Shimamura, A., and Alter, B.P. (2010). Pathophysiology and management of inherited bone marrow failure syndromes. *Blood Rev* 24, 101-122.

Simsek, D., Furda, A., Gao, Y., Artus, J., Brunet, E., Hadjantonakis, A.K., Van Houten, B., Shuman, S., McKinnon, P.J., and Jasin, M. (2011). Crucial role for DNA ligase III in mitochondria but not in Xrcc1-dependent repair. *Nature* 471, 245-248.

Smith, A.L., Alirezaie, N., Connor, A., Chan-Seng-Yue, M., Grant, R., Selander, I., Bascunana, C., Borgida, A., Hall, A., Whelan, T., *et al.* (2015). Candidate DNA repair susceptibility genes identified by exome sequencing in high-risk pancreatic cancer. *Cancer Lett.*

Smogorzewska, A., Desetty, R., Saito, T.T., Schlabach, M., Lach, F.P., Sowa, M.E., Clark, A.B., Kunkel, T.A., Harper, J.W., Colaiácovo, M.P., *et al.* (2010). A genetic screen identifies FAN1, a Fanconi anemia-associated nuclease necessary for DNA interstrand crosslink repair. *Mol Cell* 39, 36-47.

Smogorzewska, A., Matsuoka, S., Vinciguerra, P., McDonald, E.R., 3rd, Hurov, K.E., Luo, J., Ballif, B.A., Gygi, S.P., Hofmann, K., D'Andrea, A.D., *et al.* (2007). Identification of the FANCI protein, a monoubiquitinated FANCD2 paralog required for DNA repair. *Cell* 129, 289-301.

Solomon, M.J., and Varshavsky, A. (1985). Formaldehyde-mediated DNA-protein crosslinking: a probe for in vivo chromatin structures. *Proc Natl Acad Sci U S A* 82, 6470-6474.

Songur, A., Ozen, O.A., and Sarsilmaz, M. (2010). The toxic effects of formaldehyde on the nervous system. *Rev Environ Contam Toxicol* 203, 105-118.

Sonoda, E., Hochegger, H., Saberi, A., Taniguchi, Y., and Takeda, S. (2006). Differential usage of non-homologous end-joining and homologous recombination in double strand break repair. *DNA Repair (Amst)* 5, 1021-1029.

Spoendlin, M., Moch, H., Brunner, F., Brunner, W., Burger, H.R., Kiss, D., Wegmann, W., Dalquen, P., Oberholzer, M., Thiel, G., *et al.* (1995). Karyomegalic interstitial nephritis: further support for a distinct entity and evidence for a genetic defect. *Am J Kidney Dis* 25, 242-252.

Staab, C.A., Alander, J., Morgenstern, R., Grafstrom, R.C., and Hoog, J.O. (2009). The Janus face of alcohol dehydrogenase 3. *Chem Biol Interact* 178, 29-35.

Stein, S., Lao, Y., Yang, I.Y., Hecht, S.S., and Moriya, M. (2006). Genotoxicity of acetaldehyde- and crotonaldehyde-induced 1,N2-propanodeoxyguanosine DNA adducts in human cells. *Mutat Res* 608, 1-7.

Stone, M.P., Cho, Y.J., Huang, H., Kim, H.Y., Kozekov, I.D., Kozekova, A., Wang, H., Minko, I.G., Lloyd, R.S., Harris, T.M., *et al.* (2008). Interstrand DNA cross-

links induced by alpha,beta-unsaturated aldehydes derived from lipid peroxidation and environmental sources. *Acc Chem Res* **41**, 793-804.

Svendsen, J.M., Smogorzewska, A., Sowa, M.E., O'Connell, B.C., Gygi, S.P., Elledge, S.J., and Harper, J.W. (2009). Mammalian BTBD12/SLX4 assembles a Holliday junction resolvase and is required for DNA repair. *Cell* **138**, 63-77.

Thongthip, S., Bellani, M., Gregg, S.Q., Sridhar, S., Conti, B.A., Chen, Y., Seidman, M.M., and Smogorzewska, A. (2016). Fan1 deficiency results in DNA interstrand cross-link repair defects, enhanced tissue karyomegaly, and organ dysfunction. *Genes Dev* **30**, 645-659.

Tischkowitz, M., Xia, B., Sabbaghian, N., Reis-Filho, J.S., Hamel, N., Li, G., van Beers, E.H., Li, L., Khalil, T., Quenneville, L.A., *et al.* (2007). Analysis of PALB2/FANCN-associated breast cancer families. *Proc Natl Acad Sci U S A* **104**, 6788-6793.

Tome, S., Manley, K., Simard, J.P., Clark, G.W., Slean, M.M., Swami, M., Shelbourne, P.F., Tillier, E.R., Monckton, D.G., Messer, A., *et al.* (2013). MSH3 polymorphisms and protein levels affect CAG repeat instability in Huntington's disease mice. *PLoS Genet* **9**, e1003280.

Trocho, C., Pardo, R., Rafecas, I., Virgili, J., Remesar, X., Fernandez-Lopez, J.A., and Alemany, M. (1998). Formaldehyde derived from dietary aspartame binds to tissue components in vivo. *Life Sci* 63, 337-349.

Tulpule, A., Lensch, M.W., Miller, J.D., Austin, K., D'Andrea, A., Schlaeger, T.M., Shimamura, A., and Daley, G.Q. (2010). Knockdown of Fanconi anemia genes in human embryonic stem cells reveals early developmental defects in the hematopoietic lineage. *Blood* 115, 3453-3462.

Uz, E., Bayram, Y., Haltas, H., Bavbek, N., Kanbay, M., Guz, G., and Akçay, A. (2011). Karyomegalic tubulointerstitial nephritis: A rare cause of chronic kidney disease. *Nephro Urol Mon* 3, 201-203.

Van Thiel, D.H., Gavalier, J.S., Little, J.M., and Lester, R. (1977). Alcohol: its effect on the kidney. *Metabolism* 26, 857-866.

Vaz, F., Hanenberg, H., Schuster, B., Barker, K., Wiek, C., Erven, V., Neveling, K., Endt, D., Kesterton, I., Autore, F., *et al.* (2010). Mutation of the RAD51C gene in a Fanconi anemia-like disorder. *Nat Genet* 42, 406-409.

Vinciguerra, P., Godinho, S.A., Parmar, K., Pellman, D., and D'Andrea, A.D. (2010). Cytokinesis failure occurs in Fanconi anemia pathway-deficient murine and human bone marrow hematopoietic cells. *J Clin Invest* 120, 3834-3842.

Voigt, M.D. (2005). Alcohol in hepatocellular cancer. *Clin Liver Dis* 9, 151-169.

Wagner, J.E., Tolar, J., Levran, O., Scholl, T., Deffenbaugh, A., Satagopan, J., Ben-Porat, L., Mah, K., Batish, S.D., Kutler, D.I., *et al.* (2004). Germline mutations in BRCA2: shared genetic susceptibility to breast cancer, early onset leukemia, and Fanconi anemia. *Blood* 103, 3226-3229.

Walden, H., and Deans, A.J. (2014). The Fanconi anemia DNA repair pathway: structural and functional insights into a complex disorder. *Annu Rev Biophys* 43, 257-278.

Walport, L.J., Hopkinson, R.J., and Schofield, C.J. (2012). Mechanisms of human histone and nucleic acid demethylases. *Curr Opin Chem Biol* 16, 525-534.

Walsh, T., Casadei, S., Lee, M.K., Pennil, C.C., Nord, A.S., Thornton, A.M., Roeb, W., Agnew, K.J., Stray, S.M., Wickramanayake, A., *et al.* (2011). Mutations in 12 genes for inherited ovarian, fallopian tube, and peritoneal carcinoma identified by massively parallel sequencing. *Proc Natl Acad Sci U S A* 108, 18032-18037.

Wang, A.T., Kim, T., Wagner, J.E., Conti, B.A., Lach, F.P., Huang, A.L., Molina, H., Sanborn, E.M., Zierhut, H., Cornes, B.K., *et al.* (2015). A Dominant Mutation in Human RAD51 Reveals Its Function in DNA Interstrand Crosslink Repair Independent of Homologous Recombination. *Mol Cell* 59, 478-490.

Wang, A.T., Sengerova, B., Cattell, E., Inagawa, T., Hartley, J.M., Kiakos, K., Burgess-Brown, N.A., Swift, L.P., Enzlin, J.H., Schofield, C.J., *et al.* (2011). Human SNM1A and XPF-ERCC1 collaborate to initiate DNA interstrand cross-link repair. *Genes Dev* 25, 1859-1870.

Wang, M., McIntee, E.J., Cheng, G., Shi, Y., Villalta, P.W., and Hecht, S.S. (2000). Identification of DNA adducts of acetaldehyde. *Chem Res Toxicol* 13, 1149-1157.

Wang, R., Persky, N.S., Yoo, B., Ouerfelli, O., Smogorzewska, A., Elledge, S.J., and Pavletich, N.P. (2014). DNA repair. Mechanism of DNA interstrand cross-link processing by repair nuclease FAN1. *Science* 346, 1127-1130.

Wang, W. (2008). A major switch for the Fanconi anemia DNA damage-response pathway. *Nat Struct Mol Biol* 15, 1128-1130.

Wang, X., Peterson, C.A., Zheng, H., Nairn, R.S., Legerski, R.J., and Li, L. (2001). Involvement of nucleotide excision repair in a recombination-independent and error-prone pathway of DNA interstrand cross-link repair. *Mol Cell Biol* 21, 713-720.

Wang, Y., Ghosh, G., and Hendrickson, E.A. (2009). Ku86 represses lethal telomere deletion events in human somatic cells. *Proc Natl Acad Sci U S A* *106*, 12430-12435.

Ward, I.M., Reina-San-Martin, B., Olaru, A., Minn, K., Tamada, K., Lau, J.S., Cascalho, M., Chen, L., Nussenzweig, A., Livak, F., *et al.* (2004). 53BP1 is required for class switch recombination. *J Cell Biol* *165*, 459-464.

Wheeler, V.C., Lebel, L.A., Vrbanac, V., Teed, A., te Riele, H., and MacDonald, M.E. (2003). Mismatch repair gene Msh2 modifies the timing of early disease in Hdh(Q111) striatum. *Hum Mol Genet* *12*, 273-281.

Williams, H.L., Gottesman, M.E., and Gautier, J. (2012). Replication-independent repair of DNA interstrand crosslinks. *Mol Cell* *47*, 140-147.

Wyatt, H.D., Laister, R.C., Martin, S.R., Arrowsmith, C.H., and West, S.C. (2017). The SMX DNA Repair Tri-nuclease. *Mol Cell* *65*, 848-860 e811.

Wyatt, H.D.M., Sarbajna, S., Matos, J., and West, S.C. (2013). Coordinated actions of SLX1-SLX4 and MUS81-EME1 for Holliday junction resolution in human cells. *Mol Cell* *52*, 234-247.

Xia, B., Dorsman, J.C., Ameziane, N., de Vries, Y., Rooimans, M.A., Sheng, Q., Pals, G., Errami, A., Gluckman, E., Llera, J., *et al.* (2007). Fanconi anemia is associated with a defect in the BRCA2 partner PALB2. *Nat Genet* 39, 159-161.

Yamamoto, K.N., Kobayashi, S., Tsuda, M., Kurumizaka, H., Takata, M., Kono, K., Jiricny, J., Takeda, S., and Hirota, K. (2011). Involvement of SLX4 in interstrand cross-link repair is regulated by the Fanconi anemia pathway. *Proc Natl Acad Sci U S A* 108, 6492-6496.

Yan, Z., Guo, R., Paramasivam, M., Shen, W., Ling, C., Fox, D., 3rd, Wang, Y., Oostra, A.B., Kuehl, J., Lee, D.Y., *et al.* (2012). A ubiquitin-binding protein, FAAP20, links RNF8-mediated ubiquitination to the Fanconi anemia DNA repair network. *Mol Cell* 47, 61-75.

Yannone, S.M., Khan, I.S., Zhou, R.Z., Zhou, T., Valerie, K., and Povirk, L.F. (2008). Coordinate 5' and 3' endonucleolytic trimming of terminally blocked blunt DNA double-strand break ends by Artemis nuclease and DNA-dependent protein kinase. *Nucleic Acids Res* 36, 3354-3365.

Yoshida, A., Rzhetsky, A., Hsu, L.C., and Chang, C. (1998). Human aldehyde dehydrogenase gene family. *Eur J Biochem* 251, 549-557.

Yoshikiyo, K., Kratz, K., Hirota, K., Nishihara, K., Takata, M., Kurumizaka, H., Horimoto, S., Takeda, S., and Jiricny, J. (2010). KIAA1018/FAN1 nuclease protects cells against genomic instability induced by interstrand cross-linking agents. *Proc Natl Acad Sci USA* *107*, 21553-21557.

Zakhari, S. (2006). Overview: how is alcohol metabolized by the body? *Alcohol Res Health* *29*, 245-254.

Zhang, H., Kozono, D.E., O'Connor, K.W., Vidal-Cardenas, S., Rousseau, A., Hamilton, A., Moreau, L., Gaudiano, E.F., Greenberger, J., Bagby, G., *et al.* (2016). TGF-beta Inhibition Rescues Hematopoietic Stem Cell Defects and Bone Marrow Failure in Fanconi Anemia. *Cell Stem Cell* *18*, 668-681.

Zhang, J., and Walter, J.C. (2014). Mechanism and regulation of incisions during DNA interstrand cross-link repair. *DNA repair* *19*, 135-142.

Zhao, Q., Xue, X., Longerich, S., Sung, P., and Xiong, Y. (2014). Structural insights into 5' flap DNA unwinding and incision by the human FAN1 dimer. *Nat Comms* *5*, 5726.

Zhou, W., Otto, E.A., Cluckey, A., Airik, R., Hurd, T.W., Chaki, M., Diaz, K., Lach, F.P., Bennett, G.R., Gee, H.Y., *et al.* (2012). FAN1 mutations cause

karyomegalic interstitial nephritis, linking chronic kidney failure to defective DNA damage repair. Nat Genet 44, 910-915.